

The background of the cover features a large, irregularly shaped, light blue area containing a detailed histopathological image of lung cancer tissue. This area is overlaid on a solid blue background. In the upper right corner, there is a circular inset showing a magnified view of the same tissue. A dark blue curved line is visible on the left side of the cover.

HISTOPATHOLOGICAL ASPECTS OF RESECTED NON-SMALL CELL LUNG CANCER

with emphasis on Spread Through Air Spaces
and collapsed Adenocarcinoma *in Situ*

Hans Blaauwgeers

Histopathological aspects of resected non-small cell lung cancer, with emphasis on spread through air spaces and collapsed adenocarcinoma in situ

Hans Blaauwgeers

Histopathological aspects of resected non-small cell lung cancer, with emphasis on spread through air spaces and collapsed adenocarcinoma in situ

Thesis, Free University, Amsterdam, The Netherlands

Provided by thesis specialist Ridderprint, ridderprint.nl

Printing Ridderprint

Layout and design Indah Hijmans, persoonlijkproefschrift.nl

Cover design Indah Hijmans

ISBN 978-94-6483-237-2

DOI <http://doi.org/10.5463/thesis.317>

Financial support for the production and printing of this thesis was kindly provided by the Stichting Wetenschappelijk Onderzoek OLVG (SWOO)

Copyright © Hans Blaauwgeers

VRIJE UNIVERSITEIT

**HISTOPATHOLOGICAL ASPECTS OF RESECTED NON-SMALL CELL
LUNG CANCER**

with emphasis on Spread Through Air Spaces and collapsed Adenocarcinoma in Situ

ACADEMISCH PROEFSCHRIFT

ter verkrijging van de graad Doctor aan
de Vrije Universiteit Amsterdam,
op gezag van de rector magnificus
prof. dr. J.J.G. Geurts,
in het openbaar te verdedigen
ten overstaan van de promotiecommissie
van de Faculteit der Geneeskunde
op dinsdag 10 oktober 2023 om 13.45 uur
in een bijeenkomst van de universiteit,
De Boelelaan 1105

door

Johannes Lucas Gerhardus Blaauwgeers

geboren te Rijswijk (ZH)

promotor: prof.dr. E. Bloemena

copromotoren: dr. F.B.J.M. Thunnissen
dr. B.I. Lissenberg-Witte

promotiecommissie: prof.dr. S. Senan
prof.dr. P. Van Schil
prof.dr. K.M. Kerr
prof.dr. S. Lantuejoul
dr. T. Radonic
prof.dr. J.G.J.V. Aerts

Table of contents

Chapter 1	General introduction and outline of the thesis	9
------------------	--	----------

■ Part I: Histopathologic factors in the outcome and prognosis of NSCLC

Chapter 2	Complete pathological response is predictive for clinical outcome after tri-modality therapy for carcinomas of the superior pulmonary sulcus	19
------------------	--	-----------

Chapter 3	The prognostic value of proliferation, PD-L1 and nuclear size in patients with superior sulcus tumours treated with chemoradiotherapy and surgery.	35
------------------	--	-----------

Chapter 4	A population-based study of outcomes in surgically resected T3N0 non-small cell lung cancer in the Netherlands, defined using TNM-7 and TNM-8; justification of changes and an argument to incorporate histology in the staging algorithm.	47
------------------	--	-----------

■ Part II: Spread through air spaces, an artifact or reality?

Chapter 5	Ex vivo artifacts and histopathologic pitfalls in the lung	65
------------------	--	-----------

Chapter 6	A prospective study of loose tissue fragments in non-small cell lung cancer resection specimen. An alternative view to “spread through airspaces”	83
------------------	---	-----------

Chapter 7	Pulmonary loose tumor tissue fragments and spread through air spaces (STAS): invasive pattern or artifact? A critical review.	95
------------------	---	-----------

Chapter 8	To the editor: “Spread through air spaces (STAS) is prognostic in atypical carcinoid, large cell neuroendocrine carcinoma, and small cell carcinoma of the lung”	107
------------------	--	------------

Chapter 9	To the editor: “Spread through air spaces (STAS); can an artifact really be excluded?”.	111
------------------	---	------------

Chapter 10	Loose tumor cells in pulmonary arteries of lung adenocarcinoma resection specimen; no correlation with survival, despite high prevalence.	115
-------------------	---	------------

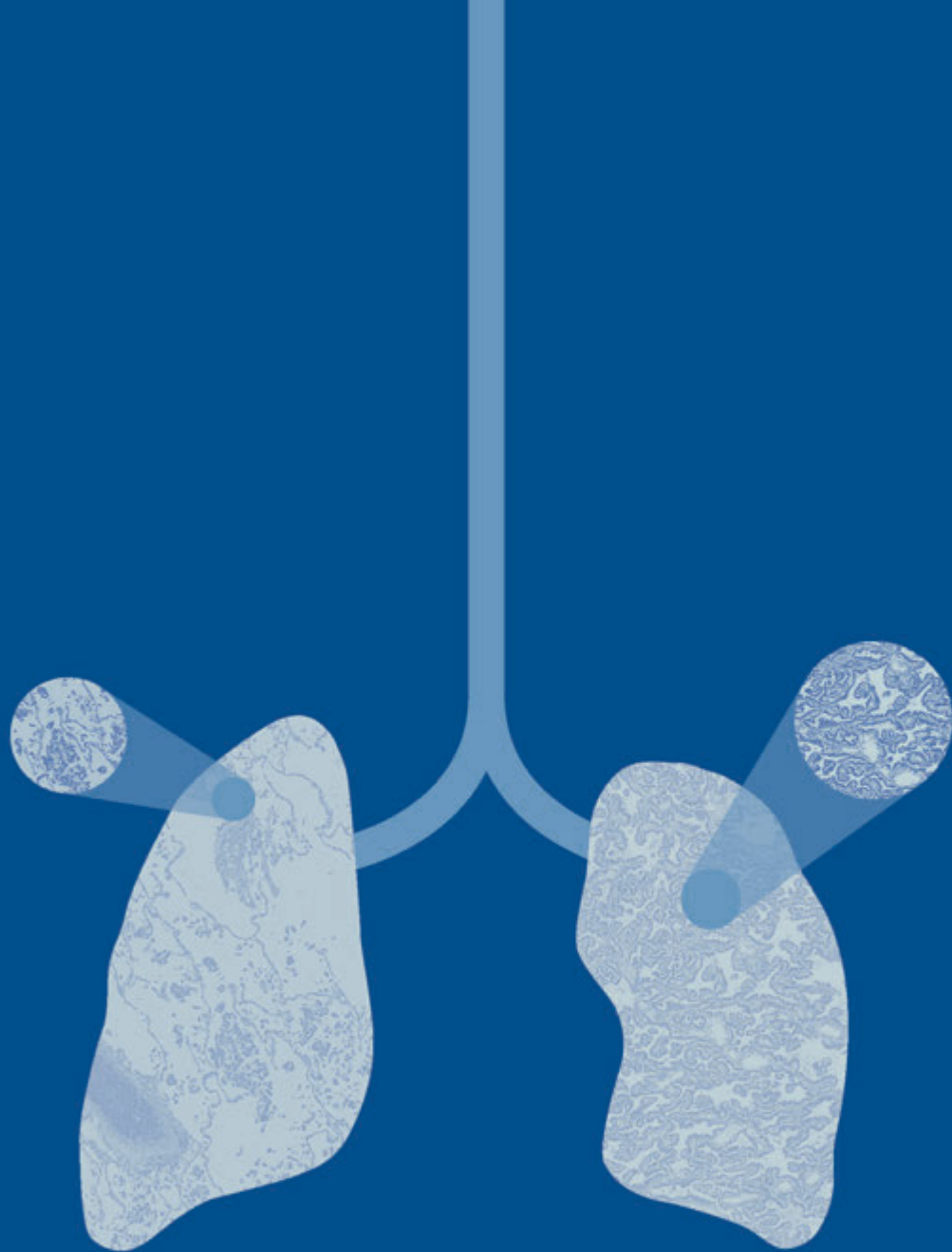
Chapter 11	Is Spread Through Air Spaces an in vivo phenomenon or an inducible artifact?	131
-------------------	--	------------

■ Part III: Collapsed adenocarcinoma in situ; the challenge of defining invasion

Chapter 12	Elastin in pulmonary pathology: relevance in tumors with lepidic and/or papillary appearance. A comprehensive understanding from a morphological viewpoint.	147
Chapter 13	Incorporating surgical collapse in the pathological assessment of resected adenocarcinoma in situ of the lung. A proof of principle study.	165
Chapter 14	3-dimensional reflection aids in understanding the fog of 2-dimensional pattern recognition in pulmonary adenocarcinomas. Proposal for a modified classification.	173
Chapter 15	Invasion measurement and adenocarcinoma <i>in situ</i> (AIS) in pulmonary adenocarcinomas of 3 cm or less. A reproducibility study according to the WHO and a modified classification.	201
Chapter 16	Arguments for non-mucinous adenocarcinoma in situ of the lung larger than 7 cm.	235
Chapter 17	General discussion and future perspectives	251

■ Appendices

Supplementary files	276
References	284
Summary	308
Nederlandse samenvatting (Dutch summary)	314
List of publications	320
Dankwoord (Acknowledgements)	326
Curriculum Vitae	329
CRediT authors statements	330



1

General introduction
and outline of the thesis

Introduction

Lung cancer is the leading cancer type among men worldwide and, after prostate and skin cancer, the most common malignancy in the Netherlands. In recent decades, there has been an increase in the incidence of lung cancer among women. Each year, over 14,000 men and women in the Netherlands are diagnosed with lung cancer, that includes non-small cell lung cancer (NSCLC) and small cell lung cancer (SCLC). Annually, about 10,000 patients die from their disease¹. The 5-year survival rate is relatively low at 17%, although small improvements have been observed recently².

Pathology plays a crucial role in the diagnosis, staging, and treatment of NSCLC, which is the most common type of lung cancer (70%). For an adequate diagnosis, pathologists use, beside cytology specimen, tissue samples obtained through biopsy or surgical resection to generate a diagnosis of lung cancer. The morphologic examination includes examination of cells and the structural relation of these cells. To this end, the initial diagnostic step is the conventional hematoxylin and eosin (H&E) staining and is often employed along with supplemental histochemical and/or immunohistochemical stainings. This pathological analysis is critical in determining the type of lung cancer and in differentiation from metastases to the lung, derived from other organs.

At the time of diagnosis of NSCLC, the extent of the disease, i.e., the stage is determined. Pathological examination can be supportive in determining the size of the tumor, and depending on where the sample is taken from, it can also help in assessing the presence of metastases, either locoregional in lymph nodes or at distant places for instance in other organs. Pulmonologists and oncologists need this information in determining the stage of the disease and treatment plan.

Classification and staging

The most prevalent type of lung cancer is NSCLC, which constitutes 70% of all pathologically diagnosed cases. Treatment for lower stage NSCLC involves a combination of surgery and other therapies. SCLC accounts for 11% of cases and is typically already metastasized at the time of diagnosis, ruling out surgical intervention. Carcinoids are rare, comprising only 1% of cases. The remaining 17% of clinically diagnosed cases are suspected to be early-stage NSCLC and are referred for treatment by stereotactic radiotherapy without a pathologic diagnosis². The recognition of the diversity of NSCLC has led to further subclassification, which was published in the 2004 and 2015 World Health Organization (WHO) classification^{3,4}. The major types of NSCLC include adenocarcinoma (AdC), squamous cell carcinoma (SqCC), and large cell carcinoma (LCC). Adenocarcinomas can be further subdivided into the most common non-mucinous variant and the mucinous variant.

The WHO classification of non-mucinous lung adenocarcinoma in 2015 states that the predominant pattern observed determines the subtype of the tumor⁴. This assessment

is based on a combination of microscopic examination, immunohistochemical analysis, and molecular/genetic analysis. Regarding NSCLC, several histopathological criteria have been linked to prognosis. For example, adenocarcinomas as a type, is associated with a better prognosis than the squamous cell carcinoma type of NSCLC⁵. Within the adenocarcinomas some subtypes, such as micropapillary and solid are associated with a worse prognosis^{6, 7}. Also within the subtypes, certain patterns are associated with worse prognosis, such as the cribriform variant of acinar adenocarcinoma⁸.

In 1960, Liebow introduced the term “bronchioloalveolar carcinoma” (BAC) to describe a well-differentiated form of adenocarcinoma that presents with one of three growth patterns: (1) a single nodular pattern, (2) a multinodular pattern, or (3) a diffuse pneumonic pattern⁹. However, the definition of bronchioloalveolar carcinoma remained somewhat unclear in terms of pathological criteria. As radiology, histology, and immunophenotyping knowledge advanced, it became increasingly crucial to distinguish certain subtypes of non-small cell lung cancer with a better prognosis and less invasive treatment from the conglomerate of cases.

In 1995, Noguchi et al. identified subtypes that exhibited 100% long term survival. Type A demonstrated growth through replacement of alveolar lining cells, accompanied by minimal or slight thickening of the alveolar septa, and an absence of fibrotic foci within the tumors, called localized bronchioloalveolar carcinoma (LBAC). Type B followed a comparable pattern, but fibrotic foci due to alveolar collapse were evident in the tumors and was called bronchioloalveolar carcinoma with foci of collapse of alveolar structure¹⁰.

In 1997, Silver and Askin examined cases that were diagnosed as having papillary or bronchioloalveolar characteristics. They identified certain cases with a worse prognosis when stricter criteria were applied, such as over 75% papillary pattern, complicated papillary growth in secondary and tertiary branches, greater cytonuclear atypia, and distortion or destruction of underlying pulmonary architecture¹¹. However, in the 1999 edition of the WHO classification, the papillary subtype is not so strictly defined, namely as “an adenocarcinoma with a predominance of papillary structures that replace the underlying alveolar architecture”¹².

In the 2015 edition of the WHO classification, the term bronchioloalveolar carcinoma (BAC) was abandoned, and instead, the concepts of adenocarcinoma *in situ* (AIS) and minimally invasive adenocarcinoma (MIA) were introduced. These new concepts have been increasingly diagnosed, particularly in lesions discovered through lung cancer screening¹³. When surgically removed, both AIS and MIA exhibit nearly 100% 5-year survival rates.

A precise and accurate diagnosis distinguishing non-invasive adenocarcinomas such as AIS and MIA from invasive carcinomas is crucial. This is because invasive adenocarcinomas may require additional therapy, while non-invasive non-mucinous adenocarcinomas can be cured through surgical resection alone, eliminating the need for further treatment.

In 2012 a reproducibility study on simple power point images of different adenocarcinoma subtypes showed that one group of pathologists consistently judged a subset of adenocarcinomas to be invasive (Invasive Group, ING), while another group of pathologists consistently judged the same subset to be non-invasive (non-ING)¹⁴. This clearly points toward a necessity for calibration or re-evaluation of the diagnostic criteria.

The concept of “loose tumor tissue fragments” as a pattern of invasion in lung carcinoma has recently been proposed and is included in the 2015 WHO fascicle on the classification of lung tumors, and was specifically called ‘spread through air spaces’ or STAS⁴. This inclusion is at least somewhat controversial, as an alternative explanation is that “loose tumor tissue fragments” represents an artifact. In the current WHO classification of lung cancer “STAS” is a criterium of invasion. The difference in consequences of both concepts warrants further research.

The main function of staging lung cancer, is to determine the extent of disease at time of diagnosis, because of the associated prognosis. The staging system for cancers is based upon anatomic primary tumor characteristics, lymph node metastasis, and distant metastasis (TNM) at time of diagnosis and has been developed to predict survival outcome in cancer patients. Stage is the main denominator for treatment planning in patients with lung cancer NSCLC¹⁵. As for many other tumors, the descriptors of the T, N and M for NSCLC evolve with time. The most recent transition from the 7th (TNM-7) to the 8th (TNM-8) editions dates in 2017^{16 17 18}. The accurate determination of the maximum diameter of the invasive part of the tumor is crucial for pathologists with regards to the T-descriptor. This is because the 8th edition of the Union for International Cancer Control (UICC)/American Joint Committee on Cancer (AJCC) TNM classification system for NSCLC recommends that the measurement of the primary tumor’s size should be based only on its invasive components¹⁹. This emphasizes the need of precise and accurate diagnosis of a non-invasive (AIS and MIA) as opposed to an invasive carcinoma.

Another aspect of staging is the examination of the response after neoadjuvant therapy in resection specimen. This may provide insight in the assessment of the efficacy of neoadjuvant treatment in NSCLC.

Aim and outline of the thesis

This thesis investigates three histopathological aspects in resected NSCLC specimens, relevant to diagnosis, prognosis, and staging.

Firstly, we aimed to establish criteria for the pathologic response effect after neoadjuvant therapy by examining whether histopathological findings such as the percentage of tumor rest, proliferative activity, and morphometric properties may lead to a refinement in the prognosis of patients with NSCLC after chemoradiation therapy.

Secondly, we sought to induce the phenomenon of “STAS” by handling the gross specimen, to investigate whether it is plausible that “loose tumor fragments” interpreted as “STAS” is not a biological way of metastasizing, but rather an artifact. We investigate the potential association between possible artifacts such as spreading tumor cells or clusters caused by mechanical knife force or collapse of lung tissue, and classification, staging, or prognosis.

Thirdly, we aimed to refine diagnostic tools that can aid in distinction between invasion and non-invasion in non-mucinous pulmonary adenocarcinoma. To achieve this, we examined the impact of iatrogenic collapse on pulmonary adenocarcinomas and its effect on invasion assessment and prognosis.

Part I of this study, comprising chapters 2-4, focuses on describing the histopathologic findings in resected specimens of patients with NSCLC, with the aim of refining pTNM staging. In chapter 2, we try to describe the histological changes after neoadjuvant therapy, analyzing a study cohort of 46 patients with sulcus superior tumors who received chemoradiation treatment followed by surgical resection. In chapter 3, we try to identify additional morphologic prognostic characteristics of residual tumors in this patient group, and examined whether proliferation, PDL-1, and nuclear size after chemoradiation in comparison to pretreatment measurements are related to prognosis. The conversion from TNM-7 to TNM-8 harbors a shift of some T-descriptors to another category. Chapter 4 presents the results of a nationwide study on T3NO NSCLC, initiated in preparation of chapter 16, which encompasses various tumor categories, including those with parietal pleura invasion or a diameter exceeding 7 cm. The aim of the study in chapter 4 was twofold: to assess the validity of this shift in the Dutch population and to investigate whether the inclusion of additional morphologic factors could improve staging accuracy.

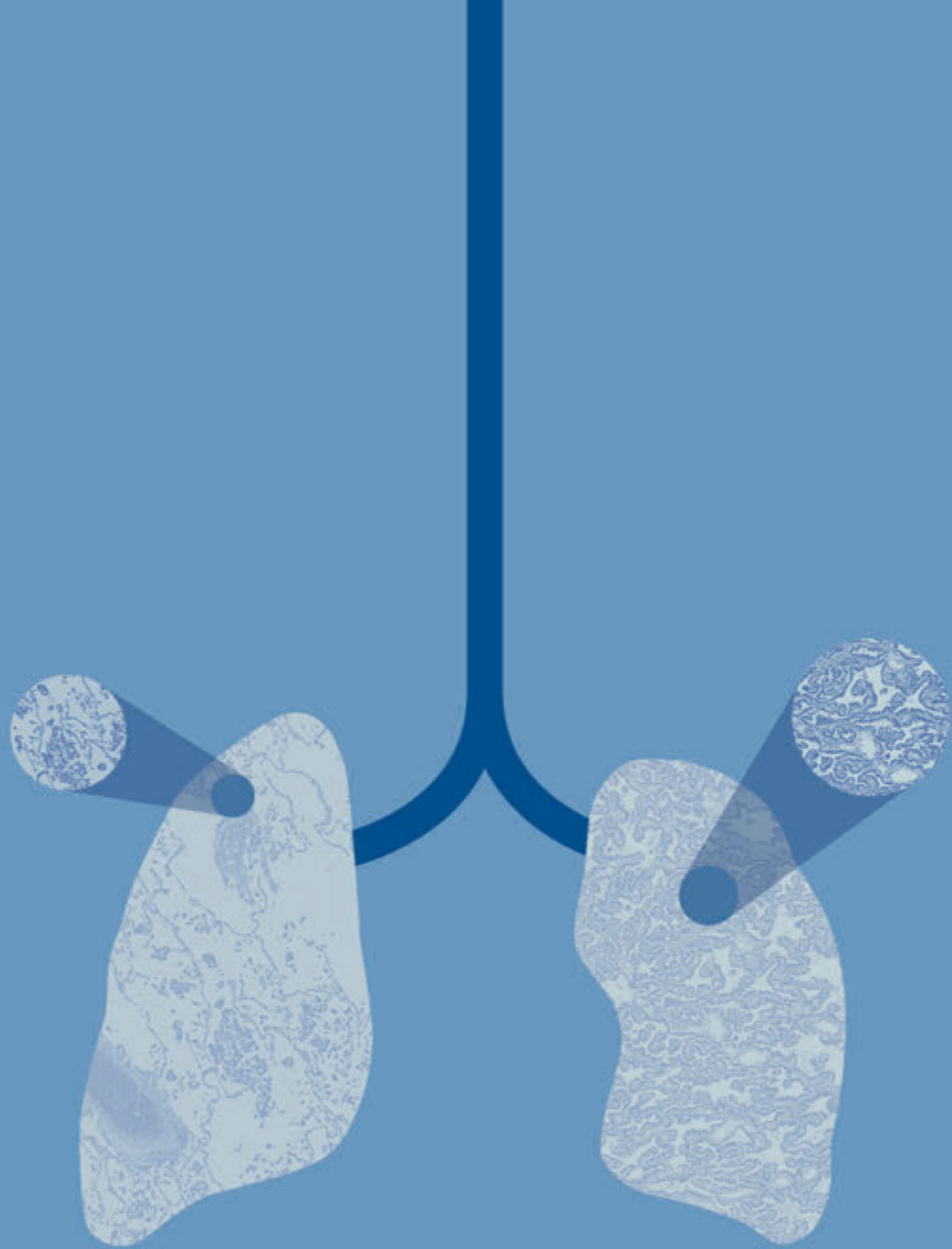
Part II concerns with the phenomenon of Spread Through Air Spaces (STAS). In the chapters 5 - 11 we focus on this phenomenon, that in the most recent WHO fascicle is classified as a new way of metastases, but is possibly an artifact.

Chapter 5 describes in general several histopathologic artifacts related to specimen handling, such as spreading (tumor) tissue through a knife, while cutting the resected specimen. Chapter 6 describes a prospective multicentered study on the investigation of the phenomenon of STAS being an inducible artifact or a new way of metastasizing. Chapter 7 is a critical review on the subject of STAS and in chapter 8 and 9 we comment on this issue, related to a study on neuroendocrine tumors of the lung and to the findings in a comparable study to ours as described in chapter 6. In chapter 10 we examine another possible artifact, namely the presence of individual tumor cells and tumor cell clusters in pulmonary artery branches in histologic sections of pulmonary resection specimen. Chapter 11 summarizes the most recent arguments about STAS as an artifact in the CON part of a Pro-Con editorial.

In part III with the chapters 12-16, we focus on iatrogenic and biological collapse as a possible pitfall in the assessment of invasion in small adenocarcinomas. In chapter 12 we describe the role of elastin in pulmonary pathology and its possible usefulness in the recognition of non-invasive patterns. Chapter 13 discusses a proof-of-principle study that explores the feasibility of considering surgical collapse when diagnosing non-invasive cases of lung cancer. This study examines whether the use of cytokeratin 7 as an immunohistochemical marker can facilitate the recognition of surgical collapse and enable the diagnosis of more non-invasive cases with excellent prognoses.

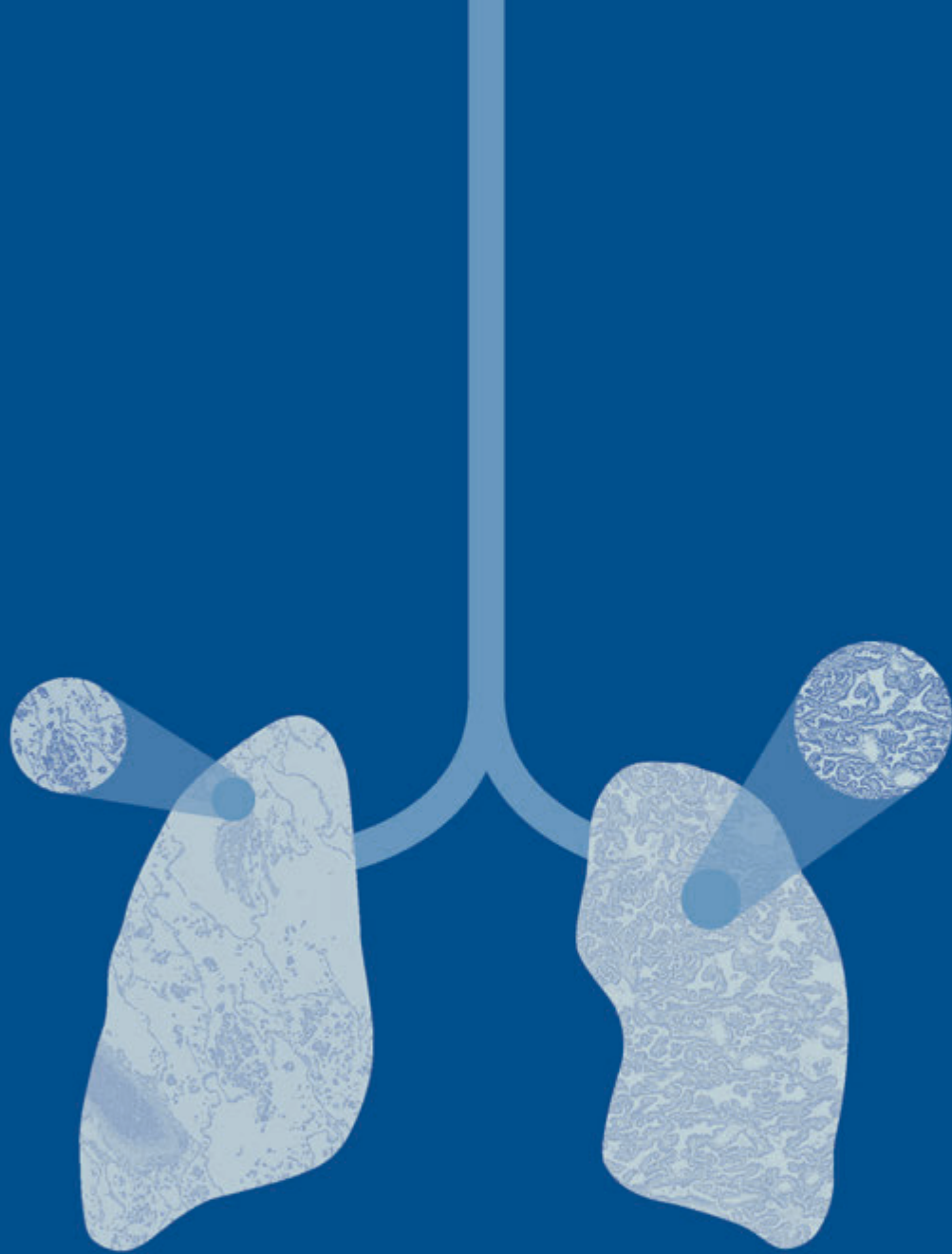
Chapter 14 details the morphological characteristics of iatrogenic and biologic collapsed AIS, incorporating lessons learned from a mathematical model and utilizing cytokeratin 7 and elastin staining to assess invasiveness. Two independent cohorts of resected adenocarcinomas measuring 3 cm or smaller were examined to investigate these aspects and their relationship to recurrence-free and overall survival was analyzed. Chapter 15 concerns a large international interobserver study, determining whether incorporating iatrogenic and biological collapse in the assessment of lung adenocarcinoma invasion using elastin and cytokeratin 7 stainings could diagnose (collapsed) AIS and reduce the interobserver variation of invasive patterns in small pulmonary adenocarcinomas.

According to the WHO for AIS has a maximum size limit of 3 cm. We wondered whether AIS may occur as a larger tumor. In Chapter 16, we examined in the nationwide subgroup of T3N0 NSCLC for the possible presence of AIS with a size larger than 7 cm.



Part I

**Histopathologic factors in the outcome
and prognosis of NSCLC**



2

Complete pathological response is predictive for clinical outcome after tri-modality therapy for carcinomas of the superior pulmonary sulcus

Hans Blaauwgeers, Ingrid Kappers, Houke Klomp, José Belderbos, Lea Dijkman, Egbert Smit, Pieter Postmus, Rick Paul, Jan Oosterhuis, Koen Hartemink, Cornelis Vos, Sjaak Burgers, Max Dahele, Erik Phernambucq, Birgit Lissenberg-Witte, Erik Thunnissen

Virchows Archives (2013) 462:547-556

DOI 10.1007/s00428-013-1404-6

Abstract

The objective was to define the relationship between histopathologic changes after pre-operative chemo-radiotherapy (CRT) and clinical outcome following tri-modality therapy in patients with superior sulcus tumors. A retrospective analysis of tumour material was performed in a series of 46 patients who received tri-modality therapy between 1997 and 2007. Median follow-up was 34 months (5 - 154). Pathologic complete response (pCR) was present in 20/46 tumors (43%). The most common RECIST score after CRT in patients with pCR was a partial response (PR; 10/17, 3 unknown) whereas in patients without a pCR, stable disease was the most common (22/26) ($p=0.002$). In 26 specimens with residual tumour, this was mainly located in the periphery of the lesion rather than the center (Spearman's correlation - 0.67, $p<0.001$). Prognosis was significantly better after a pCR compared to residual tumour (70% 5-years overall survival vs. 20%; $p=0.001$) and in patients with fewer than 10% vital tumour cells as compared to those with $>10\%$ (65% 5-years overall survival vs 18%; $p<0.001$). A low mitotic count was associated with a longer disease-free survival ($p=0.02$). Complete pathological response and the presence of fewer than 10% vital tumour cells after pre-operative CRT are both associated with a more favorable prognosis. A modification of the pathological staging system after radiotherapy, incorporating the percentage of vital tumour cells, is proposed.

Introduction

In patients with clinically resectable Non-Small Cell Lung Cancer (NSCLC), the survival rates vary, ranging from an estimated median survival of 19 months for stage IIIA to 95 months for stage IA²⁰. In locoregionally-advanced NSCLC, combined modality treatments using concurrent chemo-radiotherapy (CRT) have been associated with an increase in survival rates^{21,22}. Superior Sulcus Tumours (SST), also called Pancoast tumours, are a rare sub-set comprising 3-5% of all NSCLC and are located in the lung apex. They are locally advanced with invasion of the chest wall, adjacent structures or vertebrae, reducing the likelihood of a radical (RO) resection with primary surgery. Pre-operative induction CRT followed by resection is now considered the standard treatment option in medically fit patients^{23,24}.

This combined-modality approach is associated with 95% complete resection (RO) rates and up to 50% of tumours demonstrates pathologic complete regression (pCR)^{25,26}. Limited information is available about the histopathologic changes of such neo-adjuvant regimes on tumour and adjacent normal lung parenchyma and their relation to prognosis^{27,28,29}. The aim of this study was to describe the histopathologic pulmonary and tumour related changes after concurrent CRT and relate these to clinical outcome.

Patients and methods

A retrospective analysis was performed on a consecutive series of patients with SST treated by concurrent CRT and subsequent surgical resection in the period 1997-2007 at the VU University Medical Center (VUmc) and the Netherlands Cancer Institute (NKI-AVL), both located in Amsterdam, the Netherlands. SST was defined as a tumour growing into the thoracic wall at the apex of the lung, above the level of the second rib³⁰.

A total of 50 patients were identified, after excluding 6 patients (13%) who started CRT, but had progressive disease or were no longer clinically fit for surgery. Four cases had to be excluded because of irretrievable histological slides and tissue blocks. All but one of the 19 NKI-AVL patients received an accelerated hypo-fractionated radiation schedule of 66 Gy delivered in 24 fractions and most of them (n=17, 89%) had concurrent single agent chemotherapy consisting of daily low dose Cisplatin. The treatment at the VUmc was one cycle of cisplatin-gemcitabine, followed by concurrent CRT consisting of cisplatin-etoposide and radiation doses ranging from 39 Gy in 13 fractions to 50 Gy in 25 fractions (mean 44 Gy). All VUmc patients received chemotherapy. Combining the data from both institutes the mean absolute radiation dose was 53 Gy.

After completion of CRT, restaging (typically with some combination of CT and/or MRI of the thorax and upper abdomen, MRI scan of the brain, FDG-PET scanning and invasive mediastinal staging) and discussion in a multidisciplinary meeting, surgical resection was attempted in patients without disease progression.

Pre- and post-induction treatment tumour diameters were measured on CT/MRI scans. Response evaluation was performed according to the RECIST criteria³¹. In the surgical resection specimens, tumour size was measured on gross pathological exam and the tumour diameter was retrieved from the pathology report. Histological slides of all available paraffin blocks together with the pathology reports of the resection specimens were reviewed. In each case the number of blocks related to the tumour area was estimated.

Tumour type was based on the most classifiable specimen, either the pre-treatment histology or cytology, or the resection specimen. For example, a case with a pre-treatment biopsy diagnosis of non-small cell carcinoma not otherwise specified, and a resection specimen diagnosis of squamous cell carcinoma was classified as squamous cell carcinoma. In cases without viable tumour in the resection specimen, the tumour was classified according to the pre-treatment histology or cytology.

In order to evaluate the histopathologic changes within the tumour mass, items such as amount of viable tumour, fibrotic changes, vasculopathy and intra- and peritumoural inflammatory reaction were identified and for applicable items a semi-quantitatively scoring system was used as shown in Table 1.

■ **Table 1.** Criteria for scoring histology

Item/category	0	1	2	3	4 ¹
Tumour type ²		Squamous cell	Adenocarcinoma	Large cell	Other, specify
Viable tumour ³	no vital tumour cells	<10% vital tumour cells	10-50% vital tumour cells	>50% vital tumour	completely vital tumour
Tumour location within mass	Not relevant (no tumour)	Randomly distributed	Mainly peripherally	Mainly centrally	
Diameter macroscopical mass ⁴	≤ 2 cm	> 2 and ≤ 3 cm	> 3 and ≤ 5 cm	> 5 and ≤ 7 cm	> 7 cm
Dominant tumour growth pattern	Not relevant (no tumour)	Mainly confluent nests	Randomly distributed nests or cells	Mainly perivascular	Other, specify
Cytonuclear atypia tumour ⁵	Not relevant (no tumour)	Slight (uniform nuclei, small nucleoli)	Moderate (variation nuclear size, prominent nucleoli)	Severe (bizarre nuclei, macronucleoli)	Extreme (mainly bizarre nuclei)
Mitotic activity ⁷	Not applicable (no tumour)	Low (less than 1/HPF)	Moderate (1-3/HPF)	High (more than 3/HPF)	
Atypical mitosis ⁷	Not applicable (no tumour)	None	Few (1/HPF)	Several (more than 1/HPF)	
Amount of fibrosis - necrosis	Just fibrosis	Mainly fibrosis (> 75%)	Equal fibrosis-necrosis	Mainly necrosis (> 75%)	Just necrosis
Presence of cholesterol clefts	None	Just in alveolar spaces	Focal	Extensive	
Presence of foamy macrophages	None	Focal	Extensive		

■ **Table 1.** Criteria for scoring histology (continued)

Item/category	0	1	2	3	4 ¹
Presence of dyselastosis	None	Focal	Extensive		
Acute vasculopathy ⁸ (present in 1 or more vessels)	None	Mainly neutrophils in vessel wall, no thrombi	Mainly neutrophils in vessel wall with thrombi or necrosis	Mainly lymphocytes in the vessel wall, fibroblastic intima thickening, no thrombi	Mainly lymphocytes in vessel wall, fibroblastic intima thickening with thrombi
Chronic vasculopathy ⁹ (present in 1 or more vessels)	None	Slight intima thickening	Clear intima thickening	Nearly obliterated vessels (pinpoint lumina)	Obliterated vessels; no recanalization
Boundary tumour-lung tissue	Sharp all around	Mainly sharp (> 75%)	Mainly irregular (> 75%)	Completely irregular	
Amount of reactive changes lung parenchyma	None	Focal (close to mass)	Multifocal (one segment)	Diffuse	
Changes lung parenchyma next to mass	None	Slight (septal thickening, mild inflammation)	Moderate septal thickening or inflammation, no structure loss	Severe reactive or inflammation, structure loss ¹⁰	
Cytonuclear atypia epithelial cells in lung parenchyma ⁵	None	Slight (uniform nuclei, small nucleoli)	Moderate (variation nuclear size, stratification, prominent nucleoli)	Severe (bizarre nuclei, macronucleoli)	

¹ Items having more than 4 scores are mentioned below

² According to WHO classification 2004³², not in a semi-quantitative order

³ Modified from Dworak grading for colorectal cancer³³

⁴ Cut-off points according to the proposed IASLC staging for lung cancer 2009³⁴
Longest axis was used.

⁵ Most severe atypia accounts for the score

⁶ Pre-operative specimen not available or cytological

⁷ At least 3x HPF (1HPF=2mm²) counted³⁵

⁸ Scores 5-9 as follows:

Score 5: mainly lymphocytes within the vessel wall with fibrotic intima thickening without thrombi

Score 6: mainly lymphocytes within the vessel wall with fibrotic intima thickening with thrombi

Score 7: extensive inflammatory infiltrate within the vessel wall with fibrinoid necrosis

Score 8: vasculitis distant from the tumour mass including score 1-7

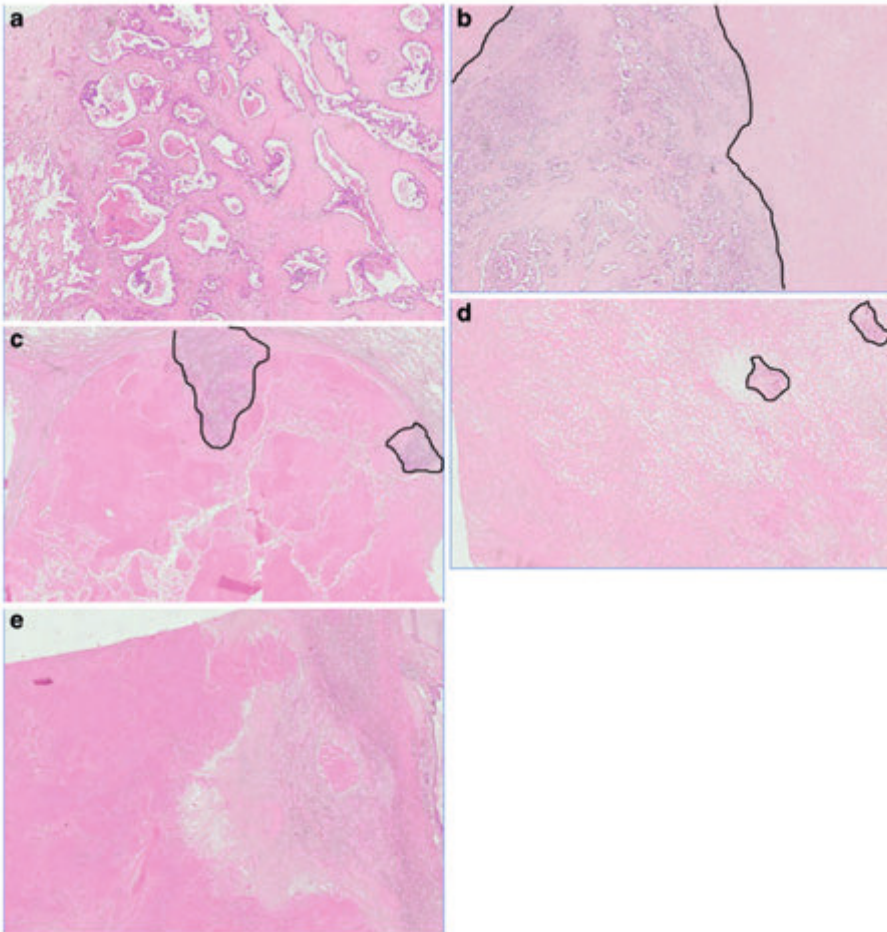
Score 9: vasculitis distant from the tumour mass including score 0

⁹ Score 5 as follows:

Score 5: obliterated vessels with recanalization (eccentric lumina)

¹⁰ Or classifiable as interstitial lung disease pattern

To estimate the percentage of vital tumour cells, the area of vital tumour cells was related to the total tumour visible in the microscopy slides, including areas of fibrosis, inflammation and necrosis (Figure 1a-e).



■ **Figure 1.** Histological overview slides: **a** complete vital tumour, **b** >50% vital tumour cells (within black lines), **c** 10-50% vital tumour cells, **d** <10% vital tumour cells, **e** no vital tumour cells (i.e. pathologic complete response)

Two experienced lung pathologists (JB, ET) independently scored all tumour area slides with respect to the items of amount of viable tumour and distribution of vital tumour cells. There were no discrepancies in their scores. A continuous area of >6 mm tumour in one slide was sufficient for scoring > 10% vital tumour cells. The percentage of vital tumour cells < 10% was defined as small focal areas in one or more sections with an estimated total area of less than 10% of the gross size of the lesion. For the other pathologic items, both pathologists independently evaluated 10 cases, also revealing no discordance. One pathologist (JB) subsequently evaluated the remaining cases. Follow-up clinical data were retrieved from the patient archives by the relevant clinicians.

Statistics

Statistical analyses were carried out by SPSS for Windows and Mac version 18.0. (IBM, New York, USA). Associations between all histological items, except for those with complete regression in which tumour characteristics were omitted, were tested using the Fisher's exact test in case of dichotomous variables with a significant level <0.05 . Spearman's correlations were calculated in case of ordinal variables with a significance level of <0.05 . Overall survival rates were estimated by Kaplan-Meier curves, and differences between curves were tested by the log-rank test. Where appropriate threshold levels of significance were adjusted for multiple comparisons by the Bonferroni's correction ³⁶.

Results

Clinicopathologic characteristics of the 46 patients are shown in Table 2.

Most patients were male (74%), almost all were smokers (87%) and the predominant histological subtype was adenocarcinoma (46%). Nineteen cases were staged as stage IIB (41%), 20 as stage IIIA (44%) and 7 as stage IIIB (15%). At the time of diagnosis 9 patients had clinical N2 disease and an additional 2 had N1 disease (table 2). After the induction treatment none of the patients had clinical N2 disease and 4 had N1 disease.

■ **Table 2.** Characteristics of all eligible patients (n=46)

Age (yrs)	
mean (range)	56.4 (31-78)
Gender	
Male	34
Female	12
Hospital	
VUmc	27
NKI-AVL	19
Smoking history	
Pack-years (yrs)	
mean (range)	30.7 (0-68)
Smoker at time of diagnosis	
Yes	40
No	3
Unknown	3
Smoker at time of treatment	
Yes	20

■ **Table 2.** Characteristics of all eligible patients (n=46) (continued)

No	18
Unknown	8
cTNM (stage)	
cT3N0M0 (IIB)	19
cT3N1M0 (IIIA)	2
cT3N2M0 (IIIA)	2
cT4N0M0 (IIIA)	16
cT4N1M0 (IIIA)	0
cT4N2M0 (IIIB)	7
Histology	
Adenocarcinoma	21
Large cell carcinoma	14
Squamous cell carcinoma	7
Unknown	4 ^a

^a Treatment based on clinical evidence without pathology diagnosis and without residual tumour in the resection specimen

Tumour related histopathologic findings

No significant differences were found between the two hospitals for the histologic items, allowing combined data analysis. The resection specimens showed that all lesions were at least 1 cm in size. No vital tumour cells (= pCR) were found in 20 cases (43%). In these 20 specimens, the presumed tumour area showed either necrosis, fibrosis with or without dyselastosis or a combination of the two. Cholesterol clefts were focally or extensively present in the majority of both the pCR and non-pCR cases. All cases showed vascular changes ranging from vasculitis-like changes to complete luminal obliteration and recanalization.

The results of the statistical analysis between all scored histological items, are shown in the table 3.

■ **Table 3.** The relationship between morphologic tumor and lung tissue characteristics is illustrated in this table.

	Tumour location in mass	Diameter macroscopic mass	Dominant growth pattern	Mitotic activity	Amount of fibrosis/necrosis	Foamy macrophages	Dyselastosis	Vasculitis-like changes	Chronic vasculitis	Amount of reactive changes	Type of reactive changes	Cytonuclear atypia lung parenchyma	Number available slides macroscopic mass
Tumor type combined pre-postOK	0,14	0,03	-0,09	0,15	0,17	-0,05	-0,23	-0,16	-0,25	0,18	-0,06	-0,09	-0,18
Regression	-0,67	0,34	-0,41	0,00	0,15	-0,39	-0,15	0,08	-0,10	0,28	0,14	0,24	0,35
pathologic Complete Response (pCR)	.	0,33	.	.	0,09	-0,34	-0,19	0,12	-0,10	0,27	0,18	0,21	0,31
Diameter macroscopic mass	-0,03	1,00	0,23	0,50	0,49	-0,04	-0,38	0,03	-0,13	-0,02	-0,06	-0,17	0,47
Cytonuclear atypia within tumour	-0,29	0,36	0,08	0,23	0,58	0,24	-0,19	-0,12	-0,18	0,18	0,14	0,18	0,10
Amount of fibrosis/necrosis	0,13	0,49	-0,16	0,36	X	0,07	-0,52	-0,06	-0,19	0,12	-0,01	0,15	0,18
Cholesterol clefts	-0,07	0,10	0,17	-0,04	0,27	0,40	0,02	-0,23	0,06	-0,03	0,00	0,14	0,10
Dyselastosis	-0,25	-0,38	0,05	-0,19	-0,52	0,15	X	0,36	0,41	0,06	0,17	0,10	-0,33
Vasculitis like changes	0,02	0,03	0,23	0,03	-0,06	0,11	0,36	X	0,33	0,15	0,31	0,12	0,04
Boundary tumour-lung	-0,25	0,12	-0,13	0,38	0,05	-0,25	0,04	0,04	0,21	0,31	0,26	0,34	-0,05
Amount reactive changes lung	-0,10	-0,02	0,01	0,10	0,12	0,08	0,06	0,15	0,26	X	0,32	0,48	0,11
Type of reactive changes lung	-0,05	-0,06	0,18	0,05	-0,01	-0,13	0,17	0,31	0,25	0,32	X	0,40	0,02

Correlation coefficients between scored items are shown (**bold/light grey cell**=significant P-values <0.05; **bold italic/dark grey cell**=significant P-values <0.01). Items without significance as well as those with a skewed distribution are not shown, except for tumor type.

Histological tumour type was not associated ($p > 0.05$) with any of the scored items. The smaller the tumour diameter and the lower the number of tumour blocks taken for histological exam, the higher chance of pCR (Spearman's correlation $r = -0.33$, $p = 0.03$ and $r = 0.31$, $p = 0.04$, respectively). In other words, from larger tumors more blocks were examined and residual tumour was more likely to be found. The numbers of blocks examined per patient varied from three to 15 with a mean of 6,8 blocks.

In cases of residual tumour, most (20/26) had less than 50% vital tumour cells. These vital cells were more frequently found in the periphery than in the center of the pathologic lesion (16/20) ($p < 0.001$). The cytonuclear atypia of tumour cells was more prominent in cases with necrosis compared to cases with mainly fibrosis ($r = 0.58$, $p = 0.002$).

A high amount of dyselastosis was associated with a smaller tumour diameter ($r = -0.38$, $p = 0.009$), as well as with more fibrosis than necrosis ($r = -0.52$ $p < 0.001$). Dyselastosis was also correlated with chronic vascular changes (i.e., from intimal fibrosis to complete luminal obstruction, $r = 0.41$, $p = 0.005$). In addition, cases with chronic vascular changes frequently occurred together with acute vasculitis-like changes ($r = 0.33$, $p = 0.03$). More type II pneumocytic cytonuclear atypia was found in lung parenchyma that showed more reactive changes ($r = 0.48$, $p = 0.001$). No correlation was found between vascular changes and histological tumour regression. When threshold levels of significance were adjusted for multiple comparisons by the Bonferroni's correction, none of the stromal related correlations showed p -values < 0.05 ³⁶. The tumour-lung boundary was predominantly sharp in nearly all cases (44/46) and no tumour foci were found outside this boundary.

Treatment response

Tumour response after CRT and before surgery could be determined on CT scans and/or MRI's in all but 3 cases. The median time between pre- and post-CRT response evaluation was 2.0 months (range 0-12 months). The median time between end of induction CRT and surgical resection was 4.0 weeks (range 0-26 weeks).

Data for the pairwise comparisons using clinical RECIST criteria for pre-treatment, post-CRT and pathological tumour sizes are shown in Table 4. More partial responses were found when the RECIST criteria were applied to pre-treatment imaging and pathological gross specimen tumour size than to pre- and post-treatment imaging ($p < 0.005$). Pathological complete response (pCR) was more frequently found in cases with clinical partial response compared to clinical stable disease and progressive disease ($p = 0.001$). Other histological changes were not associated with the extent of response.

- **Table 4.** Number of patients with tumour response based on pre and post CRT imaging using RECIST criteria, and a comparison of pre-CRT imaging and post CRT gross pathology. The number of patients in these groups with pathologic complete response (pCR) is also described.

	RECIST (Number; %) (Pathologic Complete Response: Number; %)				
	Partial Response	Stable Disease	Progressive disease	Missing	Total
Pre - post- CRT imaging	14; 30% (10; 50%)	29; 63% (7; 35%)	0	3; 7% (3; 15%)	46 (20; 100%)
Pre-CRT imaging - post-CRT gross pathology	27; 59% (16; 80%)	15; 33% (3; 15%)	4; 9% (1; 5%)	0	46 (20; 100%)

CRT chemoradiotherapy

Follow-up data

Follow-up data was available for all patients. There were no differences in follow-up status between the two hospitals or between patients with different clinical stages. Table 5 shows the follow-up status of all eligible patients according to tumour type and tumour response.

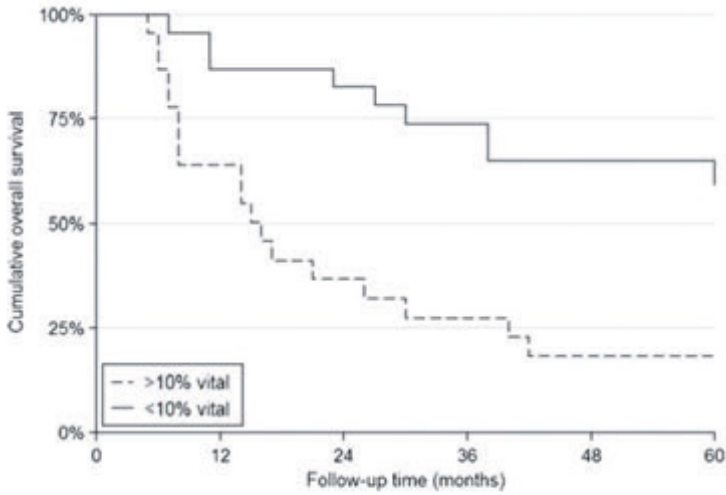
- **Table 5.** Follow up status related to tumour type and pathological response

Follow up status	AND	DND	AWD	DOD
Tumour type				
Squamous cell carcinoma	2	1	0	4
Adenocarcinoma	8	2	1	10
Large cell carcinoma	6	1	0	7
Unknown	2	0	0	2
Total	18	4	1	23
Tumour response				
Complete regression	12	1	1	6
<10% vital tumour	1	0	0	2
10-50% vital tumour	3	3	0	11
>50% vital tumour	1	0	0	4
Total	18	4	1	23

AND = Alive No Disease; DND = Dead No Disease; AWD = Alive With Disease; DOD = Dead Of Disease

The median follow-up time was 34 months (range 5 - 154 months). Prognosis was significantly better after a pCR compared to residual tumour (70% 5-years overall survival vs. 20%; $p=0.001$) and in patients with fewer than 10% vital tumour cells as compared to those with >10% (65% 5-years overall survival vs 18%; $p<0.001$; Figure

2). There were no differences in cases with 10-50% compared to >50% vital tumour cells. A low mitotic count (<1 per high power field) was associated with a longer disease-free survival ($p=0.02$). None of the other associations between histological scores and follow-up status were statistically significant.



■ **Figure 2.** Kaplan-Meier survival curves showing a significantly better prognosis in patients with less than 10% vital tumor cells in their resection specimen.

Discussion

This is the largest series reporting a detailed histopathologic evaluation of resected Pancoast tumours after tri-modality therapy. Twenty-three out of 46 patients (50%) with SST showed pathological complete response ($n=20$) or <10% vital tumour cells ($n=3$) after CRT. Pathologic complete regression or the presence of <10% vital tumour cells was associated with survival. A low mitotic rate was associated with a longer disease-free survival³⁷. The majority of patients with radiological partial response according to RECIST criteria had a pathologic complete response.

There were no statistically significant differences between the patients or outcomes from the two institutes, even though their treatment regimens differed.

Tumour regression in the lesions was associated with histologic features of necrosis and/or fibrosis, as well as variable histiocytic reactions such as foam cells and cholesterol crystal-related giant cells. These findings are similar to those of Liu-Jarin et al, who analyzed the histological patterns in 30 surgical resection NSCLC specimens after neo-adjuvant therapy²⁸. In their study, consisting of 15 cT3 tumours, the extent of fibrosis correlated with the radiologic response in patients that showed more than

10% tumour regression. We found more cytonuclear atypia in cases with more necrosis than fibrosis, in line with Yamane et al²⁹.

The pCR or minimal residual disease rate of 50% (23/46 cases), is broadly in keeping with that reported by others (Table 6), however there is some variation between studies. For example, Rusch et al²⁶ described a series of 88 patients and found up to 69% pCR or minimal residual tumour. One possible explanation for the differences might be variation in the how the pathological assessment was made (which is often incompletely described) or in histopathologic definition of response.

■ **Table 6.** Selected series of patients with non-small cell lung cancer and histopathologic evaluation after CRT

Reference	No. evaluable cases	No. patients with CRT (%)	Mean radiation dose	No. of patients with pCR (%)	No. of patients with pCR or minimal ^a residual tumour cells
This article	46	46 (100%)	53 Gy	20 (43%)	23 (50%)
Pourel ²⁵	71 ^b	71 (100%)	45 Gy	n.m.	28 (39.4%)
Rusch ²⁶	88	88 (100%)	45 Gy	32 (36%)	61 (69%)
Junker ²⁷	40	40 (100%)	45 Gy	7 (17%)	27 (67%)
Liu ²⁸	30	20 (66%)	50 Gy	5 (25%)	13 (65%)
Fischer ³⁸	44	44 (100%)	45 Gy	13 (30%)	28 (64%)

CRT chemo-radiotherapy, pCR pathologic complete response, n.m. not mentioned

^a minimal residual cells is variably defined in different studies. For example, in this study and the report by Fischer et al it was <10%

^b107 pts in the study, 105 completed CRT, 72 underwent surgery, 71 were pathologically evaluable

The results add to the growing body of evidence indicating that a complete or near-complete pathologic response is associated with a more favourable prognosis in patients with SST. This is in line with Yamane et al. who report that a smaller area of residual tumour is associated with a better prognosis²⁹.

Significantly more pCR was found in cases with a partial imaging response compared to cases with stable disease. Although the RECIST criteria were not designed to compare radiological tumour diameters with diameters measured on pathologic resection specimen, we found significantly more cases with 'partial response' when we compared the diameters on pre-treatment imaging with those in the resection specimens. The latter also tended to be smaller compared to post-treatment imaging diameters. These data suggest that pCR is more likely to be found in cases with larger diameters with subsequent significant regression on combined modality treatment, than in cases that were stable on imaging despite a smaller initial size.

Junker et al²⁷ describe a 3-grade regression scoring system for patients receiving induction therapy i.e. grade I, no or slight regression; IIA, marked but incomplete

response (>10% vital tumour); IIB, less than 10% vital tumour and grade III for complete response. We divided their grade IIA in 2 separate grades, i.e., one for more than 50% vital tumour and one for 10-50% vital tumour. This 4-tiered grading system is similar to the one used by Dworak for colorectal cancers³³. We examined whether this 4-tiered approach was associated with prognosis. This turned out not to be the case. Our data support a slight modification of the Junker classification by combining grade I and IIA into one group, which is associated with a poorer prognosis, the group with <10% vital tumour cells (=Junker IIB) and those with pCR (Junker grade III). The prognostically relevant 10% threshold has also been reported for esophageal cancer³⁹.

Interestingly, residual vital tumour was found significantly more often at the periphery of the pathologic lesion in the resection specimen. Although the center of the solid tumour is more likely to be sensitive to hypoperfused and hypoxic, a microenvironment associated with an increased chance for development of resistance to radiotherapy and anticancer chemotherapy⁴⁰, prolonged hypoxia of the tumour tissue may also lead to necrosis, a frequent finding in larger solid tumours⁴¹. In patients without pCR the margins of the surgical resection were more likely to contain vital tumour cells.

The limitations of this study include the following: (a) the total number of cases is relatively small, (b) only the available slides could be studied and (c) it is a retrospective study; therefore, the tumour lesions, for example, were sampled for reporting purposes and not more systematically for research, and in daily practice more samples may be taken from the periphery of tumour lesions than from its centre or from necrotic appearing areas. For future studies, we advocate sampling more blocks from the resected tumour mass in order to more reliably determine the absence or presence of vital tumour cells. In addition, it should be noted that the presence of histologically vital tumour cells does not necessarily predict their biological capacity to metastasize. Finally, (d) we acknowledge that there was variation in the time between pre- and post-induction CRT imaging, and the end of CRT and surgery.

In future studies of patients with neo-adjuvant CRT and surgery, we propose taking the post-CRT fraction of vital tumour cells into account. Although the IASLC Staging Manual in Thoracic Oncology advises categorization of ypT, the extent of tumour actually present at the time of pathology examination^{32,35}, detailed information on how to evaluate vital tumour cells with relevant portions of necrotic and reactive changes is not provided. For better comparison, in future studies, we suggest the following approach: firstly, record gross size of pathological lesion (including reactive changes such as fibrosis and necrosis, and if present vital tumour) to determine the size of pT. This will also allow comparison with the RECIST data with the size on the resection specimen. Secondly, for the vital tumour component, the adjunct VT is used with ranges as shown in table 7, comparable to the regression system proposed by Becker et al for gastric cancer⁴².

For example, a pathologic tumour mass at gross examination of 4 cm with no vital tumor cells, less than 10% and more than 50% vital tumour cells would then be

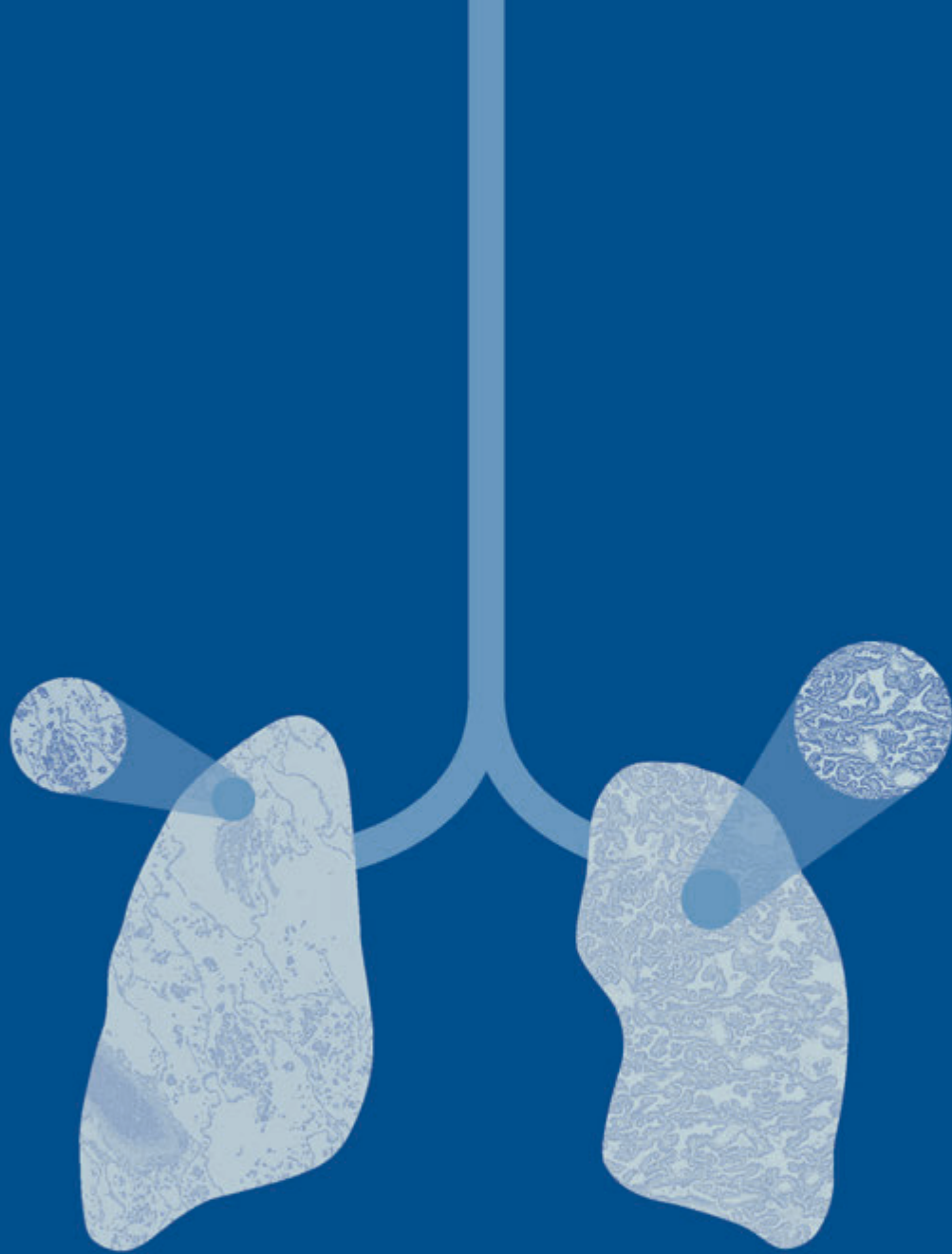
classified as ypT2a^(VT0), ypT2a^(VT1), ypT2a^(VT3), respectively. We realize that the current recommendation for no vital tumour cells should be ypT0.

■ **Table 7.** Proposed classification of the presence of vital tumour cells within a tumour after CRT

% of vital tumour cells	Notation (as superscript)
0	VT0
<10%	VT1
10-50%	VT2
> 50%	VT3

VT vital tumor cells, CRT chemoradiotherapy

In conclusion, we identified a pCR in over 40% of patients with SST undergoing induction CRT a complete or near-complete pathologic regression was associated with a more favorable prognosis.



3

The prognostic value of proliferation, PD-L1 and nuclear size in patients with superior sulcus tumours treated with chemoradiotherapy and surgery

Hans Blaauwgeers, Birgit Lissenberg-Witte,
Chris Dickhoff, Sylvia Duin, Erik Thunnissen

Journal of Clinical Pathology. 2023;76(2):111-5.

Abstract

Aims

The aim of this study was to determine the relationship between proliferative activity, PD-L1 status and nuclear size changes after pre-operative chemo-radiotherapy (CRT) and clinical outcome in patients with superior sulcus tumours.

Methods

Proliferative activity (MIB-1) and PD-L1 status was estimated by immunohistochemistry in the tumour cells of resection specimen in a series of 33 patients with residual tumour after tri-modality therapy for a sulcus superior tumour between 2005 and 2014. A morphometric analysis of both pre- and post-treatment tumour material was also performed. Results were related to disease free survival (DFS) and overall survival (OS).

Results

Low proliferative activity (<20% MIB-1) was associated with better OS: 2-year OS of 73% compared to 43% and 25%, respectively for moderate (MIB-1 20-50%) and high proliferative activity (MIB-1 >50%) (p=0.016).

A negative PD-L1 status (<1% positive tumour cells) was also associated with a better OS (p=0.021). The mean nuclear size of normal lung tissue pneumocytes was significantly smaller compared to the mean nuclear size of tumour cells of the resection specimens (median difference -38.1; range -115.2 - 16.0; p<0.001). Mean nuclear size of tumour cells did not differ between pre-treatment biopsies and resection specimens (median difference -4.6; range -75.2 - 86.7; p=0.14). Nuclear size was not associated with survival (p= 0.82).

Conclusions

Low proliferative activity determined by MIB-1 as well as a negative PDL-1 expression are significantly associated with a better overall survival in patients with residual tumour after CRT for superior sulcus tumour.

Introduction

In patients with resectable non-small cell lung cancer (NSCLC), survival rates drop with higher clinical stage, ranging from an estimated median survival of 95 months for stage IA to 19 months for stage IIIA²⁰. In locally-advanced NSCLC (LA-NSCLC), combined modality treatments using concurrent chemo-radiotherapy (CRT) have led to increased survival rates^{21,22}. For superior sulcus tumours (SST), also called Pancoast tumours, comprising 3-5% of all NSCLC, and typically invade the chest wall, induction CRT followed by resection is considered the standard treatment in medically fit patients^{23,24,30}. This combined modality approach is associated with 95% complete resection (R0) rates and up to 50% of tumours demonstrate pathologic complete regression^{25,26}. The presence of complete pathological regression was found predictive for favourable clinical outcome after tri-modality therapy in these patients⁴³. Other morphological characteristics found in pretreatment biopsies and resection specimen, such as Ki-67, MIB-1, nuclear size and PD-L1 expression, have been investigated for prognostic value in resected NSCLC, but their role in patients treated with induction and resection (trimodality treatment), and their relation to clinical outcome, is currently unknown⁴⁴. This lack of knowledge was noticed by the members of the International Association Lung Cancer (IASLC), who recently published multidisciplinary recommendations for pathologic assessment of lung cancer resection specimens after neoadjuvant therapy, stating that future studies to explore the role of immunohistochemistry on resected tumours in the neoadjuvant setting are encouraged⁴⁵.

Against this background, the aim of this study was to examine whether changes in nuclear size, expression of MIB-1 and PD-L1 in the residual tumour compared to baseline, are prognostically relevant for patients with SST treated with concurrent CRT, followed by resection.

Patients and methods

A retrospective analysis was performed on a consecutive series of patients with SST treated with concurrent CRT and subsequent surgical resection in the period 2005-2014 at Amsterdam University Medical Center, location VU Medical Center in Amsterdam. SST was defined as a tumour growing into the thoracic wall at the apex of the lung, above the level of the second rib³⁰. Patients were selected on basis of residual tumour being present in the resection specimen. For all 33 patients, a pre-treatment diagnostic biopsy was included for morphometric evaluation. Clinical data on follow-up were retrieved from the patient medical records. Part of this patient population has previously been described⁴³.

Morphometry

The method of nuclear size quantitation was performed on haematoxylin- eosin stained sections as described before⁴⁶. The measuring system was a commercially available interactive video overlay-based system (Q-PRODIT; Leica, Cambridge, UK). The microscopic image (100x objective) was recorded by a video camera and shown on a computer screen (final magnification 3000x). Biopsy area was selected by pathologist (E.T.) and nuclear area measured with manual delineation. At least 25 nuclei of neoplastic cells, and nuclei of type II pneumocytes, if present, were measured. The mean, median, 75th and 90th percentile of the nuclear size was estimated in all patients.

Immunohistochemistry

The paraffin blocks of the preoperative biopsies contained too few residual tumour tissue to perform the additional immunohistochemical analysis for MIB-1 and PD-L1. For this reason, immunohistochemistry analysis was only performed on the resection specimen. In short, immunohistochemistry for Ki67 (clone MIB-1clone (Dako/Agilent, Glostrup, Denmark) was performed in the Ventana Benchmark Ultra (Tucson, USA) diluted 1/50 and incubated for 32 minutes after antigen retrieval with Cell Conditioning Buffer 1 (CC1) 24 minutes at 100°C detection with Optiview DAB Detection Kit.

The proliferation fraction of the residual tumour in the resection specimen was estimated by scoring the overall number of positive staining tumour cells of one whole tumour section in one of three categories: <20%, 20-50% and >50%^{47,48}.

PD-L1 immunohistochemistry with the 22C3 clone was performed in a laboratory developed test (LDT) as previously described⁴⁹. The tumour proportion score (TPS) of PDL-1 positive tumour cells was assigned to one of 3 categories: <1% (negative), 1-49% (weak positivity) and ≥ 50% (strong positivity)⁵⁰.

Statistics

Statistical analyses were carried out by SPSS for Windows and Mac version 26 (IBM Corp., Armonk, NY, USA). Kaplan-Meier curves with log-rank test were used to compare overall survival (OS) and disease-free survival (DFS) between the different categories of MIB1 and PD-L1 status. OS was defined as time from diagnosis to time of death, DFS was defined as time from diagnosis to date of recurrence. Patients alive or without recurrence were censored at their last date of follow-up. Nuclear measurements in biopsies were compared to those in the resection specimens within patients using by the Wilcoxon sign rank test. Nuclear measurements in the resection specimen and normal tissue in the resection specimen from patients with and without recurrent disease were compared, using the Mann-Whitney U test. Data are described by median and range. A p-value < 0.05 was considered significant.

Results

The clinicopathological characteristics of the 33 patients are shown in table 1. Most patients were male (n=24, 73%) and adenocarcinoma (AdC) was the most frequent histological type (n= 19, 58%). In 12 cases (36%) less than 10% vital tumour was found. In 27 cases (82%) a NO lymph node status was diagnosed, whereas in 6 cases (18%) an irradical resection was found (5 R1, 1 R2). The majority of cases were staged as stage IIB (ypT3N0; n=19 [58%]). The median follow-up time was 26 months (range 4-133 months). Gender was not associated with DFS or OS (p=0.27 and p=0.33), nor was age (DFS p=0.99; OS p=0.99) and tumour type (DFS p=0.25; OS p=0.82).

A low fraction of vital tumour cells (<10%) showed a tendency for a better prognosis in OS and DFS, but did not reach significance (p=0.062 and p=0.078, respectively). In a subgroup analysis of ypT3N0 stage IIB patients (n=19), the percentage of vital tumour cells made no difference (OS p=0.18; DFS p=0.22). A lower stage (IA/B, versus IIA/B and III/IV) was associated with a better OS (p=0.002), but not with DFS (p=0.13).

Free resection margins were associated with a better prognosis: OS and DFS (p<0.001). In the ypT3N0 stage IIB subgroup this difference was also significant. (OS p=0.004; DFS p=0.003).

■ **Table 1.** Characteristics of all 33 eligible patients in relation to tumour type.

Age, mean (range)	55 years (32-73)			
Follow-up time, median (range)	26 months (4-133)			
	Tumour type			Total
	AdC (n=19)	SqCC (n=12)	NOS (n=2)	33
Gender				
Male	13	9	2	24
Female	6	3	0	9
Vital tumour				
<= 10%	6	5	1	12
>10%	13	7	1	21
N-status				
N0	17	9	1	27
N1	2	2	1	21
N2	0	1	0	1
R-status				
R0	15	10	2	27
R1	3	2	0	5
R2	1	0	0	1

■ **Table 1.** Characteristics of all 33 eligible patients in relation to tumour type. (continued)

	Tumour type			Total
	AdC (n=19)	SqCC (n=12)	NOS (n=2)	
Stage				
IA/B	4	1	1	6
IIA/B	12	9	1	22
IIIA/B	2	2	0	4
IV	1	0	0	1
MIB1				
<20%	11	2	2	15
20-50%	7	7	0	14
>50%	1	3	0	4
PDL-1				
<1%	17	6	1	24
1-50%	1	3	1	5
>50%	1	3	0	4

AdC adenocarcinoma, SqCC squamous cell carcinoma, NOS not otherwise specified

Immunohistochemistry

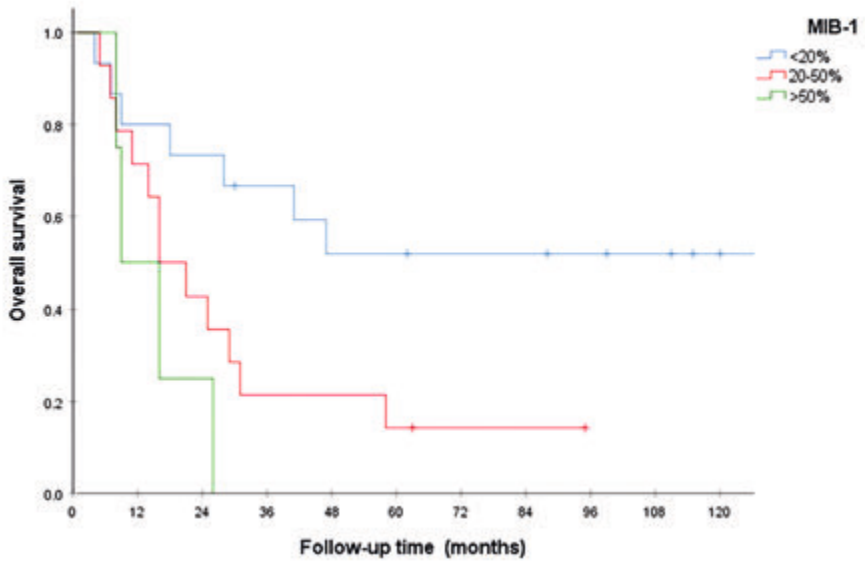
Low proliferative activity (<20% MIB-1) was associated with better OS ($p=0.016$): 2-year OS of 73% compared to 43% and 25%, respectively for moderate (MIB-1 20-50%) and high proliferative activity (MIB-1 >50%). A cut-off point of <20% MIB-1 revealed a significant difference for OS as well as DFS: $p=0.016$ and <0.001 , respectively (table 2 and figure 1).

In 24/33 of patients (73%), the number of PD-L1 positive cells was less than 1%. Of these 24 patients, 16 (66.7%) died of their disease, compared to 3 of the 5 patients (80%) with PD-L1 score of 1-50% and all 4 (100%) of those with a PD-L1 score >50% (OS $p=0.021$; DFS $p=0.066$) (figure 2).

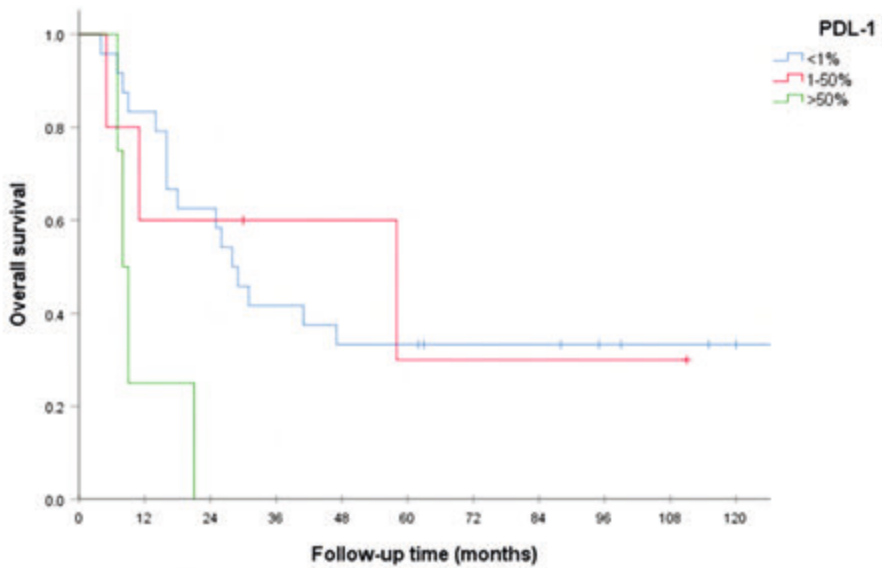
■ **Table 2.** The distribution of Mib-1 scores in the 33 resection specimen cases, related to 2-years overall survival (OS) and progression free survival (PFS)

	OS		p-value	PFS		p-value
	2-years	95% CI		2-years	95% CI	
MIB-1						
<20%	73%	51-96%	0.016	50%	24-76%	<0.001
20-50%	43%	17-69%		23%	0-46%	
>50%	25%	0-67%		0%	NE	

NE not estimated; OS overall survival; PFS progression-free survival



■ **Figure 1.** Kaplan-Meier analysis with overall survival curves for MIB-1 categories <20%, 20-50% and >50% ($p=0.016$).



■ **Figure 2.** Kaplan-Meier analysis with overall survival curves for PD-L1 categories <1%, 1%-50% and >50% ($p=0.021$).

Within the subgroup of stage IIB (ypT3N0) cases low MIB-1 tended to be associated with better OS, but not significant ($p=0.056$), whereas it was significant for DFS ($p=0.008$). For PDL-1 in this subgroup analysis it was just the other way around, a significant difference for OS ($p=0.011$), but not for DFS ($p=0.13$).

Morphometry

The mean nuclear size of normal lung tissue pneumocytes was significantly smaller compared to the nuclear size of tumour cells of the resection specimens (median difference $-38.1 \mu\text{m}^2$; range -115.2 to 16.0 ; $p<0.001$). This was also the case for median nuclear size and the 75th percentile cut-off points (table 3).

■ **Table 3.** Median difference [range] in mean nuclear size (in μm^2) of normal pneumocytes in resection specimen, pre-operative tumour cells in biopsy and post-chemoradiotherapy tumour cells in resection specimen.

	mean (μm)	p-value mean	median (μm^2)	p-value median	75th percentile (μm^2)	p-value 75th percentile	90th percentile (μm^2)	p-value 90th percentile
Tumour cells in biopsy vs resection	- 4.6 [-75.2 - 86.7]	0.14	-4.2 [-71.8 - 92.7]	0.15	- 4.9 [-107.1 - 97.4]	0.046	- 8.5 [-139.8 - 96.0]	0.085
Normal pneumocytes in resection vs tumour cells in resection	- 38.1 [-115.2 - 16.0]	<0.001	- 34.3 [-105.8 - 15.9]	<0.001	- 43.4 [-151.3 - 17.3]	<0.001	- 54.7 [-203.0 - 19.0]	<0.001

p-values in bold are significant

The mean nuclear size of tumour cells in the pre-treatment biopsies showed a tendency to be smaller than those in the resection specimens (median difference $-4.6 \mu\text{m}^2$; range -75.2 to 86.7 ; $p=0.14$), while for the 75th percentile the difference in nuclear size was significant (median difference $-4.9 \mu\text{m}^2$; range -107.1 to -97.4 ; $p=0.046$; table 3).

Nuclear size was not associated with recurrent disease. No differences were found in the mean nuclear size of tumour cells between the 10 patients who are still alive and those 23 who died of their disease, neither in the pre-treatment biopsies (median $61.7 \mu\text{m}^2$ vs $58.2 \mu\text{m}^2$; $p=0.82$), nor in the resection specimens (median $65.1 \mu\text{m}^2$ vs $69.9 \mu\text{m}^2$; $p=0.43$) (table 4).

The differences in mean nuclear size in the resection specimens of the survivors compared to their biopsies tended to be smaller than in the non-survivors; but these differences were not significant (median difference -1.1 vs -7.3 ; $p=0.33$).

■ **Table 4.** Median (and range) nuclear size (μm^2) of normal pneumocytes in resection specimen, and tumour cells in pre-operative biopsy and in resection specimen for patients with and without recurrent disease

	No recurrent disease n=11	Recurrent disease n=21	p-value
Tumour biopsy	61.7 (31.9 - 128.0)	58.2 (41.8 - 95.5)	0.82
Pneumocytes resection	31.2 (16.3 - 39.8)	32.0 (14.5 - 48.0)	0.21
Tumour resection	65.1 (20.9 - 93.0)	69.9 (47.6 - 152.2)	0.43

n number of patients

Discussion

The International Association Lung Cancer (IASLC) recently published multidisciplinary recommendations for pathologic assessment of lung cancer resection specimens after neoadjuvant therapy, stating that future studies to explore the role of immunohistochemistry on resected tumours in the neoadjuvant setting are encouraged⁴⁵.

Following these recommendations, this study demonstrates that high tumour cell proliferation (MIB-1 > 20%) and PD-L1 score of >1% are associated with a worse prognosis in patients with SST treated with trimodality therapy, including chemotherapy, radiotherapy and surgery. This finding is in line with the finding of Corzani et al.⁵¹, who report a low proliferation index determined with MIB-1 (cut-off point of 50%) associated with favorable outcome in resection specimen after neoadjuvant chemotherapy of surgically resected IIIA-N2 NSCLC. In resected NSCLC, however, several studies report conflicting results regarding the prognostic value of Ki67 or MIB-1 expression as an independent prognostic factor⁵²⁻⁵⁴.

From a theoretical point of view, one would expect that an absent PD-L1 staining in tumour cells would be associated with a better prognosis, since the tumour is more susceptible for the patient's own immune system⁵⁵⁻⁵⁸. In line with this theory, our study reports a better outcome in patients with <1% PD-L1 positive cells in the residual tumour. On the other hand, several studies did show an upregulation of PD-L1 after chemoradiation^{58,59}, suggesting it would be beneficial to add PD-L1 inhibitors to the chemoradiation therapy, hereby priming the immuno-microenvironment⁶⁰. We could not reproduce these results, since there was not enough tumour tissue left in our pretreatment biopsies to compare pretreatment and posttreatment PD-L1 expression, but adding immunotherapy to induction CRT seems promising. Furthermore, we found a relative low number of cases (4 out of 33; 12%) with a PDL1 score of >50%. This is lower than the 23% in the Keynote 010 study⁶¹, but in line with other studies, that also contained more adenocarcinomas than squamous cell carcinomas⁶². Our current results

with a worse prognosis in cases with high PDL-1, may be an argument for adjuvant immunotherapy in patients with residual tumour after trimodality therapy.

Previous studies from our group showed that patients with SST who have a pathologic complete response (pCR) in their resection specimen after trimodality therapy, do have a better prognosis when compared to patients with residual tumour^{43,63}. Whether the addition of immunotherapy to chemoradiotherapy results in higher pCR, and its mechanism of action, is currently investigated in a phase II study investigating the role of adding neoadjuvant immunotherapy to CRT in patients with T3-4N0-1 (eg, SST). The fraction of patients with a PD-L1 expression < 1% was lower than expected^{64,65} and may be explained by preanalytical factors occurring in resections specimen⁶⁶.

In addition, the translational and pathological part of this study will further help in defining the clinical significance of PD-L1 expression and up-regulation in patients treated with chemoradiotherapy and immunotherapy, and its impact on pCR⁶⁷.

In contrast to our previous study⁴³, a significant association between the percentage of vital tumour cells and prognosis was not observed. This is probably due to the selection procedure: in the current study cases with absence of vital tumour cells were not included, since this prohibited a comparison with the biopsies. The R-status and stage were, beside the above-mentioned biomarkers, the clinical parameters most relevant clinical parameters for predicting prognosis.

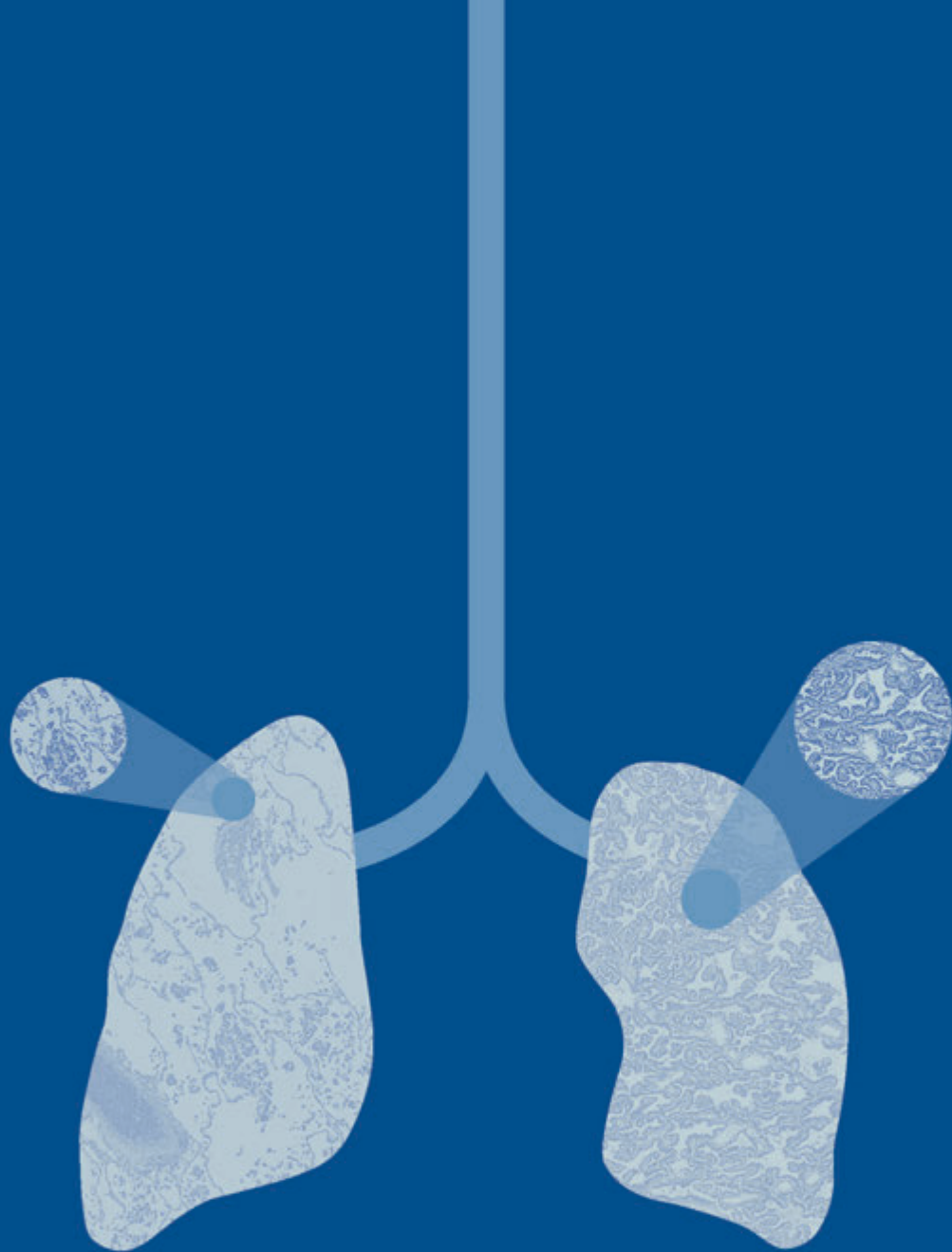
Nuclear enlargement is considered as one of the criteria of cytonuclear atypia in cancer^{68,69}, although it is not specific for cancer and could also be seen in inflammatory processes and after radiation^{70,71}. Enlarged nuclear size seems to be associated with clinical outcome in several tumour types^{72,73}. Increased nuclear size in relationship to the amount of cytoplasm (the nuclear-cell ratio) is one of the criteria for defining cytonuclear atypia and associated with a diagnosis of malignancy. Our findings of a larger nuclear size in tumour cells, both in pre-treatment biopsies and in the resection specimen, compared to normal pneumocytes is therefore not surprising. Although we found the size of tumour cell nuclei in resection specimen was larger after chemoradiotherapy compared to the pre-treatment biopsies, this was not of prognostic value.

Radiotherapy for non-small cell lung cancer induces DNA damage response in both irradiated and out-of-field normal tissues⁷⁴. This could lead to increased cytonuclear atypia, the so-called radiation atypia⁷⁰, but also to tumour cell shrinkage⁷⁵. This theoretical dual response may be a reason that we did not confirm the hypothesis that chemoradiation leads to more cytonuclear atypia. Our study did not show relevant associations between the mean nuclear area and survival in patients with residual tumour in the resection specimen. Likewise, postulating that the highest nuclear areas are associated with poorer survival, for the 75th or 90th percentiles of nuclear size we did not find a prognostic relevance. Apparently, nuclear size is too crude a measure for such associations, as many different, partly opposite, functionalities may take place in this cellular component. Examination of individual functions, such as proliferation fraction and escape from immunological surveillance, seem to be more informative.

The limitations of the study are the relatively small number of patients and the lack of sufficient preoperative biopsy tumour tissue to compare MIB-1 and PD-L1 levels before and after therapy. The relatively low numbers of cases did not allow multivariate statistical analysis between the different prognostic items such as percentage vital tumour cells, N- and R -status, stage and the immunohistochemical and morphometric results.

In summary, this study shows an increase in nuclear size of tumour cells after chemoradiotherapy, which has no prognostic significance in patients treated with trimodality for SST.

Importantly, low MIB-1 expression was associated with improved OS and DFS, and negative PD-L1 expression predicts better OS. Further study may be useful to investigate whether patients with residual tumour after trimodality therapy and high PDL-1 status may benefit from adjuvant immunotherapy.



4

A population-based study of outcomes in surgically resected T3N0 non-small cell lung cancer in the Netherlands, defined using TNM-7 and TNM-8; justification of changes and an argument to incorporate histology in the staging algorithm?

Hans Blaauwgeers, Ronald Damhuis, Birgit Lissenberg-Witte,
Joop de Langen, Suresh Senan, Erik Thunnissen

Journal of Thoracic Oncology 2018;14:459-467

doi: 10.1016/j.jtho.2018.10.164

Abstract

Objective

The objective was to study outcomes in patients in a population registry who were surgically staged as having pT3N0 NSCLC according to the seventh and eighth editions of the TNM staging classification.

Methods

Details of patients who underwent surgery for NSCLC staged as pT3N0M0 from 2010 to 2013 on the basis of the seventh edition of the TNM classification were retrieved from the Netherlands Comprehensive Cancer Organization. These data were next matched with corresponding pathology data from a nationwide registry. Patients were categorized into four major pT3 subgroups as follows: those with a tumor diameter more than 7 cm, those with separate tumor nodules in the same lobe (two or more nodules), those with parietal pleural invasion, and a mixed group (consisting mainly of those with a tumor diameter larger than 7 cm combined with parietal pleural invasion).

Results

A total of 683 patients were eligible for analysis. The 3- and 5-year overall survival (OS) rates for the subtype tumor diameter larger than 7 cm were 59.9% and 47.2%, respectively, and were comparable to the rates for the subtype with pleural invasion (50.4% and 45.3%), respectively. The mixed group has worse 3- and 5-year OS rates (37.5% and 28.7%, respectively), which were comparable to the outcomes for TNM eighth edition-staged IIIB and pT4 cases in the International Association for the Study of Lung Cancer database. For the subtype two or more nodules, the 3- and 5-year OS rates were 70.6% and 62.8%, respectively, with patients with adenocarcinoma showing a significantly better OS than did patients with squamous cell carcinoma: a 5-year OS rate of 65.1% versus 47.2%, respectively ($p < 0.001$), suggesting that the prognosis for the adenocarcinoma subgroup may be comparable to that for the pT2 category, whereas squamous cell carcinoma nodules can remain pT3.

Conclusion

This population analysis of overall survival rate by pT3N0 subcategory for NSCLC suggests that histologic type is a relevant descriptor in the category two or more nodules. The findings do not support migration of the group with a tumor diameter larger than 7 cm to the category pT4 in the eighth edition of the TNM classification, and they suggest that a combination of two pT3 descriptors (the mixed groups) merits migration to pT4.

Introduction

The TNM classification has been developed to predict survival outcome in patients with cancer⁷⁶. The T, N, and M descriptors for NSCLC have evolved over time, with the recent transition from the seventh edition of the TNM staging classification (TNM-7)^{77,78} to the eighth edition of the TNM staging classification (TNM-8) (2017)⁷⁹, based on analyses of the International Association for the Study of Lung Cancer (IASLC) database.

The T3 category for lung cancer represents a heterogeneous subgroup as shown in Table 1. In the sixth edition of the TNM staging classification (TNM-6)¹⁵, tumors with a diameter larger than 7 cm were classified as T2, whereas tumors with a separate nodule in the same lobe were classified as T4 tumors. In the TNM-7, both these categories were designated as T3, consisting of tumors with (1) a diameter larger than 7cm, (2) a second nodule or multiple lesions in the same lobe (two or more nodules), (3) parietal pleural invasion, (4) less than a 2-cm margin from the main carina, and/or (5) atelectasis or obstructive pneumonitis of the entire lung. The Staging and Prognostic Factors Committee of the IASLC published proposals to revise the lung cancer staging criteria for the TNM-8 in 2015⁷⁸. Changes to the T3 component included reclassifying tumors larger than 5 cm from T2 to T3, with tumors larger than 7 cm moved to T4. Diaphragm invasion became a T4 descriptor, but lung atelectasis, both partial and total, and all cases of main bronchus invasion, regardless of the distance from the carina were defined as T2.

The IASLC recommendations to revise the T3 category in TNM-8 were largely based on information derived from centers in Asia⁷⁹, as were the vast majority of all data in the IASLC database. As survival outcome and prognostic factors may differ between various countries/ regions, we aimed to validate the recent TNM-8 T3 recommendations in a large series from the Netherlands, using clinical data from the Netherlands Comprehensive Cancer Organization (IKNL) and pathology data from the Nationwide Network and Registry of Histopathology and Cytopathology in the Netherlands (PALGA)⁸⁰.

■ **Table 1.** Changes in NSCLC T3 descriptors between the 6th, 7th and 8th edition of the staging manual^{77, 78, 79}

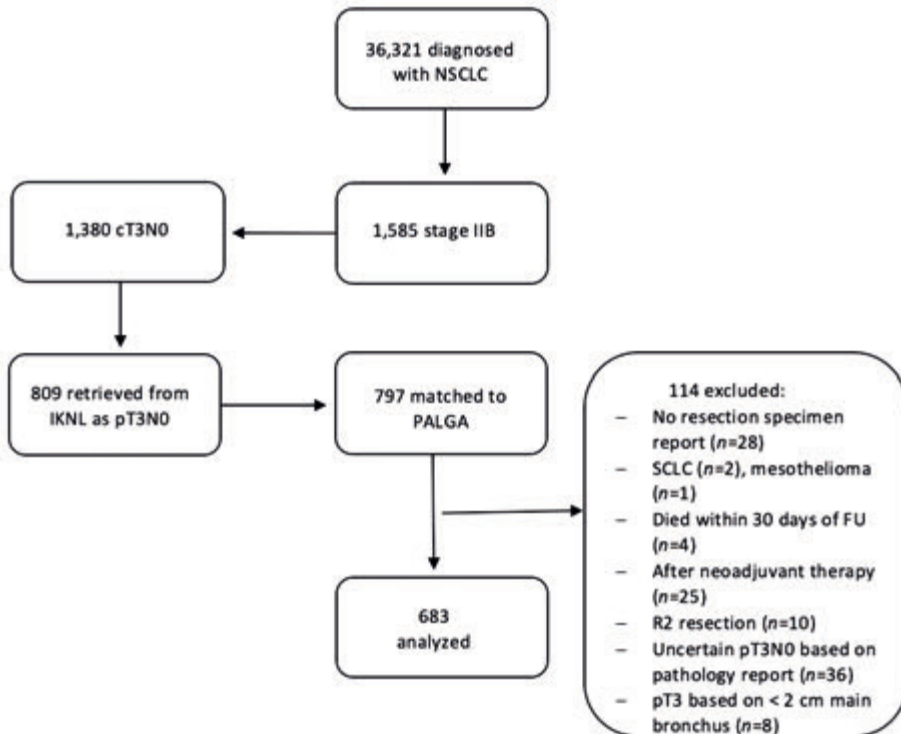
TNM-6	TNM-7	T-descriptor	TNM-8
T2	T2b	diameter 5-7 cm	T3
T3	T3	< 2 cm carina	T2
T3	T3	complete atelectasis	T2
T4	T3	separate nodules	T3
T3	T3	pleural/chest wall invasion	T3
T2	T3	diameter > 7 cm	T4
T3	T3	diaphragm invasion	T4

TNM-6, sixth edition of the TNM classification; TNM-7, seventh edition of the TNM classification; TNM-8 eight edition of the TNM classification

Materials and methods

A cohort of Dutch patients who underwent lung surgical resection for pT3N0M0 NSCLC was retrieved from the IKNL for the 4-year period from 2010 to 2013, after the introduction of the TNM-7. The study was approved by the IKNL privacy review board and performed in accordance with the regulations of the Central Committee on Research involving Human Subjects. The IKNL collects data on all cancer patients diagnosed in the Netherlands, based on notification of newly diagnosed malignancies by PALGA and hospital discharge diagnoses. The date of diagnosis was recorded as the date of retrieval of cytology specimens or tissue as mentioned in the pathology report that first confirmed the diagnosis of cancer. Information on demographics, diagnosis, staging and treatment was extracted routinely from the medical records by specially trained IKNL personnel. Clinical and postsurgical stage information was recorded according to the TNM-7. Information on survival status in the IKNL database is updated annually by using a computerized link with the national civil registry.

Of the 36,321 patients registered with NSCLC in the Netherlands during the 4-year period 2010 and 2013, a total of 1380 (3.8%) had a diagnosis of cT3N0M0, and of these, 809 (2.2%) were classified as pT3N0M0 disease. The records of these 809 patients with pT3N0M0 disease were matched to the PALGA database to obtain detailed information on the T3 descriptors. Matching was successful in 797 (98%) of the records, with one or multiple reports per patient. A total of 2179 pathology reports were retrieved from the PALGA database, with a range of one to 10 reports per patient (an average 2.7 reports per patient). The data in each report consisted of case identification number, sex, date of birth, date of diagnosis, type of material (cytology or histology) and the integral text of the conclusion of the pathology report, but not the text referring to either the gross or microscopical section reports. The detailed T3 descriptors were identified and coded after review of the reports by one investigator (H.B.). Records were excluded from analysis, if the T3-status could not be confirmed on basis of the conclusion text of the report (n=36) or when the report on the surgical specimen was unavailable (n=28). Other exclusion criteria are shown in the consort flow diagram (Fig. 1), leaving a final study database of 683 eligible patients.



■ **Figure 1.** Consort flow diagram of NSCLC patients diagnosed in the 4-years period between 2010-2013, retrieved from the Netherlands Comprehensive Cancer Organisation (IKNL), revealing 809 pT3N0 patients. After exclusion of 114 patients, 683 patients of the 797 patients retrieved after matching to the Nationwide Network and Registry of Histo- and Cytopathology in the Netherlands (PALGA) were analyzed.

Statistics

We evaluated the prognostic impact of several factors on the overall survival (OS) by using Kaplan-Meier curves and log-rank test. Post-hoc comparisons between the different groups were corrected for multiple testing, using Bonferroni's correction. Differences in OS between the T3-descriptors were also assessed after correction for age, by using a Cox regression model. A multivariable Cox regression model was built by using a backward selection procedure (p removal = 0.05), to investigate independent prognosticators of OS. The variables included in this backward selection procedure were T3 group, tumor type, residue, type of resection, and postoperative chemotherapy and radiotherapy. The multivariable model was corrected for age (continuous). Associations between pT3N0 and the other variables were tested by the chi-square test. Categorical data was described by means of frequencies and percentages. Statistical analyses were carried out with SPSS for Windows and Mac version 22 (IBM Corp., Armonk, NY, USA). The significance level was set at 0.05.

Results

General

From all 36321 registered NSCLC patients in the 4-years period between 2010 through 2013, the data of 683 pT3N0 patients (1.9%) could be analyzed after matching nationwide cancer and pathology databases.

Three major pT3N0 subtypes were present: (1) tumor diameter larger than 7 cm ($n=251$ [37%]), (2) two or more separate tumors in the same lobe (two or more nodules) ($n=173$ [25%]) and (3) parietal pleural invasion ($n=154$ [23%]). Tumors with less than a 2-cm margin from the main carina ($n=8$) were excluded from further analysis because of low numbers and because no cases with atelectasis of the entire lung were found. On the basis of the available pathology report information, no cases with pericardial or mediastinal pleural invasion were encountered. A fourth subtype was recognized. The group with this subtype, termed the *mixed subtype*, consisted of 105 patients (15%) with a mixture of any combination of the aforementioned three major subtypes major three subtypes: $n=105$ (15%); 'mixed' subtype, mainly, tumor diameter larger than 7 cm and pleural invasion ($n=94$ [89.5%]).

The frequency distribution of the clinicopathological characteristics in relation to the pT3 descriptors is shown in Table 2. Subtype was significantly associated with sex ($p < 0.001$); there were more men than women with the subtypes, tumor diameter larger than 7 cm, pleural invasion, and mixed subtype, whereas within the subtype two or more nodules, there was an almost equal distribution between men and women. A significant association between subtype and histologic type was found within the subtype two or more nodules, with more adenocarcinomas than squamous cell carcinomas ($p < 0.001$), as was also the case within the subtypes, tumor diameter larger than 7 cm and pleural invasion, whereas squamous cell carcinoma was seen more frequently within the mixed subtype.

■ **Table 2.** Frequency distribution of the clinicopathological characteristics for the Four Major pT3N0 Subtypes

pT3N0 Characteristic	>7 cm		2 nd /multiple nodule(s)		Parietal pleural invasion		Mixed		Total n (%)	p-value
	n	%	n	%	n	%	n	%		
All	251	36.7	173	25.3	154	22.5	105	15.4	683 (100)	
Gender										<0.001
male	172	68.5	86	49.7	91	59.1	77	73.3	426 (62.4)	
female	79	31.5	87	50.3	63	40.9	28	26.7	257 (37.6)	
Age (years)										0.77
< 60	65	25.9	36	20.8	38	24.7	29	27.6	168 (24.6)	
60-69	83	33.1	68	39.3	58	37.7	35	33.3	244 (35.7)	
≥ 70	103	41.0	69	39.9	58	37.7	41	39.0	271 (39.7)	

■ **Table 2.** Frequency distribution of the clinicopathological characteristics for the Four Major pT3N0 Subtypes (continued)

pT3N0	>7 cm		2 nd /multiple nodule(s)		Parietal pleural invasion		Mixed		Total	p-value
Characteristic	n	%	n	%	n	%	n	%	n (%)	
Histology										<0.001
AdC	112	44.8	107	62.2	74	48.4	28	26.7	321 (47.0)	
SqCC	94	37.6	43	25.0	65	42.5	55	52.4	257 (37.6)	
NOS	16	6.4	7	4.1	5	3.3	10	9.5	38 (5.6)	
other	28	11.2	15	8.7	9	5.9	12	11.4	64 (9.3)	
Resection										0.17
Right sided	142	56.8	106	61.3	93	60.4	51	48.6	392	
Left sided	108	43.2	67	38.7	61	39.6	54	51.4	290	
unknown	1		0		0		0		1	
Lobectomy	176		157		137		81		551	<0.001
Right upper lobe	38	21.6	67	42.7	67	48.9	28	34.6	200	
Right lower lobe	50	28.4	20	12.7	11	8.0	10	12.3	91	
Right middle lobe	1	0.6	6	3.8	2	1.5	0	0.0	9	
Right, not otherwise specified	2	1.1	2	1.3	2	1.5	1	1.2	7	
Left upper lobe	31	17.6	40	25.5	41	29.9	26	32.1	138	
Left lower lobe	51	29.0	22	14.0	12	8.8	14	17.3	99	
Left, not otherwise specified	2	1.1	0	0.0	2	1.5	2	2.5	6	
Unknown	1	0.6	0	0.0	0	0.0	0	0.0	1	
Bilobectomy	31		9		8		4		52	
Right upper and middle lobe	15	48.4	6	66.7	4	50.0	4	100.0	29	
Right lower and middle lobe	15	48.4	3	33.3	4	50.0	0	0.0	22	
unknown	1	3.2	0	0.0	0	0.0	0	0.0	1	
Pneumonectomy	44	17.8	7		9		20		80	
Right	20	45.5	2	28.6	3	33.3	8	40.0	33	
Left	24	54.5	5	71.4	6	66.7	12	60.0	47	
Residue										<0.001
Rx	91	36.3	96	55.5	65	42.2	42	40.0		
R0	150	59.8	70	40.5	52	33.8	40	38.1		
R1	10	4.0	7	4.0	37	24.0	23	21.9		

■ **Table 2.** Frequency distribution of the clinicopathological characteristics for the Four Major pT3N0 Subtypes (continued)

pT3N0	>7 cm		2 nd /multiple nodule(s)		Parietal pleural invasion		Mixed		Total n (%)	p-value
	n	%	n	%	n	%	n	%		
Chemotherapy										0.51
No	153	61.0	114	65.9	90	58.4	62	59.0		
Yes	98	39.0	59	34.1	64	41.6	43	41.0		
Radiotherapy										<0.001
No	241	96.0	167	96.5	119	77.3	83	79.0		
Yes	10	4.0	6	3.5	35	22.7	22	21.0		
Chemoradiation										<0.001
No	148	59.0	112	64.7	68	44.2	48	45.7		
Only CT	93	37.1	55	31.8	51	33.1	35	33.3		
Only RT	5	2.0	2	1.2	22	14.3	14	13.3		
Yes	5		4		13		8			

Note: the four major subtypes are as follows: larger than 7 cm; with second / multiple nodules; with pleural invasion and mixed.

AdC, adenocarcinoma; SqCC, squamous cell carcinoma; NOS, NSCLC not otherwise specified; Rx, microscopic resection margin unknown; RO, microscopic negative resection margin; R1, microscopic positive resection margin; CT, chemotherapy; RT, radiotherapy.

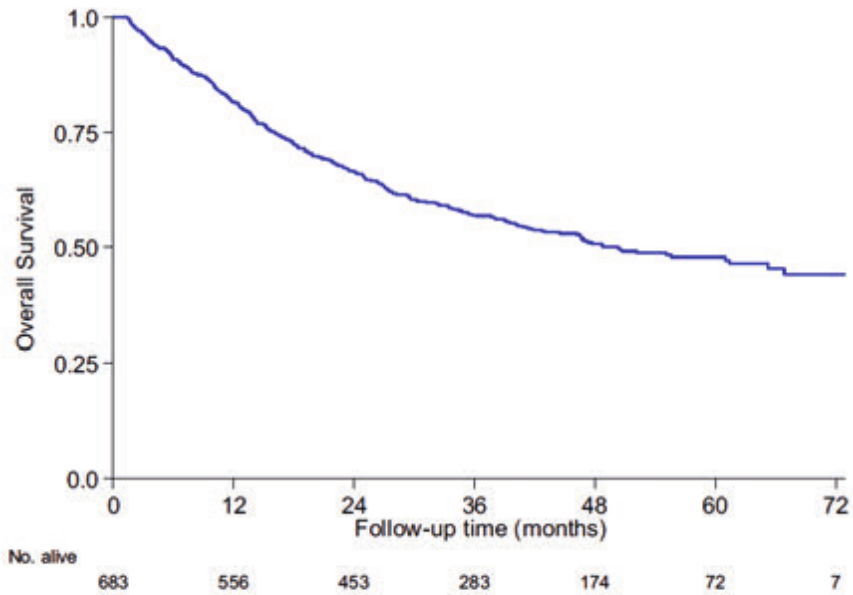
Tumors with a diameter larger than 7 cm were more often found in the lower lobes, whereas at least two-thirds of the other subtypes were found in the upper lobes ($p < 0.001$). However, no differences in OS were noted for tumors 'larger than 7 cm' found in the lower lobes, compared to those in the upper lobes ($p = 0.16$, log-rank test).

A total of 264 of the 683 (38.7%) were treated with adjuvant chemotherapy, irrespective of the pT3N0 subtype. Post-operative radiotherapy was administered in 73 patients (10.7%), but rarely to patients with pT3N0 subtypes tumor diameter larger than 7 cm and two or more nodules. However, nearly 20% of patients in the group with the pleural invasion and mixed subtypes received radiotherapy ($p < 0.001$).

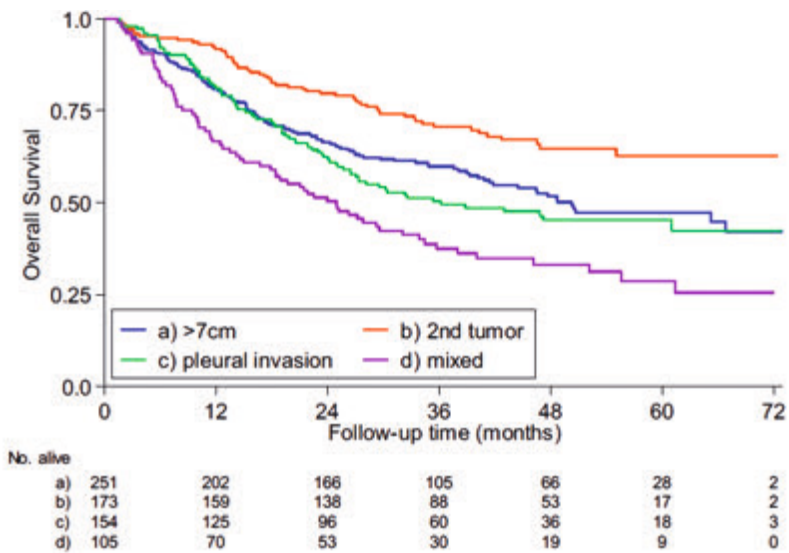
Survival

The 3- and 5-year overall survival rates for the entire study population was 57.0% and 47.9%, respectively (Fig. 2).

The four pT3N0 subtypes showed significant differences in OS ($p < 0.001$) with the best prognosis for the subtype with two or more nodules in the same lobe (5-years OS 62.8%), and the worst for the mixed subtype (5-years OS 28.7%) (Fig. 3).



■ **Figure 2.** Kaplan-Meier survival curve of the whole study population of patients with T3N0 disease (N=683).



■ **Figure 3.** Kaplan-Meier survival curves of the four major T3N0 subtypes: second or multiple nodules in the same lobe; larger than 7 cm; pleural invasion, and the mixed subtype

Post-hoc pairwise comparison showed significant differences between most T3 descriptors except between cases with pleural invasion and tumor diameter larger than 7 cm and between cases with pleural invasion and mixed subtypes (Table 3). The difference between subtypes remained significant after correction for age and gender ($p < 0.001$). The backward selection procedure identified T3 subtype, postoperative chemotherapy and age as independent prognosticators of OS (see Table 3).

■ **Table 3.** Three-year overall survival (OS) with 95% CIs for the pT3 categories and other clinico-pathological characteristics.

Characteristic	3-yr OS	95% CI	p-value	HR	95% CI	p-value	5-yr OS
pT3NO total	57.0%						49.9%
pT3NO by subtype			<0.001			<0.001	
>7cm (n=251)	59.9%	53.7% - 66.0%		1.0			
Second/multiple nodules (n=173)	70.6%	63.7% - 77.6%		0.6	0.40 - 0.76		62.8%
Parietal pleural invasion (n=154)	50.4%	42.4% - 58.5%		1.2	0.88 - 1.5		
Mixed (n=105)	37.5%	28.0% - 47.1%		1.7	1.3 - 2.3		28.7%
Age			0.004			0.010	
<60	64.3%	57.0% - 71.6%		1.02	1.004 - 1.03		
60-69	60.6%	54.2% - 66.9%					
70+	49.3%	43.2% - 55.4%					
Gender			0.001			n.i.	
Male	52.4%	47.5% - 57.3%					
Female	64.7%	58.7% - 70.6%					
Histology			0.006			n.s.	
AdC (n=321)	64.4%	59.1% - 69.8%					
SqCC (n=257)	51.9%	45.7% - 58.1%					
NSCLC-NOS (n=38)	46.4%	30.3% - 62.6%					
Other	46.5%	34.2% - 58.9%					
Resection margins			0.007			n.s.	
Rx	55.4%	49.6% - 61.2%					
R0	61.7%	56.2% - 67.2%					
R1	44.2%	32.9% - 55.6%					
Resection type			0.014			n.s.	
Lobectomy	59.1%	54.9% - 63.2%					
Pneumectomy	46.0%	34.7% - 57.3%					
Bilobectomy	52.2%	38.2% - 66.2%					

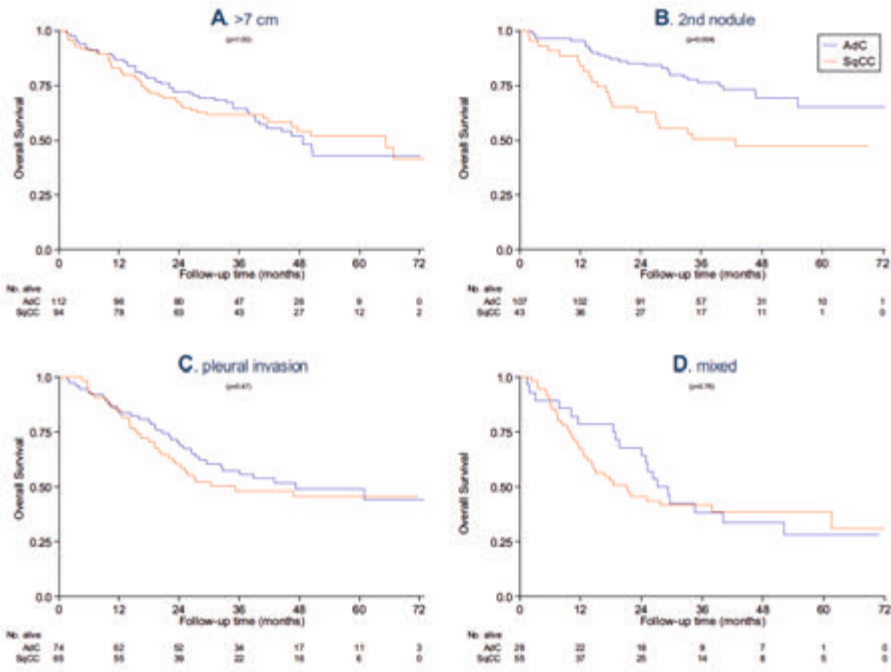
■ **Table 3.** Three-year overall survival (OS) with 95% CIs for the pT3 categories and other clinico-pathological characteristics. (continued)

Characteristic	3-yr OS	95% CI	p-value	HR	95% CI	p-value	5-yr OS
Resection side			0.38			n.i.	
Right	58.1%	53.2% - 63.1%					
Left	55.4%	49.5% - 61.3%					
Chemotherapy			<0.001			<0.001	
No	50.4%	45.5% - 55.3%		1.0			
Yes	67.5%	61.7% - 73.2%		0.6	0.45 - 0.74		
Radiotherapy			0.04			n.s.	
No	58.3%	54.3% - 62.3%					
Yes	45.9%	34.0% - 57.7%					
Chemo and/or radiation			<0.001			n.i.	
None	52.3%	47.1% - 57.5%					
Only CT	67.8%	61.8% - 73.9%					
Only RT	33.7%	19.1% - 48.2%					
Both	63.9%	45.8% - 82.0%					

Note: the four major subtypes are as follows: larger than 7 cm, second or multiple nodules in the same lobe, pleural invasion and mixed

HR, Hazard Ratio; n.s., not significant; n.i., not included in model selection; AdC, adenocarcinoma; SqCC, squamous cell carcinoma; NSCLC-NOS, non-small cell lung cancer, not otherwise specified; CT, chemotherapy; RT, radiotherapy; Rx, microscopic resection margin unknown; RO, microscopic negative resection margin; R1, microscopic positive resection margin.

Within the group with subtype two or more nodules, patients with adenocarcinoma had a better prognosis than did those with squamous cell carcinoma with 5 years OS of 65.1% vs 47.2% ($p=0.004$), respectively, whereas the differences were not significant for the other three subtypes (tumor diameter larger than 7 cm' [$p=1.00$], pleural invasion [$p=0.47$], and mixed [$p=0.76$]), (Fig. 4 and Table 4).



■ **Figure 4.** Kaplan-Meier survival curves showing overall survival and a better prognosis in adenocarcinoma (AdC) (blue) than squamous cell carcinoma (SqCC) (red) in the second nodule subtype ($p=0.004$), but not in the other three subtypes.

■ **Table 4.** Mean 5-Year OS of T3N0 NSCLC and stage IIA and IIIA as in the IASLC Database for the TNM-7 and TNM-8 with comparison to our study, Including histologic subtypes and CIs.

	TNM-7		Proposed TNM-8		Current study	
	stage	5 yrs OS	stage	5 yrs OS	5 yrs OS	95% CI
	IIB	57%	IIB	65%		
All pT3N	IIB	49%	IIB	56%	47.9%	43.5%-52.2%
All >7cm	IIB	49%	IIIA	41%	47.2%	39.9%-54.5%
AdC		n.a.		n.a.	43.0%	31.0%-55.1%
SqCC		n.a.		n.a.	51.7%	40.2%-63.3%
All 2nd tumor	IIB	49%	IIB	49%	62.8%	54.2%-71.3%
AdC		n.a.		n.a.	65.1%	52.9%-77.4%
SqCC		n.a.		n.a.	47.2%	31.8%-62.6%
All parietal pleural invasion	IIB	49%	IIB	49%	45.3%	36.8%-53.7%
AdC		n.a.		n.a.	49.0%	36.5%-61.5%
SqCC		n.a.		n.a.	45.4%	32.5%-58.2%

■ **Table 4.** Mean 5-Year OS of T3N0 NSCLC and stage IIA and IIIA as in the IASLC Database for the TNM-7 and TNM-8 with comparison to our study, including histologic subtypes and CIs. (continued)

	TNM-7		Proposed TNM-8		Current study	
	stage	5 yrs OS	stage	5 yrs OS	5 yrs OS	95% CI
	IIA	57%	IIA	65%		
All mixed	IIB	49%	IIB	49%	28.7%	18.5%-38.9%
AdC		n.a.		n.a.	28.2%	10.0%-46.4%
SqCC		n.a.		n.a.	38.4%	25.0%-51.9%
	IIIB	23%	IIIB	24%		

OS, overall survival; IASLC, International Association for the Study of Lung Cancer; TNM-7, seventh edition of the TNM classification; TNM-8, eighth edition of the TNM classification; CI, confidence interval; AdC, adenocarcinoma; SqCC, squamous cell carcinoma; na, not available

Discussion

In this retrospective population-based study we demonstrated that the subgroup of patients with the T3 descriptor two or more nodules had a better 5-years OS (62.8%) than did patients with the other T3 subtypes. This observation is conditional on histologic type, a factor not considered in the TNM classification. Adenocarcinomas of the subtype two nodules or more showed a 5-years OS of 65.1%, comparable to that for TNM-8 stage IIA tumors (65%).

On the basis on the IASLC data, the subtypes pleural invasion and two or more nodules remain allocated to the pT3 category^{16,79}. Our data on adenocarcinomas in the two nodules or more subtype may be an argument to transfer this subgroup to pT2. On the contrary, for squamous cell carcinoma the 5-years OS rate (47.2%) was similar to the survival of the pT3N0 two or more nodules subtype of the IASLC database (49%)¹⁶. In this context, our data provide a strong argument for histology to become a descriptor for pT staging.

For the T3 descriptors tumor diameter larger than 7 cm and pleural invasion, 5-years OS of 47.2% and 45.3% were found, respectively, which are in between the 5-years survivals reported for stages IIB and IIIA in the TNM-8 (56% and 41%; Table 4). However, in the IASLC database, the descriptor tumor diameter larger than 7 cm was classified as having the same prognosis as the pT4 category (stage IIIA), which was the argument for upgrading. One could argue that based on our data cases with pleural invasion should be migrated to the pT4 category, or alternatively, that cases with a tumor diameter larger than 7 cm or pleural invasion should both remain in the pT3 category.

Our finding that tumors with a diameter larger than 7 cm were more often located in the lower lobes, whereas at least two-thirds of the other subtypes were found in the upper lobes, is not easy to explain. A speculation may be that the lung volumes in the lower lobes are larger than those in the upper lobes⁸¹. In this context, tumors may

growth to a larger extent before becoming symptomatic on account of growth into structures as the pleura.

Furthermore, we recognized a T3 descriptor with a significantly different (worse) prognosis, namely the mixed type, consisting of tumors with a combination of two T3 descriptors. The mixed subtype is currently not recognized in the TNM-8 classification. In our study, this group consisted of 105 (15.4%) of the 683 patients, mainly comprising a group with tumor diameter larger than 7 cm combined with pleural invasion. This mixed subtype was associated with the worst prognosis of all T3 descriptors (a 5-years OS of 29%, which is even lower than the 41% 5-years OS of stage IIIA NSCLC, and is in fact closer to the 5-years OS of 21% for stage IIIB tumors)¹⁶. Our data suggest that future revisions of TNM should explore larger databases with patients in this category to further validate whether allocating the mixed subtype to pT4 is validated.

A possible explanation for the discrepancies between the IASLC results and our results may be a difference in the composition of the study cohorts. The IASLC database of any TNOMO consisted of a total of 26,722 pathologically staged patients, of whom 22,257 were analyzed and 2,108 were classified as pT3N0⁷⁹. As mentioned, most (79%) of the pT3N0 patients in the IASLC database came from Asia, so approximately 440 of the pT3N0 patients in this database are non-Asian. In contrast, our Dutch database consists of 683 patients. Although the ethnicity in our cohort members is unknown, in 2016 less than 1% of the inhabitants in the Netherlands had an Asian background⁸². Extrapolation to our study population would result in 5-6 patients with an Asian background. Therefore, our nationwide study population is likely to be more representative for the European/ Western population than the IASLC database. Ethnicity in this context may be an important factor influencing survival outcomes for TNM stages.

Adjuvant chemotherapy or radiotherapy could affect the OS; however, detailed information is not available in the IASLC database. Patients with pT3N0 have an indication for adjuvant chemotherapy, as mentioned in the Dutch and European Society for Medical Oncology guidelines^{83,84}. Nevertheless, of the 683 patients only 264 (38.6%) received post-operative chemotherapy.

This post-operative chemotherapy was a very strong prognosticator, unrelated to the pT3N0 subtype. An explanation for the relatively low percentage of postoperative chemotherapy may be that it is regularly withheld in frail patients, implying that part of the prognostic impact of chemotherapy may be explained in terms of confounding by indication⁸⁵. In addition, the percentage of our patients undergoing postoperative chemotherapy is comparable to that reported in a large observational study where only 40% of 31747 patients in whom chemotherapy was indicated, actually got the planned therapy⁸⁶.

Indication for postoperative radiotherapy in our study population appears mainly restricted to patients within the pleural invasion and mixed subtype, presumably as this group consists mainly of patients with pleural invasion and one of the other T3 descriptors (mostly tumor diameter larger than 7cm). This seems logical, since there

is no role for routine postoperative radiotherapy for a radically excised pT3N0M0 disease⁸⁷.

Our study has several limitations. The pT3 descriptors were based on the conclusion text of the available pathology reports. No data were available on gross examination or microscopy. This may be the explanation for the 36 excluded cases with uncertainty about the exact pT3 descriptor. Because at least two cases with SCLC and one patient with mesothelioma were registered as NSCLC in the IKNL database, other administrative errors cannot be excluded. Furthermore, the finding that the subtype two or more nodules has a better prognosis may partly reflect the fact that most of these cases represented synchronous double primary adenocarcinomas, with only a minority being true intrapulmonary metastases. Multiple stage I tumors within the same lobe are thought to have a good prognosis, with a reported 5-year OS of 82,4% for patients with multiple synchronous adenocarcinomas⁸⁸. On the basis of the available database information, we are unable to distinguish between synchronous primaries and isolated lung metastases in our study group.

In conclusion, in this population-based study of OS for pT3N0 categories in NSCLC shows that (1) there is limited support for migration of the descriptor tumor diameter larger than 7 cm from category pT3 in the TNM-7 to the category pT4 in the TNM-8, (2) histologic type deserves a role as descriptor in the two or more nodules category, where adenocarcinomas may be migrated to the pT2 and squamous cell carcinomas remain pT3, and (3) a combination of two pT3 descriptors may be migrated to pT4.

With the advent of new therapies, the relevance of proper prognostication increases and such findings, as well as ethnic bias, needs to be considered in international studies.



Part II

Spread through air spaces,
an artifact or reality?



5

Ex vivo artifacts and histopathologic pitfalls in the lung

Erik Thunnissen, **Hans Blaauwgeers**, Erienne de Cuba,
David Yick, Douglas Flieder

Archives of Pathology and Laboratory Medicine. 2016;140:212-220
doi: 10.5858/arpa.2015-0292-OA

Abstract

Context

Surgical and pathologic handling of lung physically affects lung tissue. This leads to artifacts that alter the morphologic appearance of pulmonary parenchyma.

Objective

To describe and illustrate mechanisms of ex vivo artifacts that may lead to diagnostic pitfalls.

Design

In this study 4 mechanisms of ex vivo artifacts and corresponding diagnostic pitfalls are described and illustrated.

Results

The 4 patterns of artifacts are: (1) surgical collapse, due to the removal of air and blood from pulmonary resections; (2) ex vivo contraction of bronchial and bronchiolar smooth muscle; (3) clamping edema of open lung biopsies; and (4) spreading of tissue fragments and individual cells through a knife surface. Morphologic pitfalls include diagnostic patterns of adenocarcinoma, asthma, constrictive bronchiolitis, and lymphedema.

Conclusion

Four patterns of pulmonary ex vivo artifacts are important to recognize in order to avoid morphologic misinterpretations.

Introduction

Normal lung histology including usual tissue artifacts is well described⁸⁹. Unfortunately, virtually all writings and images are concerned with “static” morphologic findings. Recently, attention has been focused on dynamic changes in the lung that cause a pitfall in the diagnosis of pulmonary papillary adenocarcinoma⁹⁰. It is certain that when one concentrates on a specific problem, one may not notice other, perhaps peripheral, issues. This “inattentional blindness” can occur in the interpretation of lung biopsies, especially when the pathologist focuses only on a particular aspect of a tissue sample and in doing so neglects other findings or even the possibility that the morphology has been altered by artifact(s)⁹¹. Ex vivo artifacts in lung samples have not been systematically investigated and it is useful to describe in detail possible mechanisms associated with several obvious changes. During the dynamic process of pulmonary resection and tissue handling several ex vivo artifacts occur, which have an impact on the histologic appearance of the lung tissue. The aim of this study is to describe and illustrate 4 mechanisms of ex vivo artifacts, namely, “surgical collapse,” “ex vivo contraction,” “clamping edema,” and “spreading through a knife surface.” These 4 mechanisms individually or in combination manifest with morphologic patterns that may lead to diagnostic pitfalls.

Mechanisms of ex vivo artifacts

Surgical Collapse

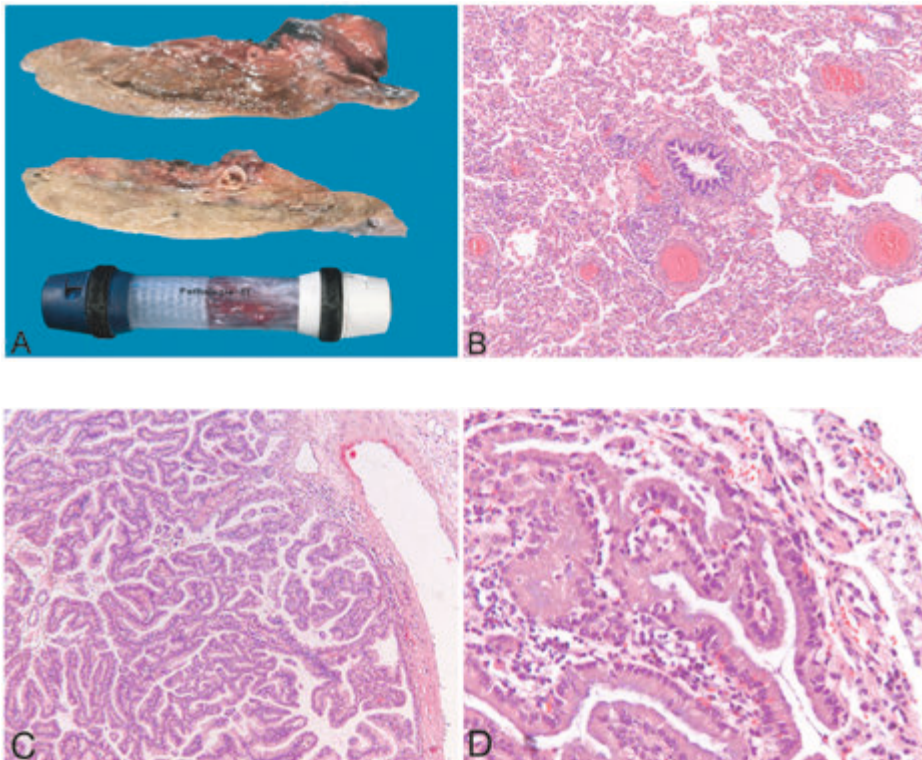
The lung is usually deflated during segmentectomy, lobectomy, and pneumonectomy, causing so-called surgical atelectasis or collapse (Figure 1A). Deflation of the surgical lung is achieved by double-lumen endotracheal intubation, allowing selective ventilation of the nonsurgical lung^{92,93}. Surgical collapse also affects the pulmonary vasculature with emptying of the blood and lymph vessels. During removal of the lung, the physiologic negative pressure between the visceral and parietal pleura is replaced by atmospheric pressure, leading to additional compression of the removed lung tissue. Manual pressure applied by the surgeon(s) may also contribute. Thus, surgical collapse encompasses 3 components. In the time frame of inspiration and expiration, approximately 3 to 4 seconds, 250 ml of air flows in and out of each lung. Interestingly, the deflation process during surgery takes longer. This is in part due to the “columns” of lymph in the superficial and deep lymphatic vessels. Emptying of the lymph into the draining lymph nodes is a slower process (minutes) compared to inspiration and expiration.

Importantly, during this process of surgical collapse not all lung parts may collapse in a similar manner. If, in addition to the abovementioned 3 aspects, adenocarcinoma in situ or atypical adenomatous hyperplasia is present, then the alveolar walls are more rigid. This reduction in compliance causes a slight reduction in lung collapse, compared

with adjacent uninvolved areas. Inspection of the lung during collapse may reveal a focally elevated pleural surface. This finding may help the surgeon identify the location of the underlying lesion and guide clamp and staple gun placement. This observation may be especially useful in cases of small nonpalpable lesions.

Surgical collapse of peripheral lung leads to approximation of the alveolar walls, possibly providing the impression of increased cellularity and more extracellular matrix. This pitfall should not be confused with interstitial fibrosis⁸⁹. This artifact can be highlighted with immunohistochemical staining for CK (cytokeratin) (eg, CK 7) and endothelium markers (e.g., CD31), or with an elastic stain.

Peripheral lung collapse may give rise to 3 pitfalls in the diagnosis of adenocarcinoma. First, depending on the amount of diminished air, the collapsed alveoli may show a pseudopapillary pattern (Figure 1B). If the alveolar walls are covered with tumor cells (ie, lepidic pattern), this may be mistaken for a papillary carcinoma^{90, 14} (Figure 1C, D).



■ **Figure 1.** Images supporting the hypothesis of the collapse artifact.

A, Lower panel: lung resection specimen in vacuum transport cassette (diameter 5 cm); upper panel: 2 gross slices of collapsed lung. The width of each slice is approximately one-third the width of the thoracic cavity. B, Overview of collapsed peripheral lung tissue. C and D, Adenocarcinoma in situ in collapsed lung, mimicking papillary carcinoma (hematoxylin-eosin, original magnifications x2 [B], x5 [C, center], and x20 [D, periphery]).

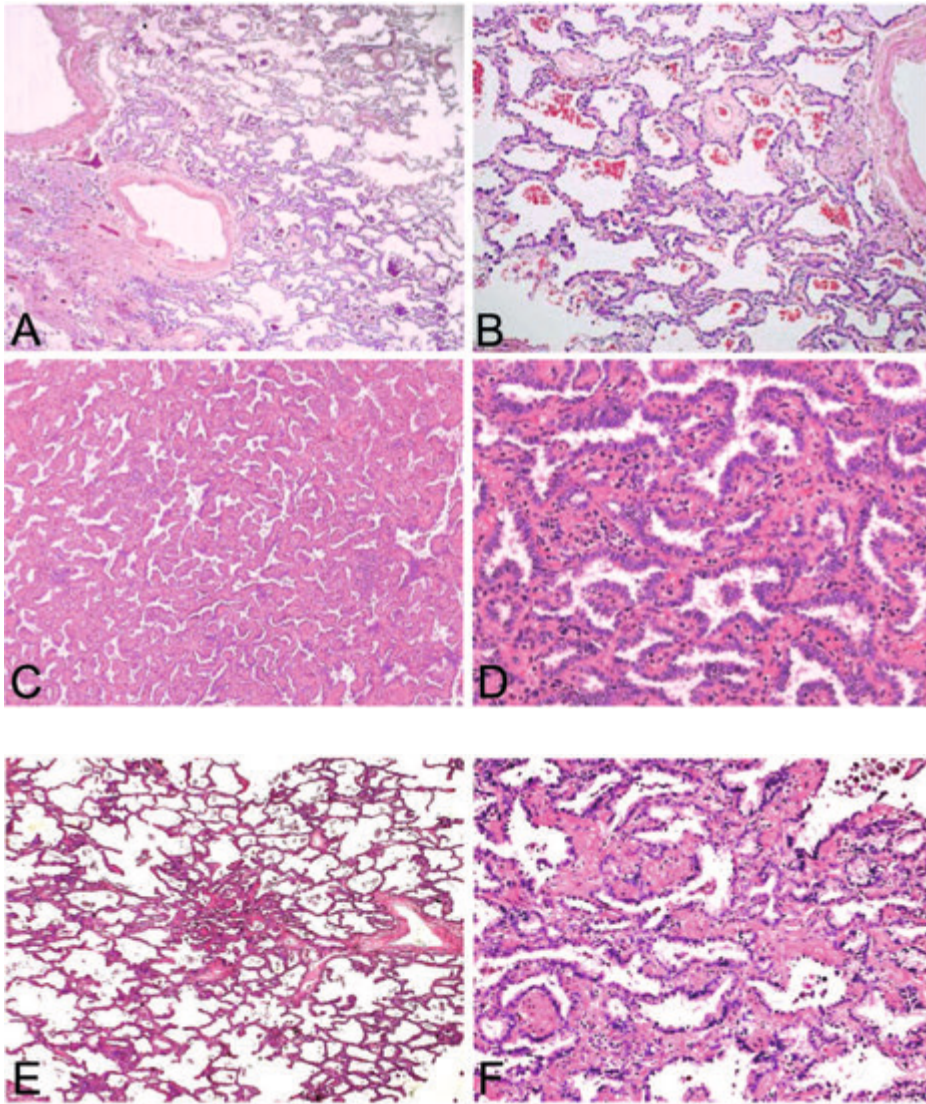
However, in 3 dimensions, these “papillae” are connected with other fragments above or beneath the plane of section, indicating that the stromal components of these “pseudopapillae” are actually the stromal components of preexisting alveolar walls.

The elastin stain is helpful in this instance, since the identification of elastin in these thin alveolar walls points to the underlying architecture of peripheral lung tissue⁹⁰. Conceptually, in statistical terms the probability of finding a straight papilla in a section of peripheral lung is low, probably as close as the probability of finding a completely straight hair in a histologic section of the skin. The probability of finding 15 papillae in 1 microscopic field of view is much smaller, providing an additional argument that the proliferation represents cross-sections of lepidic pattern as opposed to true papillae. In our opinion in case of thin “papillae” the presence of (frequently discontinuous) elastin fibers is diagnostic of lepidic pattern and supports in the distinction of a papillary carcinoma^{90, 6}.

A second pitfall may occur if preexisting fibrosis is present adjacent to lepidic patterns of adenocarcinoma. This fibrosis may be collagenous or of the infarction type with abundant fibroelastosis. Owing to the partial collapsed irregular alveolar walls, structures looking like irregular acini may mimic acinar adenocarcinoma, also seen in an earlier reproducibility study among 28 pathologists¹⁴ (Figure 2, A through F; images not published with this previous study).

This may introduce the possibility of an erroneous diagnosis of invasive adenocarcinoma adjacent to a fibrotic area¹⁴. Moreover, in lung cancer resection specimens with smoking-related lung disease, the stromal changes in remodeled lung should not be a priori attributed to lung cancer, leading one to consider any epithelial atypia as neoplastic. Preexisting scarring should be taken into account as well. Usually, this fibrosis consists of dense collagen fibers with scarce fibroblasts.

The third pitfall occurs in partial collapse giving an appearance of “tufting,” that is, the piling of the cells in airspaces without fibrovascular core formation. Sometimes this may give the impression of loose cells floating freely in alveolar spaces in close association with a lepidic growth pattern. As tufting is the morphologic hallmark of micro-papillary carcinoma, the occasional appearance of this pattern should not be diagnosed as micropapillary carcinoma. Although the minimal amount of micropapillae required for a diagnosis of papillary carcinoma is not established, practical considerations suggest that it should be extensive¹³.



■ **Figure 2.** An increase in surgical collapse parallels reduction in the amount of air, which is associated with greater doubt about presence or absence of invasion.

Note the irregular shape of the epithelial structures and lack of desmoplastic stroma. A and B, Example 1: 7% of the scores, invasion; 7%, doubt; 86%, no invasion. C and D, Example 2: 36% of the scores, invasion; 49%, doubt; 25%, no invasion. E and F, Example 3: 32% of the scores, invasion; 36%, doubt; 32%, no invasion.

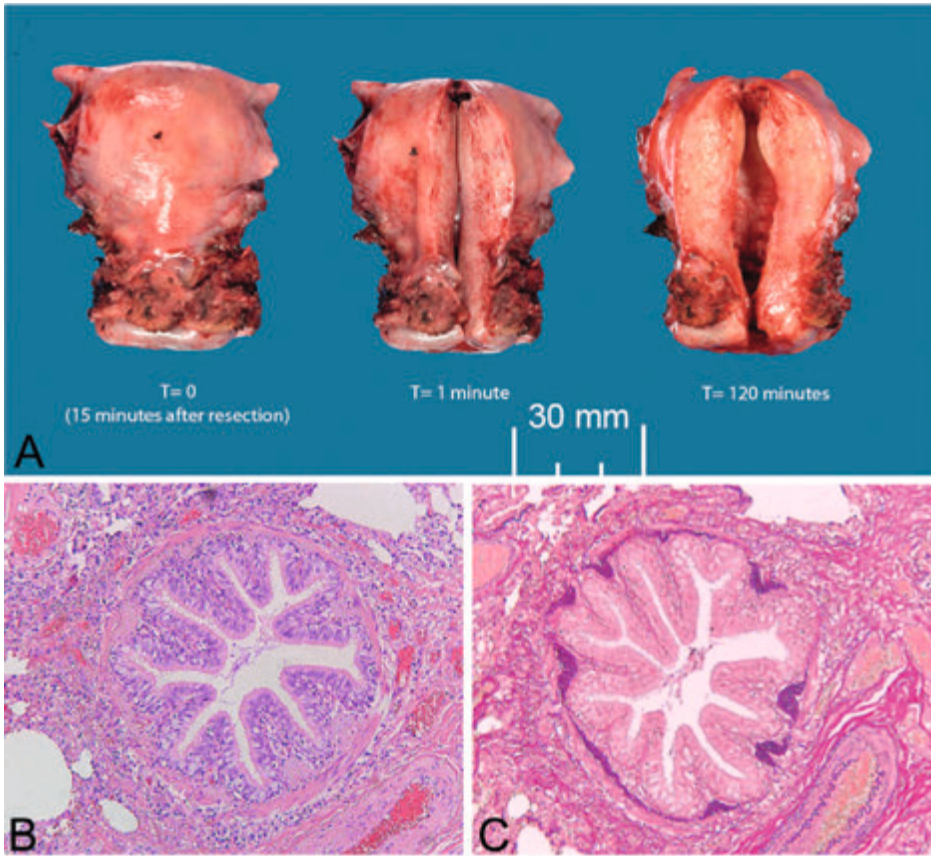
Note also the presence of alveolar macrophages in compressed alveolar lumen (hematoxylin-eosin, original magnifications x5 [A, C, and E; overview of case to reveal context]; and x20 [B, D and F; detailed image used for scoring¹⁴; images not published with previous study]).

Ex vivo smooth muscle contraction

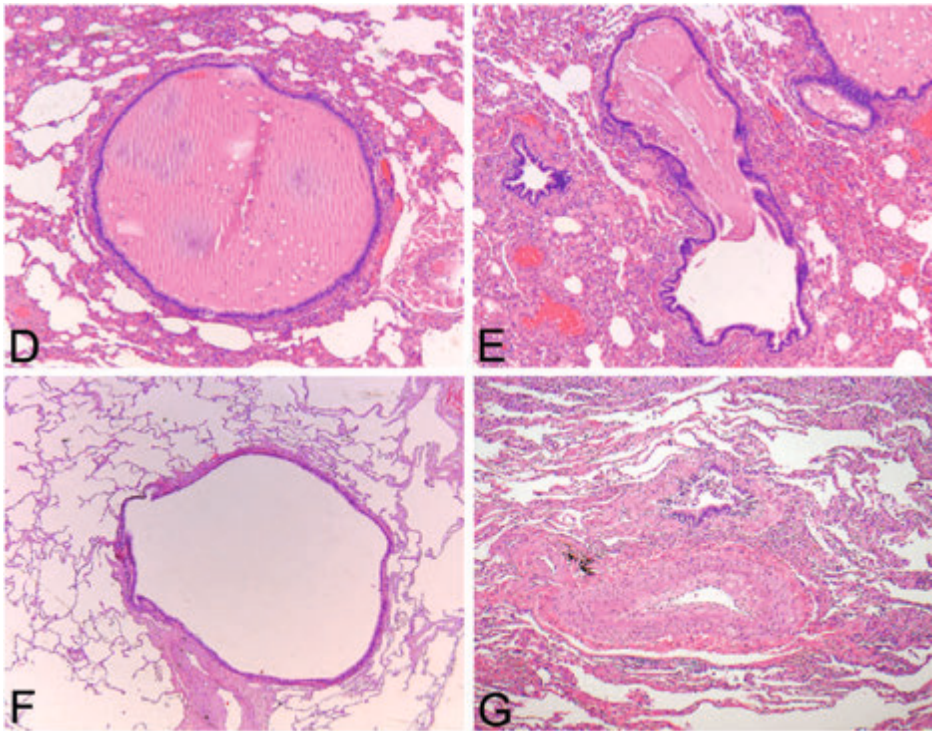
The collapse of peripheral lung tissue due to surgical atelectasis has additional morphologic consequences. While the bronchial lumens are essentially unaffected secondary to the presence of cartilaginous rings and plates, bronchiolar luminal patency is greatly affected. In vivo the bronchioles remain under physiologic conditions, expanded by the negative pressure between the parietal and visceral pleura. This “outward” force is transferred by the elastin meshwork between the visceral pleura, alveolar walls, and airways and results in circumferential traction to keep the bronchiolar lumens open. In vivo the actual bronchiolar diameter is a balance between the “outward” tension provided by the elastic fibers and “inward” contraction tension of the smooth muscle cells. At the end of expiration, a slightly lower lumen diameter is noted as compared to the end of inspiration. In the ex vivo situation the outward tension of elastin fibers is abolished, resulting in unopposed smooth muscle forces. Examples of ex vivo smooth muscle contraction are well appreciated in other organs such as uterus (Figure 3, A) and intestinal wall, where the muscle layers of the resected organs contract or shorten as compared to overlying mucosa (not shown). Smooth muscle contraction in the lung leads to a reduction in bronchiolar luminal diameter, with secondary infolding of the mucosa, including the basement membrane and elastin fibers (Figure 3, B and C). The outer diameter of the epithelium, that is, the circumference at the side of the basement membrane, should theoretically be unchanged. It is not clear whether the surface area of underlying connective tissue is unchanged. However, in the presence of a preexisting luminal mucous plug or fibromyxoid connective tissue polyp, the airway lumen is unchanged or only minimally narrowed (Figure 3, D and E). Thus, the bronchiolar epithelium will demonstrate only partial invaginations around the intraluminal material. The smooth muscle contraction was reversible by perfusion fixation (Figure 3, F).

The ex vivo bronchiolar smooth muscle contraction causes prominent narrowing of the bronchiolar lumen, which may give a false impression of constrictive bronchiolitis or other small airway diseases, including asthma⁹⁴⁻⁹⁷. This should not be called asthma because of a lack of goblet cell hyperplasia, eosinophilic granulocytes, and thickened basement membrane. In constrictive or obliterative bronchiolitis the airway has luminal narrowing due to subepithelial scarring (ie, between epithelium and smooth muscle cells, which are absent in the ex vivo contraction artifact)⁹⁷⁻¹⁰¹.

The smooth muscle cells in pulmonary blood vessels will also shrink. However, the architecture in the tunica media is different, as it is able to cope in the pulmonary artery with pressure changes between 4- and 30-mm Hg. Ex vivo during the collapse the pulmonary blood vessels will shrink in the longitudinal direction. In the cross-sectional direction the pulmonary artery will shrink ex vivo owing to the difference in structure, looking more like a rubber band without tension: there will be evidence of a (flexible) remaining lumen. This shrinking may be diminished by intimal fibrosis (Figure 3, G).



■ **Figure 3.** Images supporting the hypothesis of the contraction artifact



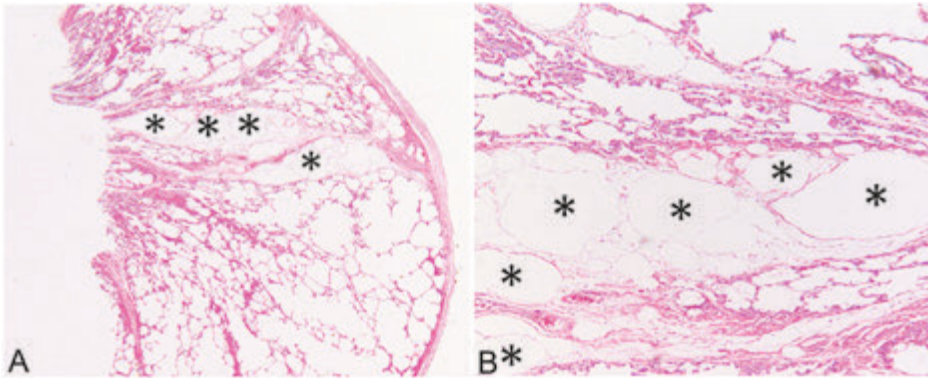
■ **Figure 3.** Images supporting the hypothesis of the contraction artifact (continued)

A, Uterus resection specimen before and after sagittal cut till cavum uteri. Note the difference in shape after 1 minute and 120 minutes at room temperature, owing to ex vivo smooth muscle contraction. B and C, Cross-section through bronchiole of collapsed lung resected for lung cancer, showing ex vivo smooth muscle contraction with folding of respiratory epithelium and underlying basement membrane and focal ex vivo aggregation of the elastin. Note that these histologic components are physiologic, except for occasional lymphocytes and surrounding edema. The pathologic diagnosis for this image may be mild chronic bronchiolitis. D and E, Images from 1 case with the same magnification of bronchioles with in vivo existing intraluminal mucus plug prohibiting the ex vivo smooth muscle contraction. Note in E also the contracted bronchiole (on the left side lumen without mucus). F, Image of another case where one part of the lobe is perfusion fixed; the nonperfused part had a similar appearance as the bronchiole left side in (E). Note that the smooth muscle contraction was reversible at the moment of perfusion fixation. G, Image from yet another case where artery and bronchiole were captured in 1 slide. Notice the difference in diameter. The intimal fibrosis prevents contraction of smooth muscle in the pulmonary artery, while the ex vivo contraction of the bronchiole remains unimpeded.

Image courtesy of Anja C. Roden, MD, Mayo Clinic, Rochester, Minnesota (original magnification x0.5 [A, see ruler in picture]; hematoxylin-eosin, original magnifications x10 [B], x5 [D and E], x2.5 [F], and x10 [G]; Elastica van Gieson, original magnification x10 [C]).

Clamping Edema

During lobectomies and pneumonectomies, lymph fluid in the lung drains into local and regional lymph nodes. However, during video-assisted thoracoscopic procedures the lymph vessels are not emptied before clamping. The staple gun compresses the lung tissue before adding the 2 rows of staples. This rapid compression squeezes the lymph in the lymph vessel columns both centrally and peripherally. The centrally directed lymph remains in vivo, but the peripherally pressed lymph dilates lymph vessels, leading to interstitial overflow. This is usually most prominent in segmental interstitium, as shown in Figure 4, A and B. This clamping artifact is only seen in video-assisted thoracoscopic specimens. One should not mistake this artifact for either septal edema or lymphatic dilatation⁸⁹.



■ **Figure 4.** Images supporting the hypothesis of the clamping artifact.

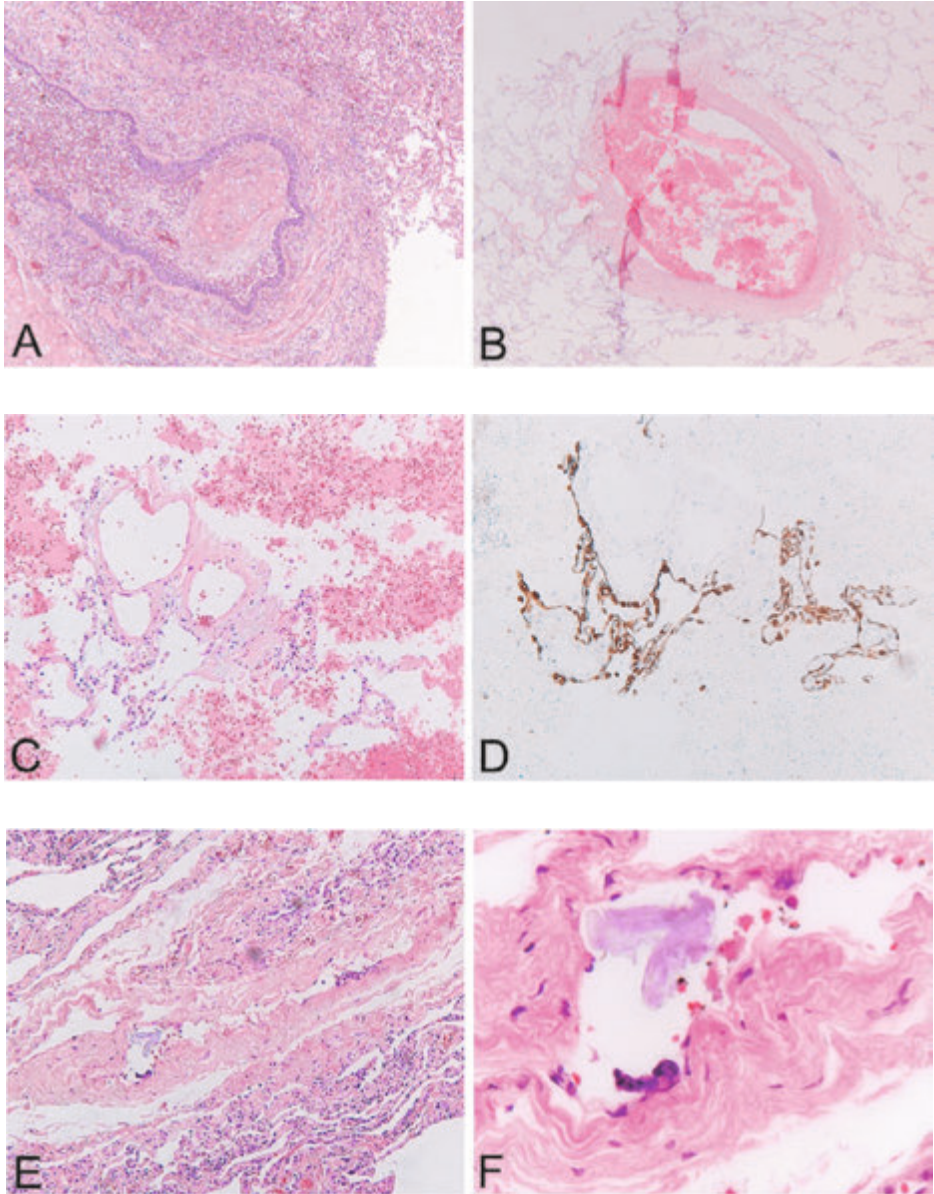
Spaces with asterisks (*) denote dilation by lymph fluid, which is most prominent in the septum and only minorly present in the pleura, emphasizing that the lymph vessels running toward the hilum are compressed during clamping (hematoxylin-eosin, original magnifications x1.25 [A] and x5 [B]).

Spreading Through a Knife Surface

An extraneous tissue contaminant on a slide is called a floater. This potential source of diagnostic confusion occurs in approximately 1.2% of prepared slides¹⁰². Floaters occur at the slide level in 73% and at the paraffin-block level in 16% of cases¹⁰³. Approximately half of these contaminations are derived from the same patient sample¹⁰³. When the origin of the tissue floater is uncertain, DNA analysis can be helpful^{104,105}. Although contamination may occur outside the pathology laboratory, it mainly happens inside the laboratory during gross handling, cutting, or slide processing^{102,106}. The location of the contamination may be from the specimen surface or from a cut surface¹⁰².

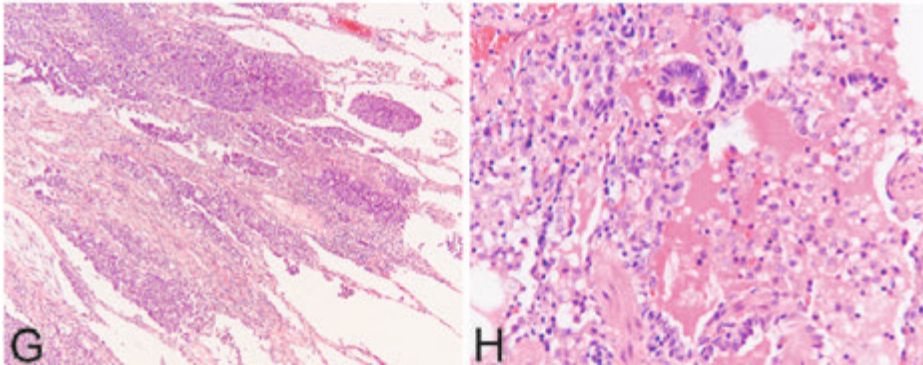
During lung resection specimen prosection, tumor cells may be displaced by the knife along the plane of sectioning: spreading through a knife surface (STAKS). The contaminants may either be displaced within the specimen or left on the surface of the tissue. Depending on the size of the loose tissue or cellular fragment, the floater

may end up in airways, blood vessels, alveolar ducts, or sacs. Microscopic examples of STAKS are shown in Figure 5, A through H. STAKS likely occurs during gross handling, as the lung contains many spaces, allowing displaced tumor fragments to settle distant from their origin.



5

■ **Figure 5.** Images supporting the hypothesis of STAKS artifact.



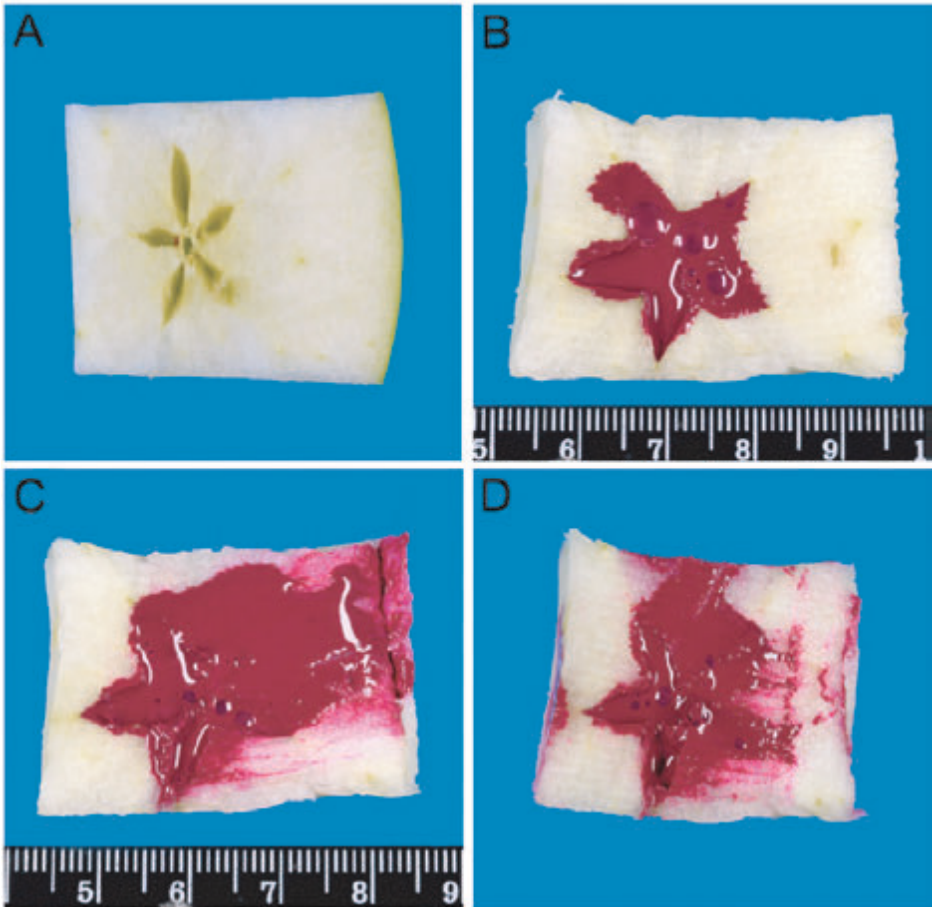
■ **Figure 5.** Images supporting the hypothesis of STAKS artifact. (continued)

A, Autopsy lung showing bronchiolus with intraluminal fragment of cartilage. B through D, Pulmonary artery with intraluminal fragment of peripheral lung tissue and erythrocytes. E and F, Largely collapsed pulmonary vein with intraluminal foreign body material. G, Lung resected for adenocarcinoma with focally loose intraalveolar parts. H, Open lung biopsy for interstitial lung disease with intraalveolar fragment of loose benign bronchiolar epithelium (hematoxylin-eosin, original magnifications x2.5 [A], x1.25 [B], x10 [C, E, and G], x40 [F], and x20 [H]; cytokeratin 7, original magnification x10 [D]).

An artificial model of an apple with ink clearly shows displaced ink in the direction of cutting (Figure 6, A through D).

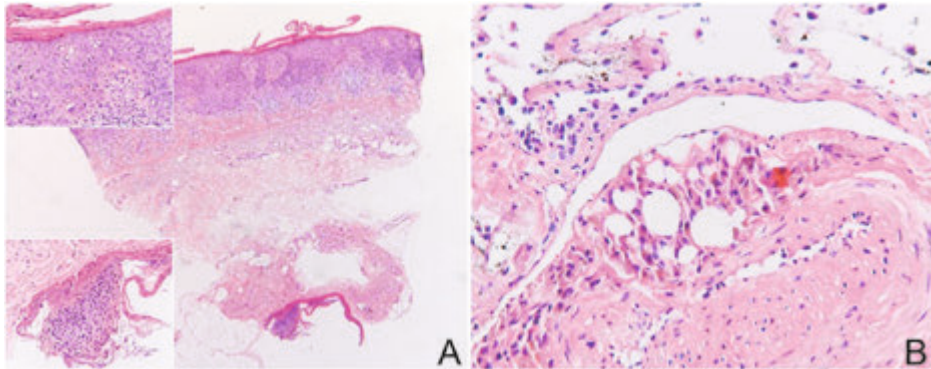
Since lung spaces are filled with paraffin during processing, the knife carryover within tissue holes is less likely to occur during microtome cutting, but may occur at the edge of the paraffin section (Figure 7, A). It is of paramount importance that the tissue floats are recognized as such and not considered separate foci of carcinoma in a lung tumor resection case. This may be challenging given the propensity for lung cancer cells to spread through vascular spaces or “presumed aerogenous spread.”

Possibly, at least a part of the STAKS effect can be avoided by quickly cleaning the knife blade after each slice with a wet sponge or tissue paper.



■ **Figure 6.** Trimmings apple model demonstrating displacement of ink during fresh cutting (original magnification x1.7 [A through D]).

A, Pits are removed from the core. B, Ink is filled in core. C, A section is cut with clean knife to the right side. D, Same knife is used for second cut in same direction (without cleaning between [C] and [D]). Note that in (D) ink is also present at the beginning of the slice (left side).



■ **Figure 7.** A, Section of skin biopsy showing part of surface displaced to deeper part of biopsy specimen. Insets show details of squamous cell carcinoma in situ. This displacement may have been caused by cutting on microtome. B, Pseudolipoid change present (central air bubbles after bronchial biopsy (hematoxylin-eosin, original magnifications x2.5 [A] and x20 [insets A, and B]).

Discussion

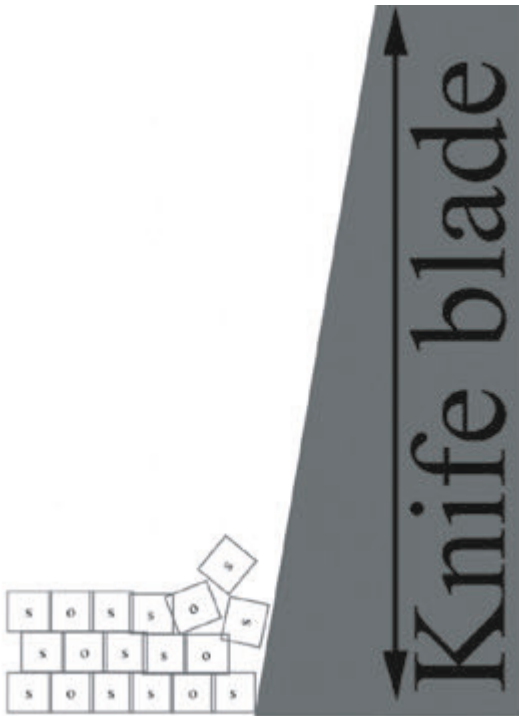
This study describes the effect of 4 patterns of ex vivo artifacts occurring in the lung. Three of the artifact patterns have to some extent been described before. Pseudolipoid change is another artifact representing air bubbles after bronchial biopsy as described before⁸⁹ (Figure 7, B). In the same textbook⁸⁹, crinkling and telescoping of epithelium are ascribed to airway compression. In our opinion these findings are a combination of the ex vivo artifacts “collapse” and “contraction.”

Recognizing “contraction” artifact may affect our perception of morphologic lung changes in asthma. Increased smooth muscle mass is consistently seen and a feature of airway remodeling; perhaps a degree of this is secondary to ex vivo artifact^{107,108}.

Intuitively, the morphology of contraction artifact is associated with functional airway obstruction. However, in most patients with folded bronchiolar epithelium there is no airway obstruction, except in airway-related diseases such as asthma and constrictive bronchiolitis, where other characteristics (increased luminal mucus, inflammation, thickened basement membrane, and/or fibrosis) explain the obstruction. The question arises as to what extent this artifact has been taken into account in previous studies measuring basement membrane thickness¹⁰⁹. In many asthma studies smooth muscle area is measured relative to basement membrane length, giving reproducible results for larger airways (but not always for smaller airways with perimeter of basement membrane, 4 mm)¹¹⁰. The contraction artifact is specifically present at the bronchiolar level, possibly being another confounder in this study, beside variation between centers in inflation procedures, presence or absence of mucus in bronchiolar lumen, selection differences in airway sizes, and differences in calibration of

measurement instruments. In a reproducibility study on the morphologic interpretation of transbronchial lung biopsies, the observer agreement was low for bronchiolitis obliterans¹¹¹. Perhaps the contraction effect played a role here too.

Artifactual knife carryover is a well-recognized phenomenon. In fact, sometimes entire strips of mucosa are displaced into bronchiolar and alveolar spaces⁸⁹. Interestingly, the 2015 World Health Organization classification of lung adenocarcinoma describes a pattern of lung cancer “spreading through the airways” (STAS)¹¹². This STAS-like pattern had also been described previously under different names¹¹³⁻¹¹⁶. Subsequently, the association of STAS and poor prognosis has been reported for larger studies¹¹⁷¹¹⁸. Warth and colleagues¹¹⁸ reported that the presence of STAS was tightly linked to specific growth patterns. In resected surgical specimens, STAS has been associated with reduced overall and disease-free survival, which was growth pattern, but not stage, independent. The study of Kadota and colleagues¹¹⁷ reports a higher risk of recurrence in patients with STAS-positive tumors than in patients with STAS-negative tumors in a limited resection group. In contrast to the study of Warth and colleagues¹¹⁸, in the lobectomy group the presence of STAS was not associated with recurrence. In STAS the underlying biologic assumption is that in an adenocarcinoma with a micropapillary, acinar, or solid component with dissociated tumor cells, tumor fragments can spread aerogenously well beyond the mass lesion and endanger the prospect of a complete resection if less than a lobectomy is performed¹¹². The STAS explanation for association between STAS and histologic patterns with poor prognosis lies in the fact that tumor cells have a tendency for dissociation. In the micropapillary pattern, the seemingly loose alveolar cells (partly dissociated tumor cells) in one section are connected to other tumor cells or to the basement membrane in the section above or below, but they are disconnected in another plane of sectioning. Moreover, the big (shovel-like) force applied during gross cutting (see Figure 8 for relative sizes) disconnects the cells or clusters of cells with a tendency to dissociate from their fixed connection, freeing them and allowing displacement, similar to the apple/ink phenomenon shown in Figure 6.



■ **Figure 8.** The relative size of epithelial tumor cells (SOS), compared to thickness of the knife blade used for cutting.

In our opinion, the reported frequency of STAS in roughly half of all resected adenocarcinomas is an indication of the frequency of STAKS. STAKS is a frequent finding in the lung, not only in adenocarcinomas but also in squamous cell carcinomas and benign lung tissue. Further validation and consideration of STAS for implementation in routine diagnostic evaluation and reporting¹¹⁸, or recognizing it as a pattern of invasion in lung adenocarcinoma¹¹⁷, is not appropriate for an artifact (STAKS). The prognostic association of STAS is in line with that of more than 100 other prognostic factors associated with poorly differentiated lung adenocarcinoma, which are not used in routine diagnostic reporting. Moreover, the radiation oncologist defines radiotherapy target volumes on the basis of microscopic tumor extent^{114 119}. In this context the STAKS pattern is likely to be a confounder, and we suggest that the target area for radiotherapy in lung cancer should not be based on displaced tumor cells during gross examination.

Diaz and colleagues¹¹⁹ described the displacement of tumor cells in breast samples. Tumor cell displacement was observed in 32% of patients who had undergone large-gauge needle core biopsies. Remarkably, the incidence and amount of tumor displacement was inversely related to the time interval between core biopsy and excision. The authors suggested that tumor cells do not survive displacement. The wall

thickness of a gauge steel needle is approximately 0.2 mm. The size of the displaced cells, as reported in the article by Diaz et al¹⁹, is smaller than the wall thickness of the needle. The thickness of the gross knife may vary, but ranges from 0.4 to 1 mm, which is 20 to 50 times larger than normal epithelial cells (see Figure 8), implying a tremendous force. In the context of breast fine-needle aspirate cytology, the force applied during smearing of the aspirate may cause separation of tumor cells from the main epithelial cluster. This loss of cohesion, also called "dissociation," is used as a feature of malignancy.

In summary, the 4 patterns of ex vivo artifacts are important to recognize so as not to compromise morphologic diagnostic accuracy.



6

A prospective study of loose tissue fragments in non-small cell lung cancer resection specimen. An alternative view to “spread through air spaces”

Hans Blaauwgeers, Douglas Flieder, Arne Warth,
Alexander Harms, Kim Monkhorst,
Birgit-Lissenberg-Witte, Erik Thunnissen

American Journal of Surgical Pathology 2017;41:1226-1230
doi: 10.1097/PAS.0000000000000889

Abstract

Introduction

The World Health Organization Classification of Lung Tumors considers “Spread Through Air Spaces” a form of invasion in lung adenocarcinoma. The recently described spread of free-floating cell clusters during lung specimen sectioning, otherwise known as “Spread Through A Knife Surface,” represents an *ex vivo* artifact.

Purpose

To prospectively investigate the presence and frequency of these free-floating tumor cell clusters in surgically resected lung cancer specimens and their possible relation to gross examination procedures. A prospective, multi-institutional study of non-small cell lung cancer resection specimen was undertaken. At prosection the first cut was made with a clean knife; the second cut was made in a parallel plane to the first. Four tissue blocks were taken from upper and lower parts of first and second cuts. Hematoxylin and eosin-stained slides were examined for displaced benign and/or malignant tissue fragments.

Results

Forty-four resection specimens were studied. The mean number of tumor clusters for blocks 1 to 4 was 0.36, 1.44, 1.86, and 1.95, respectively, and for benign fragments was 0.11, 0.11, 0.13, and 0.25, respectively. Almost all cell clusters were intra-alveolar. Comparison of tumor cell clusters in block 1 with blocks 2 to 4 was significant with *P*-values (Friedman test for repeated measures 0.03) 0.031, 0.02, and 0.05, respectively. Overall, 93% of the loose tissue fragments could be explained by mechanical forces associated with tissue handling.

Conclusion

While the 2015 World Health Organization Classification of Lung Tumors recognizes Spread Through Air Spaces as a form of lung cancer invasion, such is debatable and, in many instances, likely represents mechanical artifact, including dissemination along the prosecting knife blade.

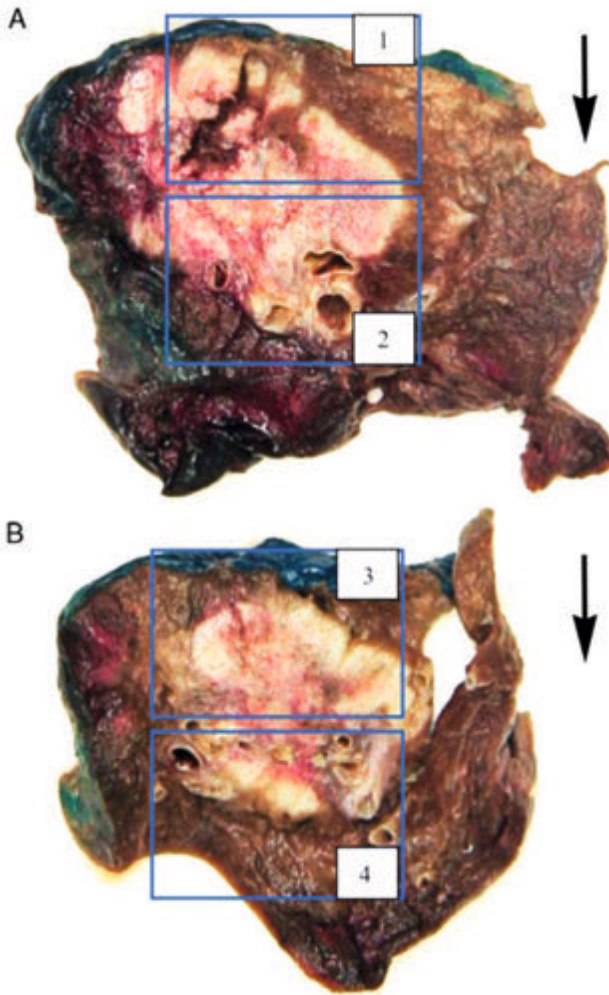
Introduction

The 2015 World Health Organization (WHO) Classification of Lung Tumors considers “Spread Through Air Spaces (STAS)”¹¹² a form of invasion in lung carcinoma. It is defined as “spread of lung cancer cells into air spaces in the lung parenchyma beyond the edge of the main tumor.” The same morphologic finding was recently described as an artifact, namely the spread of loose tissue fragments attributed to lung specimen sectioning, and designated “Spreading Through A Knife Surface” (STAKS)¹²⁰. Although this distinction has significant clinical importance regarding adequacy of resection and risk of local recurrence, this issue has only been addressed in retrospective studies.

“STAKS” is considered an artifact secondary to one of the mechanical forces at play during specimen handling. A typical prosecting knife or scalpel blade is up to 30 times wider than a human cell, leading to carry over of cells along the knife’s path. This hypothesis implies that the direction of cutting influences the number of free- floating tumor cells. Conceptually, a tissue block taken from a sample before tumor is reached should contain no or fewer loose tumor tissue fragments than a tissue block where the knife has already passed through the tumor. Generally, the information about cutting direction together with annotation of the tissue blocks is not included in pathology reports. Thus, retrospective studies cannot be used to prove or reject the hypothesis that these loose cell clusters are the result of mechanical forces and more importantly, artifactual. Furthermore, if this hypothesis holds, then it should occur in any pathology laboratory. To this end, we undertook a prospective multi-institutional study on lung resection specimens with systematic recording of cutting direction and tissue block annotation. Subsequently, the histologic sections were examined for the presence and frequency of loose tissue fragments.

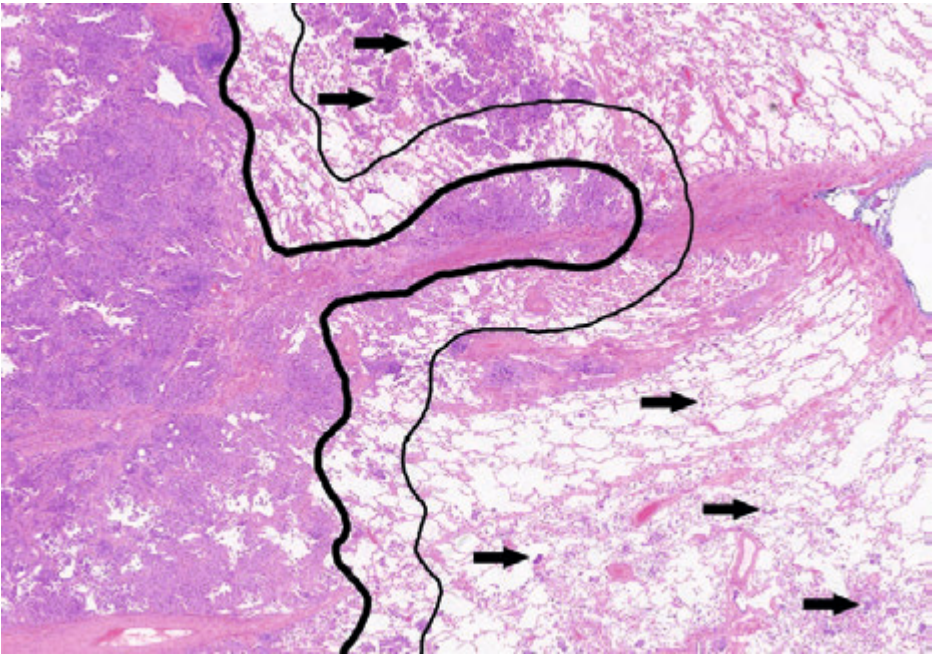
Materials and methods

A prospective, multi-institutional study of non-small cell lung cancer (NSCLC) lobectomy and pneumonectomy resection specimens was performed from January 1 through July 1, 2016. Prosection, sampling, and scoring of displaced fragments was undertaken in a systematic manner. For prosection the specimen was either cut in a fresh unfixed state, or after formalin perfusion fixation. The first cut was made with a clean long knife; the second cut was made in a parallel plane to the first cut, *without* cleaning the knife. These 2 pieces were each divided into 2 sections *without cleaning the knife* such that 4 formalin-fixed paraffin-embedded tissue blocks were procured. Block 1 was the upper part of the first cut containing normal lung tissue and then tumor tissue; block 2: the lower part of the first cut, containing first tumor tissue and then normal lung tissue; block 3: the upper part of the second cut, identical to block 1; block 4: the lower part of the second cut, similar to block 2 (Fig. 1).



■ **Figure 1.** Surface of cross-section from lobectomy resection specimen after the first (after overnight fixation) cut (slice A) and second cut (slice B); arrows indicate cutting direction. In rectangle tissue sampled with peripheral lung tissue above tumor (blocks 1 and 3) and below tumor (blocks 2 and 4).

A superficial complete hematoxylin and eosin-stained slide from each tissue block was examined for the presence of loose tissue fragments at x10 or x20 magnification. Loose benign or malignant tissue, also called displaced fragment, was scored if the fragment was at least 0.5 mm (approximately one field of view of a x40 microscope objective) from the tumor (Fig. 2) or if it was on the pleura surface in the plane of the second cut.



- **Figure 2.** Tissue section showing AdC on the left side. The tumor border is marked with thick black line. Loose fragments at a distance more than 1 high power field (0.5mm) from the tumor border (thin black line) are scored as loose fragments (arrows; hematoxylin and eosin staining, eg, block 3 of Fig. 1).

Benign and malignant loose fragments were separately noted. All loose fragments in one field of view in x10 objective count as one occurrence, independent of the actual number of loose fragments in that microscopic field. The total count of loose fragments in each block was estimated by counting all positive x10 objective fields.

Statistics

The total count of loose fragments in each block was compared by the Friedman test for repeated measures because of non-normality of the number of loose fragments. Post hoc analysis, comparing blocks 2 to 4 with block 1 separately, was performed with the Wilcoxon signed rank test and corrected for multiple testing by the Bonferroni correction. Differences between groups in number of loose fragments between different blocks were compared using the Mann-Whitney *U* test. Statistical analyses were carried out by SPSS for Windows and Mac version 18.0. (IBM, New York, NY).

Results

Clinicopathologic Characteristics

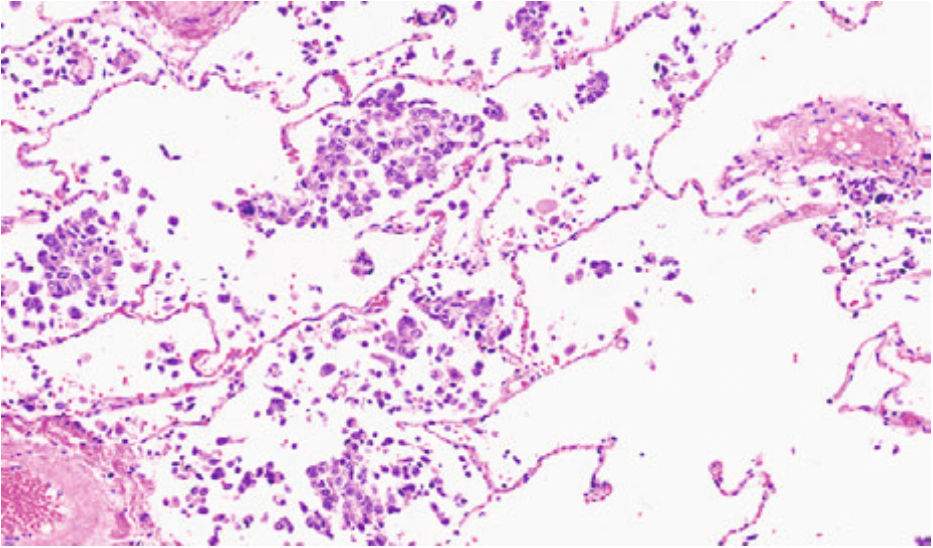
Forty-four resection specimens were included in this study. Twenty-six patients (59%) were male and 18 female (41%). The mean age of the patients was 65.7 (range: 45 to 85 y). Sixteen patients underwent a surgical lobectomy, of which 11 were freshly cut and 5 after formalin fixation; there were 21 video-assisted thoracoscopic surgery (VATS) lobectomy procedures, 6 freshly cut and 15 after formalin fixation; 3 pneumonectomies, 2 freshly cut and 1 after formalin fixation; and 4 segmentectomies, 3 freshly cut and 1 after formalin fixation. Forty-three cases consisted of primary lung carcinomas; 26 adenocarcinomas (AdC), 13 squamous cell carcinomas (SqCC), 2 large cell carcinomas, and 2 large cell neuroendocrine carcinomas. The remaining case was a segmentectomy with metastatic colonic AdC. AdC subtyping according to the WHO classification of lung tumors yielded 14 acinar predominant, 4 micropapillary predominant, 3 solid predominant, 2 lepidic predominant, 1 papillary predominant, as well as 1 invasive mucinous AdC and 1 AdC in situ. Six cases had a pure growth pattern; acinar in 2, solid in 2, mucinous in 1 and AdC in situ in 1. The other 20 cases had a secondary growth pattern; acinar in 6, micropapillary in 5, solid in 4, lepidic in 3, papillary in 2. Twelve of the 26 AdC had at least minor micropapillary patterns.

Loose Tissue Fragments

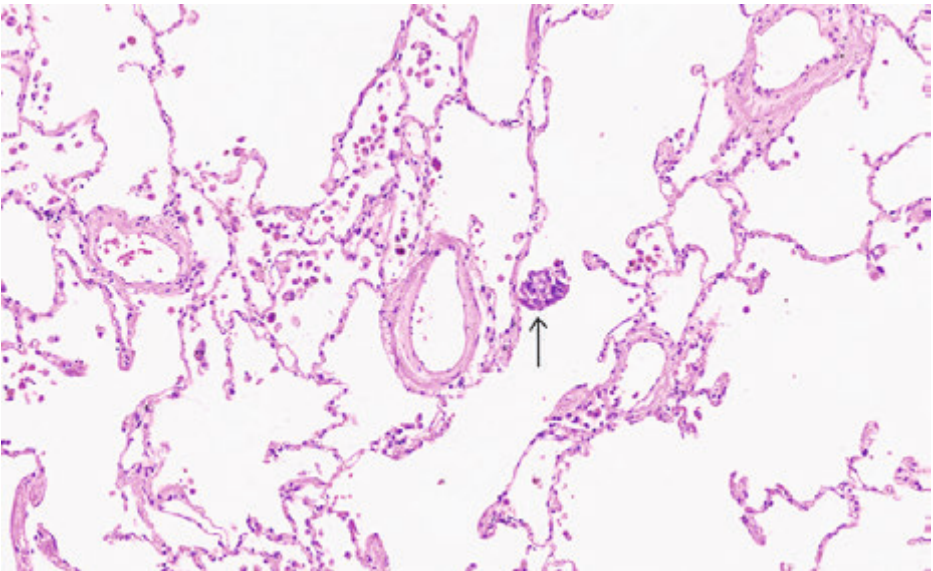
Loose tissue fragments were detected in at least one tissue block in 32 of the 44 cases (73%) with an even distribution with regard to the participating institutions. Displaced clusters of malignant cells (malignant loose fragments) were identified in 31 of those 32 cases; 244 x10 fields with malignant loose fragments were identified in the 176 histologic sections. Twenty-seven fields with displaced benign tissue fragments (benign loose fragments) were also identified in the 176 histologic sections.

Histologic Localization of Loose Fragments

In 30 of the 31 cases with malignant loose fragments, the histologic localization was intra-alveolar (Fig. 3). In the remaining case the loose fragments were on the pleural surface. Intravascular (n = 3), pleural (n = 2), and/or luminal intrabronchial (n = 1) malignant loose fragments were also noted in the 31 cases with intra-alveolar lesions. All benign loose fragments were intra-alveolar and consisted of respiratory (bronchiolar) epithelium (Fig. 4).



■ **Figure 3.** Example of multiple intra-alveolar loose fragments spread in clusters and individual tumor cells (hematoxylin and eosin staining).



■ **Figure 4.** Example of intra-alveolar loose benign fragment (arrow, ciliated cells, goblet cell; hematoxylin and eosin staining).

Distribution of Loose Fragments in Relation to Cutting Order

Five cases with malignant loose fragments were found in block 1, 18 cases in block 2, 19 cases in block 3, and 17 cases in block 4. The total number of fields with malignant loose fragments in all blocks was 244; in the blocks 1 to 4 was 16, 62, 82, and 84, respectively. Thus 93% of the malignant loose fragments were present in the blocks 2 to 4 (228/244). The mean number of malignant loose fragments for blocks 1 through 4 was 0.36, 1.44, 1.86, and 1.95, respectively. For benign loose fragments the mean number for blocks 1 through 4 was 0.11, 0.11, 0.13, and 0.25, respectively; with absolute numbers 5, 5, 6, and 11, respectively.

The number of fields with malignant loose fragments differed significantly between the blocks ($P = 0.003$). Post hoc comparisons revealed significant differences between block 1 (first cut) and blocks 3 and 4 (second cut) ($P = 0.006$ and 0.015 , respectively, after Bonferroni correction) but not between blocks 1 and 2 (deeper cut) ($P = 0.093$, after Bonferroni correction).

The number of malignant loose fragments was higher when the specimen was cut fresh in comparison with specimens cut after formalin fixation, and also significant when comparing loose fragments numbers in blocks 1 versus 3 ($P = 0.042$), but not for the blocks 1 versus 2 ($P = 0.37$) or blocks 1 versus 4 ($P = 0.79$). For benign loose fragments no significant difference was identified between the 4 blocks ($P = 0.23$). The association of loose fragments with the clinicopathologic parameters revealed a statistically significant greater number of loose fragments between blocks 1 and 4 in AdC compared with SqCC ($P = 0.028$), but not between block 1 and blocks 2 and 3 ($P = 0.24$ and 0.32 , respectively). Of the 12 cases without loose fragments, 6 were AdC (24% of the AdC cases) and 6 were SqCC (46% of the SqCC cases), but these differences were not significant ($P = 0.16$). Regarding the 26 AdC, the number of loose fragments in the 4 micropapillary predominant carcinomas was statistically significant higher from the other AdC cases between blocks 1 and 2 ($P = 0.016$). No differences were seen when the 5 cases with a secondary micropapillary component or the 12 cases with any micropapillary component were compared with the other AdC. A statistically significant difference was not seen with regard to surgical specimen type, including VATS versus thoracotomy resection when comparing block 1 with blocks 2 to 4 ($P = 0.78$, 0.056 , and 0.61). Age, sex and tumor diameter were also statistically insignificant.

Discussion

Surgical pathologists are familiar with the phenomenon of tissue floaters, not only as extraneous tissue fragments sitting on top of tissue, but also as “loose” fragments of tissue elsewhere on the slide. These pieces of tissue may originate from grossing tables, prosecting instruments, water baths, microtome blades, or tissue stainers. We were not concerned with tissue floaters of these sorts, but rather detached fragments of malignant or benign cells originating from the lung specimen. Dis- placed tumor cells

are found in many malignancies. For example, tumor cell displacement is seen in up to one third of breast cancer core biopsies^{119, 121}.

This prospective study proved that the presence of loose fragments is an inducible and reproducible phenomenon in lung cancer specimens. Tumor islands or loose tumor cells, fitting the criteria of STAKS were identified in 73% of the cases and 93% of these malignant loose fragments can be attributed to mechanical artifacts related to surgical resection and gross room specimen processing. Furthermore, benign loose fragments within alveolar spaces were also found in 61% of the cases.

It is likely that intrapulmonary spread of benign and malignant fragments is due to mechanical forces imposed on the tissue during surgery and/or specimen prosection. As lung tissue largely consists of empty spaces, that is air spaces, there are many opportunities to “trap” displaced tissue fragments. Such explains the relative low frequency of intravascular and intrabronchial as compared with intra-alveolar fragments.

Tumor cell dissociation is a recognized characteristic in malignancy related to adhesion molecule expression^{122 123 124 125 126}. There was a tendency for more loose fragments when comparing all AdC to SqCC and comparing the AdC with a predominant micropapillary growth pattern to the other types of AdC. In addition, there were also more SqCC cases without loose fragments than AdC cases. One could suggest that SqCC are more cohesive than AdC, and that the AdC micropapillary subtype is the most discohesive AdC subtype.

Interestingly, circulating tumor cells are detected in patients after undergoing lung resection, some of which are likely dislodged by the surgical procedure^{127 128}. Although we assume lung is handled “rougher” during VATS operations, where collapsed lung is removed through a small hole in the thoracic wall, our data did not demonstrate different incidences of loose fragments in the different procedure groups. Nevertheless, part of the 7% loose fragments in block 1 may be explained by intra- operative manipulations or other mechanical forces during specimen handling.

Three cases featured intravascular tumor fragments, but were not considered true angioinvasion. Artfactual presence of loose fragments in a vascular lumen mimics vascular invasion. Perhaps pathologists’ inability to discern artfactual vascular tumor from true angiolymphatic invasion muddies our ability to definitively comment on the prognostic significance of lymphovascular invasion in lung and other cancers^{129 130 131}. Morphologic clues favoring artfactual presence of loose fragments over true vascular invasion are single fragments without erythrocytes in an otherwise “empty” vascular lumen. Alternatively, clues favoring true vascular invasion are (i) tumor fragments with fibrin and or erythrocytes in the vascular lumen or (ii) multiple tumor fragments in dilated lymph vessels surrounded by clear lymph with or without occasional lymphocytes.

STAS has diagnostic criteria. The morphologic criteria for STAS are (i) micropapillary structures including ring-like structures compatible with the WHO micro- papillary pattern; (ii) solid nests or “tumor islands” consisting of solid collections of tumor cells

filling air spaces; and (iii) discohesive single cells in alveolar spaces¹¹⁷. The latter 2 criteria are not different from our findings in this prospective study, and interestingly, the frequency reported for STAS is similar to the frequency of loose tissue fragments reported in this study.

The concept of STAS as a specific pattern of invasion was added to the 2015 WHO Classification of Lung Tumors¹¹² and published with only one supporting reference (listed as “Forthcoming” in the WHO bibliography). Three-dimensional reconstruction studies demonstrating tumor islands connected to one another and with the index tumor at multiple points provides additional support. These observations suggest that tumor islands represent tumor extension through air spaces^{132 133}. While some of our 7% loose fragments in block 1 may be explained by this 3-dimensional growth, the presence of benign loose fragments, that is, normal respiratory epithelium detached from its origin in these tissue blocks, argues against this possibility and instead supports the hypothesis that this finding is artifactual. Furthermore, STAS has recently been reported in SqCC¹³³. Three-dimensional growth within alveolar spaces is a difficult concept to imagine given the nature of this tumor cell type.

“STAS” reportedly has prognostic significance and correlates with aggressive tumor behavior and poor prognosis^{115 118 114 116 134}, especially in sublobar resections¹¹⁷. However, one could argue that STAS-like artifact is simply seen in more discohesive tumors, that is more poorly differentiated tumors with fewer intercellular adhesions, such as micropapillary AdC, and this quality is responsible for the worse prognosis observed in these tumors. The presence of STAS in SqCC is also associated with poorly differentiated features such as necrosis, nuclear diameter and Ki67 labeling index¹³³. If so, then STAS is simply an epiphenomenon with a biologic explanation rather than true tumor invasion. In addition, in our study there was no apparent increase of benign loose fragments in blocks 2 to 4, in line with the more cohesive nature of benign epithelial cells.

Thus, it may be premature to recognize STAS as a morphologic pattern of lung cancer invasion. The concept of tumor invasion and lung carcinoma staging is already very complex, given the recent decision to reclassify lepidic-pattern AdC as AdC in situ, and add a superficially studied minimally invasive AdC to the morphologic classification. Our data suggests that STAS likely, in many instances, represents mechanical artifacts including knife spread during specimen prosection (STAKS).

Our study has several limitations. Although it had a detailed protocol for tissue processing, the size of the tissue sample and proportion of tumor was not constant in the different formalin-fixed paraffin-embedded blocks. This may have led to differences in amounts of normal lung tissue between the samples and therefore theoretically to a different number of detected artifactual lesions. Second, this study has no follow-up data, which precludes statistical analysis with regard to the possible prognostic relevance of the artifact vis-à-vis STAS. Lastly, this study was limited in that the AdC were mainly non-mucinous tumors. We offer no data or opinion on mucinous lung AdC and scattered detached tumor fragments.

In conclusion, this prospective study documents that the presence of loose tissue fragments is often a reproducible artifact secondary to mechanical forces caused by specimen handling and grossing, and that it manifests with greater numbers of malignant tumor clusters than benign fragments. These findings call into question the recent definition of STAS as a type of lung cancer invasion.



7

Pulmonary loose tumor tissue fragments and spread through air spaces (STAS): invasive pattern or artifact? A critical review.

Hans Blaauwgeers, Prudence Russell, Kirk Jones,
Teodora Radonic, Erik Thunnissen

Lung Cancer 2018, 123: 107-111
doi.org/10.1016/j.lungcan.2018.07.017

Abstract

The concept of tumor cell clusters or loose cells as a pattern of invasion in lung carcinoma has recently been proposed and is included in the 2015 WHO fascicle on the classification of lung tumors, so-called “spread through air spaces” or STAS. This inclusion is controversial, as there are significant data to support that this histologic finding represents an artifact of tissue handling and processing rather than a pattern of invasion.

These data are summarized in this review and support the conclusion that the inclusion of STAS in the WHO classification for lung cancer as a pattern of invasion was premature and erroneous. In our opinion, these tumor cell clusters or loose cells appear to be simply an artifact, although one which may or may not pinpoint to a high-grade tumor with discohesive cells and adverse prognosis.

Introduction

The concept of tumor cell clusters or loose cells as a pattern of invasion in lung carcinoma has recently been proposed and is included in the 2015 WHO fascicle on the classification of lung tumors, so-called ‘spread through air spaces’ or STAS⁴. This inclusion is controversial, as there are significant data to support that this histologic finding represents an artifact of tissue handling and processing rather than a pattern of invasion.

An extraneous tissue contaminant on a histologic slide is a very well-known phenomenon for pathologists and is called a floater. This can be a source of potential diagnostic error and occurs in approximately 1.2% of prepared slides¹⁰². Since at least half of these contaminants are not derived from the same patient sample¹⁰³, many of them are recognized as artifacts on morphological grounds alone. Moreover, in patients’ samples many of these contaminants are easily recognized as irrelevant, most likely produced by the biopsy procedure passing through other tissues, for instance when fragments of colonic mucosa are seen in prostate biopsies or fragments of skin are present in breast biopsies. In addition, many of these aberrant tissue fragments lie on top of the tissue to be examined, above the tissue plane of the slide, and therefore are also easily recognizable as an artifact.

“Displacement of tumor cell clusters or loose cells” in organs other than the lung have been described in the colon¹³⁵, uterus^{136,137}, and thyroid¹³⁸. In these cases, the tumor is occasionally displaced into vascular structures during biopsy procedures, surgical manipulation, or pathologic gross processing.

We question the validity of the inclusion of the presence of tumor cell clusters or loose cells as an invasive pattern in lung cancer.

In this review, we will submit the data on tumor cell clusters or loose cells in the lung and will examine whether this histologic finding should be considered an invasive pattern, a useful prognostic artifact, or simply an artifact.

The road of tumor cell clusters or loose cells to STAS

Loose tumor cell clusters or loose cells in the lung have been recognized by pathologists for a long time and have been interpreted by many as an artifact. The first study adding importance to the phenomenon of ‘tumor cell clusters or loose cells’ was that by Onozato and colleagues¹¹⁵ in 2013, adding a prognostic relevance to loose fragments. Prior to this however, in the 1990’s the concept of aerogenic spread of what was previously called bronchioloalveolar carcinoma already existed¹³⁹. While this concept uses the term ‘aerogenic spread’, an alternative explanation, in which field cancerization may be a major factor, is not excluded¹⁴⁰.

In a preparatory meeting in which issues relating to the prospective 2015 WHO classification of lung tumors were being discussed, eight of the 16 pathologists (50%) were in favor of STAS as a pattern of tumor invasion in lung adenocarcinoma, while the other half reflected that it was most likely an artifact. However, the majority of the other

experts present (e.g. pulmonologists, oncologists, radiologists, surgeons) supported the proposal as a histologic pattern of tumor invasion, although they considered that it was not sufficiently mature to enter into the WHO classification. Nevertheless, in the final version of the 2015 WHO classification of Lung Tumors, STAS has been described as a new form of invasion in the lung, namely invasion through alveolar spaces, with the concept said to be validated by two large cohorts^{117,118}. The first cohort consisted of a series of 411 Stage I adenocarcinomas in which tumor cell clusters or loose cells, called STAS, were seen usually in the first alveolar layers close to the tumor border, but also in a few dozen alveolar spaces further away. This phenomenon was associated with lymphovascular invasion and high-grade histological pattern. However, it was not significantly associated with local recurrence in the lobectomy group but was a prognosticator for any recurrence in the limited resection group¹¹⁷. In the second cohort which comprised a series of 569 Stages I-IV adenocarcinomas, STAS was associated with lymph node and distant metastasis as well as with tumor stage and high-grade histological pattern. These authors were not able to examine the effect of STAS on recurrence in patients with limited resection, as there were too few cases of sublobar resections included in their series¹¹⁸. Since then several other studies^{134,141-146} and various editorials¹⁴⁷⁻¹⁴⁹ and reviews¹⁵⁰⁻¹⁵² have supported the concept of STAS in pulmonary adenocarcinomas and more recently also in squamous cell carcinoma^{133,153}.

In the 2015 WHO Classification of Lung Tumors fascicle, STAS is defined as “spread of micropapillary clusters, solid nests, or single cancer cells into air spaces in the lung parenchyma beyond the edge of the main tumor”¹⁴. The exact distance from the main tumor is not defined. In the different studies investigating STAS, the distance from the main tumor varies, as do the criteria used to define STAS (see Table 1).

■ **Table 1.** The definitions of STAS and distance from the main tumor are shown as reported in the published studies.

Study / year	Criteria of STAS	Defined distance from main tumor
Onozato et al. 2013 ¹¹⁵	Isolated, large collections of tumor cells; no micropapillary configurations	At least a few alveolar spaces
Kadota et al. 2015 ¹¹⁷	Micropapillary clusters, solid nests, single cells	Even in the first alveolar layer from the tumor edge
Warth et al. 2015 ¹¹⁸	Small cell nest (> 5 tumor cells) Cell nests	< 3 alveoli away (limited STAS) > 3 alveoli away (extensive STAS)
Morimoto et al. 2016 ¹³⁴	A group of more than 3 small clusters containing <20 nonintegrated micropapillary tumor cells	> 3mm apart from the main tumor
Shiono and Yanagawa. 2016 ¹⁴⁴	Tumor cell cluster lying freely within alveolar spaces	At least 0.5 mm from the main tumor
Dai et al. 2017 ¹⁴³	2015 WHO definition	At least a few alveolar spaces
Lu et al. 2017 ¹³³	Tumor cell nests	Even in the first alveolar layer from the tumor edge

- **Table 1.** The definitions of STAS and distance from the main tumor are shown as reported in the published studies. (continued)

Study / year	Criteria of STAS	Defined distance from main tumor
Uruga et al. 2017 ¹⁴²	Clusters of micropapillary or solid nest, single cells	Even in the first alveolar layer from the tumor edge
Masai et al. 2017 ¹⁴¹	Single cell, small cluster, or large cluster	Not reported

The prognostic argument in favor of STAS

The claimed relevance of STAS seems to be supported by the presence of tumor cell clusters or loose cells, which, irrespective of their numbers, were frequently significantly associated with adverse clinicopathological features. The published studies and the types of clinicopathologic factors associated with STAS are summarized in Table 2.

The presence of STAS has been found to be associated with lymphovascular-, vascular- and pleural invasion as well as with criteria for higher histological grade tumors, such as solid and micropapillary adenocarcinomas. A few studies also mention the association between the presence of KRAS mutations and the absence of EGFR mutations in STAS-positive tumors. The presence of STAS has also been found to be significantly associated with poorer overall survival (OS) and/or disease-free survival (DFS), in some studies also in multi-variate analysis^{142 133}.

A more recent study has also confirmed that the presence of STAS is a significant risk factor for local recurrence in early-stage NSCLC in patients who undergo limited resections¹⁴¹. Furthermore, another recent study reported that a semi-quantitative assessment of STAS provided additional prognostic information, with shorter recurrence-free survival seen in tumors with “high STAS” on univariate analysis¹⁴². In the same study, STAS retained its significance as a predictor of survival on multivariate analysis.

But could there be an alternative explanation for the observation of loose tumor cells and tissue fragments in NSCLC with a worse prognosis?

■ **Table 2.** The frequency of STAS and type of prognostic unfavorable factor(s) which were associated with STAS are shown for the published studies.

Study / year	% STAS	Vascular invasion	High grade histology	Pleural invasion	Stage	Mutations	DFS	OS
Onozato et al. 2013 ¹¹⁵	22.2%	NS	No low nuclear grade*	NS	NS	KRAS mutation* Absence of EGFR mutation*	NS	*
Kadota et al. 2015 ¹¹⁷	38%	LVS1* VSI*	Microcapillary and solid pattern*	NS	Higher stage*	NR	NR	(in limited resection group) *
Warth et al. 2015 ¹¹⁸	51.6	NR	High Ki67	NS	Nodal metastasis* distant metastasis*	Absence of EGFR mutation* BRAF mutation* KRAS mutation NS	*	*
Morimoto et al. 2016 ¹³⁴ [18]	7%**	LVS1* VSI*	NR	NS	NS	NR	NR	*
Shiono and Yanagawa. 2016 ^{14,4} [16]	14.8%	LVS1*	NR	*	Higher stage*	Absence of EGFR mutation*	*	*
Dai et al. 2017 ¹⁴³	30.3%	NR	High grade*	NR	NR	NR	*	(in < 3cm tumors) *
Lu et al. 2017 ¹³³	29.7%	LVS1* Vascular invasion*	High nuclear grade* High Ki67*	NR	Higher stage*	NR	\$	NS
Uruga et al. 2017 ¹⁴²	47.6%	LVS1* VSI*	Solid*	*	NR	NR	\$	(in high STAS) \$
Masai et al 2017 ⁴¹	15%	LVS1*	High grade*	*	NR	NR	NR	NR

LVS1 = lymphovascular space invasion; VSI = vascular space invasion; * = statistically significant in univariate analysis, but not in multivariate analysis (p < 0.05); \$ = statistically significant in multivariate analysis (p < 0.05); NS = statistically not significant; NR = not reported; DFS = disease free survival; OS = overall survival
** estimated in 67 microcapillary adenocarcinoma of 444 adenocarcinomas

The alternative explanation for ‘tumor cell clusters or loose cells’

In vivo spread of tumor cells in oncologic surgery is a well-known phenomenon and therefore the general approach is to avoid cutting through a tumor, as if this occurs, the whole field of operation is then considered to be contaminated. In a model system, the chance of tumor recurrence was instrument dependent¹⁵⁴. In medicine, tumor contamination of a biopsy path with subsequent outgrowth of the tumor along that path is seen in different tumor types such as NSCLC¹⁵⁵⁻¹⁵⁹, mesotheliomas¹⁶⁰, sarcomas¹⁶¹ and is a well-recognized phenomenon of tumor spread by instrumental forces.

The need to collect data for an alternative explanation for ‘tumor cell clusters or loose cells’ evolved after the WHO classification suddenly included STAS as a new pattern of invasion in pulmonary adenocarcinomas at the end of 2015.

One alternative hypothesis is that tumor cell clusters or loose cells may be derived from the handling procedure of resection specimens secondary to size differences between the thickness of the knife (~ 1 mm) and tumor cells, which are smaller by factor of 50-100. Cutting may disrupt the smaller cells and spread them along the new surface created by the knife. The ‘tumor cell clusters or loose cells’ in this hypothesis are no more than an artifact, similar to the already mentioned floaters, but caught in the many ‘holes’ present in the lung, the alveolar spaces.

A recent prospective, multi-institutional study demonstrated the presence of tumor cell clusters or loose cells in 73% of cases examined with scrutiny¹⁶². In contrast, most retrospective studies report the presence of STAS as not higher than in 15-51.6% of cases^{115 117 118 142 143 146 148 133}. Importantly, 93% of all tumor cell clusters or loose cells were found in blocks sampled from the downward side, i.e., after cutting through tumor tissue, both in adenocarcinomas and squamous cell carcinomas and only in a small minority of the lung tissue sampled before the knife cut through the tumor.

Remarkably, benign cell clusters or loose cells were also found in this study, mainly consisting of small clusters and strips of normal (not malignant) bronchial epithelium. Although in severe asthma the respiratory epithelium may shed¹⁶³, the cases in this study did not show signs of asthma in the bronchial mucosa. The fact that the low frequency of benign cell clusters or loose cells has not been reported in the studies examining STAS is possibly explained by the mental focus of the researchers on malignant cell clusters, which might lead them to overlook the benign loose clusters. Overall, this prospective study provides a strong rationale that loose benign and malignant cell clusters or loose cells are a reproducible artifact due to mechanical forces caused by specimen handling and gross cut-up in the pathology laboratory¹⁶².

An argument in favor of STAS reported in this prospective study is that some tumor cell clusters or loose cells were found in areas on the slide that were cut before passing through tumor tissue. However, this theoretically could also be explained by in vivo mechanical forces other than a knife, for instance due to surgical handling, either during a video assisted thoracoscopic surgical (VATS) procedure or after this procedure during manual handling. In this context, STAS may also stand for “Spread Through A Surgeon”, as coined in a recent review¹⁵⁰.

Moreover, the biological implication of the term 'spread through air spaces' has no comparable accepted biological connotation, except with micro-organisms such as viruses and bacteria. However, micro-organisms or cells growing along alveolar walls with all cellular nutrition available from the underlying capillaries is not the same as growing into the air. A distance of more than 100 microns from a capillary, leads to cellular apoptosis, of which high grade ductal carcinoma in the breast is a clear example. The implication in STAS that tumor cells can live on air alone is biologically not plausible. Moreover, pathologists are aware that when a bronchial biopsy is taken from the lung and it is not immediately fixed, the cells may appear dried out under the microscope e.g., after placing the biopsy on a piece of gauze during transport to the laboratory rather than into formalin. This has been compared to the difference between raisins and grapes. Peculiarly, in the published photomicrographs of examples of STAS the tumor cells appear viable and not dried out. This is another argument that the presence of loose tissue fragments is a phenomenon associated with the moment of resection, and not present for days. In addition, lung cancer is not a contagious disease, i.e., it is not distributed to other human beings by air spreading.

In a recent review of STAS, the authors acknowledge that whilst 'invasion of air' by a tumor is an unconventional concept, the presence of tumor cells and tumor cell clusters floating in pools of mucin in cases of mucinous and colloid adenocarcinomas, such as in lung and colon, is "internationally accepted" as evidence of tumor invasion despite the lack of stromal invasion¹⁴⁸. However, in morphological terms tumor cells and tumor cell clusters do not invade pre-existing mucin but produce the mucin themselves. Furthermore, these mucin pools are also present within the confines of the tumor, sometimes at the tumor's edge, but still recognized to be within the microscopic boundaries of the tumor. Similarly, in the colorectum, mucin pools are not normally present in the bowel wall but develop in mucinous adenocarcinomas due to secretion of mucin by tumor cells within the bowel wall and not by air movements within the bowel wall. Therefore, we look upon this comparison as an argument for STAS as a fallacy.

Overall, there are no accepted similar morphological criteria in other situations that would not require stromal, vascular or pleural invasion as evidence of invasion, so the concept of air invasion is unprecedented.

Mimickers of 'tumor cell clusters or loose cells'

Yet *other* explanations of 2-dimensional representations of tumor cell clusters or loose cells are i) poor fixation and ii) collapse of certain adenocarcinoma subtypes.

In pulmonary specimens subjected to a delay in fixation resulting in poor fixation, the bronchial epithelium frequently detaches from the underlying basement membrane and can be displaced by handling, with displacement occurring into the adjacent alveolar spaces. This phenomenon is well known, especially in autopsy specimens, but may also occur in lobectomy and pneumonectomy specimens. One would expect this phenomenon to be more pronounced in freshly cut specimen, compared to properly formalin fixed ones. This is indeed found in the above mentioned prospective study¹⁶².

In this study more tumor cell clusters or loose cells were found in specimen freshly cut, compared to formalin fixed ones.

Pulmonary collapse on the other hand is a more general phenomenon in pulmonary resections. During pulmonary resection, the air, lymph and probably also a certain amount of blood will flow out of the lung and give rise to a smaller handling volume of lung tissue. The extent of the volume reduction depends on the size of resection and the extent of disease. In any case, collapse resulting from reduction in the amount of air is recognized as close approximation of the alveolar walls. In invasive adenocarcinomas, a specific growth pattern of tumor cells along alveolar walls is called the lepidic pattern. If this is the only pattern present within a tumor smaller than 3 cm, this tumor is classified as adenocarcinoma in situ (AIS)⁴. A 2-dimensional representation of an AIS may mimic a papillary pattern in collapsed lung⁹⁰. In collapsed lung, the compressed alveoli do not have the original open air-space presentation, but show variable shapes due to the very flexible nature of lung tissue. Therefore, in collapsed lung tissue in which there is a proliferation of tumor cells along the alveolar walls, the so-called lepidic pattern, cutting of slides in a 2-dimensional (2-D) plane will result in seemingly loose tumor cells or fragments. Most pathologists would agree that this should certainly not be given a special designation, apart from recognizing it as a cutting artifact¹²⁰. Three-dimensional reconstruction studies of pulmonary adenocarcinomas also demonstrated that seemingly tumor cell clusters were frequently interconnected to each other and with the main tumor mass at multiple points, when examined in 2-D^{145,132}. Other authors have demonstrated similar findings using multiple serial sections of tumors, showing that many seemingly separate micropapillary tumor clusters present in alveolar spaces were in fact connected to the main tumor^{40,41}. These reconstruction studies may explain part of the 7% of seemingly tumor cell clusters present in the blocks before tumor cutting, as reported in the previously mentioned prospective study¹⁶².

How to explain the association of ‘tumor cell clusters or loose cells’ with poor prognosis?

A plausible biological explanation for the association of tumor cell clusters or loose cells with poor prognosis is that disruption of tumor cells is simply seen in poorly differentiated, highly discohesive tumors. It has been postulated that such poorly differentiated discohesive tumors have fewer intercellular adhesions between tumor cells, such as in micropapillary adenocarcinomas and poorly differentiated squamous cell carcinomas^{124,125,165,166}. Interestingly, in micropapillary carcinoma (frequently associated with STAS) one study suggests that the loose cells have most likely acquired resistance to apoptosis and facilitated anchorage-independent growth, which are advantageous for proliferation during lymphatic cancer metastasis¹⁶⁴. Dissociation of tumor cells is not a rare phenomenon and is recognized in diagnostic breast cytology where dissociation of epithelial cells is a useful artifact in favor of malignancy¹⁶⁷.

Moreover, studies that show a correlation between STAS and poor prognosis also demonstrate correlations between STAS and other prognosticators. In all these

studies STAS is correlated with other prognostically unfavorable factors, such as lymphovascular invasion, pleural invasion, high grade histology (such as micropapillary and solid patterns) and EGFR-negative status (see table 2), and associated with poorly differentiated features such as necrosis, higher grade, nuclear diameter and Ki67 labeling index.

In daily practice the prognosis of patients diagnosed with lung cancer is guided by the TNM system. Pathology factors relevant in the TNM system are tumor size, lymph node metastases and pleural invasion. The value of another prognostic pathology factor based on an artifact may be appreciated in the context of more than 100 additional prognostic factors have been published, none of which have made it into the TNM^{168,169}.

After its rapid embrace by pathologists, the concept of aerogenous spread has been inhaled by the radiologists, starting with a radiological definition: intrapulmonary discontinuous spread of neoplastic cells through airspaces and airways, with the discontinuous foci seen close to the primary tumor as satellite foci or at distance, including in the contralateral lung¹⁷⁰. Remarkably, the size of the tumor clusters seen microscopically defined STAS are below the current detection limit of CT scanning.

There is sufficient evidence to support that tumor cell clusters or loose cells are an artifact caused by displacement from surgical manipulation and gross processing - particularly from a knife blade. Thus, tumor cell clusters or loose cells should neither be interpreted as "spread through air spaces" (aerogenic or pneumonic metastasis) or as a novel pattern of tumor invasion.

The most compelling argument for recognition of this histologic finding is its correlation with poor survival. However, this prognostic association often loses its significance when high-grade histologic patterns are included in multivariate analyses. Despite this fact, the recognition of tumor cell clusters or loose cells is useful and should be a telltale sign for pathologists, that there is likely a high-grade neoplasm nearby.

In conclusion, we believe that, while well-intentioned, the inclusion of STAS in the WHO classification for lung cancer as a pattern of invasion was premature. These loose tissue fragments are simply an artifact, that often reveal the presence of a high-grade neoplasm.



8

To the editor: "Spread through air spaces (STAS) is prognostic in atypical carcinoid, large cell neuroendocrine carcinoma, and small cell carcinoma of the lung"

Erik Thunnissen, Alberto Marchevsky, Giulio Rossi, Prudence A. Russell, **Hans Blaauwgeers**, Teodora Radonic, Jan von der Thüsen, Douglas Flieder, Giuseppe Pelosi

Journal of Thoracic Oncology 2020, 15:e116-7.
doi.org/10.1016/j.jtho.2019.11.027

To the Editor

Since the concept of “spread through air spaces” (STAS) was included in the 2015 WHO book on classification of lung cancer, the manuscript by Aly et al.¹⁷¹, is the first study proposing detailed histologic criteria to distinguish STAS from other forms of “loose tumor fragments”: tumor floaters and artifacts¹⁷¹ in lung neuroendocrine neoplasms. These expert opinion criteria are not supported by evidence showing prognostic differences in cases that exhibit STAS versus loose tumor fragments. In addition, the proposed criteria rely mostly on the detection of loose tumor fragments with smooth edges in spatial continuity with the tumor and within a certain distance to the lesion. Loose tumor fragments with jagged or ragged margins and/or those located far away from the tumor (“more than four airspaces away,” as shown in Fig. 2) or at the edge of a tissue section are designated as an artifact¹⁷². The proposed criteria depend on an arbitrary distance between the tumor and the loose fragments, and the ability of pathologists to distinguish smooth from jagged or ragged edges. The difficulty of interpreting the characteristics of tumor borders is underscored by looking at the examples of STAS provided in Figure 1, taken at x100. In our opinion, it is difficult at this magnification to evaluate whether the fragments have round or jagged/ragged edges. The proposed criteria also raise questions as to why a tumor would always spread only through fragments with smooth borders. Indeed, previous studies have shown that the knife can disseminate tumor fragments with smooth or ragged margins radially from tumor edges into holes in tissue or into the edge of tissue sections. A previous study of the presence of STAS on frozen section did not find sufficient evidence to support the routine reporting of STAS during intraoperative consultations¹⁷². To our knowledge, there are no clinical trials supporting the use of STAS as a predictive feature. Previous studies have used variable definitions for the identification of STAS on tissue sections, precluding the use of meta-analysis to aggregate available evidence about the association between STAS and prognosis¹⁷². Moreover, in the article by Aly et al.¹⁷¹, at least 88% (43 out of 49) of the STAS in typical carcinoids is present in cases without recurrence or lung cancer-specific death. Recent reports^{173,174} (and references herein), have described as artifacts the presence of loose fragments in different neoplastic and non-neoplastic lesions such as in diffuse idiopathic pulmonary neuroendocrine cell hyperplasia¹⁷⁴. Studies performing 3D reconstructions evaluating the continuity between the main tumor and the detached cells have shown that the latter represent tentacles of inherently fragile structures¹³².

In summary, the diagnostic criteria for the distinction between STAS and artifacts proposed by Aly et al.¹⁷¹, need to be defined in more detail with studies showing diagnostic reproducibility and correlation with prognosis and prediction before the controversy as to whether pathologists can distinguish the so-called STAS from artifacts is put to rest.



9

To the editor: "Spread through air spaces (STAS); can an artifact really be excluded?".

Hans Blaauwgeers, Erik Thunnissen

American Journal of Surgical Pathology 2021;45(10):1439

doi: 10.1097/PAS.0000000000001787

To the Editor

With great interest we read the study of Metovic et al¹⁷⁵ "Gross specimen handling procedures do not impact the occurrence of spread through air spaces (STAS) in lung cancer" in search for scientific truth in the discussion about spread through air spaces (STAS), whether STAS is an artifact or a biological reality. The authors deserve a compliment for performing a more controlled prospective study than the study of Blaauwgeers et al¹⁶² also published in your journal, with respect to the use of a clean knife for every cut. Nevertheless, we have 2 questions about the interpretation of their data.

The first one deals with the statement in the discussion "As it is against physical laws that the possibility of neoplastic cell clusters to be misplaced in the reverse direction of an acting physical force, as that produced by a cutting blade, it seems virtually impossible to interpret STAS images in the upper parenchymal portion as a knife-induced artifact." The authors seem to think of only a vertical cut into the tissue without relevant mechanical force on the tissue. A possible confounder may, beside the downward displacement also be a slight sideward movement of an oblique knife. Moreover, using an ~800 µm thick knife there has to be a physical downward force at cellular level¹²⁰. This force does not exclude a sideways and possibly upward wave in a tissue structure that consists of 70% water. Think about examples like a bow wave of a ship sailing in the water, the upward rain-drop image when it rains "cats and dogs" and, for example, the guillotine, with a vertical controlled, yet oblique knife. In these examples, there is besides a sideways also an even upward movement of water/blood.

The second question deals with the extravasated erythrocytes around the loose displaced tumor cells (interpreted as "STAS") present in all the figures. Of note, Pelosi et al¹⁷⁴ interpreted the presence of such erythrocytes around the also displaced benign neuroendocrine cells as an artifact. On the basis of the confounder of hard to prove but not difficult to imagine crude cutting force (including the effect of extravasated erythrocytes) we think that the suggestion in the title "Gross specimen handling procedure do not impact the occurrence of spread through air spaces (STAS) in lung cancer" should be downsized. Future studies are warranted.



10

Loose tumor cells in pulmonary arteries
of lung adenocarcinoma resection
specimen; no correlation with survival,
despite high prevalence.

Hans Blaauwgeers, Federica Filipello, Birgit Lissenberg-Witte,
Claudio Doglioni, Teodora Radonic, Idris Bahce, Yuko Minami,
Andreas Schonau, Julien Vincenten, Arthur Smit,
Chris Dickhoff, Erik Thunnissen

Archives of Pathology and Laboratory Medicine, accepted May 2023

Abstract

Context

Loose tumor cells and tumor cell clusters can be recognized in the lumen of intratumoral pulmonary arteries of resected non-small cell lung cancer (NSCLC) specimens. It is unclear whether these should be considered tumor-emboli, and as such could predict a worsened prognosis.

Objective

To investigate the nature and prognostic impact of pulmonary artery intraluminal tumor cells.

Design

This multicenter study involved an exploratory pilot study and a validation study from 3 institutions. For the exploratory pilot, a retrospective pulmonary resection cohort of primary adenocarcinomas, diagnosed between Nov 2007 and Nov 2010, were scored for the presence of tumor cells, as well as potentially other cells in the intravascular spaces using hematoxylin-eosin (H&E), and cytokeratin 7 (CK7) stains. In the validation part, 2 retrospective cohorts of resected pulmonary adenocarcinomas, between Jan 2011 and Dec 2016, were included. Recurrence free survival (RFS), and overall survival (OS) data were collected.

Results

In the pilot study, CK7 positive intravascular cells, mainly tumor cells, were present in 23 out of 33 patients (70%). The 5-year OS for patients with intravascular tumor cells was 61% compared to 40% for patients without intravascular tumor cells ($P=0.19$). In the validation study, CK7 positive intravascular tumor cells were present in 41 out of 70 patients (58.6%). The 5-years RFS for patients with intravascular tumor cells was 80.0% compared to 80.6% in patients without intravascular tumor cells ($P=0.52$). The 5-year OS rates were respectively 82.8% and 71.6% ($P=0.16$).

Conclusion

Loose tumor cells in pulmonary arterial lumina were found in most NSCLC resection specimens and were not associated with a worse RFS or OS. Therefore, most probably they represent an artifact.

Introduction

Lung cancer is associated with a high incidence of pulmonary embolism, caused by thrombotic emboli, as a paraneoplastic phenomenon, but also caused by real tumor-emboli¹⁷⁶.

In general, pulmonary tumor embolism can be categorized by size, into large, proximal emboli and smaller emboli in the microvasculature. Tumor-emboli occurring in large branches of the pulmonary artery, are associated with an acute deterioration of clinical performance. Pulmonary tumor embolism localized in smaller branches of the pulmonary arteries is described by two different entities: pulmonary tumor micro-embolism and pulmonary tumor thrombotic microangiopathy¹⁷⁷⁻¹⁷⁹. These two conditions are likely to represent a spectrum of the same disease and may be associated with pulmonary hypertension^{177,180}.

Although pulmonary tumor-emboli are a known specific entity and can be diagnosed in tumor biopsies or tumor resection specimen, it is unclear whether all intravascular tumor cells in pathology slides can be considered tumor-emboli. In our experience, a substantial incidence of tumor cells can be recognized in the lumen of intra-tumoral pulmonary arteries in many resected non-small cell lung cancer (NSCLC) specimens, albeit with a morphological aspect, distinct from regular tumor-emboli. We hypothesized that these 'common' loose intravascular tumor cells may be caused by technical artifacts through displacement in the preparation process of the slides. Therefore, we aimed to investigate the prognostic impact of these intravascular tumor cells and to substantiate the claim that these intravascular tumor cells may be caused by iatrogenic artifacts.

Materials and methods

Design

This study involved an exploratory pilot study and a validation study. While studying a previously described cohort of patients with adenocarcinoma of the lung (diagnosed on biopsies and 195 resections from different institutes), between November 2007 and November 2010¹⁸¹, we observed the presence of intravascular tumor cells in a high number of cases. We conducted an exploratory pilot study on a subset of this cohort (n=33) to confirm our findings. The selection of participants was based on the availability of slides and paraffin blocks for additional staining of resections performed at the Vrije Universiteit Medical Center (VUmc) in Amsterdam, the Netherlands. Additionally, participants were included in the study based on the availability of clinical follow-up. Hematoxylin and eosin (H&E) stained slides were retrieved from the archive and for each resected tumor 1 or 2 most representative tumor slides were selected. Cytokeratin 7 (CK7) staining was performed as described below on the sections of the same paraffin block(s).

The presence of loose tumor cells and other cells, in pulmonary arteries was scored in H&E and CK7 stained slides by two experienced pulmonary pathologists (HB, ET). Follow-up data were retrieved from patient files.

Because the exploratory study contained a relatively small number of patients and consisted of a not uniformly defined set of patients, we expanded the study with two retrospective separate cohorts in search of validation of the initial findings: patients with resected pulmonary adenocarcinoma diagnosed between the 1st January 2011 and the 31th December 2016 in the (1) Onze Lieve Vrouwe Gasthuis (OLVG) Hospital, Amsterdam, The Netherlands and (2) San Raffaele Scientific Institute, Milan, Italy.

The inclusion criteria for both of these cohorts were different from the exploratory cohort and included resection specimens with a primary pulmonary adenocarcinoma of a pathological tumor diameter 3 cm or less and available follow-up information. The exclusion criteria were the presence of nodal or hematogenous metastases at the time of resection, treatment with neoadjuvant chemotherapy, multiple nodules in the same or other lobes, synchronous previous lung carcinoma, and invasive mucinous adenocarcinoma or other special type patterns (intestinal and fetal adenocarcinoma). Freshly cut sections of the selected paraffin blocks from both institutes were stained for H&E, elastica von Gieson (EvG or elastin) staining, and CK7 immunohistochemistry at the department of Pathology of the VUmc. Both institutes used neutral buffered formaldehyde for the fixation of their resection specimens. It was estimated that a total of 70 to 80 cases would be sufficient to validate the initial finding. Therefore, after determining suitable cases in both institutes, a minimum of 40 cases in each were randomly selected.

Age, sex, total tumor size, tumor location, pathological stage adjusted to the 8th edition of the Union for International Cancer Control/American Joint Committee on Cancer (UICC/AJCC) TNM classification system for non-small cell lung cancer (NSCLC)^{B2}, time to recurrence, death, and cause of death were determined by retrospective chart review after approval by the Institutional Review Board (OLVG: ACW021-044; VUmc 2022.0269 [biobank 2017.023]; Milan CE 284/2022).

In the OLVG in Amsterdam 218 cases of resected adenocarcinoma in the lung between January 1st 2011 and December 31st 2016 were retrieved from the pathology archives. One hundred fifty-eight cases were excluded, because they did not meet inclusion criteria (47 with nodal metastases, 26 metastases from other organ [mainly colorectal carcinoma], 20 with multiple nodules, 2 subjected to neoadjuvant therapy, 47 with a diameter > 3 cm, 4 with previous or synchronous lung cancer, 12 mucinous or other type). The remaining 60 cases were included for random selection.

A total of 365 cases of resected primary lung adenocarcinoma between 1st January 2011 and 31th December 2016 were retrieved from San Raffaele archive in Milan. A total of 223 were firstly excluded because did not meet the inclusion criteria of the study (122 with nodal metastases, 12 without lymph nodes histologic examination, 6 subjected to neoadjuvant treatment, 8 with multiple lung nodules at the time of resection, 18 mucinous and 1 enteric adenocarcinoma, 18 mixed mucinous and non-mucinous

adenocarcinoma and 38 cases with tumoral diameter > 3 cm). Of the remaining 142 cases, 48 had short or no accessible follow up information, for 2 cases cause of death was unknown and for 17 cases material was not available or insufficient. The remaining 75 cases from San Raffaele Scientific Institute were included for randomization.

After randomization, 80 cases were included. Histological review of these cases was performed by 3 pathologists. For each case, one representative tumor block was selected and digitized. The digital images were uploaded on the collaborative platform for on-line teaching, training and quality assurance in pathology, Pathogate (<https://pathogate.net>).

After technical review of the cases, 10 were excluded, because of insufficient quality of the slide or out-of-focus areas after scanning. Therefore, 70 cases, 35 from each institute, were analyzed.

Since in the original pathology reports subtyping of the adenocarcinomas was rarely reported, this was done by 2 pathologists in the categories adenocarcinoma in situ (AIS), lepidic predominant adenocarcinoma, low grade adenocarcinoma (acinar, papillary) with or without more than 10% high grade component and high-grade adenocarcinoma (micropapillary, solid). Cases with discrepancies (dominant pattern, presence of high-grade component) were reviewed, reaching consensus.

Cytokeratin 7 (CK7)

The immunohistochemical stain for CK7 (clone OVTL12/30 (Agilent/Dako (Glostrup, Denmark, catno. M701801)) was performed in a Roche/Ventana benchmark Ultra (Roche, Basel Switzerland) with 3µm tissue slides mounted on TOMO-glass slides (Roche, Basel, Switzerland). Antigen retrieval was applied with high pH-buffer CC1 (32 minutes at 100°C) and the antibody was diluted 1/100 (incubated for 32 minutes at 36°C) and detected with the Optiview DAB kit under standard conditions. Sections were dehydrated with ethanol 100%, cleared with Xylene and coverslipped with Tissue-Tek coverslip film on the Sakura coverslipper (Sakura Finetek Europe B.V, Alphen aan de Rijn, The Netherlands). Internal positive controls were pneumocytes and respiratory epithelial cells. Internal negative controls were e.g., smooth muscle cells in vessel walls and bronchioli. Occasional CK7+ endothelial cells were not scored as luminal positive cells.

Statistical analysis

The presence of tumor cells within the lumen of pulmonary arteries was evaluated using H&E and CK7. Continuous variables were described by mean and standard deviation, categorical variables by frequency and percentage. For relapse free survival (RFS) and overall survival (OS) analysis Kaplan-Meier curves were estimated and compared using the log-rank test. Statistical analysis was performed in SPSS version 26 (IBM Corp., Armonk, NY, USA). P-values <.05 were considered statistically significant.

Results

Exploratory pilot study

Clinicopathological characteristics

In the pilot study from a total of 33 patients, 74 histological sections of 40 tumors were analyzed. The clinicopathological characteristics of the patients are presented in table 1. A total of 7 patients had 2 tumors; in 4 of them located in 2 separated wedge excisions, 1 in a lobectomy and a wedge excision and 2 patients with a double tumor in 1 lobe. The histological diagnosis was invasive carcinoma for most tumors, except for 3 with a diagnosis of adenocarcinoma in-situ, of which 1 was in combination with a separate invasive carcinoma.

■ **Table 1.** Clinicopathological variables of pilot study patients.

		n (%)
Age (mean - SD)		63 (10)
Sex	Male	14 (42%)
	Female	19 (58%)
Previous malignancy	Squamous cell carcinoma larynx	2 (6%)
	Adenocarcinoma sigmoid	1 (3%)
	Mantel cell lymphoma	1 (3%)
	None	29 (88%)
Surgery procedure	Lobectomy	23 (70%)
	Bilobectomy	1 (3%)
	Wedge resections (n=12) ^a	8 (24%)
	Lobectomy and wedge	1 (3%)
Pathological stage	1	11 (33%)
	2	10 (30%)
	3	10 (30%)
	4	2 (6%)
Histological diagnosis (patients)	AIS	2 (6%)
	Invasive	31 (94%)

Adenocarcinoma subtypes (n=40)^b		
AIS		3 (8%)
Lepidic		13 (33%)
Papillary		0 (0%)
Acinar		6 (15%)
Micropapillary		2 (5%)
Solid		16 (40%)

Comments: ^a 4 patients with 2 wedge excisions in the same surgical procedure; ^b 4 patients with 2 tumors in 2 wedges, 1 patient with 2 tumors in a lobectomy and 1 in wedge, 2 patients with a double tumor in lobectomy

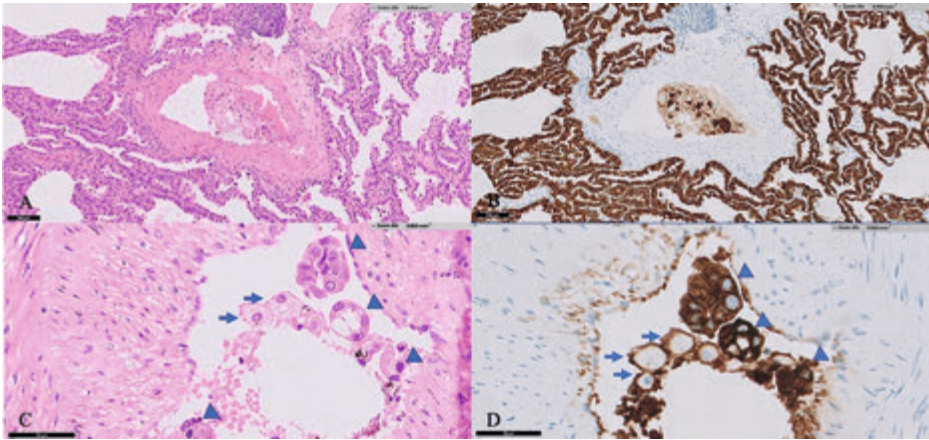
Abbreviations: SD = standard deviation; AIS = adenocarcinoma in situ

Microscopic findings

All the histological sections contained alveolar walls covered with tumor cells located near branches of the pulmonary artery. Frequently, in the routine H&E stain, a few clusters of tumor cells, focal remaining erythrocytes, and rare alveolar macrophages, were observed. The cytonuclear appearance of the tumor cells in the arterial lumen was similar to the adjacent alveolar wall lining tumor cells.

Immunohistochemical staining with CK7, which is reactive to the cytoplasm of most pulmonary adenocarcinomas, revealed immunohistochemical positive single tumor cells or small clusters in the 'looking like air' partially empty lumen of the larger pulmonary arteries, without fibrin (Figure 1). This finding was present in 41 out of 74 (55%) histological sections, 26 out of 40 (65%) tumors and in 23 out of 33 patients (70%). In the smallest branches of the pulmonary arteries tumor cells were not discerned. Intravascular tumor cells were found in 2 of the 3 of tumors without invasion (AIS) (67%) and in 19 of the 37 tumors (51%; $P=0.61$) with invasion.

No tumor cells were observed neither in venous, nor in lymphatic vascular structures.



- **Figure 1.** A: Example of partially collapsed peripheral lung in which alveoli are covered with epithelial tumor cells. Classified as non-invasive, adenocarcinoma in situ (AIS). Centrally a pulmonary artery with clusters and isolated tumor cells. Hematoxylin & Eosin (H&E) 200x, B: Same area as in figure A. Cytokeratin 7 (CK7) immunohistochemical stain, 200x. C: Example of another pulmonary artery with clusters of tumor cells (blue arrow heads), alveolar macrophages (blue arrows) and some erythrocytes. H&E stain, 400x. D: same artery as in figure C. CK7 immunohistochemical stain, 400x.

Validation study

Clinicopathological characteristics

In the validation study a total of 70 tumor slides of 70 patients were analyzed. The clinicopathological characteristics of the patients are presented in table 2. The histological diagnosis was invasive carcinoma for 60 tumors. A total of 10 patients were classified as non-invasive/ AIS (14.3%).

- **Table 2.** Clinicopathological variables in the two validation cohorts.

	Milan	OLVG	Total
Number of patients	35	35	70
Age (mean±SD)	67.2 ± 9.9	61.5 ± 7.6	64.4 ± 9.2
Sex (%)			
Male	25 (71.4%)	12 (34.3%)	37 (52.9%)
Female	10 (28.6%)	23 (65.7%)	33 (47.1%)
Mean follow up time ^a (range)	61 (11-113)	81 (28-132)	69.5 (11-132)
Resection type (%)			
Segmentectomy	9 (25.7%)	4 (11.4%)	13 (18.6%)
Lobectomy	26 (74.3%)	31 (88.6%)	57 (81.4%)

■ **Table 2.** Clinicopathological variables in the two validation cohorts. (continued)

	Milan	OLVG	Total
Pathological stage^a (%)			
pTis	2 (5.7%)	8 (22.8%)	10 (14.3%)
pT1a	7 (20.0%)	6 (17.1%)	13 (18.6%)
pT1b	15 (42.9%)	13 (37.1%)	28 (40.0%)
pT1c	11 (31.4%)	8 (22.6%)	19 (27.1%)
Adenocarcinoma predominant subtype (%)			
AIS	2 (5.7%)	8 (22.8%)	10 (14.3%)
Lepidic predominant	7 (20.0%)	6 (17.1%)	13 (18.6%)
Acinar	10 (28.6%)	9 (25.7%)	19 (27.1%)
Micropapillary	2 (5.7%)	3 (8.6%)	5 (7.1%)
Papillary	3 (8.6%)	1 (2.8%)	4 (5.7%)
Solid	11 (31.4%)	8 (22.8%)	19 (27.1%)

^a months; ^b according to the TNM 8th edition; AIS, adenocarcinoma in situ

Although there were significant differences between the two cohorts with respect to age (Milan mean 67.2, OLVG 61.5, $P=.009$); gender (Milan 25 male and 10 females, OLVG 12 male and 23 females, $P=.002$) and follow-up time (Milan mean 61 months, OLVG 81 months, $P=.005$), the RFS-time in cases with a relapse between the 2 cohorts did not differ (Milan mean 26.7 months [$n=7$]; OLVG mean 34.9 months [$n=8$]; $P=.49$), nor did the dominant tumor type ($P=0.66$). Therefore, for the analysis of the presence of intravascular cells, the 2 cohorts were combined.

Microscopic findings

The presence of intravascular cells in the combined cohorts both for invasive and non-invasive (AIS) cases are shown in table 3.

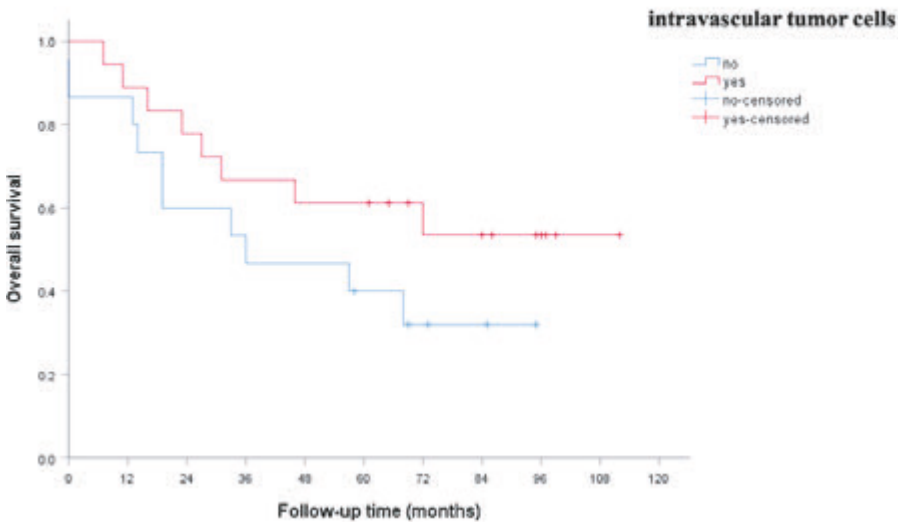
■ **Table 3.** Presence of intravascular cells (CK7+ and/or macrophages) in both validation cohorts, in invasive and adenocarcinoma in situ (AIS) cases.

	AIS n=10	Invasive n=60	Total (%) n=70
Intravascular cells			
CK7+ tumor cells	3	10	13
macrophages	3	6	9
CK7+ and macrophages	2	17	19
Present (total)	8	33	41 (58.6%)
Absent	2	27	29 (41.4%)

In a total of 41 out of 70 patients (58.6%) intravascular tumor cells, tumor cell clusters and/or macrophages were found. These were also found in 8 of the 10 tumors without invasion (AIS) (80.0%) and in 33 of the 60 invasive tumors (55.0%; $P = .18$). No tumor cells were observed neither in venous nor in lymphatic vascular structures.

Survival outcomes

The median follow-up time in the pilot study was 58 months (range 1-112 months). The OS for intra-arterial tumor cells is shown in figure 2. In the exploratory cohort, the mean 5-year OS rate for the patients with intravascular tumor cells was 61% compared to 40% for the patients without intravascular tumor cells ($P = .19$).



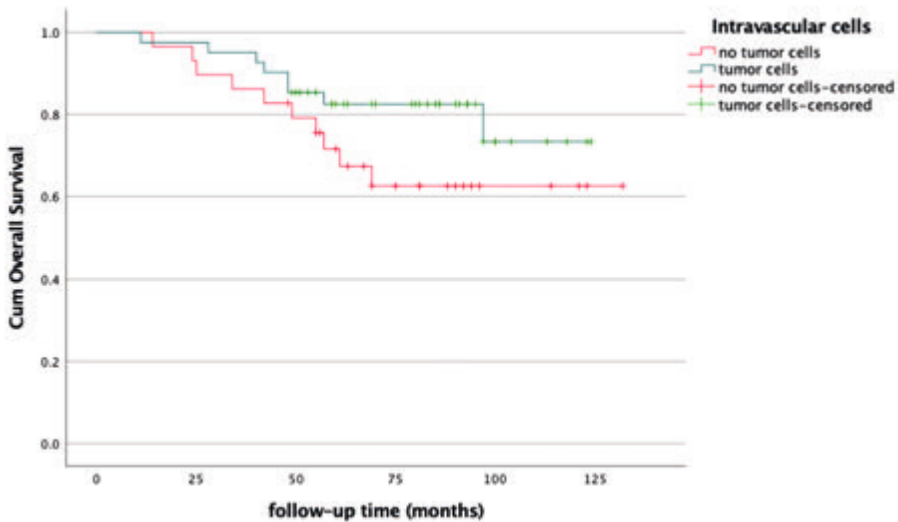
■ **Figure 2.** The Kaplan-Meier curves for overall survival in the pilot study are shown for tumor cells in lumen of the pulmonary arteries ($P = .19$).

In the cohorts of the validation study, the median follow-up time was 61 months (range 11-113) for the Milan cases and 81 months (range 28-132) for the OLVG cases.

In the Milan cohort, the 22 cases with intravascular tumor cells had a 5-years OS of 85.6% compared to 41.5% for the 13 cases without intravascular tumor cells ($P = .002$). In the OLVG cases, the 5-year OS for the 19 cases with and the 16 cases without intravascular tumor cells was 78.9% and 93.8%, respectively ($P = .35$). In both cohorts combined, the 5-years OS for cases with intravascular tumor cells was 82.5% versus 71.6% for cases without ($P = .16$) (Figure 3). The 5-years RFS data for both cohorts showed no significant differences, neither for the separate cohorts, nor combined (80.0% with and 80.9% without intravascular tumor cells; $P = .52$).

Discussion

In this multicenter retrospective study, we conducted an exploratory pilot study and a validation study in 2 separate cohorts. Our findings showed that intravascular tumor cells were present in a surprisingly high number of resected early-stage non-small cell lung cancer (NSCLC) patients. In the pilot study, individual tumor cells, small clusters of tumor cells, and/or macrophages were found in 70% of the 33 patients and in 65% of the 40 resected tumors. This finding was confirmed in the validation cohort, where intravascular tumor cells were found in 41 out of 70 (58.6%) cases. Interestingly, the presence of arterial tumor cells was associated with a seemingly better survival outcome in the pilot study and in one of the validation cohorts.



■ **Figure 3.** The Kaplan-Meier curves for overall survival in the validation cohorts are shown for CK7+ tumor cells and or macrophages in lumen of the pulmonary arteries (P = .16)

However, this finding was contradictory to the expected biological phenomenon. We also observed the presence of intravascular tumor cells in cases without invasive carcinoma (adenocarcinoma in situ/AIS) in both the pilot study and the validation cohort.

The morphological diagnosis of tumor cells within pulmonary arteries, as we found in our study, can be distinguished from five other pathological entities, as discussed below:

First, direct invasive growth through the arterial wall of tumor cells. In none of the cases in our study, direct tumor invasion in the adventitia, media, or intima layer was observed, either in the H&E stain or in the cytokeratin 7 stain.

Secondly, tumor cells in smaller branches with or without occlusive fibro-intimal remodeling in small pulmonary arteries, which are usually a sign of metastases from other organs in the form of pulmonary tumor micro-embolism and pulmonary tumor thrombotic microangiopathy. In the pilot study, only 4 of the patients had a history of cancer, of which only 1 had a colonic carcinoma (Table 1), which is a tumor type that is infrequently CK7+. In the validation cohort, the presence of a previous malignancy was an exclusion criterion. Additionally, none of the cases with luminal tumor cells showed intimal fibro-remodeling.

Thirdly, the morphological features in our study differ from tumor emboli in larger vessels from metastases of other organs in several ways. (1) In our cases, the alveolar walls surrounding the pulmonary artery were covered with tumor cells extending from the adjacent tumor, with a similar cytonuclear appearance as in the lumen of the artery. In metastatic emboli, the adjacent alveolar walls do not contain tumor, and the cytonuclear details of the metastases have a similarity with the primary tumor, which is usually different from a primary lung adenocarcinoma. (2) The amount of tumor cells was small (i.e., isolated tumor cells or small clusters) and without surrounding fibrin or other blood components, as discussed above in point 2. In cases of metastasis, the lumen of the larger pulmonary artery is usually slightly extended by the filling of the tumor embolus, while in our study, a large part of the occasionally indented lumen was 'empty'. In patients with clinical suspicion of pulmonary emboli on preoperative imaging, the differential diagnosis includes sarcoma of the pulmonary artery¹⁸³, which was not present in our patients.

Furthermore, hydrophilic coats on medical interventional devices may dissociate from the device surface during endovascular manipulation and give rise to hydrophilic polymer embolism¹⁸⁴⁻¹⁸⁶. These are morphologically characterized by intraluminal foreign body material surrounded by thrombosis, with or without inflammatory response, and are usually located in smaller arteries. Foreign body material was not present in our study.

A last distinction can be made from circulating tumor cells that may appear similar, but these cells in the pulmonary artery of the resection specimen should then be derived from a primary source elsewhere in the body and flow via the heart to the lung. Morphologically, the circulating tumor cells should be surrounded by blood components, while in our study, the arterial lumen looked 'empty' with occasional tumor cells without a lot of blood components. Moreover, in most patients, a primary tumor of other origin than the lungs was not present at the time of resection and during follow-up (median time > 5 years). In addition, circulating tumor cells are rare in the bloodstream. For analysis of circulating tumor cells, enrichment and isolation methods have been developed¹⁸⁷, while in our study, there was a relatively high frequency in histological sections of both the pilot study and the validations cohorts.

In the lung, a pilot study of blood sampling from tumor-draining pulmonary veins at the time of tumor resection was previously performed with the hypothesis that patients with detectable circulating tumor cells in the pulmonary vein would have a higher risk

for disease recurrence¹⁸⁸. While the concept of venous drainage from a pulmonary carcinoma is plausible, involvement of arterial tumor cells in this context is not.

The morphological and clinical diagnostic aspects discussed above support the idea that our findings are different from clinical entities described so far, except for the report by Pechet and colleagues¹⁸⁹, who described arterial invasion in stage I NSCLC. Pechet and colleagues defined the presence of tumor within the lumen of a muscular vessel with a clearly defined internal or external elastic lamina in at least two anatomically distinct vessels as a positive score for arterial invasion. They found that patients without arterial invasion had significantly better survival than those with arterial invasion (73% versus 38%, $P < .001$). However, their study did not include histopathological images for comparison. In our study, we specifically searched for tumor cells using CK7 immunohistochemical staining in at least one pulmonary artery, while Pechet's study required at least two vessels (i.e., 39 of the 100 [39%] of the patients). Complete data on recurrence in their study was available for 64 patients, of which 16 had arterial invasion. Remarkably, 6 of the 16 were alive at 5 years (2 with and 4 without recurrence). Although the selection criteria and follow-up in Pechet's study were different from ours, this does not exclude the possibility of an iatrogenic artifact in their study.

Several findings from our study are remarkable. One is the high incidence of intratumorally intravascular tumor cells compared to previous literature (25-50%)^{190,191}. Another is that we only found intra-arterial vascular tumor cells and no intravenous or lymphovascular invasive tumor cells. A third notable finding is that we also found intra-arterial tumor cells in 3 of the 33 cases in the pilot study and also in 8 of the 10 cases in the validation cohorts that were classified as adenocarcinoma in situ (AIS) and also on revision showed no other criteria of invasiveness. This supports the idea that at least some of the intravascular tumor cells we found were not a true representation of vascular invasion, but most likely an artifact. We believe that isolated tumor cells in pulmonary arteries with adjacent abundant tumor cells are easily overlooked in routine H&E staining, but are more clearly recognized in CK7 immunohistochemical staining. This raised the question of whether our observation is a clinically relevant reality or an artifact. Based on the following arguments, we strongly favor the idea that our findings are the result of an iatrogenic artifact during gross handling rather than a clinically relevant reality: (1) the lack of morphological similarities with known clinical entities; (2) the lack of clinical signs of metastases in our patients (also in the 5 year follow-up period); (3) the association with a counterintuitive, better prognosis for patients with intra-arterial tumor cells than those without; (4) the presence of occasional 'alveolar macrophages' in the lumen of pulmonary arteries adjacent to tumor cells; (5) the detection in resections specimen and (7) its presence in cases of adenocarcinoma in situ.

Moreover, for loose tumor cells in alveolar spaces criteria have been mentioned that might be associated with artifacts such as jagged edges¹¹⁷. These characteristics were not present in the tumor cells located in the pulmonary artery. Of note, rounded

clusters / isolated tumor cells can also be an artifact as well. A possible explanation may be that during cutting of the resection specimen a knife is used. The width of the knife is around 10-15 times bigger than that of tumor cells¹²⁰, inducing a tremendous force with mechanical displacement of tumor cells at the cutting edge. Apparently, the 'empty' arterial vascular lumen forms a niche that is fillable, probably due to the still flexible structure of the pulmonary arterial wall compared to veins and lymph vessels. The example of a peripheral pulmonary tissue fragment in the lumen of a pulmonary artery strongly supports this explanation (see Figure 5, B through D, in Thunnissen et al¹²⁰).

We do not have the intention to call isolated tumor cells in pulmonary arteries of resection specimen 'spread through vascular space', but rather 'spread through a knife surface' as described in a study as 1 of the 4 ex-vivo artifacts in pulmonary resection specimen¹²⁰. The possibility of artifacts has been described in several organs as well, such as in thyroid resections, in which the artifactual displacement of adenoma and non-malignant epithelial cells has been reported¹⁹². But also in resection specimen for prostate cancer it could be a pitfall¹⁹³. In colon cancer, extramural venous invasion was associated with a worse prognosis^{194,195}, in contrast to the presence of intramural venous invasion that revealed a similar prognosis when compared to no venous invasion¹⁹⁴. In laparoscopic abdominal hysterectomy specimens, vascular pseudo-invasion of malignant and benign cells was reported^{136,137}. In one of these studies a suggestion was made that pathologists may be generating postoperative pseudo-invasion by mechanically transporting tumor into vascular spaces during the grossing process¹³⁶.

Recently Metovic and colleagues¹⁹⁶, published an interesting article stating that "STAS is without any doubt, no artifact that can be induced by gross specimen handling." The authors are to be complimented with the careful designed methodology. Nevertheless the effect of cutting (including the manual pressure) combined with the tendency of dissociation of tumor cells, remains open for discussion¹⁹⁷.

In short, there are no defined morphological criteria to distinguish true invasive tumor cells or small clusters from mechanically dragged tumor particles. Taking the morphological, clinical, and literature information, including from other organs, into account, we interpret the presence of tumor cells floating in the arterial lumen detached from the vessel wall and without associated thrombus in resection specimens of primary pulmonary adenocarcinomas in the presented cases as an artifact, although true vascular invasion may occur.

The study's limitations include its retrospective design and the use of available tumor blocks, which may not have included the entire tumor for histopathologic examination, even for small tumors. Additionally, because all cases had a low stage and non-mucinous adenocarcinomas, resection alone may lead to a cure. The study did not conduct multivariate analysis to account for potential clinical confounders, which requires at least 20 events for RFS and OS. However, our study did not fulfill the minimum requirements with only 14 RFS events and 18 OS events. Further larger prospective studies examining also higher stages are warranted.

Conclusions

In most NSCLC resection specimens, CK7+ tumor cells were detected in the lumen of pulmonary arteries. The presence of these tumor cells was not associated with worse OS. The arguments discussed are strongly in favor of an iatrogenic artifact, probably created during gross handling of the resection specimen. It is important to be aware of this artifact as a frequent cause of intravascular tumor cells, observed in resection specimens.



11

Is Spread Through Air Spaces (STAS) an in vivo phenomenon or an inducible artifact?

Hans Blaauwgeers, Chris Dickhoff, Giuseppe Pelosi, Wim Timens, Federica Filipello, Yuko Minami, Giulio Rossi, Erik Thunnissen

Journal of Thoracic Oncology, accepted, October 2022

Since the introduction of spread through air spaces (STAS) as a new invasive pattern in the 2015 WHO classification on non-small cell lung cancer (NSCLC)¹¹², there has been a debate on whether STAS is a true biological phenomenon or mainly an artifact induced by surgical and pathological handling of the resected specimen¹⁷³.

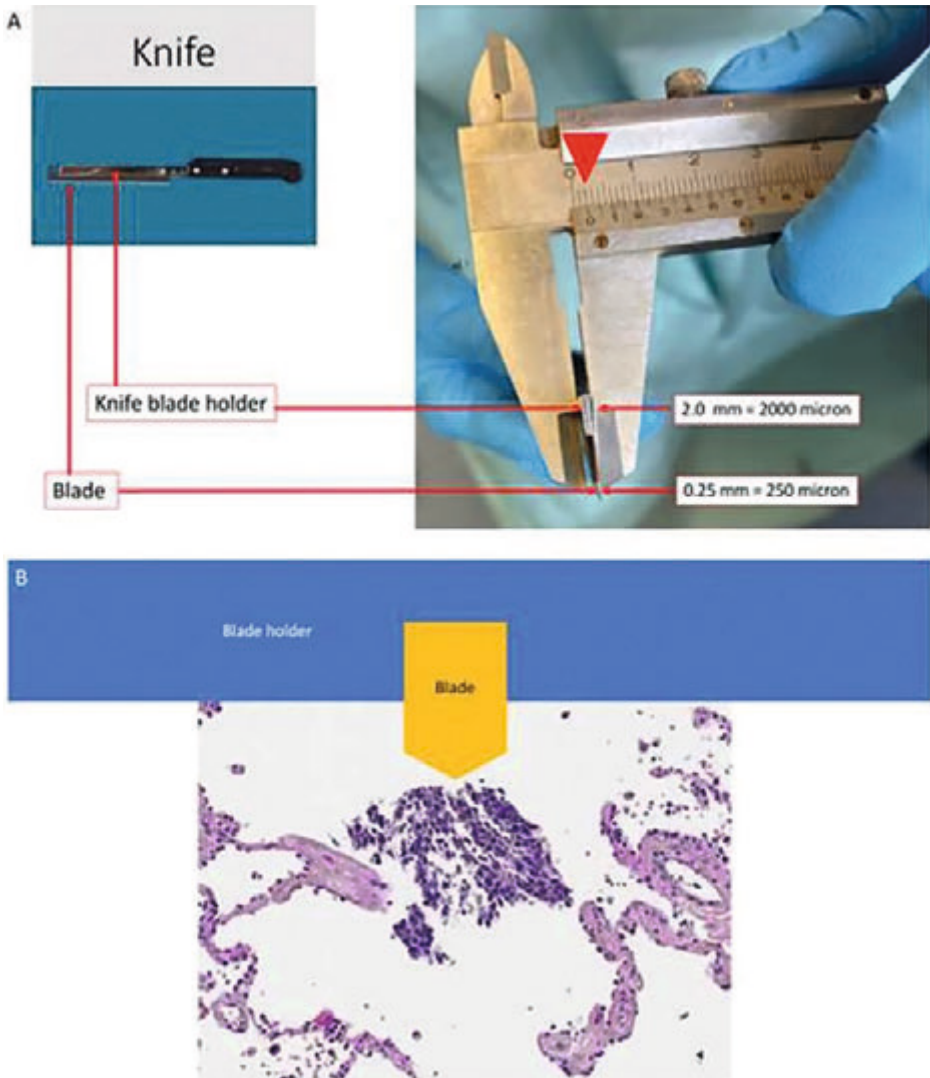
The definition of STAS is blurred by semantics and imaginary interpretations and lack thereof.

In morphological terms pathologists may recognize "loose tumor cells" as single cells or clusters in airspaces. The definition of STAS has several peculiarities and implications¹⁹.

- A) The actual definition of STAS has two components: a morphological and a topological component. In the identification of STAS three so called "patterns" are recognized: single cells, micropapillary and solid tumour cell clusters¹¹⁷. For the topological component one of these "patterns" of intra-alveolar tumor cells need to be demonstrated in a continuum of airspaces containing intra-alveolar tumor cells back to the tumor edge (or viewed from the other direction "beyond the main tumor edge"). However, if the tumour cells fitting in this "pattern" description are localized at a distance from the main tumor (without the continuum), then these tumor cell "patterns" are regarded as an artifact. In other words, although there is no morphological or cytological difference between these "patterns" the topological distribution denotes whether they are interpreted as artifact or STAS. Of note: the term "pattern" is in the lung not synonymous for "morphology".

Beside the above definition other aspects are relevant of the distinction of STAS:

- B) Tumour floaters shown by the presence of clusters of cells often randomly scattered over tissue and at the edges of the tissue section are favoured to be interpreted as an artifact¹¹⁷. However, no diagnostic clues are provided how to make the distinction between when (a few) tumor cells close to the tumor, when they are randomly scattered or "real" STAS. In a more recent publication, the refinement of "more than one tumor cell nest involvement of at least one air space beyond the tumor edge, and continuous alveolar spread from the tumour edge to the furthest STAS."¹⁷¹ was made. The minimum number should be two "cells or clusters".
- C) The presence of "jagged edges" of tumour cell clusters suggested tumour fragmentation or edges of a knife cut during specimen processing. In practice the knife blade has a width of 250 micron and the blade holder a width of 2000 micron (2mm). The blade itself has a width of at least 10x the size of a tumor cell, while the blade holder is broader than 80 tumor cells in a row (Figure 1).

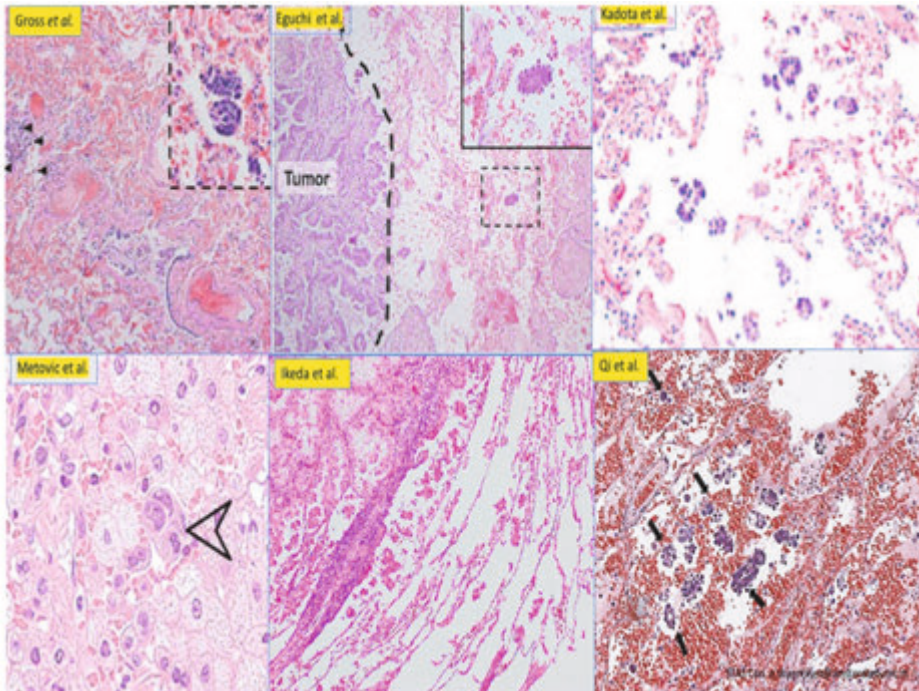


■ **Figure 1.** A: Grossing knife on the left side and the thickness of the blade holder in the caliper on the right side (arrow head). B: The relative size of blade holder (blue) and blade (orange) compared to 'loose tumour fragment' in peripheral lung tissue.

During cutting a prominent force is applied on the section. An unsolved question will be whether the jagged or ragged edges are caused by the knife itself or by the force during cutting. The "jagged" or "ragged" description is at a macroscopic level appealing, like an imaginary cut in a finger, but is at microscopic level taking the broad blade into account only understandable if sheared cutting forces tear clusters apart.

- D) This cutting force may cause benign and malignant cells to be displaced. In the first manuscript macrophages were mentioned¹¹⁷. In the more recent manuscript of the same institute pneumocytes and bronchial epithelial cells were specifically mentioned, as an artifact when displaced from their normal environment^{19 171}.
- E) Linear strips of cells, that were lifted off of alveolar walls are also interpreted as an artifact^{117 171}. In specimen with a fixation delay the epithelial lining may be detached¹⁹⁸.

This is a frequent finding in resection and autopsy specimen. However, the detachment of cells is not restricted to benign cells, as this general effect will also affect tumour cells creating individual tumour cells. This may lead to an overinterpretation of STAS.



■ **Figure 2.** A compilation made of STAS images in 6 different scientific publications (Gross¹⁹⁹, Eguchi²⁰⁰, Kadota²⁰¹, Metovic¹⁷⁵, Ikeda²⁰² and Qi²⁰³). Note: in the alveolar spaces are beside the “loose tumour cells” extravasated erythrocytes discernible.

- F) The elephant in the room is in this context the erythrocyte: a benign cell that is present in practically all publications that contain microscopic examples of STAS, in the neighbourhood of the as STAS interpreted cells (Figure 2). Most pathologists will see these erythrocytes and immediately skip these for diagnostic purpose and mentally regard this as artifact. Recently, spreading of neuroendocrine epithelial cells and erythrocytes were regarded as an artifact¹⁷⁴. The question is here: why are the erythrocytes interpreted as artifact and the adjacent loose tumour cells as STAS?

In short, these considerations around the definition of STAS is actually based on topology of at least two “loose tumor cells”, which are on itself on morphological/cytological grounds indistinguishable from what the leading authors call “artifacts”. In addition, inconsistency in interpretation of loose erythrocytes from adjacent tumour cells is arbitrary.

Reproducibility of STAS in frozen section

To be useful for pathology diagnosis in daily practice, the criteria for that diagnosis have to be clear allowing a pathologist to be consistent in time (intra-observer reproducibility) as well as lead to the same diagnosis between different pathologists (inter-observer variability). Studies on interobserver reproducibility can be divided in local and global approach: studies reporting on reproducibility between a few pathologists within an institute or within a region and studies involving pathologists from around the globe. The latter will be most informative.

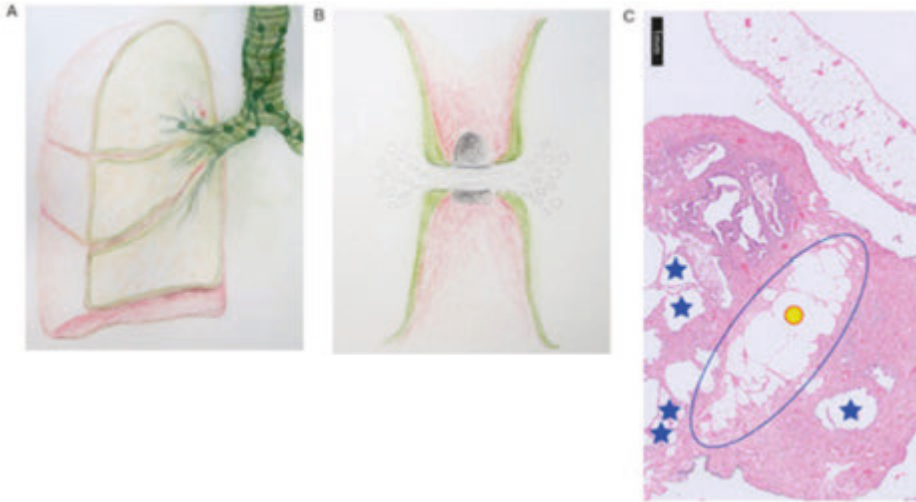
A possible application of STAS could be the use in frozen sections. The sensitivity for STAS in four studies ranged from 55 to 86%^{204 205 172}.

One study mentions a worrying lack of consistency in sampling: STAS was only consistently present in i) frozen section, ii) paraffin section of frozen section and iii) other tumor sections in 39% of the cases¹⁷². The reproducibility studies of STAS assessment in frozen sections revealed kappa scores of 0.51 and low 0.34, respectively^{204 205}. The concerns of STAS analysis in frozen sections are clearly expressed in the summary of the paper by Villalba and colleagues, which are regional pathologists with specific interest in pulmonary pathology: “As current accepted definitions for STAS and artifactual clusters are variably interpreted by pathologists, more precise criteria should be established and standardized, before the assessment of STAS can be implemented globally in the intraoperative setting to aid surgical decision making”²⁰⁴.

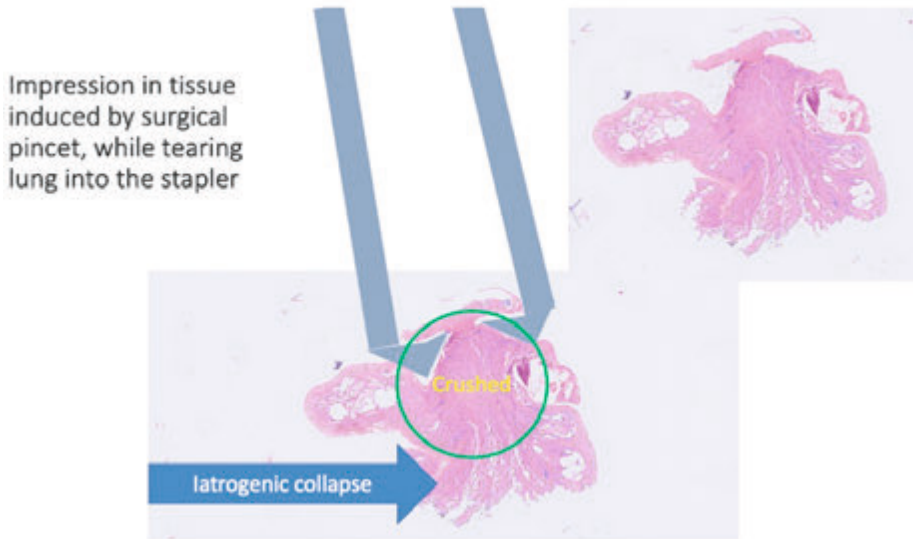
Alternative explanation for the occurrence of loose tumour cells

Given the tendency of dis cohesion in malignant cells and the notion that the consistency of the cells is like a raw egg without a shell, other explanations for spreading of tumor cells may be the surgeon’s i) hand, ii) instrument (Figure 3 and 4), iii) (eventual) localization procedure, iv) tearing tissue through a pinhole in video assisted thoracic

surgery (see below, 'displacement during surgery handling'), v) iatrogenic collapse²⁰⁶, the pathologist's vi) hand and vii) knife²⁰ (see below 'pathology aspects').



- Figure 3.** A: Cartoon with cross section of the right lung. Note that under the pleural surface is a network of lymph vessels (green) present. Lymph vessel also accompany the pulmonary artery towards the centre of the lobe. B: Cartoon of clamp compressing during the clamping. The lymph in between the clamps will be pressed to both sides, causing dilatation and extravasation of lymph in surrounding tissue (interstitium and alveoli). C: Histological example of clamping artifact in an open lung biopsy. The blue oval denotes the septal area with the stretched lymph vessels and interstitial lymph. On the upper left side iatrogenic collapsed alveoli and interstitial inflammatory cells are visible. The asterisks denote the dilated alveolar spaces, probably due to the clamping. Note that a difference between empty space filled with lymph or air cannot be made in histological slides. The similarity in overdistension between the alveoli and adjacent septum strongly supports the interpretation of intra-alveolar lymph. The yellow circle denotes the normal size of the lymph vessels. Of note, the area covered by the yellow circle approximates the size of a cluster of around 50-100 tumour cells.



- **Figure 4.** Example of an impression by a surgical pincet in an open lung biopsy taken for diagnosis of interstitial lung disease. The pincet marks are visible with adjacent crushed tissue and iatrogenic collapsed alveolar walls.

Displacement during surgery handling

Another possible cause of iatrogenic displacement of tumour cells is manipulation of the tumour during surgery or grossing of the fresh (unfixed) specimen. A 'no touch' technique is impossible during lung surgery or pathology grossing.

During surgery not only clamping may be a cause, but also manipulation with a hand or an instrument (e.g., for tearing parenchyma into the clamp) (Figure 4). Moreover, opening of the thorax will abrogate the negative pressure between the parietal and visceral pleural leaves. This will reduce the physiologic lymph flow and thereby increase the interstitial pressure. The deflation process may have an incremental effect on the (also intratumorally) interstitial pressure. This process, combined with possible manipulation, may lead to an increase of circulating tumour cells (CTCs)²⁰⁷. Although studies on CTC's during surgery for NSCLC collect blood samples at various sites (peripheral vein, radial artery during anaesthesia, pulmonary draining vein in the beginning and at the end of resection) and examine different biomarkers, the findings point more or less in the same direction: increase in CTCs during surgery^{208 209 210 211 212 213}, increase in clusters of CTC^{128 212 214}, association with adverse clinicopathologic parameters: higher stage^{215 212}, microscopic lymphatic tumour invasion²⁰⁹, N+ vs NO²¹⁵, reduced disease free survival^{216 217 218}. Several manuscripts mention the word manipulation explicitly, expressing awareness in the surgical community. Moreover, the finding of normal epithelial cells in the pulmonary vein was also reported in a few

patients and was considered an additional argument for its cause by manipulation during surgery²¹⁹.

In short, the unwelcome possibility and understandable concern exist that tumour-cell release during surgery contributes to metastatic colonization²⁰⁷. At least some force is executed during manipulation by the surgeon.

Pathological aspects of STAS

In the proposed STAS concept it is argued that STAS tumour cells can attach to the alveolar walls rather than appearing free floating, as seen on the two-dimensional sections, thus suggesting that tumour cells detach from the main tumour, migrate through air (= alveolar) spaces, and reattach to the alveolar walls through vessel co-option, allowing them to survive and grow²²⁰. The main question is if the provided arguments are persuasive enough to definitively accept STAS as a biological property related to tumour growth and invasion.

The argument of 3-dimensional analysis and loose tumour cells

In 2012 Onozato and colleagues reported a 3-dimensional analysis of four adenocarcinoma resection specimens, and in two cases they found islands of tumour cells being detached in alveolar spaces that had not been described in any of the existing adenocarcinoma classifications¹³². In serial sections islands of tumour cells extended into a deeper area of the tissue and were interconnected with each other and the main tumour with a solid pattern that was surrounded by the islands. In other words, they found seemingly detached tumour cells localized at some distance from the main tumour, which were connected to the main tumour in a tentacular way. In a subsequent study they extended the number of analysed cases with a mainly 3-dimensional approach and reported a prognostic relevance to this finding¹¹⁵.

Yagi and colleagues performed 3-dimensional image analysis of serial sections from 4 archived formalin and paraffin embedded samples by using different stains: haematoxylin and eosin (H&E), immunohistochemistry (IHC), and immunofluorescence (IF) staining²²⁰. These sections were cut from retrospectively collected specimen with iatrogenic collapsed tissue. Although the results section mentioned "the STAS cells are focally in close apposition to the pre-existing capillaries in the alveolar septa", in the accompanying figure the text is extended with the interpretation" (i) *attached* to the alveolar wall, (ii) *replacing the normal pneumocytes*" as well as "*attached to and (iii) penetrating the alveolar wall*".

Actually, at least one of the reasons that the 3-dimensional study was performed was related to the question how these loose tumour cells get their energy, while seemingly free floating in the air space. The authors argue that focally there is a close approximation of some cells with the pre-existing alveolar wall and they applied for this observation the biological term 'vessel co-option'. Vessel co-option was previously defined as incorporation of pre-existing vessels from surrounding tissue by cancer cells as opposed to generating new vessels (= angiogenesis)^{114 221}. Remarkably, the lack

of signs of the suggested “vascular co-option” seen in most cases of purported STAS, makes this observation unlikely to be a biological constant phenomenon.

Possible alternative explanations

For the observation “(i), the attachment to the alveolar wall”, gravity is likely to play a role, causing detached tumour cells to get in touch with alveolar walls. The term “in close approximation” to the alveolar wall, is scientifically probably more accurate than “attached” to the alveolar wall. For phrase “(ii) regarding replacement of pneumocytes”, an image is provided with a magnification²²⁰, that by itself is insufficient to judge the replacement of pneumocytes type I, because the alveolar wall including the pneumocytes type I at the gas exchange interface is very thin (between 0.2 and 0.6 μm). In the published figures, type I pneumocytes as an alternative explanation may be present in between the endothelial cell staining and the tumour cells. Thus, the scientific proof that IHC stains demonstrate the focal absence of pneumocytes at the “attachment points” is clearly lacking.

For the phrase “(iii) dealing with the penetration of the alveolar wall”, in the provided image, an alternative explanation could be that this discontinuation may well correspond to physiological pores of Kohn²²².

In our opinion the suggestion that “tumour cells detach from the main tumour, migrate through air spaces, and reattach to the alveolar walls through vessel co-option, allowing them to survive and grow” is an overinterpretation or misconception, which is not incontrovertibly supported by the presented data.

The argument of retained tumour cells in the unresected lobe after segmentectomy

In a recent study Gross and colleagues observed that occult STAS tumour cells can be detected in the lung tissue of the remaining unresected lobe after segmentectomy¹⁹⁹. Ten patients were examined who initially had a local resection with STAS and subsequently another local resection or a completion lobectomy. In all ten patients, STAS was found in the additional resection. As different knives were used in the cases a strong argument is put forward against the pathologist’s knife as a plausible cause. The authors concluded that “our study provides evidence that STAS is not an ex-vivo artifact of the pathologic tissue-grossing process and adds to the growing evidence that STAS is an in vivo biological process.” However, if there are other explanations, the last interpretation is definitely a jump to far.

An alternative explanation

At this point it is essential to realize the physiology of the lymph flow in the lobes. A cross section of a lobe with subpleural lymph vessels is shown in Figure 3A. Columns of lymph are filled during inhalation in the lymph vessel, which are subsequently reduced in length during exhalation, pushing the lymphatic flow centrally, where the larger lymph vessels have valves. These prohibit backflow during the next inhalation. As the

lymph vessels have their anchoring fibers attached to the during inhalation stretched elastic fibers, the negative pressure in the lymph vessels sucks the intercellular oedema into the lymph vessel lumen¹²⁰.

During a limited resection the surgeon clamps part of the lobe. The normal size of the clamp is up to 6 cm long and 1.2 cm width (Ethicon parenchyma stapler, Johnson & Johnson, USA; ENDO GIA™ Ultra, Medtronic, Eindhoven, NL))

The clamping (e.g., during segmentectomy, wedge resection), by pressing the tissue in between the clamps, will be likely to cause a lymph flow to both sides of the clamp (see Figure 3B). This clamping of pulmonary parenchyma will cause an artifact upon histology: beside iatrogenic collapse of the alveoli, the lymph between the clamps is pressed into the adjacent parenchyma, causing so called “clamping edema” (see Figure 3C)^{120 223}. If a lymph vessel has tumour cells in the lumen, they may be displaced by the surgical clamping force quite a distance (also in adjacent alveolar spaces). In the study of Gross and colleagues a cartoon shows the location of the tissue sampling for microscopy: close to the staple margin. This location perfectly matches the area with the forcefully clamped dispersed lymph.

In the study of Gross and colleagues 5 out of the 10 patients had clear lymphovascular invasion and an additional patient had pleural invasion. Other conventional morphological signs of invasion were not mentioned (such as bronchial, arterial and stromal invasion). IHC analysis (e.g., D2-40) supporting possible lymph vessel invasion in the remaining cases was not performed.

In addition, the detailed cytonuclear image of STAS in the completion lobectomy shows condensed chromatin and eosinophilic cytoplasm, more looking like a proapoptotic state than a vital tumour. In this respect, a direct comparison of the STAS-assigned tumour cells in the completion lobectomy with the tumour cells of the initial resection would be useful. In addition, extravasated erythrocytes are abundantly present in the shown examples (see paragraph below). Compared to previous publications of this institute^{200 117} the 10 cases in the study of Gross and colleagues¹⁹⁹ is biased towards lymph vessel invasion.

Considering all arguments, clamping displacement is a more likely explanation for tumour cells seen in the completion lobectomy specimen. In addition, if vascular cooption was essential for tumour cell to survive and grow (as previously stated by the same research group), such a phenomenon should be somehow recognizable on the provided microscopic pictures documenting STAS, but this is not persuasive by showing small inserts inside them. Another observation is that elapsed time between primary and additional (subsequent) resection for all investigated patients was immediate to one month later, with STAS occurring in completion specimens upon wedge resection of primaries. This is again in line with STAS as an artifact via the underrecognized role of lymphatic vessel drainage alterations upon surgical clamping, as above stated.

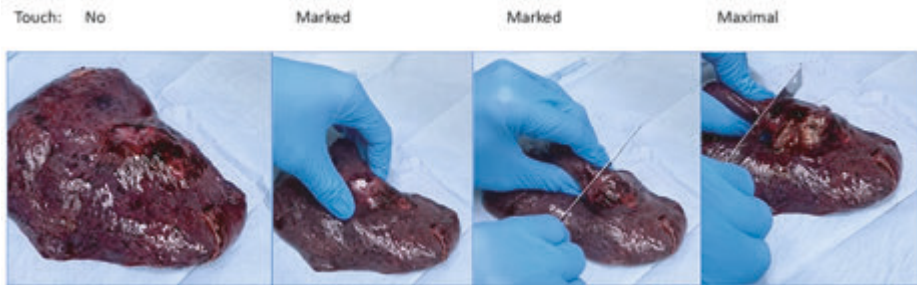
Displacement during pathology handling

The use of a knife during grossing has been reported as a possible cause of displaced tumour (and benign) cells in tissue¹²⁰. As a reaction upon STAS appearing in the WHO classification¹⁹, a prospective study by Blaauwgeers *et al.* was performed about loose tumour cells and tissue sampling from a proximal and distal side from cutting direction¹⁶². The authors hypothesized that, if the grossing knife (blade thickness 250-micron, blade holder thickness 2000 micron = 2 mm.) was a possible cause of STAS, the first block would have less displaced tumour cells (tumour cell size range around 20-40 micron) than the other three blocks in sequence when the same knife was used. They showed in this multi-institutional study significantly more displaced tumour cells in the other three blocks compared to the first sampled tissue fragment (*i.e.*, tissue cut by the knife before the knife reaches the tumour). During grossing there was no obligation to clean or change the knife.

Subsequently, a carefully designed study of Metovic and colleagues¹⁷⁵ was published, where a new clean blade was used for each cut, and the sequential analysis of fresh and formalin-fixed specular samples containing the lung tumour and the peritumoural parenchyma performed. No difference was found between the proximal and distal samples in the cut of the fresh sample, nor in the cut after 24 hours fixation.

One of the issues that does not cause a difference between studies of Blaauwgeers *et al.* and Metovic *et al.* is the method of counting. Metovic and colleagues used the method of Kadota as well as the method used by Blaauwgeers and colleagues and showed almost the same scores (correlation coefficient >0.90)²²⁴, indicating that the differences in reported STAS data from other studies cannot be attributed to differences in these counting methods.

This study of Metovic and colleagues claims to perform vertical cuts only by the pathologist^{175 224}. However, we have the experience that perfectly vertical cuts are practically impossible to perform because of resistances generated by entire cutting edge (a knife as a second kind of lever) and the soft consistency of lung parenchyma, preventing thin slices to obtain (it is not just like a paraffin block fixed on a microtome with moving blade in the same direction of cutting), since there is always a transversal movement necessary to sequentially reduce in single cutting lines the tumour mass as a whole, sometimes even accidental and imperceptible subjectively, which is thus inherent to cutting procedure by itself¹⁹⁷. It is impossible to account for vertical and lateral-transversal cut, even if it is minimal and apparently controlled. It is likely that at the tumour edges the tumour cells have the soft consistency of a raw egg or like an amoeba, and are prone to be dissociated under minimal pressure while cutting or by unavoidable traumas even occurring during the preoperative biopsy process. In Metovic's study another possible source of detachment is the manipulation by the pathologist itself while handling¹⁷⁵, sampling or simply describing the sample (touch and palpation are commonly performed while grossing (Figure 5). Likely, interfering cut procedures are probably the last ones to intervene.



- **Figure 5.** Lobectomy specimen with elevated pleura above the tumour and different moments of gross cutting. Photos made in Italy received with the courtesy of M. Papotti M.D. PhD. and Alessandra Pittaro, M.D. Note that with the intention to cut in the vertical direction only, the distance between two fingers of the left hand holding the tumor mass is getting progressively smaller, indicating increasing pressure on the tumor.

In a third prospective study, Xie and colleagues examined 83 patients and collected an upper and a lower block²²⁵. In 45 patients STAS was noted, but only consistently present in upper and lower block in 60% of the cases. In the remaining 40% STAS was only present in the lower block. Remarkably, Xie and colleagues interpreted in these (inconsistent) cases the presence of STAS as an artifact: in patients with real STAS, the upper blocks still had fewer fields of STAS compared to lower blocks ($p=0.016$), emphasizing an effect of the cutting direction. In addition, EBUS needles may also displace tissue fragments²²⁶.

In short, the prospective studies on sampling blocks related to the gross cutting direction at the pathology laboratory is still a matter of debate: beside the needle displacement two studies find more loose tumour fragments in the blocks after cutting through the tumour, while the other did not show this difference.

Biology of loose tumour cells

Wild type epithelial cells are attached to each other with adhesion molecules. Detachment will lead to apoptosis. Adhesion molecules play a role in the apoptotic process. In pulmonary adenocarcinoma downregulation of E-Cadherin is a frequent finding with increased risk for metastases, which is supported in model systems and leads to a reduction in cohesion, a characteristic of malignant cells, what is also recognized in other organs. For example, discohesion of tumor cells in cytological samples of breast cancer is used as a criterium for malignancy, not as a prove for invasion, as ductal carcinoma in situ may show the same dissociation. Remarkably, in the lung the discohesion of loose tumor cells is, if interpreted as STAS, in the WHO 2021 classification arbitrarily interpreted as invasive¹⁹.

The discohesion is a clear morphological characteristic of the micropapillary pattern. Peculiar is in this context is that in the study of Yagi and colleagues E-cadherin

remained present²²⁰ a feature fitting more with radial non-invasive growth as seen in lepidic featuring adenocarcinoma of either precursor or outgrowth type.

STAS and prognosis

Since STAS was included in the WHO classification of 2015, close to 200 manuscripts have been published on this subject.

Many of them show a significant association with recurrence free and overall survival.

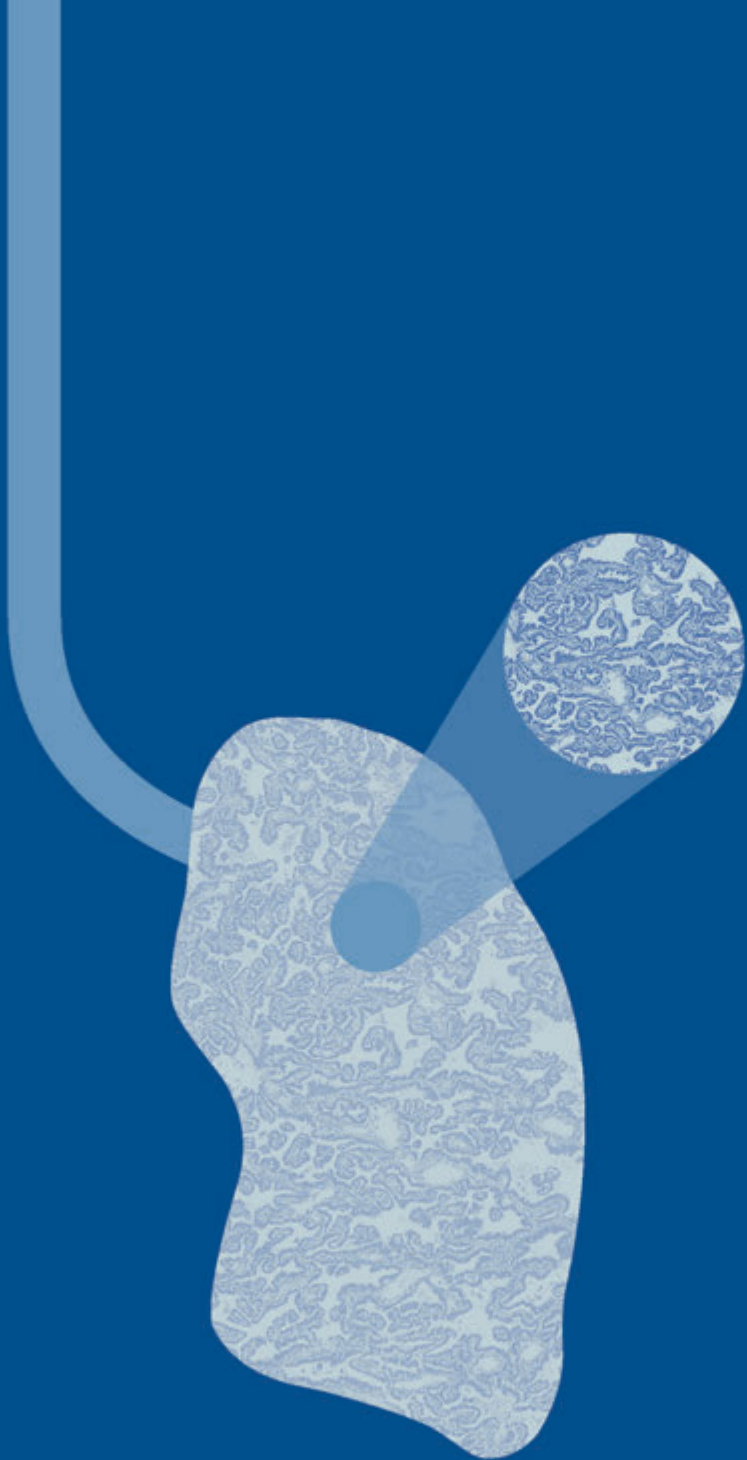
Not surprisingly, STAS is significantly associated with many of the known adverse prognostic factors: tumour size^{117 227 143 133 228 229 230 231 232 233 234 235 236 237 238}, lymph node metastases^{236 239 240 241}, lymphovascular invasion, vascular invasion^{133 228 229 232 234 235 236 242 134 243 244 245 246 247}, micropapillary and solid adenocarcinoma growth patterns^{228 235 248 249 250 251}. This is not surprising if STAS, whether biological or artefactual, reflects poorly differentiated adenocarcinoma with easy decohesion of tumour cells, likely because of reduced intercellular adhesion. Importantly, STAS was in an extensive study about grading in 3 independent cohorts in comparison with other histological parameters NOT selected as relevant parameter for the IASLC grading system²⁵². This substantially weakens the application prospect of STAS as prognostic factor.

In summary, there is no incontrovertible evidence that STAS as currently presented, is indeed a biological phenomenon and not rather an inducible artifact with inconsistency in sampling. On top of this, the reproducibility of its presence is at best moderate. Inclusion of STAS in the WHO classification as an established and widely agreed-upon phenomenon is premature¹⁷³. STAS, including the underlying biology of dissociation, need further investigation.



Part III

**Collapsed adenocarcinoma in situ;
the challenge of defining invasion**



12

Elastin in pulmonary pathology: relevance in tumors with lepidic and/or papillary appearance. A comprehensive understanding from a morphological viewpoint.

Erik Thunnissen, Noriko Motoi, Yuko Minami, Daisuke Matsubara, Wim Timens, Yukio Nakatani, Yuichi Ishikawa, Ximena Baez-Navarro, Teodora Radonic, **Hans Blaauwgeers**, Alain C Borczuk, Masayuki Noguchi.

Histopathology. 2022 Feb;80(3):457-467. doi: 10.1111/his.14537.

Abstract

Elastin and collagen are the main components of the lung connective tissue network, and together provide the lung with elasticity and tensile strength. In pulmonary pathology, elastin staining is used to variable extents in different countries. These uses include evaluation of the pleura in staging, and the distinction of invasion from collapse of alveoli after surgery (iatrogenic collapse). In the latter, elastin staining is used to highlight distorted but pre-existing alveolar architecture from true invasion. In addition to variable levels of use and experience, the interpretation of elastin staining in some adenocarcinomas leads to interpretative differences between collapsed lepidic patterns and true papillary patterns. This review aims to summarise the existing data on the use of elastin staining in pulmonary pathology, on the basis of literature data and morphological characteristics. The effect of iatrogenic collapse and the interpretation of elastin staining in pulmonary adenocarcinomas is discussed in detail, especially for the distinction between lepidic patterns and papillary carcinoma.

Introduction

In pulmonary pathology, elastin staining is used to variable extents in different countries. In some settings, it is used to distinguish collapsed alveoli from papillary adenocarcinoma. This practice is not uniformly accepted, and, as a result, this has not been incorporated into the World Health Organization (WHO) definitions of lepidic and papillary adenocarcinoma.

The theoretical basis for the use of elastin staining is that normal lung tissue and pleura have elastic tissue that helps to delineate the histology of these lung structures. As a result, pathological conditions involving the lung and pleura can alter this architecture, and this alteration can be exploited diagnostically. However, there are differences in opinion on the value of the presence or absence of elastin once normal lung tissue has been altered by disease. In pulmonary adenocarcinoma, some use the presence of elastin as an argument for pre-existing structure [implying the diagnosis of adenocarcinoma *in situ* (AIS) or a lepidic pattern as part of a minimally invasive adenocarcinoma or lepidic-predominant adenocarcinoma (LPA)] to highlight the retention of existing architecture. Others emphasise the lack of elastin as an argument for papillary carcinoma, whether by destruction of elastic tissue or the lack of it in a new proliferation; in either event, this pattern would indicate invasion. These considerations are critical, as a collapsed lepidic pattern would not be included in the T stage assessment of invasive size. To complicate matters further, the term 'collapse' is used in different ways in the literature.

This review aims to describe the morphological structure and function of elastin in normal and diseased lung, and apply this to unravel interpretation issues mentioned above in pulmonary adenocarcinomas.

Elastin components and structure

The human lung is an intricate organ whose architecture includes the vasculature, conducting airways, and terminal airspace compartments, which need an elastic and balanced extracellular matrix to support repeated movements of extension and recoil throughout life²⁵³. Elastin and collagen are the main components of the lung connective tissue network, and together provide the lung with elasticity and tensile strength²⁵⁴.

The extracellular matrix has been defined as the structural network of collagens, elastin, glycoproteins and proteoglycans surrounding stromal cells and underlying endothelial and epithelial cells. In addition to having structural properties, the extracellular matrix functions as a dynamic modulator of various biological processes¹. This is accomplished through the selective binding and subsequent release of growth factors and cytokines, and through its interaction with cell surface receptors^{255 256}. Although collagen and elastic fibers are the major constituents of the extracellular matrix, the overall function is defined by the interrelationships between all of the various components.

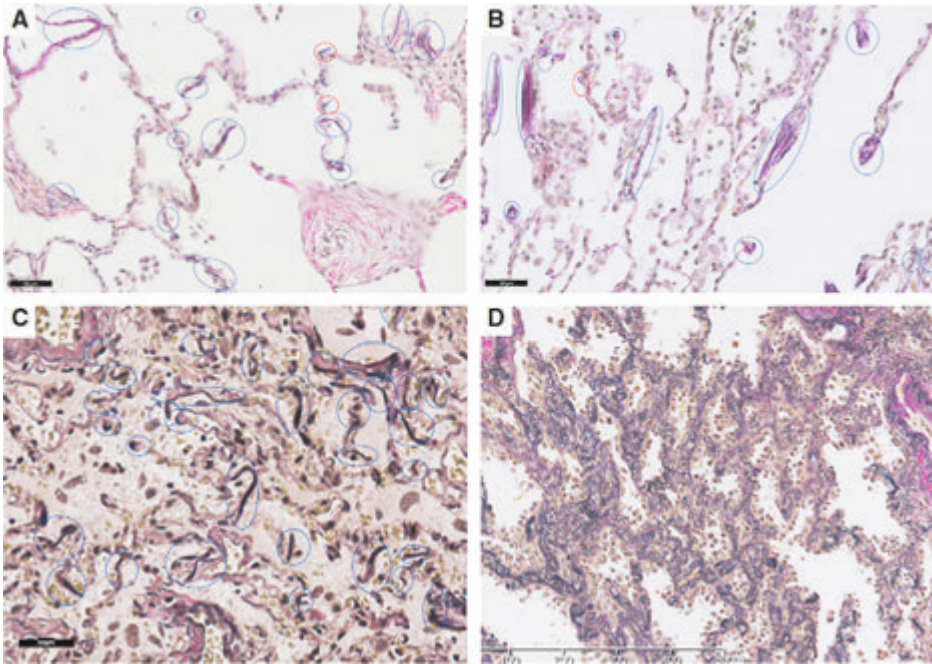
Tropoelastin is the soluble monomer precursor of elastin, and is secreted as a 60-kDa mature protein produced, through variable splicing, by diverse elastogenic cell types in the lung, including chondroblasts, myofibroblasts, mesothelial cells, and smooth muscle cells⁵. Tropoelastin self-aggregates on the cell surface before being deposited onto fibrillar microfibrils and crosslinked to form elastic fibers, in a complex multistep process collectively referred to as elastogenesis^{255 257 258 259}. Tropoelastin has a unique structure, possessing a mosaic of domains in various states of order. The free energy landscape of tropoelastin encompasses multiple energy minima with no sizeable barriers between them^{257 260}. The molecule transitions easily between these low energy minima, giving rise to a conformational ensemble that comprises a wide array of structurally related but dissimilar states. This allows flexibility at a molecular level, providing, at the end of elastogenesis, the functional elasticity required in lung parenchyma for breathing, i.e., maintaining the patency of alveoli, small airways, and adjacent lymph vessels.

Elastin expression occurs over a narrow window of development, beginning in mid-gestation and continuing at high levels throughout the postnatal period²⁶¹. The mature elastic fiber is an insoluble and stable protein with a very long lifespan of ~ 80 years^{262 263}, consistent with the lack of tropoelastin expression in adults (animal model²⁶¹). Furthermore, elastin is extensively distributed in most human lung compartments, including the pleura, alveolar septa, large vessels, and cartilage²⁶¹. The crude connective tissue dry weight concentrations of elastin are 20-30% in the respiratory parenchyma, 7-16% in the pulmonary blood vessels, and 3-5% in the airways.

The elastic fiber scaffold is known to be an important supportive structure of the normal alveoli⁹. Alveolar size increases with age²⁵⁴. The delicate three-dimensional network forms a looping system encircling the alveoli and alveolar duct, and ensures that applied forces will be transmitted equally to all parts of the lung²⁶¹.

In functional terms, during exhalation the elastic fibers recoil and maintain a regular, spaced alveolar structure and the diameter of the small airways. A histochemical elastic fiber stain may be useful for recognition of the underlying pulmonary architecture.

Two forms of elastic fiber have been described in ultrastructural and three-dimensional image studies: thick and thin elastic fibers. The main framework of the alveoli is constructed of thick elastic fibers, forming the alveolar orifice and also the sides of the polygonal alveoli where three neighboring alveoli join. Thin elastic fibers branch from the thick elastic fibers intercrossed in the alveolar wall, and support the alveolar wall^{264 265 265}. Type II pneumocytes are located along thick elastic fibers²⁶⁵.



- **Figure 1.** A,B, Two examples of elastin staining in a non-malignant peripheral lung with minimal iatrogenic collapse (perfusion-fixed). A, a 31-year-old male with organizing pneumonia. B, a 39-year-old female with invasive mucinous adenocarcinoma. C, a specimen submerged in fixative with prominent iatrogenic collapse. The diagnosis was made on other sections of the same resection specimen. Circles (blue) encompass elastic fibers. Note: (i) the reduction in the amount of air because of collapse; (ii) that the number of discontinuous elastin fragments is dependent on the number of alveolar cross-sections in the field of view; (iii) that the alveolar cross-sections sometimes result in a pseudopapillary appearance; and (iv) that if one were to replace all pneumocyte type I cells lining the alveolar walls with a monolayer of cylindrical tumour cells, the proper diagnosis would be adenocarcinoma in situ (AIS), whereas, in terms of patterns, this may be perceived as a mixture of a lepidic pattern and a papillary pattern. The use of an elastin stain would reveal the underlying architecture of the preexisting lung, as proven by the inherent distribution of fragmented elastic fibers, including some of the alveolar wall parts without elastin. D, Elastin staining of AIS showing the pre-existing alveolar structure with mild iatrogenic collapse (perfusion-fixed). Note the continuous sheets of elastin (compatible with Noguchi type B¹⁰).

In elastin-stained histological 3-5- μm sections, thick elastic fibers may easily be recognized, whereas thin elastic fibers cannot readily be discerned. The light-microscopic literature on elastin usually deals with thick elastic fibers, which will be subsequently referred to as 'elastic fibers'. In two-dimensional histological sections of normal alveolar walls, the elastic fibers appear discontinuous curvilinear or dot-like^{254 266} (Figure 1A-C). It is of note that these seemingly fragmented elastic fibers form part of the three-dimensional elastin network (scaffold); that is, in serial sections they are connected to each other.

Pathophysiology of elastin

Alveolar myofibroblasts are located underneath the alveolar epithelium, and are defined by expression of α -smooth muscle actin and the production of elastin and collagen²⁶⁷. In alveolar development, deposition of elastin is an essential process for septation. Elastin allows alveoli to stretch during inhalation²⁶⁸. After birth, elastin forms a matrix, serving as a scaffold on which alveolar myofibroblasts adhere and mark the sites of secondary septa²⁶⁷. Cyclic mechanical stretch is important to maintain the alveolar myofibroblast state²⁶⁹. In a model system of pulmonary fibrosis, the mechanical stretch is reduced and myofibroblast differentiation is increased²⁶⁹. Moreover, pre-existing elastin has been shown to induce an increase in extracellular elastin production by myofibroblasts. This explains the focal increase in the amount of elastin in areas with pre-existing elastin. As well as the increased expression of elastin, expression levels of the $\alpha 1$ chain of type V collagen and tenascin C are increased²⁶⁹. In chronic obstructive pulmonary disease, abnormal fibulin-5 metabolism is suggested to play a role in disturbed elastogenesis²⁷⁰.

In pleuroparenchymal fibroelastosis, the combination of increased numbers of subepithelial myofibroblasts and increased amounts of elastin in continuous sheets was demonstrated in areas with mild non-specific interstitial pneumonia²⁷¹. This distribution of elastic fibers is similar to that seen in some cases of AIS and lepidic adenocarcinoma. These findings suggest that: (i) in AIS and non-specific interstitial pneumonia, an interaction between epithelial cells, extracellular matrix components and subepithelial myofibroblasts leads to increased elastin production; and (ii) the light-microscopic demonstration of continuous elastic fibers (corresponding to 'elastin sheets' in the third dimension) cannot be used as a criterion for invasion.

In pulmonary adenocarcinomas, Matsubara *et al.*²⁷² emphasized two locations of myofibroblasts, i.e. the above-mentioned alveolar subepithelial myofibroblasts and the stromal myofibroblasts, often in areas of central fibroelastosis. The subepithelial myofibroblast pattern is associated with a favorable prognosis²⁷³.

Terminology of elastin degradation

In 2000, Fukushima *et al.* used the term 'degradation of elastin' in an electron-microscopic study for the examination of pulmonary carcinomas. On ultrastructural examination (high magnification), some thick elastic fibers showed vacuolar changes and electron-dense granular deposits²⁷⁴. These changes were called 'degradation' of elastic fibers. Thus, the term 'elastin degradation', in this sense, constitutes an electron-microscopic definition of individual fibers, referring to features that are not readily recognisable with light microscopy.

In pulmonary adenocarcinomas, Eto *et al.*²⁷³ performed a light-microscopic histological image analysis study using elastin stains, and noticed, in the central fibrotic 'invasive' part of peripheral adenocarcinomas, a disrupted pattern of the elastotic framework related to invasion and a poor prognosis. It is of note that they described, in the periphery of the tumour, a thin-walled elastic framework similar to normal alveolar walls. Fukushima *et al.*²⁷⁴ compared elastin in non-malignant peripheral lung with that

in well-differentiated adenocarcinomas, and found a normal pattern or an increase in the amount of elastin, but not a decrease in the latter.

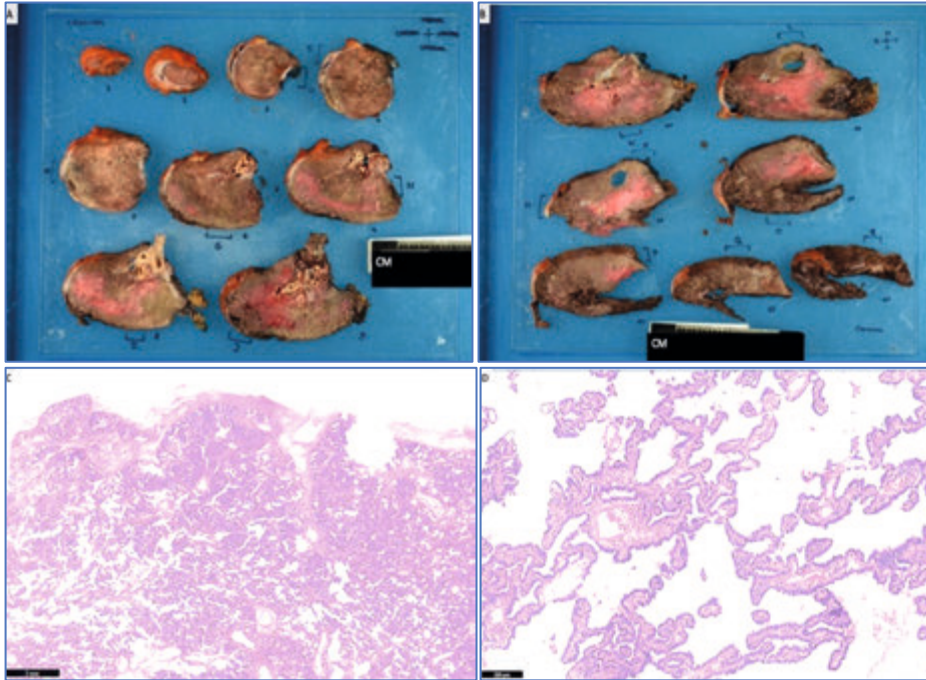
Overall, these findings indicate that normal lung and lepidic-pattern tumours either retained normal elastin or showed thick elastin, but that disruption/degradation of elastic fibers occurred in central fibrotic areas only, in association with invasion.

Collapse

In the pulmonary pathology literature, two different descriptions have been used for 'collapse'. In 1985, the term 'collapse' was used in adenocarcinomas with a central 'scar', showing a recognisable collapsed alveolar framework within condensed elastic tissue on elastin staining. With haematoxylin and eosin staining, the condensed elastic tissue could be mistaken for fibrosis. In fact, elastin staining emphasised the preponderance of elastic over collagenous tissue²⁷⁵. This was also noted by Shimosato *et al.*^{276 10} and supported by Yamashiro *et al.*²⁷⁷: the central part of the tumour shows collapsed alveolar spaces (absence of air) with condensation of elastin. However, these condensations of elastic fibers with some fibrosis are not infrequent. In this setting, fibrosis is defined as collagenous²⁷⁸, whereby elastosis is not an essential component of the fibrotic reaction. In the Japanese literature, the central part may be fibrotic as well as elastotic, whereas, in the above-mentioned 1985 study, this central area was characterized by elastin condensation without fibrosis. This meaning of collapse is a 'biological' collapse with loss of alveolar architecture. This alteration is present before the surgical procedure, and does not include the area outside the scar with peripheral lepidic growth and possible increased alveolar wall thickness.

Another definition of collapse¹²⁰ involves 'iatrogenic collapse'—i.e. an artefact of deflation—whereby the alveolar air, vascular blood and lymph volumes are reduced during surgery. Owing to the lack of negative pressure between the pleural leaves, the natural recoiling of the elastic fibers places alveolar walls in close proximity to each other¹²⁰. This effect can be seen as an 'iatrogenic' or 'mechanical' 'collapse'; here, the alveolar architecture is maintained but is harder to evaluate morphologically. Examples of collapse involving areas with lepidic growth have recently been published²⁷⁹. The effect of iatrogenic collapse can be reduced during gross handling, e.g. by bronchial and/or transpleural perfusion with formalin. The distance between the alveolar walls will be enlarged by the perfusion process, but the effect of the iatrogenic collapse may not be fully mitigated. The enlarged formalin-containing spaces between the alveolar walls are, light-microscopically, the equivalent of air-filled (clear) spaces. Gross handling differs between laboratories throughout the world: Japanese laboratories^{280 273 281} and some laboratories outside Japan perform perfusion fixation¹⁹⁸, whereas many pathology laboratories in the world will have the influence of prominently collapsed lung tissue in the diagnostic process. Perfusion fixation of the human lung has been performed for research^{282 283 284 285 286} and clinically²⁸⁷ in the past. For optimal preservation of the alveolar architecture, a perfusion fixation method may be chosen^{281 198}. For an understanding of the published images of adenocarcinoma, it is useful if these studies

mention the routine handling procedure for pulmonary resection specimens (including wedge resections). Overall, in contrast to biological collapse involving a central area of the tumour, the structural change of iatrogenic collapse is most prominent in light-microscopic evaluation at the level of the alveolar walls.



■ **Figure 2.** Example of tumor atelectasis*)

In A and B sequential slices of a lobectomy specimen after 24+ hours buffered formaldehyde fixation. The orientation of 16 slices was as described before [33]. The fibrous adhesion on the left(upper) side was during gross examination colored with red ink. The slices were numbered from crania(a)l (1) to cauda(a)l (16) direction. The slice orientation is shown in the right upper corner (Media(a)l = m; Ventra(a)l = v; Dorsa(a)l = D; Latera(a)l = L). The letters D-G adjacent to the slices denote location of sample taken for initial microscopic analysis. Note i) that peripheral areas were fixed (grey) and some central areas are unfixed (red). In addition, ii) the slices do not show a solid lesion (which is associated with a firm consistency). iii) The bronchial and vascular resection margins as well as lymph nodes were sampled before cutting the 16 slices. In C and D microscopic images of haematoxylin-eosin stained section (sampled from slice 12, location N) showing overview (C) and detail (D) with monolayer of tumor cells on the alveolar wall (compatible with AIS). Note i) the variability in the amount of 'air' space: more collapse is less 'air'; and ii) in these images there are no signs of invasion.

*) Shown upon request of a few reviewers²⁷⁹.

In some cases of AIS and LPA, the elastic fibers are increased in number and lie in sheets²⁶¹, which, light-microscopically, are characterised by continuous elastic fibers. Noguchi type B is a clear example¹⁰. This increase in the number of elastic fibers emphasises the pre-existing lepidic (alveolar) structure (Figure 1D). Eto *et al.*²⁷³

demonstrated centrally, in what is now called AIS, an increase in the elastin content, contraction of the alveolar wall, and a consequent marked reduction in the amount of remaining alveolar air. This phenomenon of possible *in-vivo* collapse of peripheral lung tissue was recently given support in a radiological-pathological correlation, whereby the radiological solid appearance could only be explained by collapse of the lepidic parts of adenocarcinomas²⁷⁹. A gross picture of the resection specimen associated with *in-vivo* collapse is shown in Figure 2.

Thus, collapse of the peripheral lung will not only occur *ex vivo* during surgery, but may also happen *in vivo*.

Pathology of elastin

The diseases in pulmonary pathology with a change in elastin configuration are summarized in Table 1.

■ **Table 1.** Diseases in pulmonary pathology with a change in elastin configuration

Elastin	Disease	Morphology	Reference
Loss	Emphysema	Irregular enlarged airspaces and reduction in peribronchiolar alveolar wall attachments	Wright <i>et al.</i> ²⁸⁸ Kawabata <i>et al.</i> ²⁸⁹
	Langerhans cell histiocytosis	Focal emphysematous change	Fukuda <i>et al.</i> ²⁹⁰
	Granulomatous inflammation	Initial reticulin fiber increase in and around granuloma, resulting in hyalinosis	Mariani <i>et al.</i> ²⁹¹
	Idiopathic interstitial pneumonias	Fibrotic areas: focal elastolysis	Honda <i>et al.</i> ²⁹²
Increase	Adenocarcinoma*	Increased elastin in alveolar walls and/or the collapsed center	Noguchi <i>et al.</i> ¹⁰
	Elastosis†	Dense disorganized deposits of elastin	Fukushima <i>et al.</i> ²⁷⁴ Starcker <i>et al.</i> ²⁹³
	Apical cap	Subpleural increase in alveolar walls	Lagstein ²⁹⁴
	Pleuropulmonary fibroelastosis	Subpleural and septal increase	Tsubosaka <i>et al.</i> ²⁷¹ von der Thüsen <i>et al.</i> ²⁹⁵ Kinoshita <i>et al.</i> ²⁹⁶
	Idiopathic interstitial pneumonias	Increased vascular elastin	Parra <i>et al.</i> ²⁹⁷
	Organized infarct	Collapsed entangled elastic fibers within a collagenous stroma	Kawabata <i>et al.</i> ²⁹⁸ Groshong <i>et al.</i> ²⁹⁹

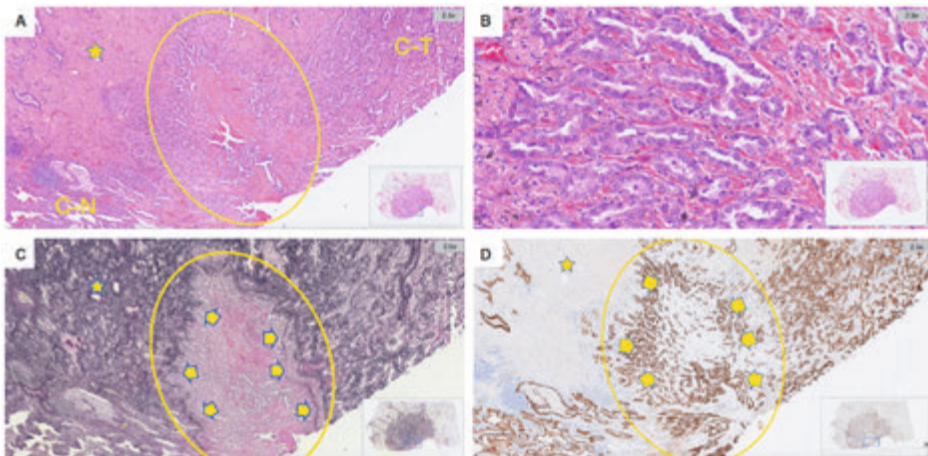
*Some, but not all, adenocarcinomas have increased amounts of elastin in alveolar walls and/or the collapsed center.

†Elastosis is defined as 'large aggregates of elastin fibers'/'diffuse increase in elastin mass', similarly as in other organs: breast, stomach, and papillary thyroid carcinoma³⁰⁰. The prognosis of patients with adenocarcinomas in the breast^{301 302} and lung²⁷⁴ is better in patients with elastosis than in those without elastosis.

In pulmonary adenocarcinoma, elastin staining can be used to demonstrate invasion in several ways. The most obvious are pleural and vascular invasion. Also, in pre-existing disease the elastin pattern can be helpful. The elastin pattern in seemingly papillary structures, which could be either true papillary or pseudopapillary because of iatrogenic collapse, requires more explanation.

Pleural invasion

Recognition of the normal pleural elastin layer is used for staging. In small adenocarcinomas, elastin staining plays a role in determining the presence or absence of pleural invasion, defined as cancer cells infiltrating beyond the outer elastic layer or beyond the outer elastic layer and onto the visceral pleural surface¹⁷. Tumours ≤ 30 mm with pleural invasion are upstaged to pT2a (Figure 3).



■ **Figure 3.** A,B, Overview (A) and detail (B) of the pleural invasive area: haematoxylin and eosin staining of the submerged fixed specimen shows invasive adenocarcinoma with pleural retraction (yellow oval) and a fibroelastotic scar (*yellow star). C, Corresponding elastin staining of A, showing elastin (black) in the lung as well as fibrosis (red) in the pleural retraction invaded by small acinar adenocarcinoma beyond the outer elastic layer (yellow arrowheads). D, Corresponding cytokeratin 7 staining to A, highlights cytokeratin 7-positive cells (brown). C-N, collapsed non-malignant area; C-T, collapsed tumour area.

Vascular invasion

If a pathologist is in doubt about whether a histological structure is an artery or a vein, elastin staining may help in the recognition of vascular structure and thereby invasion by tumour cells: the elastic fibers in the tunica media of the pulmonary arteries will designate the vascular lumen.

Pre-existing disease

Adenocarcinoma may arise as a secondary disease on top of other pre-existing diseases, such as emphysema, so there may be an already modified tissue architecture. When the pattern of remodeling in the adenocarcinoma component is similar to that in the adjacent non-malignant lung with pre-existing disease, remodeling is probably due to the pre-existing disease and not to adenocarcinoma.

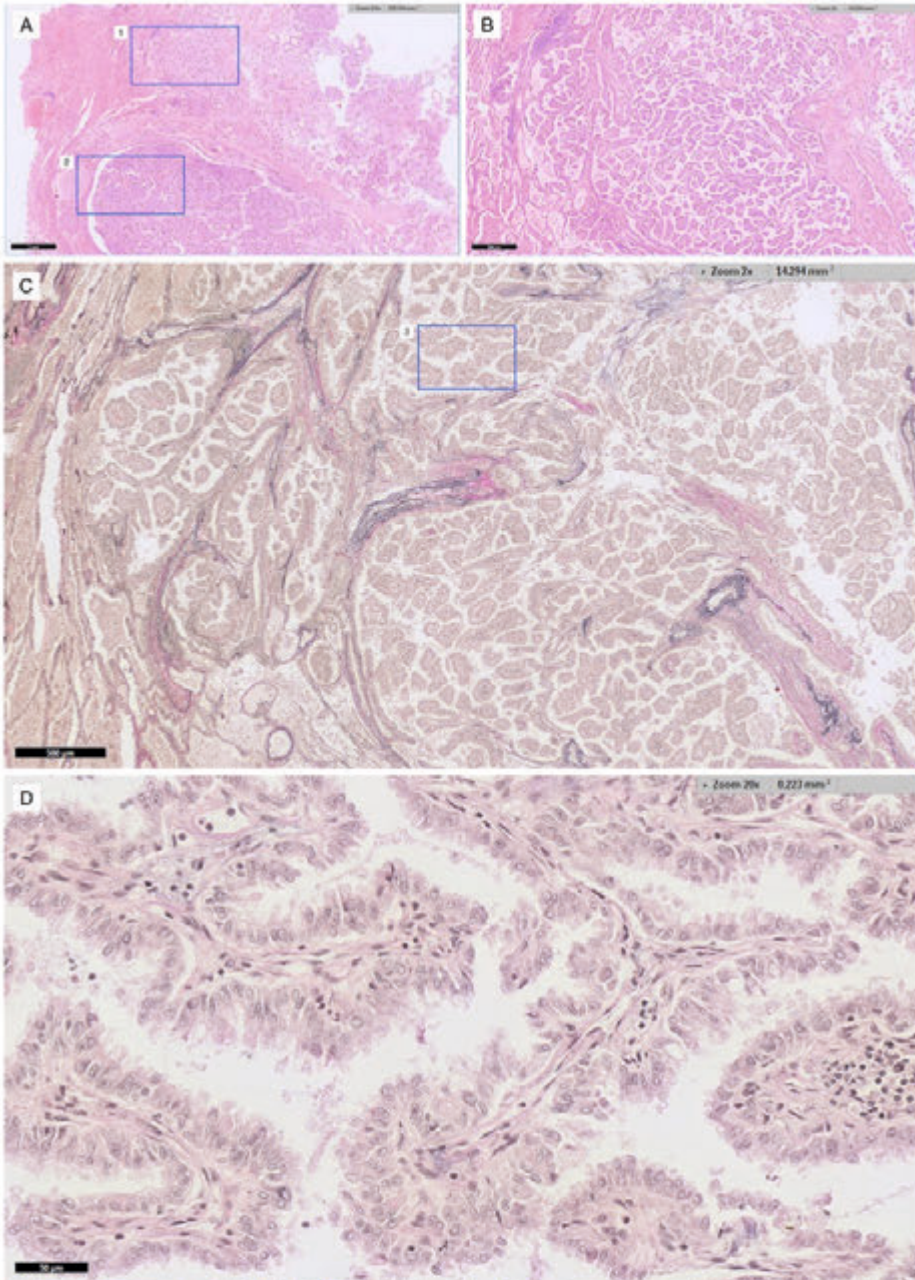
Adenocarcinoma, including mimickers of papillary adenocarcinoma

Iatrogenic collapse in a lung with non-mucinous AIS may mimic a papillary and/or acinar pattern as defined according to the WHO classification⁴. In this differential diagnosis, the presence of elastin shows that these structures represent pre-existing collapsed alveolar walls, and should be interpreted as part of the pre-existing peripheral pulmonary framework⁹⁰, supporting the diagnosis of AIS or, if invasion is present elsewhere, a lepidic pattern of adenocarcinoma.

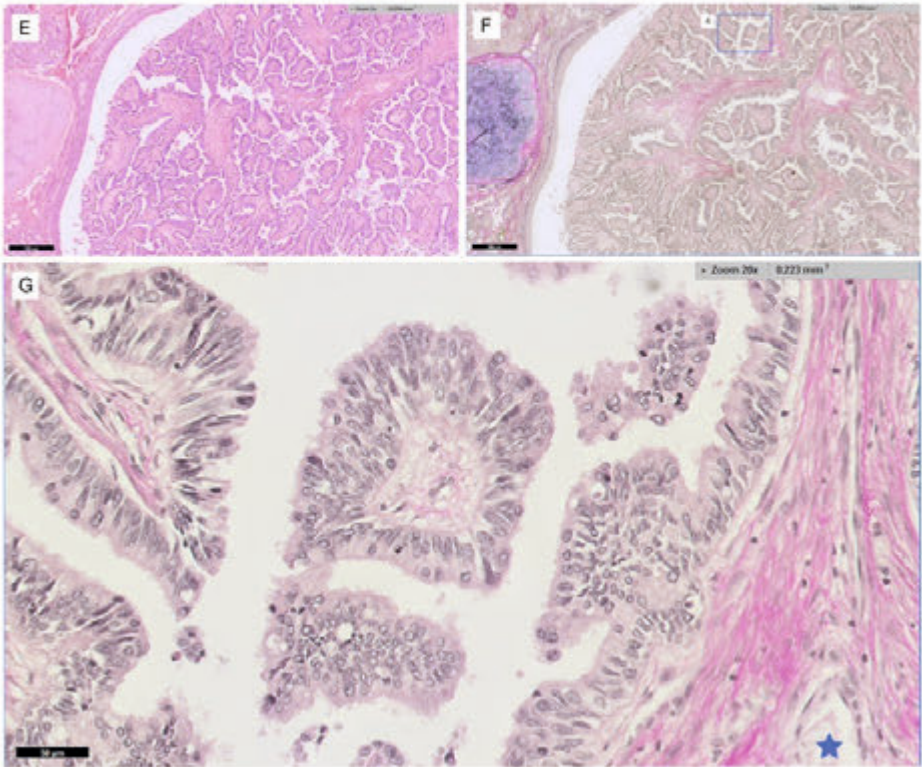
At the center of the controversy is the fact that true papillary cores include endothelial and fibroblastic cells with extracellular matrix, but elastic fibers are not structural components in papillary adenocarcinoma, unless there is pre-existing elastosis (Table 1). An example of a true papillary carcinoma of the lung is shown in Figure 4.

The papillary carcinoma with partly intrabronchial location was chosen, so that it could not be confused with alveolar collapse.

AIS is influenced by iatrogenic collapse, and has a simple pattern with an epithelial monolayer and, frequently, thin alveolar stromal cores (Figure 5).

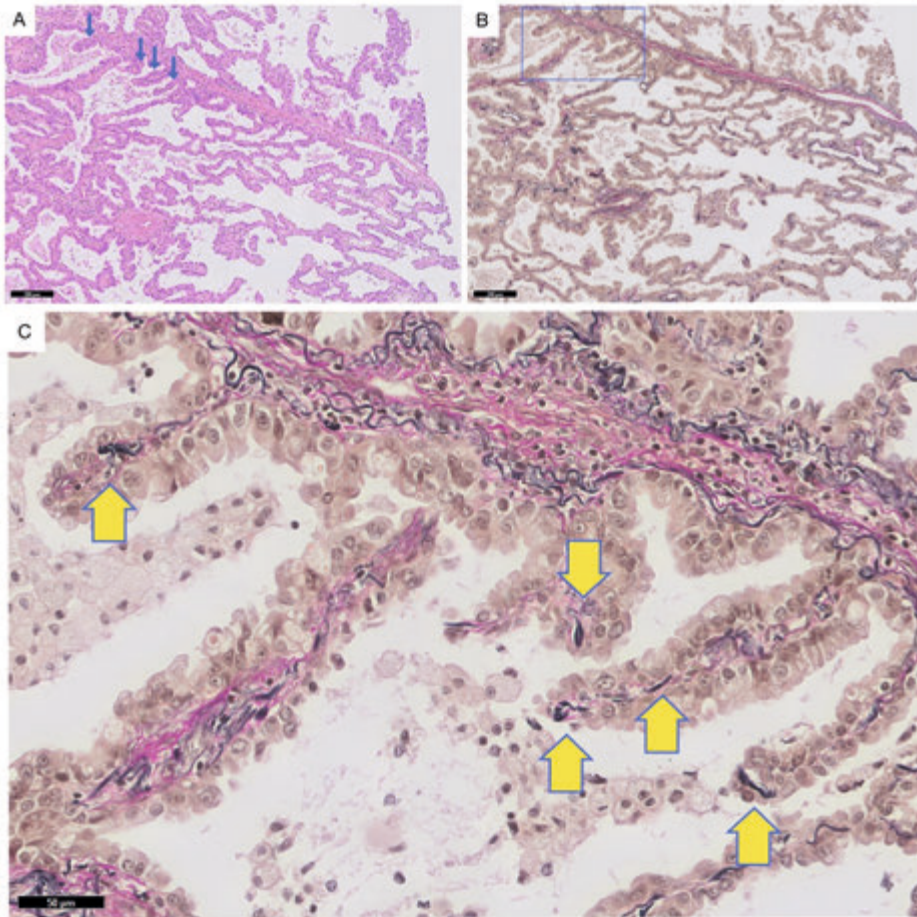


■ **Figure 4.** A submerged fixed resection specimen with papillary carcinoma.



■ **Figure 4.** A submerged fixed resection specimen with papillary carcinoma. (continued)

A, A haematoxylin and eosin (H&E) overview with both peripheral (around rectangle 1) and intrabronchial (around rectangle 2) growth. Note the iatrogenic collapse in peripheral non-malignant lung tissue in the left of rectangle 1. B,C, H&E (B) and elastin (C) staining show details of rectangle 1. Note the presence of elastin-containing remnants of the pre-existing architecture (including vessels and alveolar walls). Rectangle 3 is depicted in (C). D, Higher magnification of elastin staining of rectangle 3. Note the absence of elastin in all of the small papillae. E,F, H&E (E) and elastin (F) staining show details of rectangle 2. The internal control of the elastin staining (around the cartilage; below the bronchial epithelium and vessels) is positive. Rectangle 4 is depicted in (F). G, Higher magnification of elastin staining of rectangle 4. Note the complete absence of elastin intrabronchially, in the small papillae as well as in a slightly larger vessel (lumen with asterisk).

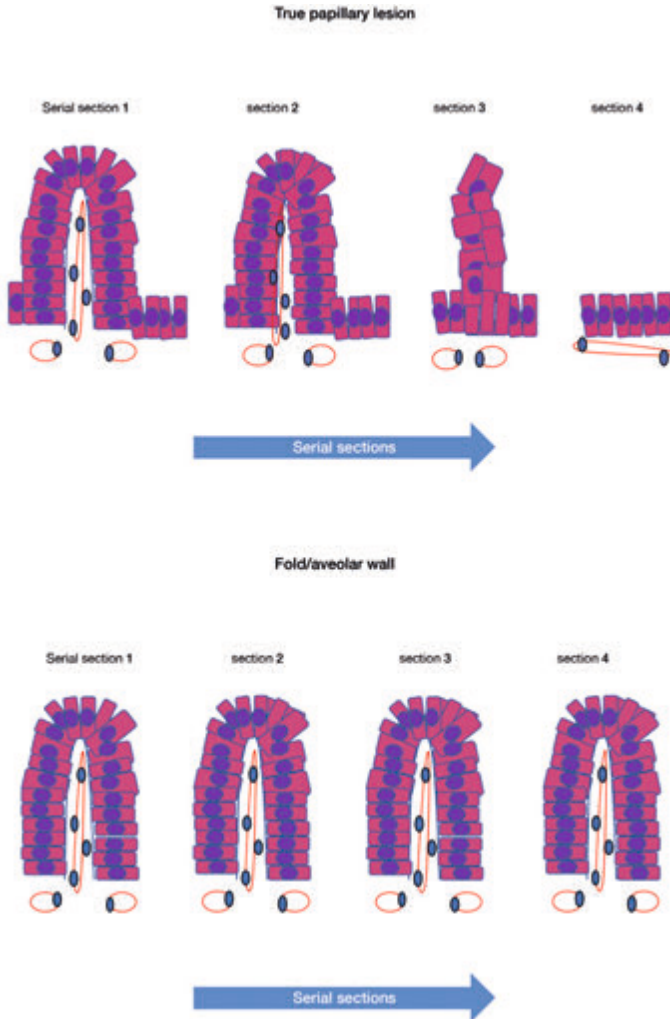


■ **Figure 5.** A, B, an example of lepidic adenocarcinoma with a pseudopapillary pattern (A, haematoxylin and eosin; B, elastin) with a focal papillary mimicker (blue arrows). C, Elastin staining shows the same pseudopapillae with focal elastin (yellow arrows). The stromal part of papillary carcinoma is mainly collagenous and focally desmoplastic. Note that the elastin in the interlobular septum is curly, as opposed to being stretched during maximal inhalation.

The non-invasive nature of this papillary mimicker was recognized in 2005 by Ishikawa *et al.* as 'Non-invasive papillary adenocarcinoma of the lung: a proposal of new entity'³⁰³. These pseudopapillary structures result from iatrogenic collapse but should not be considered as a distinct pathological entity. Instead, this entity represents a gap in the definition of the 1999 WHO classification¹², in which specific architectural and stromal constituents, such as desmoplasia, were not incorporated¹¹.

Importantly, cross-sections of these papillary mimickers have a diameter of ~46 μm (range, 36-54 μm ; Motoi and Thunnissen, unpublished data). The microscopic two-

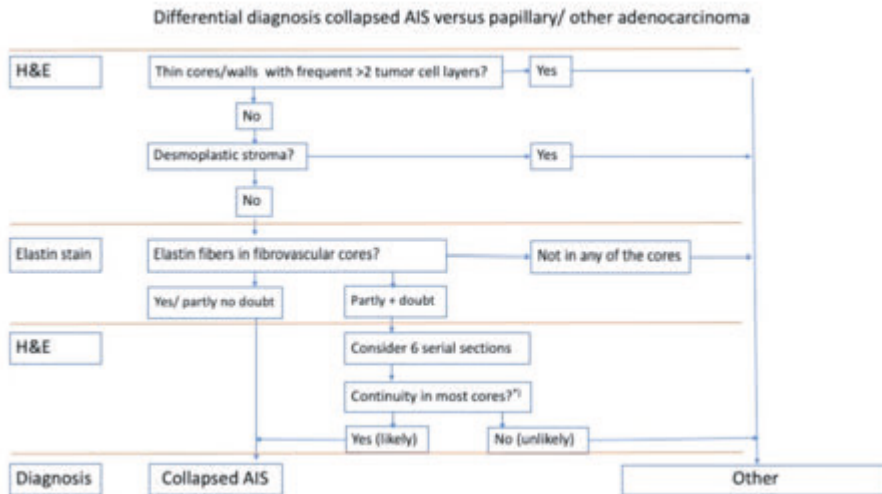
dimensional view of a papilla is approximately representing the middle of the three-dimensional papillary structure. One would expect that cutting deeper sections from the paraffin block would lead to disappearance of the papillary structure in four to five serial sections (Figure 6).



- **Figure 6.** A: cartoon with change of true papillary structure in consecutive series of sections. Note that a true papillary structure (with a radius of about 23 μm) should disappear after 4 - 6 sections. B: Cartoon with cross-section of alveolar wall. Although the shape may change, the cross section can be followed in serial sections.

The morphological criteria in the above-mentioned differential diagnosis, i.e. (i) the presence of elastin in alveolar walls, (ii) the absence of elastin in true papillary carcinoma⁹⁰, and (iii) the three-dimensional size of these papillary mimickers, point to AIS or a lepidic pattern.

The application of the current WHO classification was discussed among the authors. A case with iatrogenic collapse with tumour cells in one or two layers along a thin wall led to agreement. However, when elastin was absent in similar structures, opinions ranged from a lepidic pattern to possible papillary outgrowth (and therefore invasion) (Figure 7).



■ **Figure 7.** A flow chart with thought process for the differential diagnosis between collapsed AIS versus papillary/ other adenocarcinomas. *) In serial sections of collapsed AIS continuity of the alveolar walls is visible, with the exception of cross sections of alveolar duct endings. "Of note, in desmoplastic stroma elastic fibers may also appear discontinuous due to degradation of elastin by elastase containing inflammatory cells (see text for location of elastin degradation). Moreover, the desmoplastic stroma is a morphologic clue towards invasion."

The difference in interpretation may result from arguments based on a retained background architecture (i.e., the collapsed underlying microscopic anatomy), whereas the criteria used in the WHO classification of lung cancer since 1999 are based on microscopically visual tumour cell patterns. Although it is realized that the iatrogenic collapse may have an effect on measurements of tumour size¹⁷, the WHO does not incorporate in the current lung cancer classification the effect of iatrogenic collapse on pulmonary adenocarcinomas¹²⁰. It is clear that more data on this subject with sufficient follow-up are needed to resolve this uncertainty, in order to reach the level required for an evidence-based pathology classification.

Desmoplastic stroma

A mixture of tumour cells and dot-like or fragmented elastic fibers in combination with an increase in the number of loose collagen fibers (desmoplastic stroma³⁰⁴;

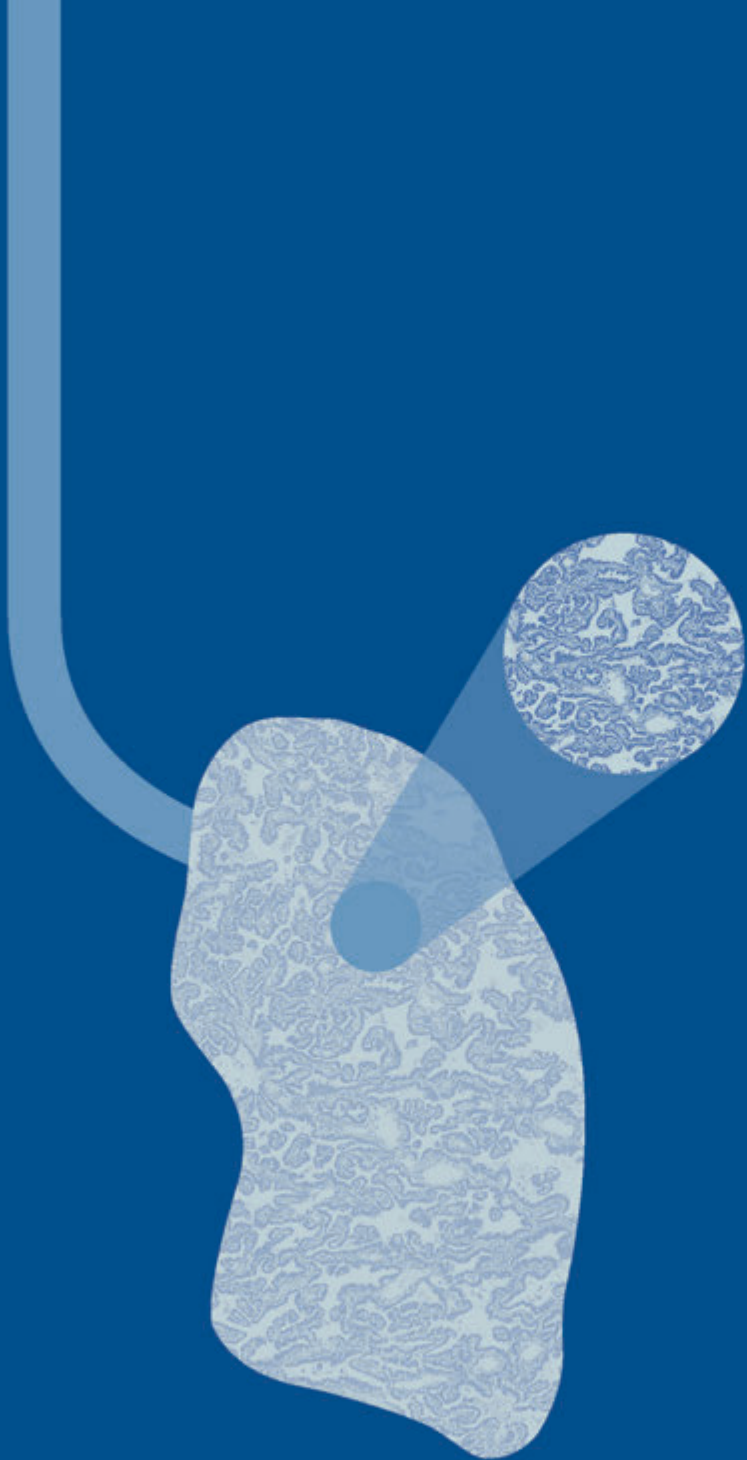
neofibrogenesis) is characteristic of stromal invasion. Usually, these tumour cells have high-grade atypia. Tumour areas with desmoplastic stroma and/or other classic characteristics of invasion do not form part of the above discussion regarding a collapsed AIS/lepidic pattern and papillary adenocarcinoma.

Artefact

A seemingly focal increase in elastin content occurs in cases of pulmonary collapse after surgery as an *ex-vivo* artefact: the bronchiolar epithelial layer folds because of the smooth muscle contraction. Underneath this folded epithelial layer is an accumulation of recoiled elastin¹²⁰. Remarkably, the simple epithelium lining *in vivo* is flexible enough to pile up as small folds in in the bronchiolar lumens of lungs with iatrogenic collapse. It is not excluded that, in collapsed AIS, some piling of the tumour cells on alveolar walls may occur. If this does not consistently exceed a thickness of two cell layers, early data support an excellent prognosis³⁰⁵.

Conclusions

Overall, iatrogenic collapse may have a profound effect on the microscopic appearance in pulmonary adenocarcinomas. Perfusion fixation, as routinely used in some centres, may mitigate this effect. Elastin staining is useful for the distinction between AIS with iatrogenic collapse and papillary carcinoma. Use of elastin staining should be considered, in order to make the most accurate diagnosis.



13

Incorporating surgical collapse in the pathological assessment of resected adenocarcinoma in situ of the lung. A proof of principle study.

Hans Blaauwgeers, Teodora Radonic, Birgit I. Lissenberg-Witte, Idris Bahce, Julien P.L. Vincenten, Chris Dickhoff, Erik Thunnissen

*Poster presentation at the IASLC WCLC September 2021
Journal of Thoracic Oncology 2021; 16 (10): S985*

Abstract

Introduction

The 8th edition of UICC/AJCC TNM classification system for non-small cell lung cancer (NSCLC) tumors recommends that size measurement of the primary tumor should be based solely on the invasive components. The distinction between adenocarcinoma in-situ (AIS) and other patterns, which are regarded as “invasive”, is of the utmost importance. In AIS, surgical collapse could alter architectural patterns, e.g., papillary, thus simulating invasive growth. The purpose of this study was: a) to examine the effect of surgical collapse in hematoxylin and eosin (H&E) stained slides on the WHO classification of pulmonary adenocarcinomas and b) to examine the additional value of cytokeratin 7 (CK7) immunohistochemical (IHC) staining for recognition of surgical collapse.

Material and methods

A retrospective, proof-of-principle study was performed, including early-stage NSCLC patients with resected primary adenocarcinomas, diagnosed between November 2007 and November 2010 at the Department of Pathology, Amsterdam UMC, location VUmc. H&E readings (using on average 2 slides (range 1-3)) without and with knowledge of surgical collapse were performed, blinded for clinical outcome. In a first scoring, pattern recognition according to the WHO was performed by one pathologist (HB). Subsequently, incorporating knowledge on surgical collapse, a second consensus scoring of the same slides was performed by two pathologists (HB & ET). An AIS with surgical collapse pattern was interpreted as non-invasive when a compressed pre-existing alveolar pattern was recognizable. Additionally, CK7 immunohistochemical stained slides of the same block were independently scored based on recognition of a regular collapsed pattern and monolayer of tumor cells. For survival analysis, patients with more than one tumor were categorized as ‘invasive’ if at least one of the tumors was invasive.

Results

A total of 74 histological sections of 40 tumors from 33 patients were scored.

After the first H&E scoring according to the WHO classification, the 5-year overall survival (OS) rate for patients with a non-invasive pattern (n=2) versus invasive pattern (n=31) was respectively 100% and 48% (p=0.18). When surgical collapse was considered, 5 invasive cases were downgraded to non-invasive AIS. The 5-year OS rate for all those non-invasive cases (n=7) remained 100% and for the invasive cases (n=26) became 39% (p=0.019). After CK7 staining the same 7 cases were scored as non-invasive. The CK7 reading was perceived as an easy tool.

Noteworthy, this shift of cases to the non-invasive category did NOT affect the 100% 5-years overall survival of this non-invasive category.

Conclusion

This proof-of-principle study shows that taking surgical collapse into account when scoring H&E and IHC-CK7 slides can enable re-classification of WHO invasive NSCLC cases into non-invasive AIS cases. In this study, the shift in recognition improved the prediction of survival outcomes, highlighting the need to recognize surgical collapse in pathological readings, as this may prevent underdiagnosing AIS.

Introduction

According to the 2015 WHO classification of non-mucinous lung adenocarcinoma, the predominant pattern present in any case is used for subtyping the tumors³⁰⁶. The concepts of adenocarcinoma in situ (AIS) and minimally invasive adenocarcinoma (MIA), first established in the 2015 WHO classification, are now recognized more frequently, particularly in patients taking part in lung cancer screening protocols. Both AIS and MIA are associated with 100% 5-years survival.

The 8th edition of UICC/AJCC TNM classification system for non-small cell lung cancer (NSCLC) tumors recommends that the size measurement of the primary tumor be based solely on the invasive components³⁰⁷. The distinction between adenocarcinoma in situ (AIS) from other patterns, which are regarded as "invasive" is therefore of the utmost importance.

Surgical collapse or compression of the alveolar structure/lepidic pattern was recognized recently as a frequent phenomenon in pulmonary resection specimen²⁷⁹. This pattern may affect the shape of normal alveoli as well as alveoli lined by tumor cells and can significantly modify the morphology of the tumor. Artefactual compression of alveolar structures lined by tumor cells may lead to folding or tufting in deflated lung parenchyma. As a consequence, it is possible that collapsed folds (alveolar walls) may mimic a papillary architecture when cross-sectioned^{90 308}. Our assumption is that not all pathologists realize that collapse may mimic certain patterns of pulmonary adenocarcinoma classification such as papillary and acinar patterns. The clinical consequence is that some in-situ carcinomas are diagnosed as invasive lung cancer, with the implication of greater invasive tumor diameters leading to possible differences in staging or even neoadjuvant therapy.

Our hypothesis is that cases with surgical collapse in AIS will have a favorable prognosis. For the interpretation of surgical collapse, the recognition of the pre-existing architecture is of utmost importance. Currently there is no information whether a cytokeratin stain is supportive for the recognition of the pre-existing architecture.

Therefore, we performed a proof of principle study to examine the recognition of surgical collapse as a pseudo-invasive pattern in cases of AIS and the possible supportive role of CK7 in the recognition of these pseudo-invasive patterns, that should correlate to an excellent prognosis.

Materials and methods

A retrospective, proof of principle study was performed on a previously described cohort of patients with adenocarcinoma of the lung (diagnosed on biopsies and 195 resections from different institutes submitted originally for mutation analysis), between November 2007 and November 2010 at the VU University Medical Center¹⁸¹.

Follow-up was retrieved from patient files. Hematoxylin and eosin (H&E) stained slides were retrieved from the archive.

Cytokeratin 7 (CK7)

The immunohistochemical stain for CK7 (clone OVTL12/30 (Agilent/Dako (Glostrup, Denmark, catno. M701801) was performed in a Roche/Ventana benchmark Ultra (Roche, Basel Switzerland) with 3µm tissue slides mounted on TOMO-glass slides (Roche, Basel, Switzerland). Antigen retrieval was applied with high pH-buffer CC1(32 minutes at 100°C) and the antibody was diluted 1/100 (incubated for 32 minutes at 36°C) and detected with the Optiview DAB kit under standard conditions. Sections were dehydrated with ethanol 100%, cleared with Xylene and coverslipped with Tissue-Tek coverslip film on the Sakura coverslipper (Sakura Finetek Europe B.V, Alphen aan den Rijn, The Netherlands). Internal positive controls were pneumocytes and respiratory epithelial cells. Internal negative controls were e.g., smooth muscle cells in vessel walls, bronchioli.

Morphologic evaluation

A first scoring of H&E-stained slides was performed based on pattern recognition as advocated according to the WHO by one pathologist (HB). Subsequently, a consensus score was made by two pathologists incorporating surgical collapse (HB, ET).

Surgical collapse with AIS was characterized as compressed lung tissue where tumor cells were lining compressed alveolar walls with reduced or minimal air remaining. This pattern has a regular, occasionally streaming appearance with a monolayer of tumor cells. Tangential cutting of tumor cells (focal seemingly > 2 cell layers in an area otherwise fitting with collapsed AIS) was interpreted as collapse and not classified as 'focally > 2 cell layers'.

Surgical collapse was taken into account to interpret some seemingly papillary or acinar patterns as non-invasive.

After reading of H&E and a washout period of >2 weeks the CK7 slides were scored for the same items as the H&E. The assumption was that most adenocarcinoma cases were CK7 positive and when lined on alveolar walls a consistent architectural pattern could be present and be supportive of non-invasive growth. In addition, characteristics of invasive growth such as individual tumor cells, and more luminal proliferation than fitting with AIS, such as prominent multilayering, cribriform and/or solid growth we decisive for invasion.

Statistical analysis

Continuous variables are described by mean and standard deviation, categorical variables by frequency and percentage. For each tumor H&E and CK7 data was compared, using the McNemar test. Patients with >1 tumor were in Kaplan-Meier curves categorized as 'invasive' if one of the tumors was invasive. Curves were compared using the log-rank test. Statistical analysis was performed in SPSS version 26 (IBM Corp., Armonk, NY, USA). P-values <0.05 were considered statistically significant.

Results

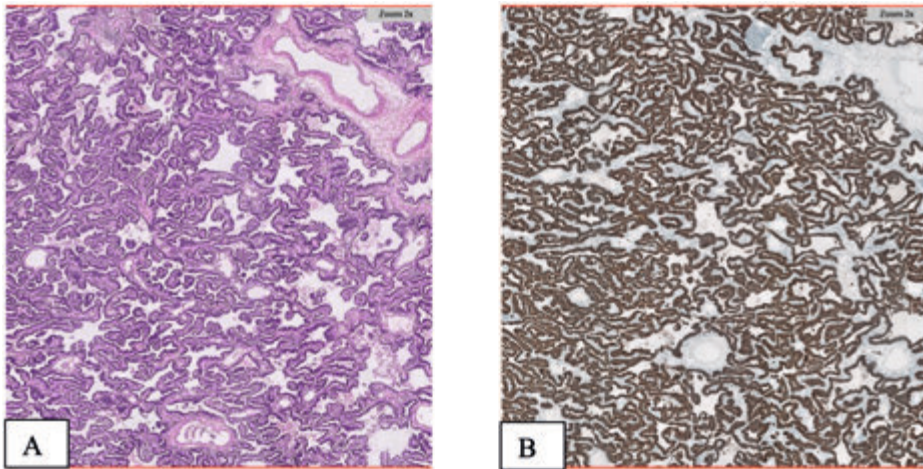
A total of 74 histological sections of 40 tumors from 33 patients were scored. The clinicopathological characteristics of the patients are presented in table 1. The mean age of the patients was 63.1 ± 10.3 . There were 19 females and 14 males. The pathological stage distribution for stage I - IV was 11, 10 and 2, respectively. The median follow-up time was 57 months (range 0 - 112).

■ **Table 1.** Clinicopathological characteristics of the 33 patients

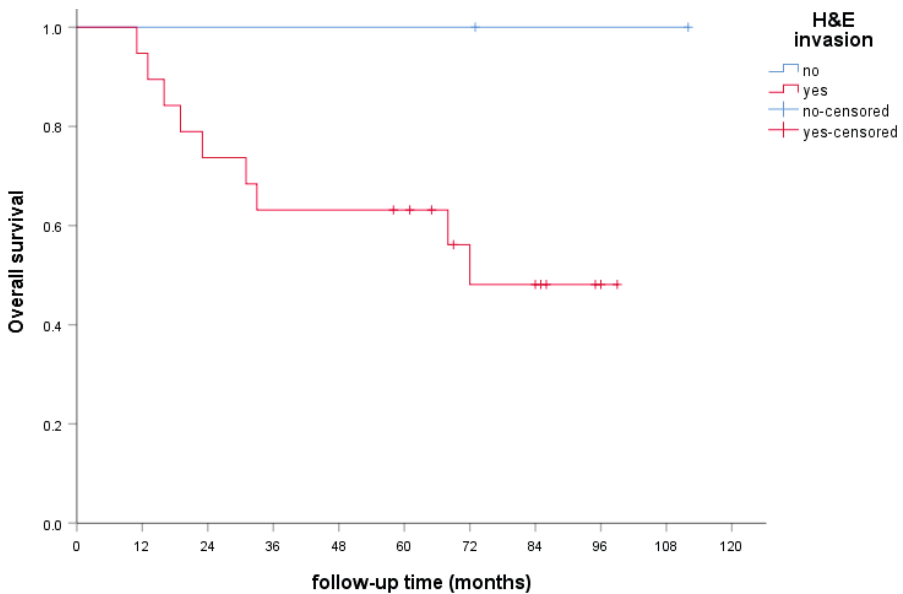
		n (%)
Number of patients		33
Mean age (SD)		63.1 (± 10.3)
Gender	male	14 (42.4%)
	female	19 (57.6%)
Pathological stage	1	11 (33.3%)
	2	10 (30.3%)
	3	10 (30.3%)
	4	2 (6.0%)

n = number; SD = standard deviation

In the first H&E reading 2 out of 21 patients were diagnosed as having a non-invasive adenocarcinoma. In the second H&E reading including iatrogenic collapse an additional 5 patients out of the 21 were diagnosed as non-invasive (Figure 1A). In the CK7 reading the same 7 out of 21 patients were diagnosed as non-invasive, based on a recognizable pattern of pre-existing architecture (Figure 1B).



■ **Figure 1.** H&E (A) en cytokeratin 7 (B) showing a regular pattern in a collapsed non-invasive adenocarcinoma.



■ **Figure 2.** The overall survival is shown in a Kaplan-Meier curve for H&E reading incorporating iatrogenic collapse

Survival

After the first H&E scoring according to the WHO classification, the 5-year overall survival (OS) rate for patients with a non-invasive pattern (n=2) versus invasive pattern (n=31) was respectively 100% and 48% (p=0.18). When surgical/iatrogenic collapse was considered, 5 invasive cases were downgraded to non-invasive AIS. The 5-year OS rate for all those non-invasive cases (n=7) remained 100% and for the invasive cases (n=26) became 39% (p=0.019) (Figure 2). After CK7 staining the same 7 cases were scored as non-invasive. The CK7 reading was perceived as an easy tool.

Discussion

In this 'proof of principle study' we used surgical/iatrogenic collapse morphology to recognize non-invasive areas, while these can also according to the WHO be interpreted as invasive acinar or papillary patterns. The overall survival of the patients with *in-situ* reclassified adenocarcinomas remained 100%.

The assessment of invasion as acknowledged by the WHO and as borne out in numerous studies, may be challenging in more than occasional cases of resected adenocarcinoma^{14,309-311}.

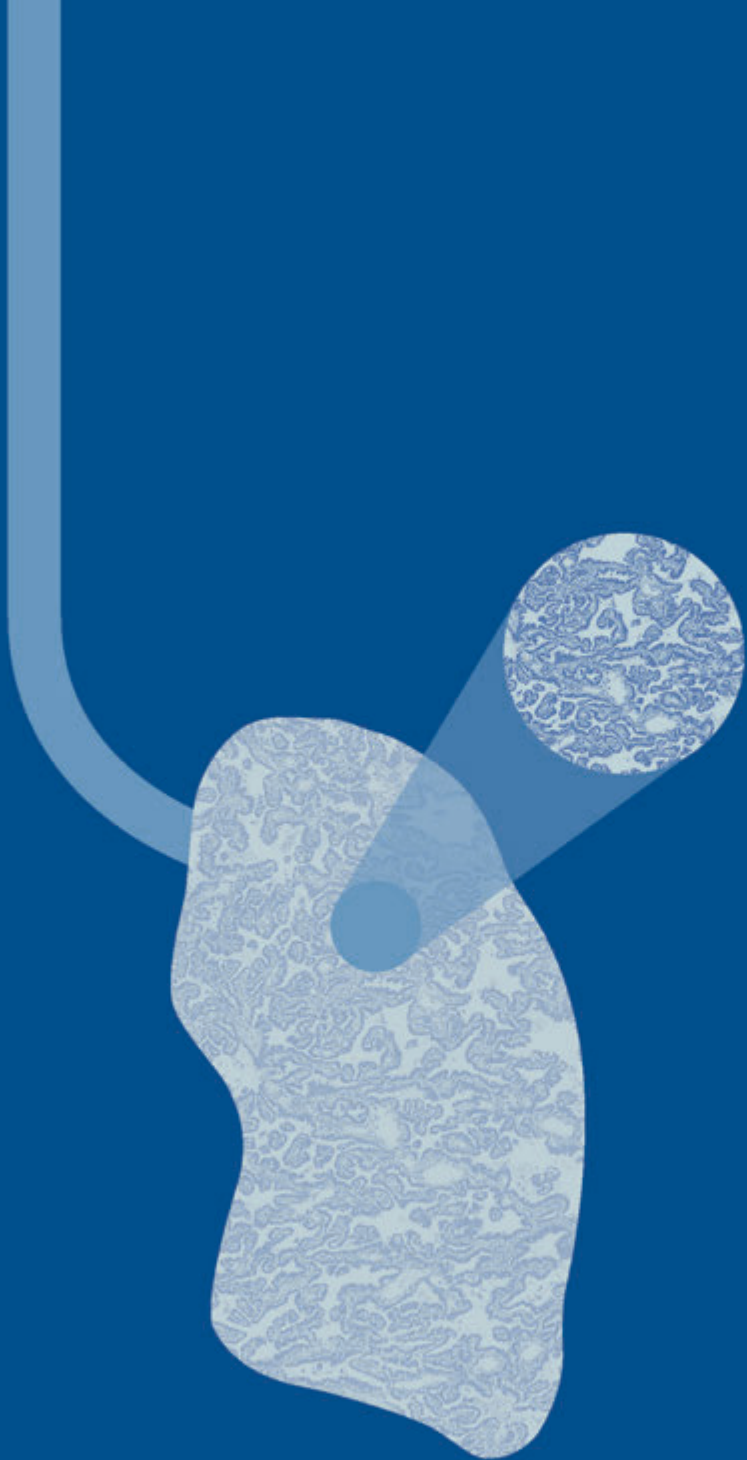
CK7 regularity clearly aids in understanding the folded architecture of surgical collapse.

Boland and colleagues show for assessment of pulmonary early adenocarcinomas a difference in survival curves between readings of two pathologists³¹². One has 100% probability of overall survival for AIS compared to 80% for the other. Moreover, they suggested that "tumors with disagreement between 'minimal invasive adenocarcinoma' and 'invasive adenocarcinoma' had survival similar to agreed 'minimal invasive adenocarcinoma', and thus, borderline cases can be confidently classified as 'minimal invasive adenocarcinoma'." Although with the recognition of surgical collapsed adenocarcinoma *in situ* 'minimal invasive adenocarcinoma' should not be used, their findings are in line with our study.

Limitations of this study are i) the raked together sample set from a larger cohort collected for another purpose (mutation analysis in a period with only focal availability of mutation testing); ii) the sample size, which was reduced by limited availability of follow-up.

Conclusion

In this proof of principle study recognition of surgical/iatrogenic collapse with the aid of CK7-IHC are supportive in the assessment of (non)invasive adenocarcinoma. Further study on this topic is needed.



14

3-dimensional reflection aids in understanding the fog of 2-dimensional pattern recognition in pulmonary adenocarcinomas. Proposal for a modified classification.

Federica Filipello#, **Hans Blaauwgeers**#, Birgit Lissenberg-Witte, Andreas Schonau, Claudio Doglioni, Gianluigi Arrigoni, Teodora Radonic, Idris Bahce, Arthur Smit, Chris Dickhoff, Antonio Nuccio, Alessandra Bulotta, Yuko Minami, Masayuki Noguchi, Francesca Ambrosi, Erik Thunnissen
equally contributed

Submitted

Abstract

Introduction

For resected non-small cell lung cancer specimens, recognizing non-invasive growth patterns is necessary to correctly estimate their T-stage and to distinguish between invasive and non-invasive adenocarcinoma, as prognosis varies greatly. In particular, after resection due to iatrogenic collapse, this distinction can be difficult. The aim of this study is to investigate the complex morphology of non-mucinous non-invasive patterns of adenocarcinoma *in situ* (AIS) in resection specimen with iatrogenic collapse, and to relate this to follow-up.

Material and methods

The effects of iatrogenic collapse on the morphology of collapsed AIS were examined on a mathematical model, and subsequently re-examined with a revised classification using also cytokeratin 7 and elastin as additional stainings in two independent retrospective cohorts of primary pulmonary small (≤ 3 cm) adenocarcinomas resection specimen with available follow-up information.

Results

The morphometrical model demonstrated that wrinkling of alveolar walls occurs during iatrogenic collapse, leading to significant increase in tumour cell heights in maximal collapse areas. Out of a total of 70 resection specimen 10 were (re)classified as iatrogenic collapsed AIS. Patients with AIS showed a 100% recurrence-free survival after a mean follow-up time of 69.5 months.

Conclusions

Iatrogenic collapsed AIS forms a morphologic complex, wrinkled pattern with in the cytokeratin 7 a regular pattern and in the elastin staining a preserved elastin framework. A classification with refined criteria facilitates the diagnosis of iatrogenic collapsed AIS.

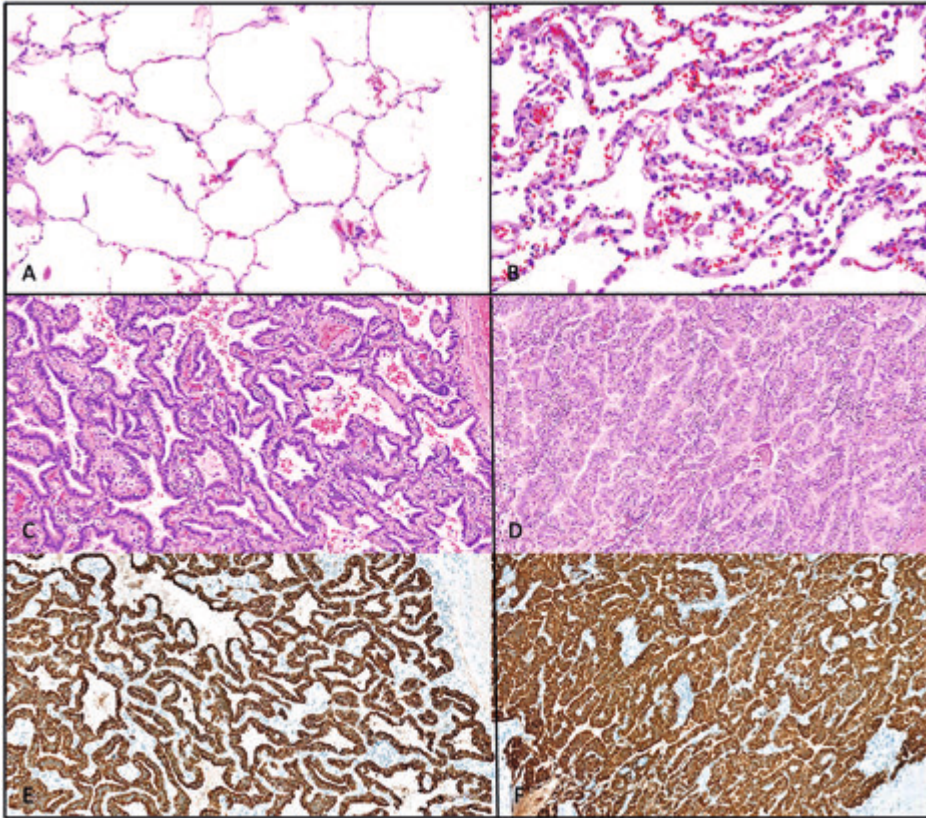
Introduction

According to the World Health Organization's 2021 classification of non-mucinous lung adenocarcinoma, the predominant pattern is used to subtype the tumours³¹³³¹⁴. Adenocarcinoma *in situ* (AIS) and minimally invasive adenocarcinoma (MIA) are associated with a 100% 5-year recurrence free survival (RFS) rate⁷³¹⁵. AIS is defined as growth of a monolayer of tumour cells along pre-existing alveolar structures with focal cell overlap or mild stratification³¹⁴, i.e. pure lepidic growth without any invasive feature, in tumours that are 30 mm or smaller³¹⁶.

The 8th edition of UICC/AJCC TNM classification system for non-small cell lung cancer (NSCLC) recommends that the size of the primary tumour should be determined by the invasive components only³⁰⁷. It is therefore crucial to differentiate between a lepidic growth pattern, specifically AIS, and other patterns that are deemed "invasive". However, assessment of invasion has a poor reproducibility¹⁴. Moreover, the Pathology Committee of the International Association for the Study of Lung Cancer (IASLC) recently published a proposal for defining morphologic features of invasion in pulmonary non-mucinous adenocarcinoma with lepidic growth, involving also the effects of collapse on morphology³¹⁷. It appears that, in the past decade, the fog around adequately recognizing invasion patterns implicitly present in the WHO classification of pulmonary adenocarcinomas has not lifted as their recent publication stimulates research on this topic³¹⁷.

Typically, when identifying pre-neoplastic lesions, *in situ* carcinomas, and invasive patterns, pathologists compare the observed tissue to its normal physiological state as a reference. For example, to recognize mild cervical dysplasia, pathologists compare the abnormal epithelium with the adjacent normal non-keratinized squamous epithelium, or if absent, with their mental visualization of the normal squamous epithelial surface. Unlike the cervix, where tissue structure remains largely unchanged following biopsy or resection, the peripheral pulmonary parenchyma undergoes significant morphological alteration during resection. This alteration in morphology is similar to the impact of compression atelectasis observed in tension pneumothorax³¹⁸.

When the thorax is opened during surgery, the negative pressure in the pleural cavity is reversed, leading to a positive atmospheric pressure. As a consequence, the lung parenchyma deflates, and there is a decrease in vascular blood and lymph flow, which ultimately results in peripheral lung collapse¹²⁰ (see Supplementary Figure S3 in ³¹⁷). In addition, when a tissue sample is taken from its natural context, such as during surgical resection, the natural recoil of the elastic fibers changes the shape and length of the alveolar walls³⁰⁸. As a consequence, so called iatrogenic collapse of the lung parenchyma occurs, which is identifiable under microscopy by the close proximity of alveolar septa with little or no air retained between them (Figure 1 A, B).



■ **Figure 1.** A, B. Histology of normal expanded alveolar lung parenchyma (left) and iatrogenic collapsed parenchyma (right). Although the patterns are different, samples were taken from the same specimen, with (left) and without (right) transpleural perfusion fixation before submerging fixation. Tumor cells are absent (H&E, 100x). C-F. Two cases of collapsed AIS (adenocarcinoma in situ) are shown (C and D in hematoxylin and eosin (HE) staining; corresponding cytokeratin 7 immunohistochemistry (CK7, IHC) E and F). The case shown in C and E has moderate collapse, with alveolar walls and alveolar spaces that are still recognizable. D and F show an example of prominent collapsed AIS, in which the alveolar walls are compressed against each other and the alveolar “air” space is hardly recognizable. Note I) a regular pattern in both cases and II) collapsed AIS may easily be interpreted as an acinar or papillary pattern

The underlying alveolar architecture is distorted by this phenomenon of iatrogenic collapse, which makes it more difficult to evaluate the morphology³⁰⁸. Iatrogenic collapse is more prominent in resection specimen than in biopsies, with usually minimal collapse and open alveolar ‘air’ spaces. In the past, different descriptions were used for ‘collapse’ in pulmonary pathology literature³⁰⁸. In the 1980s, the term ‘collapse’ was used to describe adenocarcinomas with a central ‘scar’ that still showed a recognizable collapsed alveolar framework within condensed elastic tissue on elastin staining^{276, 319}.

In hematoxylin and eosin (H&E) staining, the condensed elastic tissue may be mistaken for fibrosis, while in elastin staining, the preponderance of elastic over collagen fibers is easily recognizable. This parenchymal collapse is referred to as 'biological collapse', as opposed to iatrogenic collapse. In 1995, two Japanese studies showed that non-mucinous adenocarcinomas with tumour cell growth along alveoli and central biological collapse, had a favorable prognosis^{10,277}. In 2016, the collapse of peripheral lung during surgery was described as having an effect on the pre-existing morphology¹²⁰. More examples of this iatrogenic collapse involving areas with lepidic growth, consistent with AIS have recently been published²⁷⁹. If the amount of collapse is minimal, with a clear number of airspaces between the alveolar walls, the diagnosis of AIS can be readily made. However, if the collapse is more prominent, overlap may occur with diagnostic criteria for papillary and acinar adenocarcinoma patterns in particular⁹⁰. Therefore, according to the WHO classification, collapsed AIS may be (over)diagnosed as invasive adenocarcinoma (Figure 1 C-F).

The aim of this study is to improve understanding of the complex 3-dimensional morphology of lung adenocarcinoma, especially for non-mucinous AIS in resection specimens, under conditions of iatrogenic and biological collapse. To this end, we first used a mathematical approach to evaluate morphological changes on alveolar walls and tumour cells during iatrogenic collapse.

Subsequently, we investigated diagnostic criteria for collapsed AIS using hematoxylin and eosin (H&E), cytokeratin 7 (CK7) and elastin staining and considered more extensive intra-alveolar growth patterns as surrogate markers for invasion. By using the proposed criteria, we investigated whether cases could be reclassified as AIS and whether this was supported by follow-up outcomes. Modifications lead to a proposal for a revised classification of pulmonary adenocarcinoma.

Material and methods

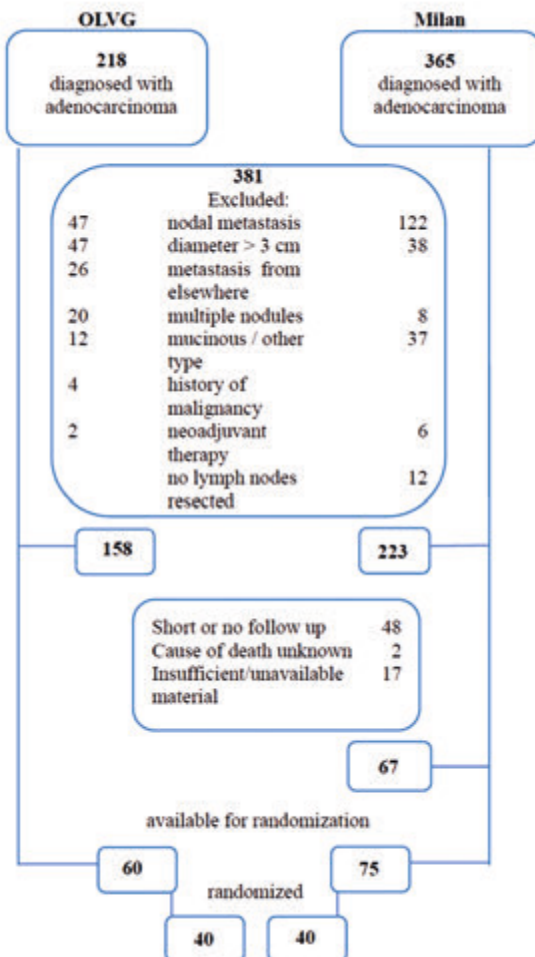
Patient cohorts

Two retrospective cohorts of patients with resected pulmonary adenocarcinoma diagnosed between the 1st January 2011 and the 31st December 2016 were collected in: A) OLVG Hospital, Amsterdam, The Netherlands and B) San Raffaele Scientific Institute, Milan, Italy. The inclusion criteria for the cases were: resection specimen with a primary pulmonary adenocarcinoma of a pathological tumour diameter of 3 cm or less and available follow-up information. Exclusion criteria were the presence of nodal or hematogenous metastases at the time of resection, treatment with neoadjuvant chemo(radio)therapy, multiple nodules in the same or other lobes, previous lung carcinoma, and invasive mucinous adenocarcinoma or other special type patterns (intestinal and fetal adenocarcinoma).

Assuming the fraction of cases to be downgraded to AIS to be around 20%³²⁰ and a 95% confidence interval between 10-30% the minimum sample size required is 70

cases. Therefore, after determining appropriate cases in both institutes, a minimum of 40 cases in each were randomly selected.

The following information was retrieved by retrospective chart review after approval by the Institutional Review Board (OLVG: ACWO21-044; VUmc 2022.0269 [biobank 2017.023]; Milan CE 284/2022): age, gender, total tumour size, tumour location, pathological stage adjusted to the 8th edition, time to recurrence, death, and cause of death.



■ **Figure 2.** Flow diagram of patient selection from OLVG and Milan cohorts, revealing 583 cases with resected adenocarcinoma. After exclusion of 448 patients, 135 patients with an adenocarcinoma of 3 cm or smaller and available follow up were included for randomization.

In the OLVG Amsterdam, 218 patient cases were retrieved from the pathology archives, whereas from San Raffaele archive in Milan 365 patient cases were retrieved. The flow diagram of selection of suitable cases is shown in figure 2. A total of 135 fulfilled the study criteria.

After random selection in total 80 cases were included. Freshly cut sections of the selected paraffin blocks from both institutes were stained for H&E, elastin (Elastica von Gieson, EvG) staining²⁰⁶ (see for Standard Operation Procedure (Dutch) Supplementary files), and CK7 immunohistochemistry (IHC) at the department of Pathology of the VUmc.

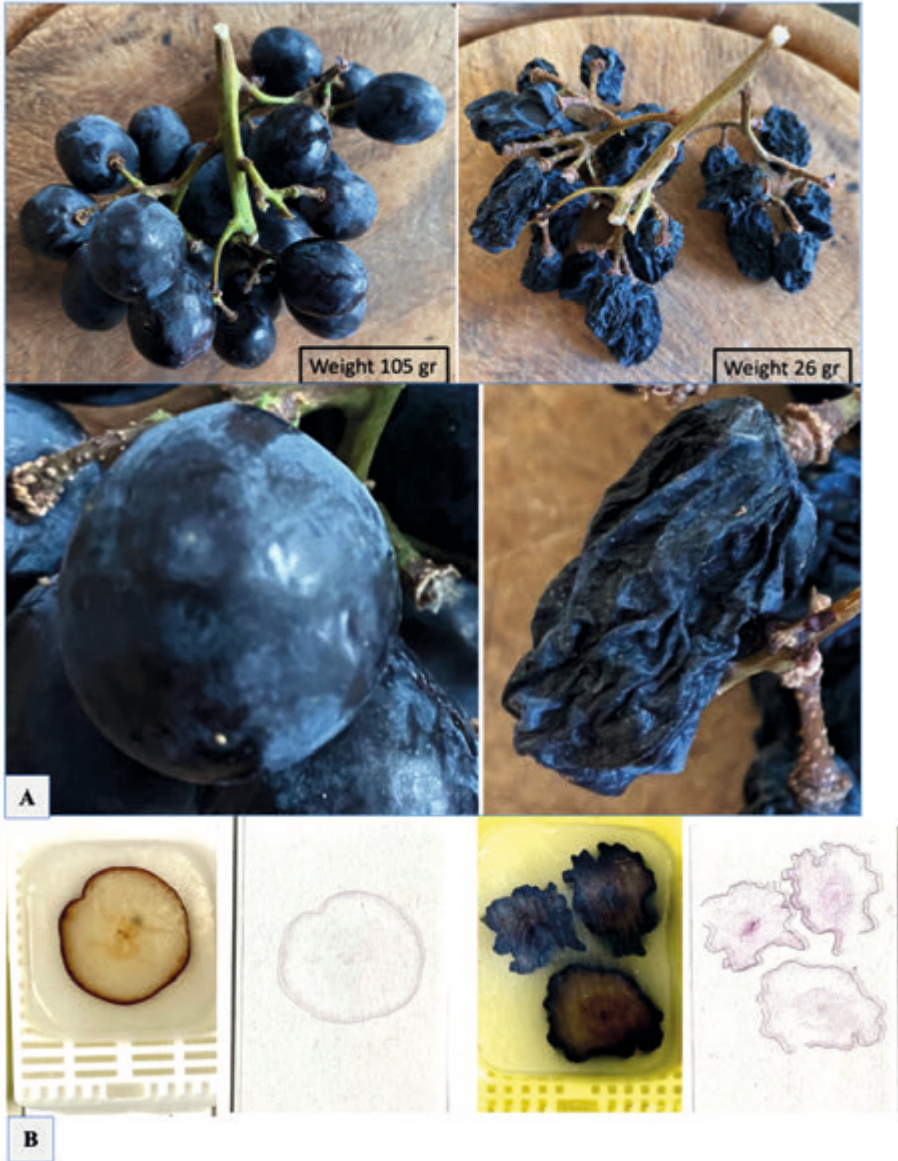
Both institutes used neutral buffered formaldehyde for the fixation of their resection specimens. Histological review of these cases was performed by three pathologists (HB, FF, ET). For each case, one representative tumour block was selected and digitized. The digital images were uploaded on the collaborative platform for on-line teaching, training and quality assurance in pathology, Pathogate (<https://pathogate.net>). After technical review of the cases, 10 were excluded, mainly because of insufficient quality of the slide, including out-of-focus areas after scanning. Therefore, 70 cases, 35 from each institute, were further analyzed.

Subtyping of the adenocarcinomas according to the WHO was performed by 2 pathologists (HB, FF) in the categories AIS, lepidic predominant adenocarcinoma (LPA), low grade adenocarcinoma (acinar, papillary) with or without > 10% high grade component and high-grade adenocarcinoma (micropapillary, solid). Cases with discrepancies (dominant pattern, presence of high-grade component) were reviewed, reaching consensus.

Mathematical model

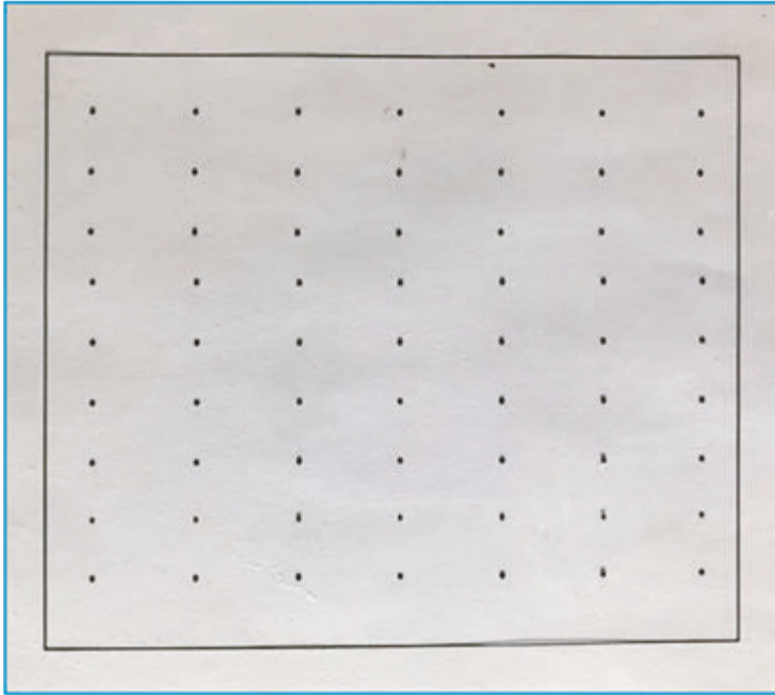
In order to understand and demonstrate the effect of collapse, we tried to construct a mathematical model, starting from a cube with equal ribs as an approximation of an alveolar space. In this model, an approach was used with reduction in size to a progressively flatter box, where the total circumference of the ribs remains the same. The effect of progressive flattening on surface area and volume was calculated. As the alveolar architecture is sometimes compared to a bunch of regular and dried grapes,³¹⁸ the analogous example of grapes and raisins is shown in Figure 3. Pictures were taken from grapes, both fresh and after 3 weeks of dehydration. Slices were embedded in paraffin blocks and section were stained with H&E.

We formulated the following hypothesis: i) alveolar walls will be folded in iatrogenic collapse and ii) due to increased pressure by decrease of alveolar surface, the tumour cells may increase in length in prominent collapse.



■ **Figure 3.** A. Bunch of grapes, comparable to the alveolar structure with airways³¹⁸ and alveoli, fresh with a smooth surface (left) and after 3 weeks of dehydration to a 75% reduced weight/volume (right). B. Cross section in a paraffin block and histologic slide of a fresh, fully extended grape (left) and in dehydrated state (right). Note that wrinkling of the surface is the way to cope with the reduced volume in the dehydrated state.

To test both hypotheses, morphometry was performed on cases from two cohorts of resection specimen with a primary pulmonary adenocarcinoma of a pathologic tumour diameter ≤ 3 cm. CK7 stained slides were digitized and the point counting method performed according to Weibel³²¹ (see for methodology Figure 4).



■ **Figure 4** and methodology according to Weibel³²¹.

A rectangle of 14,7x12,5 cm containing 63 dots of 1x1 mm, all within equal distance, was designed and printed on a plastic sheet, see photo. The overhead sheet with dots was superimposed on the screen showing the digital tumour image. The dots were projected on top of either "air", "cell", "nucleus" or "stroma". Four tumour areas on CK7 were chosen for each case: two different areas with a prominent amount of "air" (or the largest "air" spaces present) and two severely iatrogenic collapsed areas with minimal "air". Each area was counted at the same (20x) magnification. The number of dots in the air spaces, on the cells (both nucleus and cytoplasm) and in the stroma were recorded. Dots on alveolar macrophages or cellular debris floating in the alveolar space were regarded as "air" spaces dots. Dots that fall on structures that were not clearly recognizable, because of technical artifacts as one of the three components (cells/stroma/air) were not assigned. The relative fractions of a) air, b) cells (including dots on nuclei) and c) stroma were calculated.

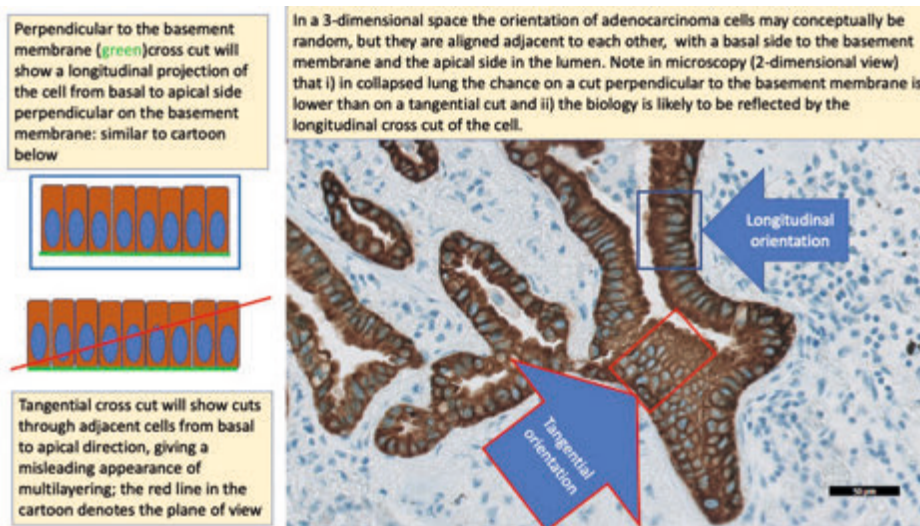
The relative fractions of a) air, b) tumour cells and c) stroma were calculated. Subsequently, the minimum and maximum apicobasal tumour cell height was measured in microns with a ruler available in the software (Philips IntelliSite Pathology solution, Image management system 3.3 (1.4). For the latter measurement, only cells with clearly discernible profiles were selected, while for instance areas of tangential cutting with

multilayering were excluded. The measurements were performed on the two cohorts. The Milan set was used as a test set and the OLVG cases for validation.

Criteria of iatrogenic collapsed adenocarcinoma in situ in a proposed modification of the adenocarcinoma classification

Iatrogenic collapsed AIS was defined as a folded alveolar wall lined with a monolayer of non-mucinous adenocarcinoma cells. Within “the alveolar wall” in the elastin stain fragmented or linear elastin fibers should be present. Moreover, in CK7 staining, a regular pattern of collapsed alveolar septa is visible.

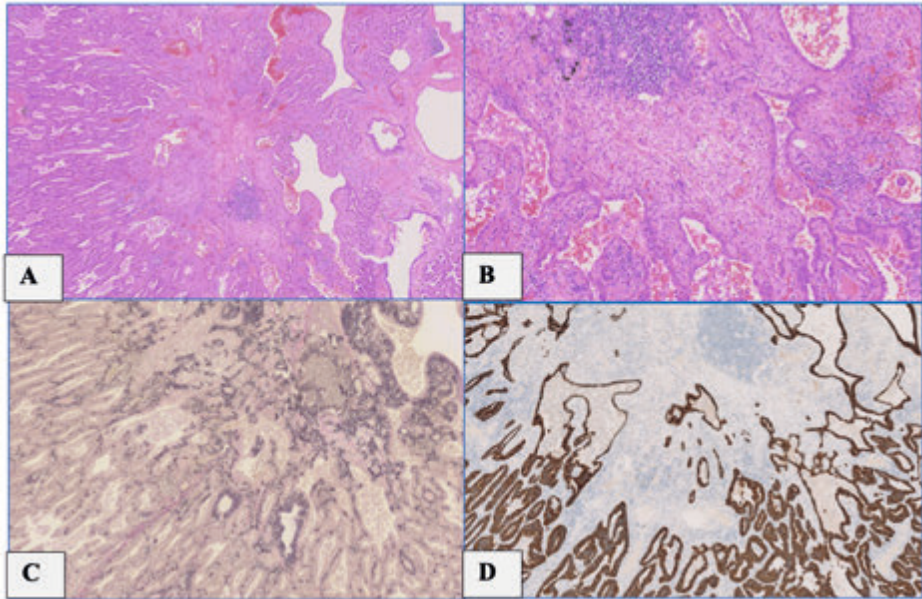
In AIS with iatrogenic collapse without scar, the *in vivo* structure is altered from straight alveolar walls to an undulated, folded, focally pseudopapillary or wavy appearance. On low power view, the tumour growth in AIS respects the physiological contours of the bronchovascular bundles and interlobular septa. The lining tumour cells can focally overlap with mild stratification³¹⁴ and this effect is even accentuated by tangential cutting (Figure 5). The tumour cells in (iatrogenic collapsed) AIS have usually low nuclear grade³²².



■ **Figure 5.** Illustration of the phenomenon of tangential cutting.

In AIS with scar, two components are discerned: fibrosis with dense collagen, and biological collapse with increased elastin. The latter is recognized by the pre-existing pulmonary architecture, previously described as Noguchi 1995 type B¹⁰ or Type II by Goto et al, both concluded to be non-invasive³²³. In AIS, the area with collagen rich scar lacks invasive tumour cells in the H&E and CK7 stain.

The pattern of iatrogenic collapsed AIS adjacent to the scar is more or less similar to AIS without scar, except for the border zone between scar and AIS. In the border zone, a reduction of glandular structures may be observed (Figure 6A and B). The sometimes-angulated compressed alveoli may mimic an acinar pattern³¹⁷, but the elastin containing structures support non-invasive nature (Figure 6C). In the CK7 this change in glandular size also shows a regular pattern (Figure 6D), in line with the WHO classification¹⁹.



- **Figure 6.** Case of adenocarcinoma in situ showing at the periphery a regular pattern of a monolayer of tumour cells with a central “scar” (A, H&E, 100x). At the border area of the scar a reduction of alveolar structures is seen, but no desmoplastic stroma (B, H&E, 200x). In the elastin staining there are elastin fibers in the peripheral preexisting alveolar septa, while in the “scar” area remnants of alveoli with increased elastin are visible (C, Elastin, 100x). In cytokeratin 7 staining at the periphery regular pattern is seen, with condensation of alveolar or “gland-like” structures towards the edge of the “scar” (D, CK7, 200x). Note that the “scar” area fits in the description of biological collapse with smaller alveoli with increased elastin.

In the proposed modified classification, the elastin staining is used for the differential diagnosis between true papillary carcinoma and collapsed AIS: the presence of elastin demonstrates that these structures represent pre-existing collapsed alveolar walls³⁰⁸ and should, without other signs of invasion, be interpreted as part of the pre-existing peripheral pulmonary framework, supporting the diagnosis of AIS. When invasion is present in other areas, the growth pattern that occurs along the alveolar surfaces of adenocarcinoma is referred to as “lepidic”. We distinguish several other forms of intra-alveolar growth, besides a monolayer as in collapsed AIS or papillary carcinoma:

a) complete alveolar filling tumour growth is a solid pattern similar to the WHO; b) cribriform pattern is made of multiple small lumina visible within an alveolar space which fit in an invasive acinar pattern^{324 325 326}; c) micropapillary growth shows tufting with discohesive tumour cells^{327 328 329}; and d) a grey zone refers to an alveolar growth that exceeds the criteria of a monolayer of collapsed AIS but does not meet the criteria for options a-c. These alveolar growth patterns are surrogate markers of invasion, as opposed to true morphologic invasion which is frequently associated with desmoplastic stromal reaction. Examples of the latter are invasive growth of individual, small tumour cell clusters or glands, usually surrounded by desmoplastic stroma and lacking elastin. A summary is shown in table 1.

■ **Table 1.** Revised adenocarcinoma classification based on evaluation of H&E, CK7 and elastin stainings.

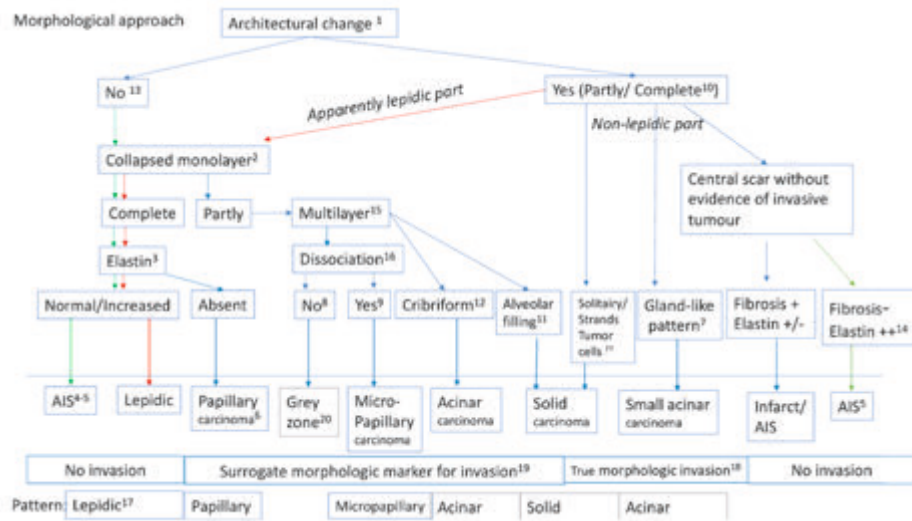
Revised adenocarcinoma classification*)	Remarks	
AIS ± collapse	Regular pattern, monolayer of tumour cells, elastin in alveolar wall	Iatrogenic collapse is collapse of flexible parts of the parenchyma. Biological collapse is associated with an increase of elastin (Noguchi type B). Without increase of elastin is Noguchi type A ¹⁰ . Minor collagen fibers may be present in biological collapse between elastin and tumour cells. This observation needs further study. In CK7 stain a regular pattern of CK7 positive tumour cells. Borders of bronchovascular bundles and interlobular septa are respected. Any irregularity in the CK7 pattern should be scrutinized for focal true invasion. Tangential cutting of a monolayer may lead to focal pseudo-stratification. This should not be interpreted as micropapillary or grey zone.
	Iatrogenic collapsed AIS has pseudo-papillary and pseudo-acinar appearance	Carcinomas do not produce elastin. Segmented (or continuous) elastin fibers in relatively thin alveolar walls point to growth on alveolar wall. Luminal alveolar macrophages may vary in number. When abundantly present the iatrogenic collapse is less pronounced.
True invasion in:	Bronchovascular bundle	Expansion in size, also visible in elastin staining
	Interlobular septum	Delineated by elastin on both sides.
	Alveolar space, accompanied by desmoplastic stroma	Desmoplastic stroma may be focal or very extensive (solid). The CK7 supports in the recognition of individual tumour cells. Some pulmonary adenocarcinomas lack or have reduced CK7 staining intensity ³³⁰ .
	Visceral pleura	Elastin criteria, similar as in WHO 2021
	Interstitium = stroma of alveolar walls	When alveolar walls are lined with alveolar type II cells, think of metastases. Small acinar adenocarcinoma has glands <<200 µm and usually not surrounded by elastin.

■ **Table 1.** Revised adenocarcinoma classification based on evaluation of H&E, CK7 and elastin stainings. (continued)

Surrogate markers of invasion "alveolar filling growth"		
All subtypes	Growth within alveoli in ≥ 3 adjacent alveolar spaces	The threshold of 3 adjacent alveolar spaces implies that the type alveolar filling growth should be consistently present and avoids the overlap with tangential cutting, especially in marked iatrogenic collapse.
Solid	Complete alveolar filling	Complete alveolar filling is not seen in iatrogenic collapse.
Cribriform	Gland in gland formation	The almost complete alveolar filling is not seen in iatrogenic collapse. Overlap with solid pattern may occur.
Micropapillary	Tufting, dissociation	Beware of artifacts due to delayed fixation, which may not only be observed by detachment of tumour cells from the underlying stroma, but also by diffuse single cells.
Papillary	Fibrovascular cores without elastin	Growth in alveolar space. Occasionally also in lumen bronchus/ bronchioles. Disturbed homeostasis of elastin is visible by variable amounts of elastin in pre-existing alveolar wall. In lumen of bronchus or bronchioles: lack of elastin. Alveolar macrophages usually absent.
Grey zone	Multilayering more than in tangential cut AIS, but not enough to fall in one of the other subtypes	Recently, a slightly different approach was proposed and the "in between" zone was called "extensive epithelial proliferation" ³¹⁷ .

*) Minimal invasive adenocarcinoma and the so-called invasive pattern of STAS are not used in this classification.

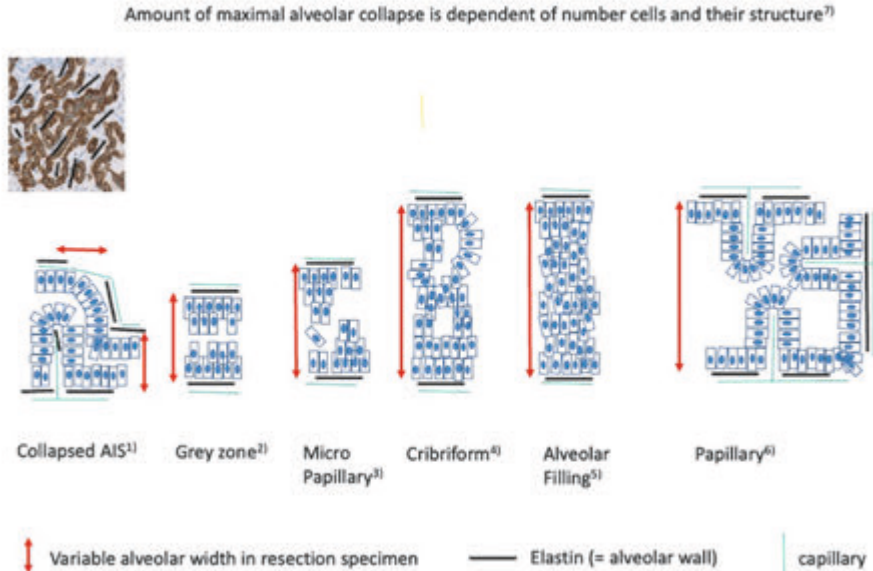
A flow chart of this morphologic approach is shown in Figure 7.



■ **Figure 7.** Flow Diagram with morphological approach on invasion in pulmonary adenocarcinoma

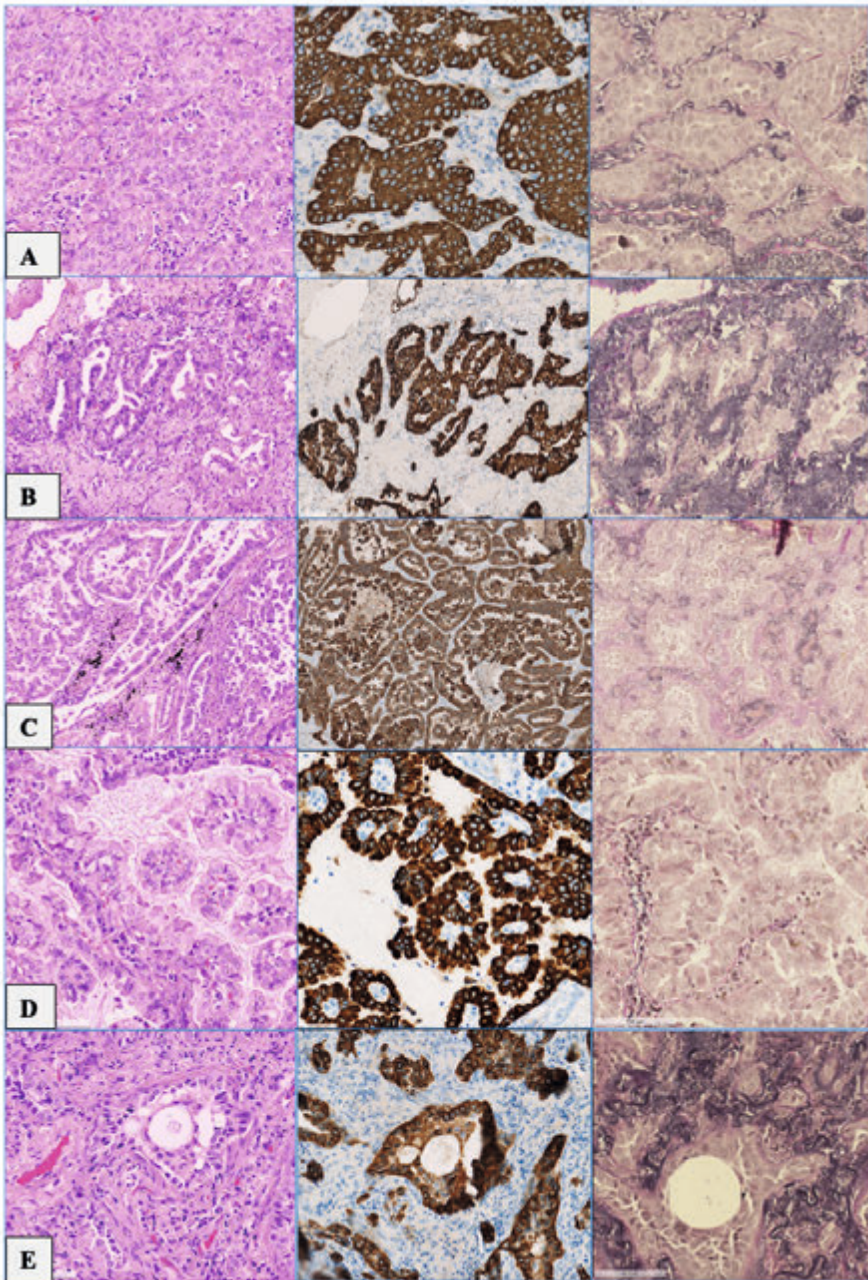
- 1) Architectural change by the tumour also determined in CK7 and elastin stain
- 2) Iatrogenic collapse and monolayer of cells. Due to tangential cutting multilayering may occur in part of alveolar structures
- 3) Elastin stain info in review Histopathology 2021²⁰⁶
- 4) Noguchi type A: AIS with lepidic growth on thin alveolar septa.
- 5) Noguchi type B: AIS with increased amount of elastin causing slightly thickened alveolar septa (iatrogenic +/- biological collapse)
- 6) Papillary carcinoma does not produce elastin; fragmented elastin is normal and denotes alveolar walls.
- 7) Gland-like structures, in area without pre-existing alveoli, usually have a "glandular" diameter <<200 µm (size of average alveolus) and is therefore called "small" acinar adenocarcinoma; usually no elastin in between the gland-like structures. Small acinar adenocarcinoma may also invade in the interstitium of alveolar walls.
- 8) No dissociation and distinct multilayering in several adjacent alveoli: uncertain, more data required; for time being designated as invasive.
- 9) This typically is the micropapillary pattern lining the pre-existing alveolar wall
- 10) implies cases with complete effacement of pre-existing architecture, but may also be cases with lepidic growth and focal features invasion.
- 11) Solid adenocarcinoma contains alveolar filling with tumour cells, invasion of individual tumour cells, small strands of tumour cells and/or larger interstitial fields of tumour. Individual cells and strands of cells are frequently embedded in desmoplastic stroma (loose fibromyxoid stroma).
- 12) Cribiform is intra-alveolar growth with epithelial proliferation with a "gland-in-gland" formation. This prevents iatrogenic collapse and has in the elastin stain only elastin on the outside.
- 13) Only growth on alveolar walls (lepidic growth) with or without iatrogenic collapse.
- 14) Increased elastin and no other signs of invasion (NOSI): Biological collapse, where in the elastin stain the pre-existing alveolar structure can easily be recognized usually in association with increased elastin in alveolar walls with lepidic growth: Also Noguchi type B. In this pattern the CK7 stain may show comma like CK7 positive structure in the region close to collapse without CK7 positivity.
- 15) The area with multilayering is defined as fully present in at least a few adjacent alveoli. Not infrequently the lobular unit has the same appearance.
- 16) Loss of cellular cohesion.
- 17) Lepidic in association with true morphological signs of invasion in non-lepidic part 18) Beside lympho-, bronchial- and pleural invasion
- 18) No real invasion observed but presence is associated with other signs of invasion (true invasion, lymphogenic and/or haematogenic invasion
- 19) Multilayering / stratification in >=3 alveolar structures, which fall short of the minimum criteria for micropapillary (3 cells tall, 2 cells wide)
- 20) MIA is not used, see discussion.
- 21) STAS is not undisputed; not used.

A graphical display and histologic examples of this morphologic approach are shown in the Figures 8 and 9.



■ **Figure 8.** Schematic drawing of intra-alveolar growth

- 1) In collapsed AIS the pre-existing alveolar wall is recognizable by the elastin fibers (black). Above the schematic drawing is a CK7 staining with added elastin fibers. Seemingly papillary or acinar structures with thin walls containing elastin fibers are pre-existing alveolar walls (pseudo-papillary /pseudo acinar). In collapsed AIS the tumour growth is essentially a monolayer, where tangential cutting is a focal effect (part of an alveolus) that may lead to seemingly multilayering.
- 2) In the grey zone stratification is present in at least 3 adjacent alveolar spaces. This may also be seen close to the transition with non-malignant pneumocytes.
- 3) In micropapillary dissociation is frequently present. Tufting / micropapillae are minimally 3 cells tall and 2 cells wide.
- 4) "Gland-in-gland formation" also called "cribriform" is a form of acinar adenocarcinoma
- 5) Alveolar filling growth is a form of "solid" pattern. The cribriform and solid pattern prohibit alveolar collapse during resection.
- 6) Papillary carcinoma has fibrovascular cores, where the cores and the vessels therein do NOT contain elastin.
- 7) Note A): the amount of alveolar collapse in the tumour area is dependent of the number and structure of the tumour cells. If there are also alveolar macrophages present, this may reduce the possible collapse as well. Note B): all criteria associated with invasive growth should be present in at least 3 alveolar spaces.



■ **Figure 9.** Histologic examples of the intra-alveolar surrogate invasive growth patterns

In each row respectively from left to right H&E, Cytokeratin 7 and elastin stainings. Note in the elastin stainings in all patterns a preserved pre-existing alveolar architecture with elastin fibers present.

A, solid with alveolar filling; B, cribriform; C, micropapillary; D, papillary; E, grey zone in biological collapse.

Furthermore, the presence of a scar, defined as a (peri)centrally in the tumour located, recognizable area of fibrosis and/or collapse with elastosis was estimated in each tumour. The composition of the scar was scored as only fibrotic, only biological collapse or the combination of both. In each case the presence of invasive growth into the scar area was scored as absent, extensively present, focal in the fibrotic or biological collapse part or in both.

The immunohistochemical stain for Cytokeratin 7 (CK7) (clone OVTL12/30 (Agilent/Dako (Glostrup, Denmark, catno. M701801) was performed in a Roche/Ventana benchmark Ultra (Roche, Basel Switzerland) with 4 µm tissue slides mounted on TOMO-glass slides (Roche, Basel, Switzerland). Antigen retrieval was applied with high pH-buffer CC1(32 minutes at 100°C) and the antibody was diluted 1/100 (incubated for 32 minutes at 36°C) and detected with the Optiview DAB kit under standard conditions. Sections were dehydrated with ethanol 100%, cleared with Xylene and coverslipped with Tissue-Tek coverslip film on the Sakura coverslipper (Sakura Finetek Europe B.V, Alphen aan den Rijn, The Netherlands). Internal positive controls were pneumocytes and respiratory epithelial cells. Internal negative controls were e.g., smooth muscle cells in vessel walls and bronchioli.

Statistical analysis

In the morphometrical part, Pearson's correlation coefficients were estimated between amount of air dots and tumour cell height. In the 2 cohorts, survival times, measured as a) recurrence free survival (RFS, time from initial surgery to recurrence); b) overall survival (OS, time from surgery to death from any cause)³³¹, were compared between cases identified as collapsed AIS and invasive cases using the log rank test. Survival times are plotted with Kaplan-Meier curves, 5-year survival were reported with corresponding 95% confidence interval (CI). The significance level was set at 0.05. All analyses were conducted in SPSS version 26 (IBM Corp., Armonk, NY).

Results

Morphological consequences of the mathematical model

In the mathematical model the 3-dimensional configuration, comparable to alveolar structures was used. A graphical display with a 2-dimensional and a 3-dimensional approach is shown in Figure 10.

Figure 1 A

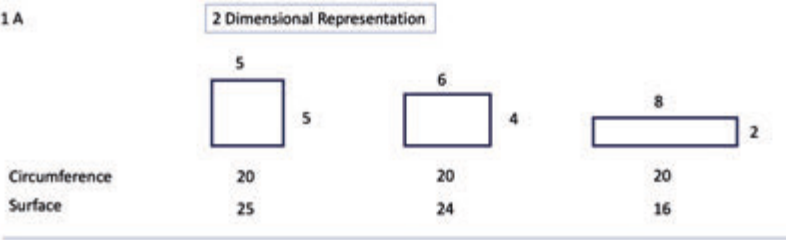
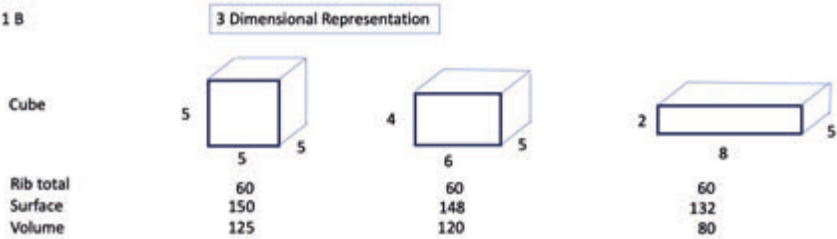
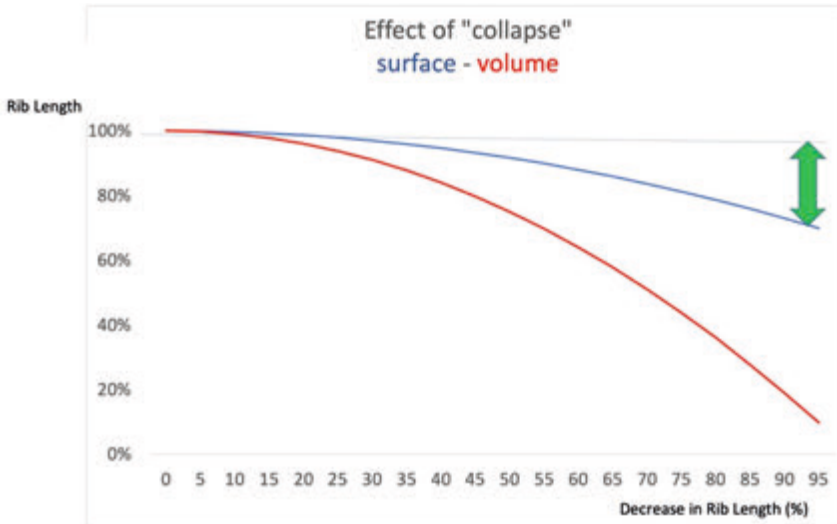


Figure 1 B



■ **Figure 10.** The effect of collapse in a 2-dimensional representation (A) is shown where the square has a higher surface area than a rectangle with the same circumference length. B. Examples of three different boxes are shown: left a box with equal length of the ribs and right two flatter boxes with different sizes of the ribs, but the total size of the ribs in each of the three boxes is the same.

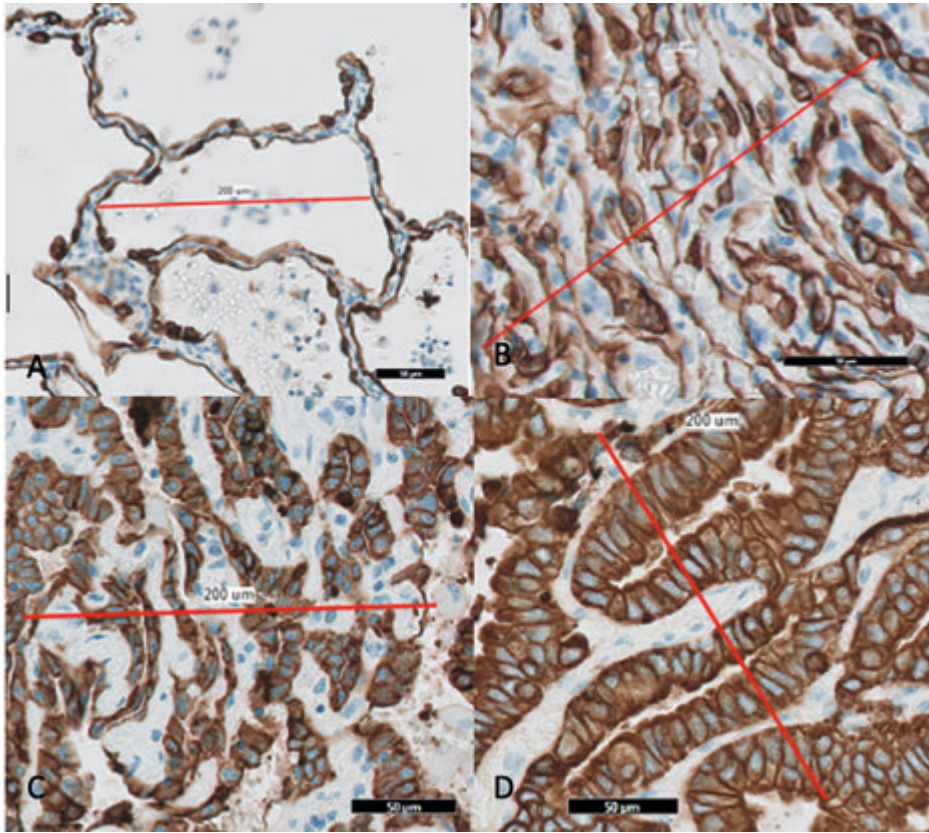


■ **Figure 11.** The relation between volume (red line) and surface (blue line) is shown for boxes of different shapes involving progressive reduction in size of one rib and similar increase of a second rib while the third rib remained unchanged. A smaller box requires less surface. As during iatrogenic collapse, the alveolar surface does not change, the relative excess of surface is shown by the green arrow.

The effect on the box surfaces and volumes with progressive decrease in size of one rib and increase in size of another rib is shown in Figure 11.

According to the model's prediction, near maximal collapse, there is an estimated decrease in surface area of approximately 15-20% and a decrease in volume of 95-100%. This decrease in surface and volume is similar across boxes of sizes 200, 300, and 400 μm , indicating that this reduction is independent of the original size of the box, i.e., alveolar size.

To quantify the maximal collapse of pulmonary parenchyma, a sample without malignancy and virtual absence of air was used, where the pneumocytes type I of an alveolar wall practically touch the pneumocytes of the opposing alveolar wall. The measurements revealed that 12 alveolar wall cross sections fit in nearly complete iatrogenic collapsed normal lung parenchyma in a length of 200 μm (the size of an average alveolus) (figures 12 A and B), as well as that the alveolar septa showed an undulated appearance. In adenocarcinoma resections with lepidic growth, a mean of 4.8 (range 3 to 7) and 4.3 (range 3 to 6) alveolar walls were measured in Milan and Amsterdam cohort, respectively (figures 12 C and D).



■ **Figure 12.** Examples of CK7 IHC in normal lung parenchyma (A), normal expanded alveoli, collapsed normal parenchyma (B) and collapsed AIS (C, D). The red line has a length of 200 μm , equivalent to the diameter of a normal air-filled alveolar space as shown in A. In the collapsed normal lung parenchyma (B), up to 12 alveolar septa were counted along a line of 200 μm . In pulmonary adenocarcinoma with lepidic growth approximately 4-5 cross sections of alveolar walls lined with tumour cells fit into a length of 200 μm .

This model apparently has two implications for lung morphology.

Firstly, due to iatrogenic collapse, an alveolus shrinks to less surface area than in-vivo. As the alveolar wall membrane surface will not decrease during iatrogenic collapse, the only option for the alveolar walls is to spatially fold (Figure 1, 12 and the grape as an analogous example in Figure 3).

Secondly, the folding of the lining epithelial cells may result in sideways tension on these cells. When the collapse is at its maximum, all of the tumour cells will be subjected to maximal compression. However, if the collapse is less prominent, then the pressure on the tumour cells may be lower. As tumour cells typically make contact with the basement membrane on the basal side and are surrounded by neighbouring tumour

cells, the only potential way to handle the sideways pressure during iatrogenic collapse is the displacement of cellular material towards the alveolar lumen on the apical side. If this hypothesis is correct, it is possible that tumour cells may exhibit an increased apicobasal height in instances of more pronounced collapse.

In the test set, 20 cases were suitable for measurements, while in the validation cohort 16 cases could be measured. The measurements of apicobasal tumour cell length and relative air surface are shown in Table 2.

- **Table 2.** The mean \pm standard deviation (SD) of minimum tumour cell length, relative air surface and stroma is shown for Milan (test cohort) and Amsterdam cases (validation cohort).

Cohort	Minimum TC length	Relative air surface	Stroma
	Mean \pm SD	Mean \pm SD	Mean \pm SD
Test, n=20	8.3 \pm 2.6	18.8 \pm 14.6	18 \pm 6.9
Validation, n=16	9.6 \pm 2.9	23.2 \pm 15.8	13.5 \pm 6.2

The correlation coefficient between the relative amount of air and minimal tumour cell height in the Milan cohort's test set showed an inverse relationship. Put differently, the smaller the amount of air (i.e., more pronounced collapse), the larger the apicobasal tumour cell length ($r = -0.44$; $p < 0.001$). In the independent OLVG cohort, this finding was validated ($r = -0.42$; $p = 0.001$).

For the maximal tumour cell length, the correlation values were similar for both test and validation set, $r = -0.43$ ($p < 0.001$) and $r = -0.39$ ($p = 0.002$), respectively. The correlation coefficient for stromal area with minimal tumour cell length was not significant in both data sets (p values in test and validation set: 0.50 and 0.64, respectively).

Reclassification of cases

The clinical characteristics of the two cohorts that were tested are shown in table 3.

Out of the 70 cases, 56 contained a scar (80%), of which 38 (54%) had a combination of biological collapse and fibrosis. The remaining cases showed biological collapse ($n=11$, 16%) or fibrosis only ($n=7$, 10.0%). Of the 10 AIS cases, 5 did not show scar signs and the remaining showed biological collapse ($n=3$) or a combination of biological collapse and fibrosis ($n=2$). In 48 of the 56 cases (86%) with a scar, tumour infiltration was seen within the scar. In all 7 "fibrosis only" scars invasion was present (100%), while this was the case in 35 of the 38 cases with a combined scar (92%). In 6 of the 11 (55%) "biologic collapsed only" scars, invasion was discerned.

■ **Table 3.** Clinical variables in both cohorts.

	Milan	OLVG	Total	p-value
Number of patients	35	35	70	
Age (years, mean ± SD)	67.2 ± 9.9	61.5 ± 7.6	64.4 ± 9.2	P=.009
Gender (%)				P=.002
Male	25 (71.4%)	12 (34.3%)	37 (52.9%)	
Female	10 (28.6%)	23 (65.7%)	33 (47.1%)	
Mean follow-up time (months, range)	61 (11-113)	81 (28-132)	69.5 (11-132)	P=.005
Resection type (%)				
Segmentectomy	9 (25.7%)	4 (11.4%)	13 (18.6%)	P=.128
Lobectomy	26 (74.3%)	31 (88.6%)	57 (81.4%)	

Note that the cohorts differ with respect to age, gender and follow-up time. According to the initial reports, only one of the cases was diagnosed as AIS. After revision, 9 of originally classified invasive cases were reclassified as AIS. Three were originally classified as acinar with a lepidic component, three as lepidic predominant with an acinar component, one as papillary, one as MIA and one as acinar. Subtyping after revision is shown in Table 4.

■ **Table 4.** revised subtyping of the adenocarcinomas in both cohorts

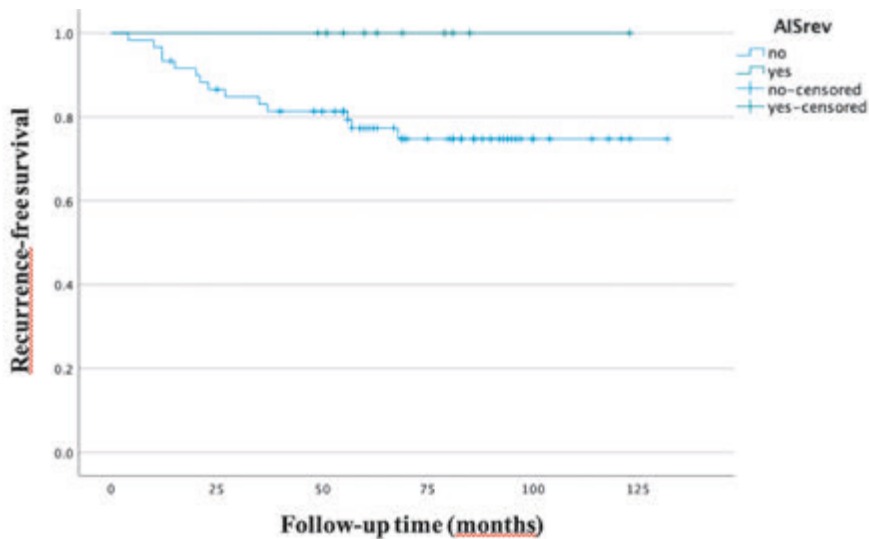
Adenocarcinoma predominant subtype (%)	Milan cases	OLVG cases	Total (n=70)
AIS	2	8	10 (14.3%)
Lepidic predominant	7	6	13 (18.6%)
Acinar	10	9	19 (27.1%)
Micropapillary	2	3	5 (7.1%)
Papillary	3	1	4 (5.7%)
Solid	11	8	19 (27.1%)
Pathologic stage ¹⁾ (%)			
pTis	2	8	10 (14.3%)
pT1a	7	6	13 (18.6%)
pT1b	15	13	28 (40.0%)
pT1c	11	8	19 (27.1%)

¹⁾According to 8th edition of UICC/AJCC TNM classification system

Survival data

The RFS-time in patients with a relapse between the two cohorts did not differ significantly (Milan mean 26.7 months (n=7); OLVG mean 30.0 months (n=7; p=0.77).

Therefore, in analysis of follow-up of AIS, the two cohorts were combined. The 5-years RFS of the 10 patients with AIS was 100% as compared to 77% of the 60 patients with invasive adenocarcinoma ($p=0.11$, Figure 6). The 5-year OS for the patients with AIS was 100% and with invasive adenocarcinoma 74.5% ($p=0.072$). In one of the reclassified cases, 6 years after the primary resection, there was suspicion of recurrent disease in a mediastinal lymph node (N7). After further analysis, this turned out to be a second primary with a different cytology and immunohistochemistry: large cell neuroendocrine carcinoma. Survival analysis in patients with or without scars revealed no significant differences in RFS and OS.



■ **Figure 13.** Kaplan-Meier curves of the RFS of the 10 patients with AIS cases compared to the 60 invasive adenocarcinomas ($p=0.11$).

Discussion

This study, using a mathematical model and histologic arguments, explained how iatrogenic collapsed pulmonary parenchyma causes wrinkling of the alveolar walls and alteration in tumour cell height. Taking into account the changes in iatrogenic collapsed AIS histology, led to reclassification of 9 patients with small pulmonary adenocarcinoma (13.0%) to AIS, supported by the 100% recurrence-free survival rate. Furthermore, we described in detail revised classification criteria using elastin and keratin 7 immunohistochemistry in this study and recognized other intra-alveolar growth patterns, other than the monolayer like in AIS in the revised classification, that could be surrogate markers of invasion.

The maximum degree of iatrogenic collapse that may occur is influenced by the thickness of both the alveolar epithelial lining and wall. In cases of lepidic adenocarcinoma, the increased thickness of the lining reduces the flexibility of the alveolar walls, but the tumour cells themselves remain relatively flexible. This also explains the difficulty for surgeons to localize, i.e., by palpation, ground glass opacities during surgery. On the other hand, acquired desmoplastic stroma has a solid texture that cannot be compressed, making it easier to feel during palpation.

The physiological variation in surface and volume during breathing is neglectable. In contrast, the morphology drastically changes during iatrogenic collapse, not only at architectural, but also at cellular level. A possible minor adaptation during collapse of the peripheral pulmonary parenchyma may be that the recoil of the elastic fibers support surface reduction to some extent. The contracting activity of myofibroblasts, normally placed under the pneumocytes, and adaptation in length of the smaller airways may also play a minor role.³¹⁸ However, this is not sufficient to prevent the here described wavy/undulatory appearance of the alveolar walls.

Tangential cutting leads to pseudostratification, which may add to the confusion with invasive adenocarcinoma. In practice, this tangential cutting effect is present in focal areas of the collapsed alveolar space, and not in the whole alveolar space. The biology of the lesion is likely to be represented by the monolayer, whereby focal cell overlap or mild stratification is a known feature¹⁹.

Undulating appearance may give rise to over-interpreting collapsed AIS as a papillary or acinar predominant pattern³³². Therefore, to understand the in-vivo growth patterns of pulmonary adenocarcinomas, the pathologist requires beside a mental image of the normal microanatomy of the inflated lung, also a mental image of the deflated wrinkled alveolar walls as this modification inevitably occurs during the surgical procedure. The presence of (discontinuous) elastin fibers in a tumour with fibrovascular cores lined by tumour cells, denotes the fibrovascular core as a 2-dimensional cross cut of alveolar wall. Without other invasion characteristics, the diagnosis is than (iatrogenic collapsed) AIS.

The minimum criterion of alveolar filling growth patterns as surrogate marker of invasion is that at least a few adjacent alveoli should contain this pattern, to avoid overdiagnosis of invasive adenocarcinoma. This approach is in line with that in the breast: e.g. in the diagnosis of lobular carcinoma in situ³³³ and the differentiation from (atypical) hyperplasia. In such cases, the criteria is that more than 50% of the acini in a terminal duct lobular unit must be filled and expanded by the neoplastic cells to qualify as lobular carcinoma in situ.

MIA is not used in the revised classification, as 2 mm true invasion may be associated with a recurrence in the follow-up. In addition, the recognition of elastin in pre-existing alveolar wall may induce downgrading to AIS if signs of invasion are absent. The overdiagnosis in application of the WHO classification explains the improved prognosis of papillary carcinoma and some acinar carcinomas and also the recognition of the MIA category.

A scar could be relevant as a sign of invasive growth and has been described as a potentially unfavourable prognostic feature in the 1980's by Shimosato et al.²⁷⁶, whereby the composition of the scar itself was also identified as a prognostic criterion. Hyalinized scars in patients with a resected adenocarcinoma of 3 cm or less were associated with more lymph node metastasis or pleural invasion than those without scar or more fibrotic scars.

Suzuki et al. found that patients with a central scar of less than 5 mm had a 100% 5-year overall survival rate³³⁴. More recently, Bittar et al. showed that adenocarcinoma with a scar was associated with a better prognosis³³⁵. Interestingly, their discussion mentions: "From a morphological standpoint, there is no histologic feature that could separate pre-existing subpleural scar/apical cap from scars associated with carcinomas". This suggests that they observed increased elastin in line with biological collapse and associated good prognosis¹⁰.

Comparable to Bittar et al.³³⁵, our study consisted of a cohort without lymph node metastasis and an occasional case with pleural invasion, but their cases also included tumours larger than 3 cm (range 1-5). Also, in our study the majority of scars had a fibroelastic appearance (80%). Similar to Noguchi type B, we found in 5 of the 10 AIS cases a scar-like area¹⁰. In H&E staining, fibroelastosis is not always easily recognizable, while in the elastin staining, prominent increase of elastin supports proper interpretation. In those cases, with fibrotic and biologic collapsed scars, most (85.7%) had at least focal areas of invasion. Invasion was observed in all 7 'fibrosis only' cases and a lower fraction in the 'biological only' cases (54.5%). In contrast to the studies of Shimosato and Bittar, nor the presence of a scar, neither the composition of it, was correlated with RFS nor OS in our study. This could be explained by the fact that in our study, cases with lymph node metastasis were excluded and the cohorts contained just one case with pleural invasion and contained just tumours of 3 cm or smaller.

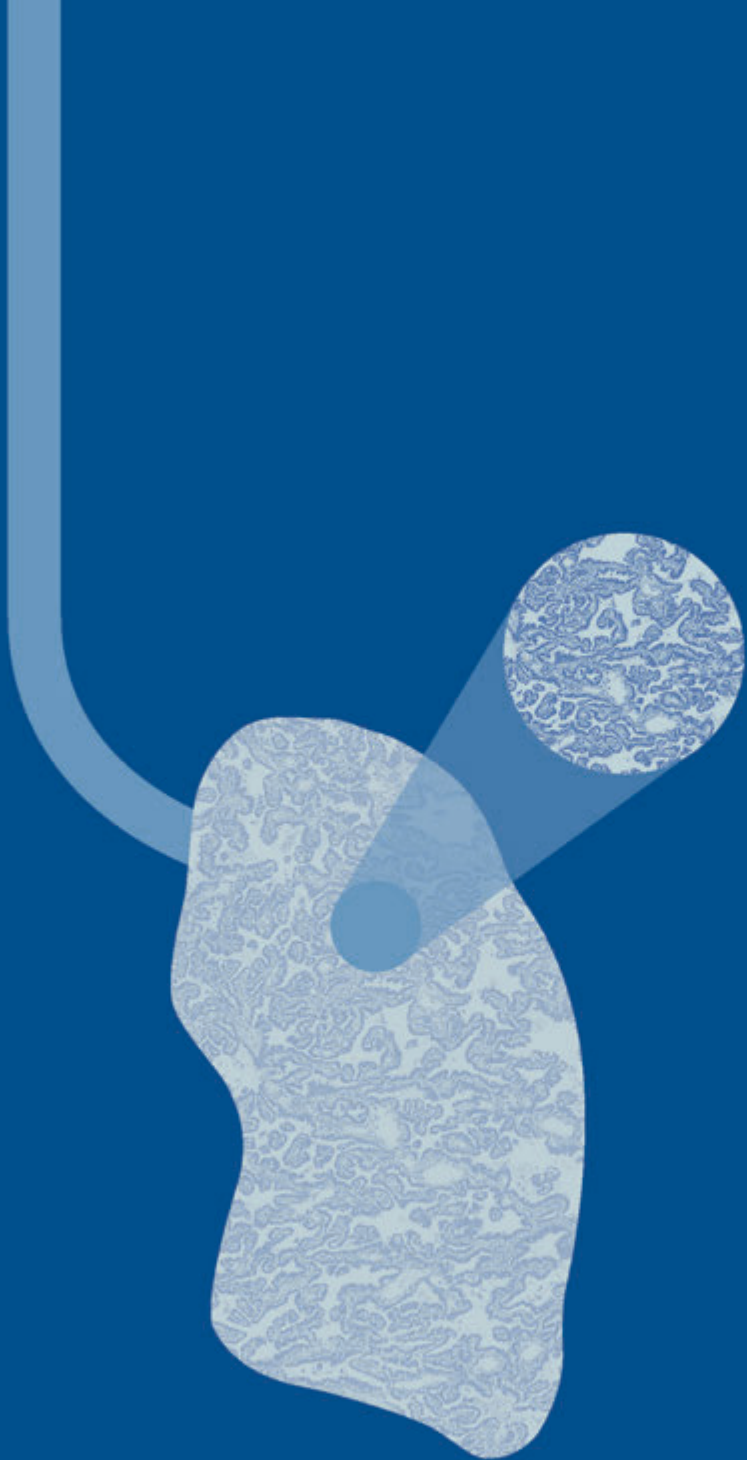
Recently, Yambayev and colleagues performed a study in the same pulmonary adenocarcinoma domain, searching for a "low malignant potential" subgroup with a better prognosis³³⁶. Their proposed criteria for "low malignant potential" adenocarcinoma among non-mucinous adenocarcinoma were a total size of ≤ 3 cm, exhibiting $\geq 15\%$ lepidic growth, and lacking non-predominant high-grade patterns ($\geq 10\%$ cribriform, $\geq 5\%$ micro-papillary, $\geq 5\%$ solid), >1 mitosis per 2 mm^2 , angiolymphatic or visceral pleural invasion, spread through air spaces or necrosis³³⁶. They followed the managerial process of the current WHO classification¹⁹ and did no attempt to distinguish morphological invasion. Interestingly, they accepted high grade patterns, but with low thresholds: "low malignant potential" may have up to 10% cribriform and micropapillary and 5% solid pattern. In comparison with our study this may encompass cases with tangential cutting of lepidic AIS, which may mimic focal high-grade (solid) patterns and explain the prognostic association in their study. It is likely that cases in our study may represent the same subgroup as in the study of Yambayev and colleagues. For example, in their figure 1D, diagnosed as acinar predominant adenocarcinoma, we would diagnose this as collapsed AIS.

The prevalence of AIS in our study cohort was high with 10 out of 70 cases (14.3%) is higher than previously reported incidences of AIS in NSCLC (1-8%)³³⁷, but similar to the 16% reported by Murikami et al⁷ and by Yambayev et al. for adenocarcinoma when “low malignant potential” is included³³⁶.

Verifying the hypotheses regarding iatrogenic collapsed AIS with 100% recurrence-free survival has a limitation. Resection of non-mucinous adenocarcinomas may lead to cure, and the presence of invasive characteristics without metastases is not excluded by the disease-free survival rate. This implies that the lack of recurrence is not synonymous with the absence of invasion.

Conclusion

Our results showed that iatrogenic collapsed AIS forms a complex wrinkled morphology. The use of elastin and CK7 staining aids in the recognition of iatrogenic collapsed AIS and the distinction from invasive adenocarcinoma. Awareness of iatrogenic collapsed AIS is important, as these patients are cured after resection. Further studies are necessary to determine whether the proposed modified classification improves pattern recognition accuracy, and lifts the long-lasting fog.



15

Invasion measurement and adenocarcinoma *in situ* (AIS) in pulmonary adenocarcinomas of 3 cm or less. A reproducibility study according to the WHO and a modified classification.

Erik Thunnissen#, **Hans Blaauwgeers**#, Federica Filipello, Birgit Lissenberg-Witte, Yuko Minami, Masayuki Noguchi, Willem Vreuls, Jan H. Von der Thüsen, John Le Quesne, Mauro Giulio Papotti, Wim Timens, Irene Sansano, David Moore, Sabina Berezowska, Aleš Ryška, Giuseppe Pelosi, Luka Brcic, Kirk Jones, Noriko Motoi, Yukio Nakatani, Christiane Kuempers, Paul Hofman, Veronique Hofman, Vibeke Grotnes Dale, Giulio Rossi, Francesca Ambrosi, Daisuke Matsubara, Yuichi Ishikawa, Birgit Weynand, Fiorella Calabrese, Izidor Kern, Sven Perner, Diana Gabriela Leonte, Siobhan Nicholson, Douglas Flieder, Marc Ooft, Mariel Brinkhuis, Nicole Bulkman, Shaimaa Al-Janabi, Aino Mutka, Sanja Dacic, Mary Beth Beasley, Gianluigi Arrigoni, Rienke Britstra, Hendrik Hager, Andreas Schønau, Federica Pezzuto
equally contributed

In preparation to be submitted

Abstract

Background

The definitive identification of the invasive component of mixed pattern non-mucinous adenocarcinoma of the lung is crucial, as only the invasive size is used for staging. The separation of true invasion from iatrogenic collapse is difficult. This study aims to investigate whether incorporating additional histopathological criteria for collapse enhances the identification of genuinely invasive regions in non-mucinous adenocarcinomas, and whether this impacts invasion measurements and subtype classification.

Design

Cases were obtained by combining two retrospective cohorts of pulmonary non-mucinous adenocarcinoma from institutes in different countries. Tumors were resected between the 1st January 2011 and the 31th December 2016, had a tumor diameter ≤ 3 cm, no metastases, and were linked to follow up data. Freshly cut sections of 70 cases were stained for H&E, elastin and CK7, scanned to digital image files, and uploaded to the Pathogate website. The cases were reviewed twice by 42 pulmonary pathologists to determine the presence of invasion: firstly, according to the 2021 WHO classification, and secondly using an alternative approach recognizing collapsed AIS. In between the 2 rounds an on-line tutorial was presented, together with written materials. The parameters recorded were presence of invasion, growth pattern percentages, total tumor size, location invasive area, invasive size, and an uncertainty score about decision of invasion. The heatmap analysis revealed areas more or less commonly scored as invasive in each case. Based on feedback from 41 peers in the first two rounds, which included scores and heatmaps highlighting the underlying histology of hotspots of invasion, a third round was conducted with the expectation that an updated classification system would result in improved consensus.

Results

A total of 42 pathologists from 13 countries scored all 70 cases in the first 2 rounds, while 36 pathologists scored 41 non-unanimous cases in the 3rd round. The kappa values for rounds 1, 2 and 3 were, 0.27, 0.45 and 0.62, respectively.

In the first round, more than 21 pathologists scored “No Invasion” in 3 cases, and this increased to 10 cases in the 2nd and 3rd rounds; crucially none of these cases recurred. In measurements of total tumor size, the mean coefficient of variation was 6% in two rounds (range 1st round 1-26%; 2nd 1-29%). In contrast, when measuring invasive tumor size, the mean coefficient of variation rose from 34% in the first round to 40% in the second round, and these changes were for each case visualized by heatmap analyses. Growth pattern subtyping showed least variation for “solid” pattern: kappa 0.65 and for the others <0.3.

Conclusions

There is significant interobserver variation in the measurements of invasive size and assignment of invasive patterns among pathologists. However, using refined morphological criteria along with CK7 and elastin staining can help improve recognition of collapsed AIS. The formal recognition of collapsed AIS can aid in identifying low-risk lesions that are wholly non-invasive.

Introduction

According to the 2015 WHO classification of non-mucinous lung adenocarcinoma, the predominant histological growth pattern present determines tumour subtype⁴. Furthermore, these patterns are used to assign tumour grade in recent IASLC recommendations²⁵². The concepts of adenocarcinoma *in situ* (AIS) and minimally invasive adenocarcinoma (MIA), first established in the 2015 WHO classification, are being recognized increasingly frequently, particularly in lesions identified through lung cancer screening. When resected, both AIS and MIA show essentially 100% 5-years survival³⁰⁶ and their definitive identification is crucial to prevent overtreatment with, for example, adjuvant chemotherapy.

The 8th edition of UICC/AJCC TNM classification system for non-small cell lung cancer (NSCLC) tumors recommends that the size measurement of the primary tumor be based solely on the invasive components¹⁹. The distinction between adenocarcinoma AIS from other patterns, which are all regarded as “invasive”, is therefore of utmost importance.

The poor reproducibility of invasive pattern recognition in adenocarcinomas was shown by an IASLC pathology committee study in 2012¹⁴.

During surgical resection deflation is part of the procedure and specimens typically arrive at the pathology laboratory in a collapsed state, often being compressed to less than half of their *in vivo* width. This iatrogenic collapse changes the morphology of the resected adenocarcinoma as well as background tissue. In particular, the histological criteria of the WHO pattern classification, especially papillary and acinar subtypes, show overlap with iatrogenic collapsed adenocarcinoma *in situ* (IC-AIS).

Our hypothesis is that the use of additional histopathological criteria may delineate IC-AIS from higher risk patterns currently designated as being invasive adenocarcinomas.

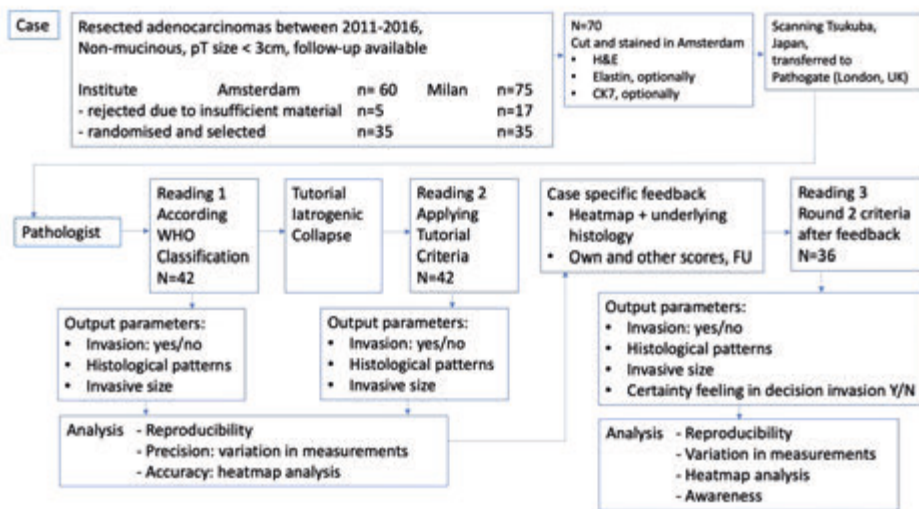
The aim of the study was to examine if such additional histopathological criteria can improve the recognition of non-invasive growth, with or without iatrogenic collapse, in non-mucinous adenocarcinomas, and to determine the effect of these criteria on invasion measurements and subtype classification.

To evaluate the potential of a revised classification, a group of 42 pathologists from different parts of the world were asked to interpret a series of adenocarcinomas twice. The first interpretation was based on the 2021 WHO classification, while in the second

interpretation additional criteria were provided and used. It is generally expected that reproducibility is higher within a single institute, so pathologists from multiple countries were included in this study. In a third round of interpretation, conducted under optimal conditions, the effectiveness of the revised classification was further assessed.

Materials and methods

An overview of the study design is shown in Figure 1.



■ **Figure 1.** Flow chart of study design including case selection

A retrospective multi-institutional study was performed on patients with resected pulmonary adenocarcinoma diagnosed between the 1st January 2011 and the 31st December 2016 in the Onze Lieve Vrouwe Gasthuis (OLVG), Amsterdam, the Netherlands and San Raffaele Scientific Institute, Milan, Italy.

Inclusion criteria were pathologically assessed tumor diameter ≤ 3 cm and complete follow-up information. Exclusion criteria were the presence of regional lymphogenic and/or distant hematogenous metastases at the time of resection, treatment with neoadjuvant chemotherapy and mucinous adenocarcinoma. The study was approved by ethical committees (VUmc: 2022.0269; OLVG: 21.044; San Raffaele Scientific Institute Milan 284/2022).

From 89 cases from San Raffaele Scientific Institute and 85 cases from OLVG all formalin-fixed paraffin-embedded (FFPE) blocks containing tumor were retrieved from the archive and send to Amsterdam. Two pathologists (ET and FF/HB) reviewed

the hematoxylin-eosin (H&E) stained slides and selected for the study 1 FFPE block containing the largest amount of invasive tumor from each case. Using the selected block, serial 4 μm sections were cut and stained with H&E, Elastin Van Gieson and immunohistochemically for Cytokeratin 7 (CK7) (clone OVTL12/30 (Agilent/Dako (Glostrup, Denmark, catno. M701801 performed in a Roche/Ventana benchmark Ultra [Roche, Basel Switzerland]), at UMC-VUmc. Cases with excessive delay in tissue fixation were excluded from the Amsterdam and Milan series (n=17 and n=5, respectively)³³⁰. From the remaining cases of Amsterdam (n=55) and Milan (n=75), 40 samples from each laboratory were selected after randomization. After digitizing 10 cases were omitted due to poor digitization with focus issue or fixation problems.

All slides were sent to Tsukuba, Japan (MN, YM) and scanned [with 40x objective] as described before³¹⁷. Subsequently, files were transferred to a server of UKNEQAS and the pathogate.net platform was used to organize the patient cases and served as the interface for data collection (A.S.).

Morphologic evaluation

All cases were initially read twice. For both readings the H&E image was supplied, and elastin and CK7 stain were optionally available for all cases. The data requested were: i) whether invasion was present (yes/no/not sure), ii) percentage of growth patterns, iii) total size, iv) invasive size, determined in two ways: A) by calculation according to the WHO (maximum diameter multiplied by invasive proportion) (according to WHO¹⁹ page 67) and B) by direct measurement using a digital ruler available in the image viewer, where the location and the length of the line was also recorded. Up to 3 lines designating separate invasive areas could be recorded. If >1 line was designated, the sum of all lines was used in further analysis. The first round of case scoring was performed according to current histopathological practice, as governed by the WHO pattern recognition criteria. After the first reading a tutorial was provided (see Supplementary file), which explained the distinctions between iatrogenic and biological collapse, and the morphological differences between them. For the second reading the morphological features of iatrogenic collapsed AIS were taken into account when determining non-invasive areas.

Heatmaps were created on the platform in the following way. The drawn line(s) for total tumor and invasive size were interpreted as diameters of a circle. For each position in the image, the number of overlapping circles was calculated, and the numbers were normalized. Finally, an arbitrary digital color scale was added for visual purpose. The color-range from low to highest number of invasion scores for a pixel was blue, green, yellow orange, red. This implies that an overlay with regional preference for invasion is obtained for those pathologists who assigned invasive line(s).

Sample size consideration

Assuming the fraction of cases that could be downgraded to non-invasive would be around 15-20%³²⁰ with a 95% confidence interval between 10-30% the minimum sample size required was 70 cases. For this study 80 cases were digitized and 70 cases read.

Post-virtual feedback round

In a virtual feedback session, the results of the first two rounds were presented and contained i) overall data: near-unanimous diagnosis, variation in measurements of total tumor size and invasive size and ii) case-specific information: including heatmaps, invasion scores from round 1 and 2, measures of variation in invasion measurement (CV-inv), distribution of pattern scores in both rounds, morphological details of hotspots and other key areas and iii) information about focal invasive growth in biological collapse. To establish the measure of uncertainty about the assessment of invasion one “uncertainty” question was added to each case for the 3rd round: score 1: very uncertain about invasion assignment; score 2: somewhat certain; score 3: neutral; score 4: somewhat certain about invasion (presence or absence); score 5: very certain about presence or absence of invasion. As 29 cases were scored in round 1 and 2 as unanimous invasion, the specific request was to read in the 3rd round the remaining 41 cases.

Statistical analysis

Statistical analysis was performed in SPSS version 28 (IBM Corp., Armonk, NY, USA) and R Statistical Software version 4.2.1 (R Core Team 2022). P-values <0.05 were considered statistically significant. Invasion scores of first and third and second and third round were compared with the McNemar test. For comparison of coefficient of variation (CV = standard deviation / mean *100%; CVinv: mean) the modified signed-likelihood ratio test in the R CV equality package was used³³⁸. This test for comparison coefficient of variations at case level was applied on total tumor size and invasive size measurements as well as for comparison of coefficient of variations between largest invasive size (CV-inv) measurement and the sum of 2 or 3 lines. To obtain an impression about the precision of CV-tot and CV-inv the relative invasive size (ratio invasive size divided by total tumor size) was compared to the mean CV-inv and for case corresponding mean CV-tot. The distribution for ranking the pathologists for the frequency of invasive scores in lowest third, middle and highest third was compared with the region of work using the chi-square test. For Fleisch kappa analysis in the third round the scores from the 29 unanimous invasion cases in the first two rounds were added to the 41 cases. The average pathologists feeling about the decision of invasion was calculated as follows. Four points were assigned to “very uncertain”, 3 points to “somewhat uncertain”, 2 points for “neutral”, and 1 point to “somewhat certain”. The sum of all points divided by the number of pathologists scoring that case resulted in an average uncertainty score per case. For correlation analysis Pearson’s correlation coefficients calculated. For relapse free survival (RFS) and overall survival (OS) Kaplan-Meier curves were estimated and compared using the log-rank test.

Results

A total of 42 pathologists from 13 countries scored all 70 cases in 2 rounds, before and after a tutorial on iatrogenic collapse. There are 33 pathologists working in academic hospitals and 9 in non-academic hospitals, and they all share a common interest in pulmonary pathology. The median and standard deviation of the experience in pathology is 20 ± 10.6 years (range 4-40 years).

Round 1 according to WHO classification

Summary data of invasion scoring, measurement of total and invasive size and kappa analysis is shown in Table 1.

- Table 1.** Overview data of 3 rounds: 1st according to the WHO classification, 2nd after tutorial about revised classification and 3rd round repeat revised classification after feedback of the results in the 1st and 2nd rounds including case specific heatmap analysis, underlying histology, biological collapse and recurrence.

	Round 1	Round 2	Round 3
Number of pathologists	N=42	N=42	N=37
Invasion score	Total (%)	Total (%)	Total (%)
“No”	291 (9.9%)	516 (17.6%)	342 (15.2%)
“Yes”	2572 (87.7%)	2315 (78.7%)	1856 (82.7%)
“Not sure”	69 (2.4%)	109 (3.7%)	46 (2.0%)
	Mean \pm SD	Mean \pm SD	Mean \pm SD
Total tumor size*)	14.9 \pm 4.5 mm	14.9 \pm 4.6 mm	14.8 \pm 4.4 mm
Invasive size*)	10.3 \pm 5.2 mm	9.1 \pm 5.7 mm	9.6 \pm 5.4 mm
	Mean \pm SD (range)	Mean \pm SD (range)	Mean \pm SD (range)
CVtot	6 \pm 5% (1-25%)	6 \pm 5% (1-29%)	\pm 5% (1-25%)
CVinv Largest, incl “0”	46 \pm 45% (2-190%)	71 \pm 85% (3-370%)	41 \pm 29% (6-120%)
CVinv Largest, excl. “0”	30 \pm 22% (2-88%)	36 \pm 29% (3-150%)	32 \pm 25% (3-110%)
CVinv Sum1-3, incl “0”	42 \pm 44% (1-180%)	68 \pm 88% (1-370%)	33 \pm 32% (2-120%)
CVinv Sum1-3, excl. “0”	26 \pm 22% (1-81%)	32 \pm 30 (1-130%)	30 \pm 29% (2-110%)
Kappa scores			
Invasion (70 cases, 42 pathologists)	0.27	0.45	0.62
Invasion (41 cases, 36 pathologists)	0.21	0.35	0.56
MIA	0.11	NA	NA
Pattern Lepidic	0.21	0.34	NA
Pattern Papillary	0.21	0.27	NA

- **Table 1.** Overview data of 3 rounds: 1st according to the WHO classification, 2nd after tutorial about revised classification and 3rd round repeat revised classification after feedback of the results in the 1st and 2nd rounds including case specific heatmap analysis, underlying histology, biological collapse and recurrence. (continued)

	Round 1	Round 2	Round 3
Pattern Micropapillary	0.27	0.24	NA
Pattern Acinar	0.28	0.27	NA
Pattern Solid	0.65	0.62	NA

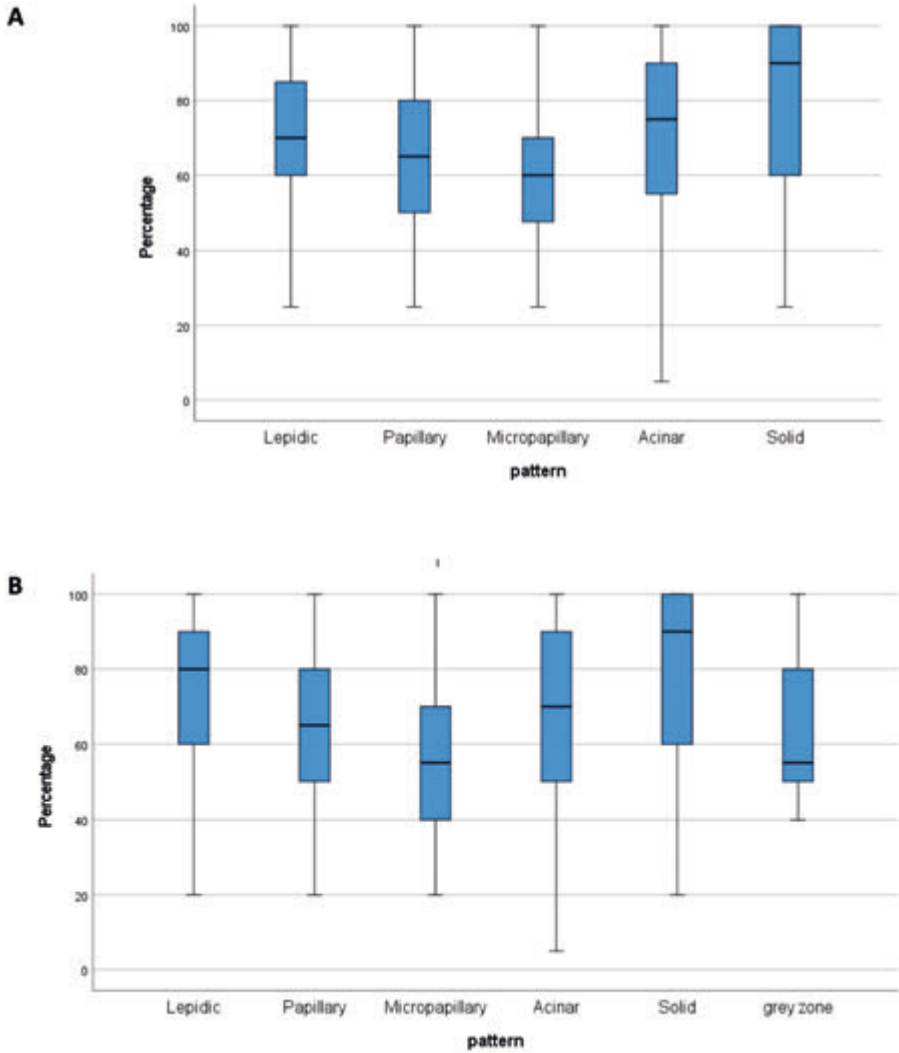
*₁) Size determined with digital mouse in histologic image.

The coefficient of variation of invasive measurement (CV_{inv}) was determined for the largest invasive line (Largest) and for sum of maximum 3 invasive lines (Sum1-3). The CV_{inv} was calculated over all cases including "0" for diagnosis of "No invasion" (incl. "0") and separately only for the drawn invasive lines (excl. "0"). The coefficient of variation for total tumor size (CV_{tot}) is low compared to CV_{inv}. SD = standard deviation, MIA = minimal invasive adenocarcinoma

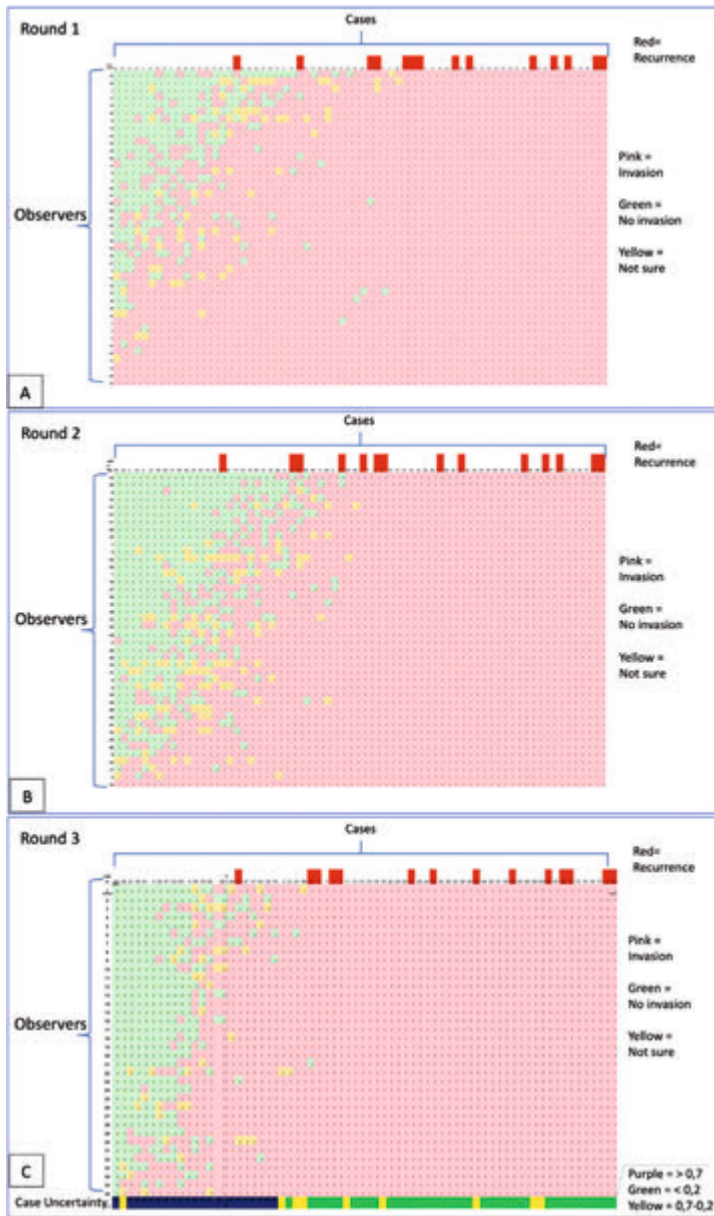
In the first reading of the 70 cases according to the WHO classification unanimous invasion "yes" was scored in 31 cases (44%). In 5 cases (7%) at least one score was given for invasion "yes" and "not sure", while in another 6 cases (8%) invasion was scored as "yes" and "no". In the remaining 26 cases (37%) all options were scored at least once. So, in about half of cases, there was disagreement between pathologists in the diagnosis of invasion.

The distribution of pathologists' WHO pattern scores across 70 cases is shown for round 1 in Figure 2A. The assignment of the dominant (lepidic, papillary, micropapillary, acinar and solid) revealed a near unanimous score (>39 pathologists) in only 6 cases: five cases with solid and 1 with acinar pattern, while in 21 cases 70% of the pathologists scored the same dominant pattern: n= 13 solid, n=7 acinar and n=1 papillary.

The distribution of pathologists' scores for 'invasion', 'no invasion' or 'not sure' is for each case shown in Figure 3A. Of note, in about half of the cases all pathologists agreed on invasion. However, in a about a third of the cases there is variation across samples and individual pathologists. This is not explained by geographical differences (Table 2).



■ **Figure 2.** Distribution of pathologist's pattern scores across 70 cases is shown for the first round in A. Note that a score close to 100 is considered maximal concordance. In the second round (B) the 'grey zone' was added for areas that contained more epithelial stratification than fitted for iatrogenic collapsed AIS and not enough to fit into one of the other patterns. Note the large variation on the quantitative scores for a pattern: this covers not infrequently a range of 70% between pathologists.



■ **Figure 3.** Distribution of 42 pathologist's scores in 70 cases for 'invasion' (pink), 'no-invasion' (green) or 'not sure' (yellow) is shown for three rounds (A, round 1; B round 2; C, round 3). (continued)

Note the variation across samples and pathologists as well as a change towards more 'no-invasion' in the 2nd round. Recurrence is shown with a red box. In the image of round 3 the average case uncertainty score has been added. Note the high association between uncertainty about the decision on invasion and the discordant scores between invasion "yes" and "no".

- **Table 2.** The distribution for ranking the pathologists for the frequency of invasive scores in the lowest third, middle and highest third for round 1 and 2 was compared with the region of work and did not reveal a significant difference.

		Frequency of invasion score						
		Low		Middle		High		
Round	Region	n	%	n	%	n	%	p-value
1	USA	1	25.0%	2	50.0%	1	25.0%	0.84
	Europe	11	34.4%	10	31.3%	11	34.4%	
	Japan	2	33.3%	3	50.0%	1	16.7%	
2	USA	1	25.0%	2	50.0%	1	25.0%	0.36
	Europe	11	34.4%	13	40.6%	8	25.0%	
	Japan	1	16.7%	1	16.7%	4	66.7%	

The low concordance is also reflected in the low kappa score for most of the patterns, except for solid adenocarcinoma, see Table 1.

The measurement of total tumor size has a low coefficient of variation for all 70 cases (mean 6%, range 1-25%, indicating that pathologists can and do measure total tumor size consistently. In contrast, the measurement of invasive size has a 4-7-fold higher coefficient of variation depending on the measure calculated. These invasion and measurement findings are in line with a recent publication from the IASLC pathology panel³¹⁷. Apparently, the criteria as defined in the WHO classification permit large variations in interpretation, leading to poor reproducibility on a world-wide scale. There is a clear need for more detailed guidance in the assessment of invasion in pulmonary adenocarcinomas.

Round 2

A live online tutorial as well as additional literature was provided between the first and second rounds of assessment, which focused on the mechanism of iatrogenic collapse and its recognition and other criteria (see supplementary file and suggested literature on elastin and collapse^{206 279}, as well as a concept version of chapter 14 of this thesis). In the second round the 'grey zone' category was added for areas that contained more alveolar filling growth than was consistent with iatrogenic collapsed AIS but not enough to conform to one of the other surrogate markers of invasion. As focal multilayering is one of the effects of tangential cutting, a surrogate marker of invasion should be consistently present in at least three adjacent alveolar spaces to avoid overdiagnosis of invasiveness. Similarly, to the first round, in the 2nd round 45 cases with invasion scored near-unanimously. The second-round summary data of invasion scoring, measurement of total and invasive size and kappa analysis are also shown in Table 1. The distribution of pathologists' WHO pattern scores across 70 cases is shown for round 2 in Figure 2B.

The case-based comparison of invasion scores in 1st and 2nd round is summarized in Table 3. In a total 19 out of 70 cases there was a significant shift towards assessment of

being non-invasive in the second round. The mean and standard deviation of invasive size for these 19 cases is in the 1st and 2nd round 15.6 +/- 4.1 and 5.1 +/- 3.0, respectively. For the other 51 cases these were 14.6 +/- 4.6 and 12.2 +/- 4.5, respectively. Most pathologists scored in the 2nd round less invasion than in the 1st round, except for one, who scored all cases 'invasive' in both rounds. The kappa score improved from 0.27 to 0.45, including a shift in a selected group of cases towards "no invasion". The decrease in invasive size essentially happened in the cases reclassified as non-invasive by several pathologists. The distribution of pathologists' scores for 'invasion', 'no invasion' or 'not sure' is for each case shown in Figure 3B.

■ **Table 3.** The distribution of invasion scores in 1st (R1) and 2nd round is shown for each case.

Invasion round 2						
Number of cases	Case	Invasion R1	"no"	"yes"	"not sure"	p-value
25	80 +	yes		42		-
4	77, 29, 34, 15	yes		41		-
2	24, 26	yes		41	1	-
1	68	yes	2	40		-
1	11	yes	2	39	1	-
1	22	no		1		-
		yes		41		
2	7, 25	yes		41		-
		not sure		1		
1	72	no		1		-
		yes		40		
2	10, 16	no		1		-
		yes		40		
		not sure		1		
1	2	no R1	0	2		-
		yes 1	2	37		
		not sure 1	0	1		
1	48	yes	2	37	1	-
		not sure	0	1	0	
1	49	yes	3	34	3	-
		not sure	0	2	0	
1	58	yes	4	35	0	-
		not sure	0	2	1	
1	64	no	0	1	0	1,00
		yes	1	36	3	
		not sure	0	1	0	
1	31	no	0	2	0	0,69
		yes	4	33	1	
		not sure	1	1	0	

■ **Table 3.** The distribution of invasion scores in 1st (R1) and 2nd round is shown for each case. (continued)

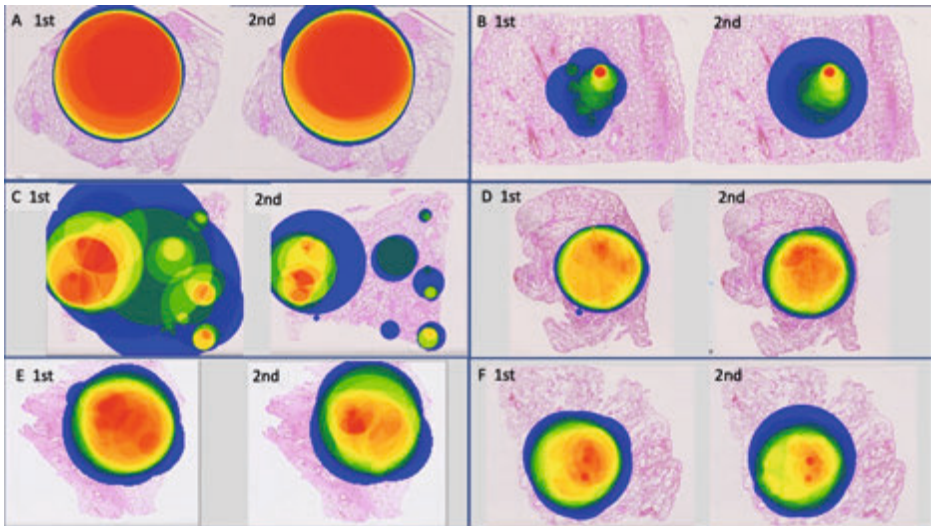
Number of cases	Case	Invasion R1	Invasion round 2			p-value
			"no"	"yes"	"not sure"	
1	26	no	0	3	0	0,51
		yes	6	27	4	
		not sure	0	2	0	
1	69	no	1	2	0	0,29
		yes	6	26	5	
		not sure	0	1	1	
1	57	no	3	4	2	0,27
		yes	9	17	3	
		not sure	1	3	0	
1	74	no	3	3	0	0,23
		yes	8	22	1	
		not sure	1	1	2	
1	42	no	0	1		0,22
		yes	5	36		
		not sure				
1	33	no	3	0	0	0,06
		yes	5	28	2	
		not sure	0	3	0	
1	23	no	9	2	2	0,04
		yes	10	12	5	
		not sure	1	1	0	
1	43	no	2	1	1	0,04
		yes	8	26	1	
		not sure	1	2	0	
1	60	no	26	1	1	0,04
		yes	8	1	2	
		not sure	3	0	0	
1	37	no	3	0	0	0,03
		yes	6	30	1	
		not sure	0	2	0	
1	21	no	22	1	2	0,02
		yes	9	7	1	
		not sure				
1	19	no	2	0	0	0,02
		yes	7	31	2	
		not sure				
1	62	no	12	2	2	0,01
		yes	12	8	3	
		not sure	2	1	0	
1	59	no	10	1	2	0,01
		yes	10	14	2	
		not sure	1	0	2	

■ **Table 3.** The distribution of invasion scores in 1st (R1) and 2nd round is shown for each case. (continued)

Number of cases	Case	Invasion R1	Invasion round 2			p-value
			"no"	"yes"	"not sure"	
1	38	no	25	0	2	0,01
		yes	8	5	0	
		not sure	2	0	0	
1	53	no	6	2	1	0,01
		yes	13	14	5	
		not sure	1	0	0	
1	47	no	13	2	1	0,01
		yes	13	10	3	
1	65	no	10	2	2	0,01
		yes	13	13	1	
		not sure	0	1	0	
1	63	no	6	0	1	0,00
		yes	9	20	3	
		not sure	2	0	1	
1	41	no	3	1	2	0,00
		yes	12	22	0	
		not sure	0	1	1	
1	79	no	3	1	1	0,00
		yes	12	14	6	
		not sure	3	1	1	
1	61	no	16	1	0	0,00
		yes	13	4	4	
		not sure	2	1	1	
1	45	no	16	0	3	<0,001
		yes	12	7	1	
		not sure	2	0	1	
1	3	no	19	0	0	<0,001
		yes	15	5	1	
		not sure	1	1	0	
1	6	no	13	0	1	<0,001
		yes	17	7	3	
		not sure	0	0	1	

Numbering according to the 1st round (excluded 10 cases) for feedback purposes, will be adjusted in time (1-70). The p-value was calculated for a 2X2 table without the 'not-sure' category. The discordant scores (false negative) with a recurrence are depicted in red.

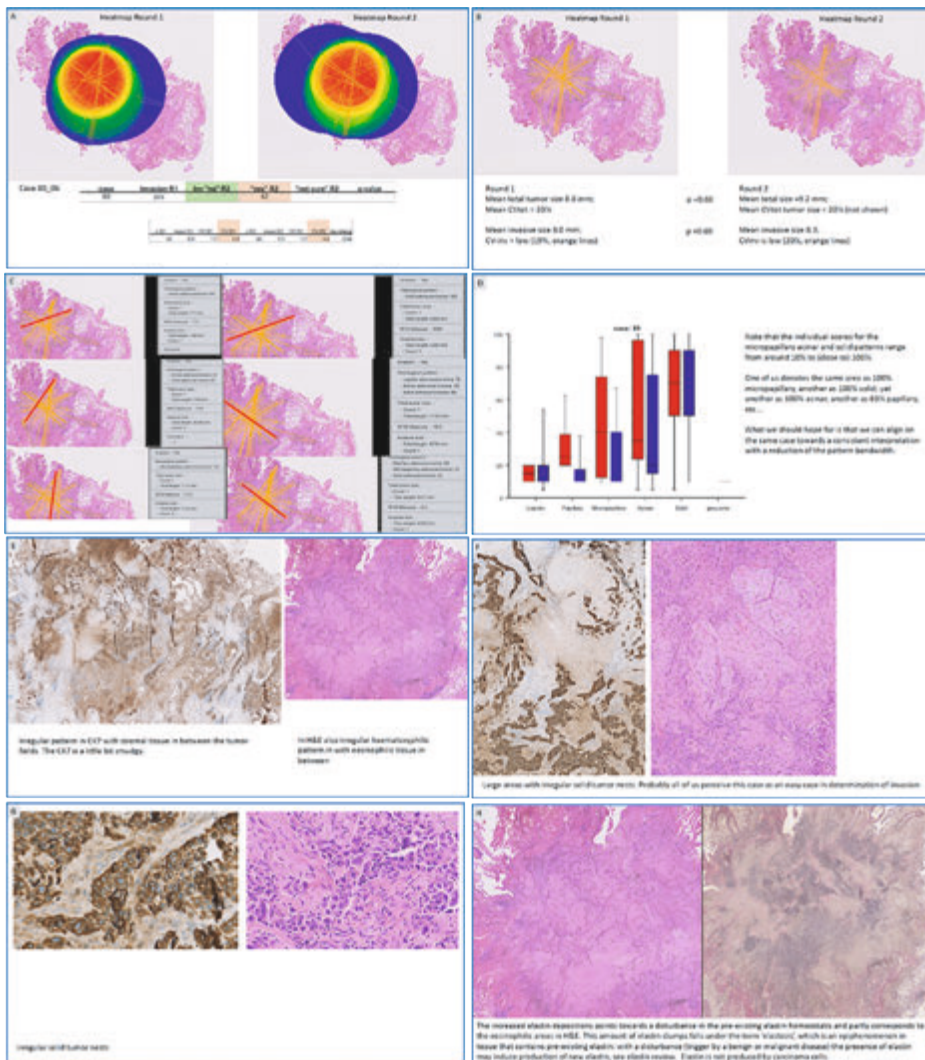
To examine the location of the invasive areas assigned by all pathologists within each case we developed a method of heatmap analysis. A visual summary with a color scheme shows areas with low and high agreement for invasiveness. Heatmaps were generated for all cases, and examples of unanimous invasive cases and on the cases with discordance in invasion assessment, are shown in Figure 4. A round shape of the hotspot (red) area denotes agreement among numerous pathologists.



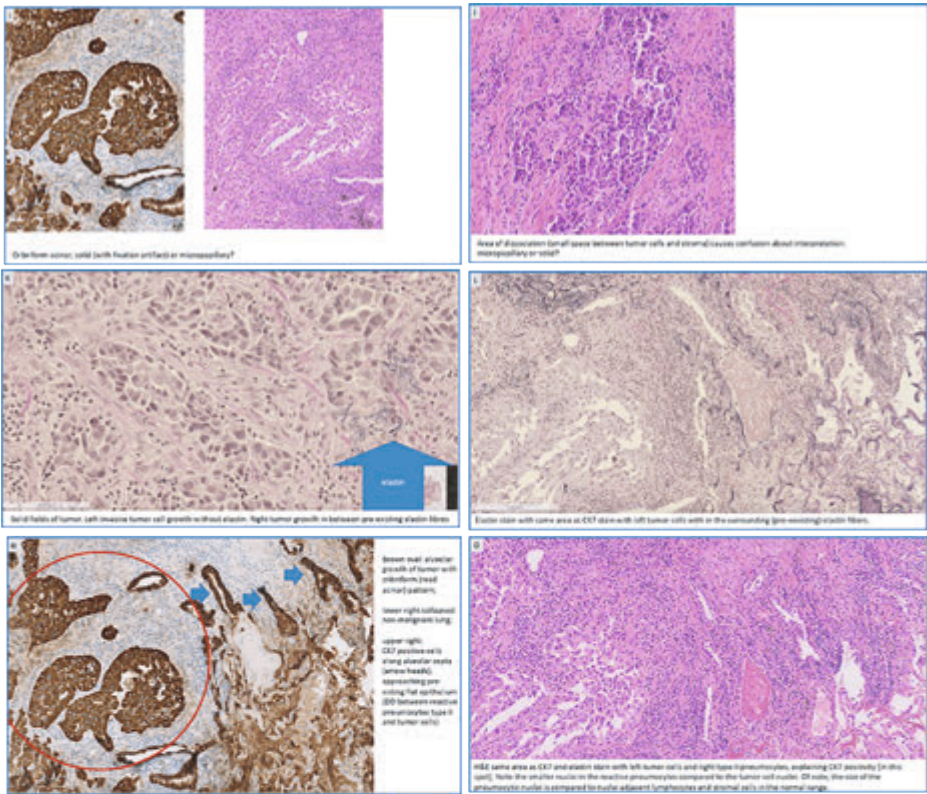
■ **Figure 4.** Examples of heatmap overlays are shown for 6 cases in 1st and 2nd round.

Note the similarities between the 1st and 2nd rounds. A: Tumor with large invasive area and high concordance. B: Tumor with focal area of invasion; C: Relatively low number of invasive scores with smaller focus of possible invasion in the 2nd round; D: relative increase in areas of possible invasion without a focus; E: separation and reduction of possible invasion focus; F: Sharp focus of two rounds of possible invasive areas in the 2nd round. Of note, a round hotspot area (red) denotes invasion by more than a few pathologists, while dispersed, angulated red areas point to variation in location and length of invasive size. The heatmap does not provide information about the pathologists scoring a case as non-invasive.

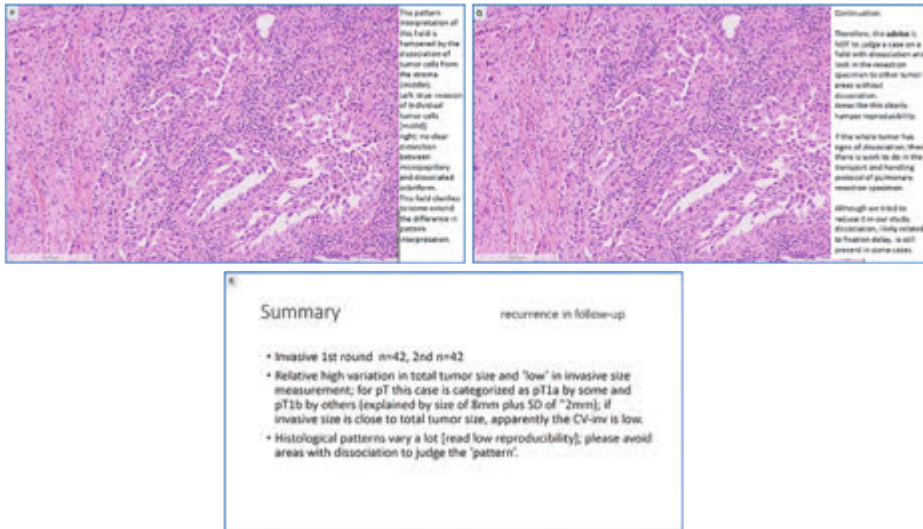
The highest agreement occurred in cases with clear invasion in practically the whole tumor, resulting in low measurement variation (Figure 5).



■ **Figure 5.** An example is shown of heatmap analysis in a case with a uniform diagnosis of invasion. In addition, the measurements and variations are discussed as well as the underlying histology.



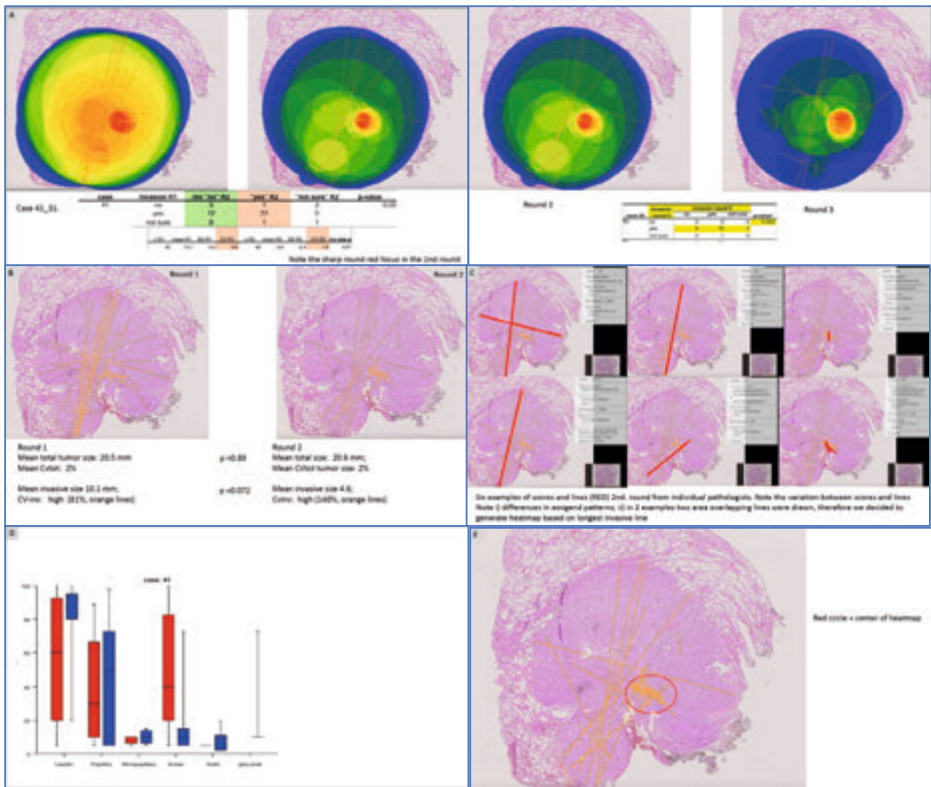
■ **Figure 5.** An example is shown of heatmap analysis in a case with a uniform diagnosis of invasion. In addition, the measurements and variations are discussed as well as the underlying histology. (continued)



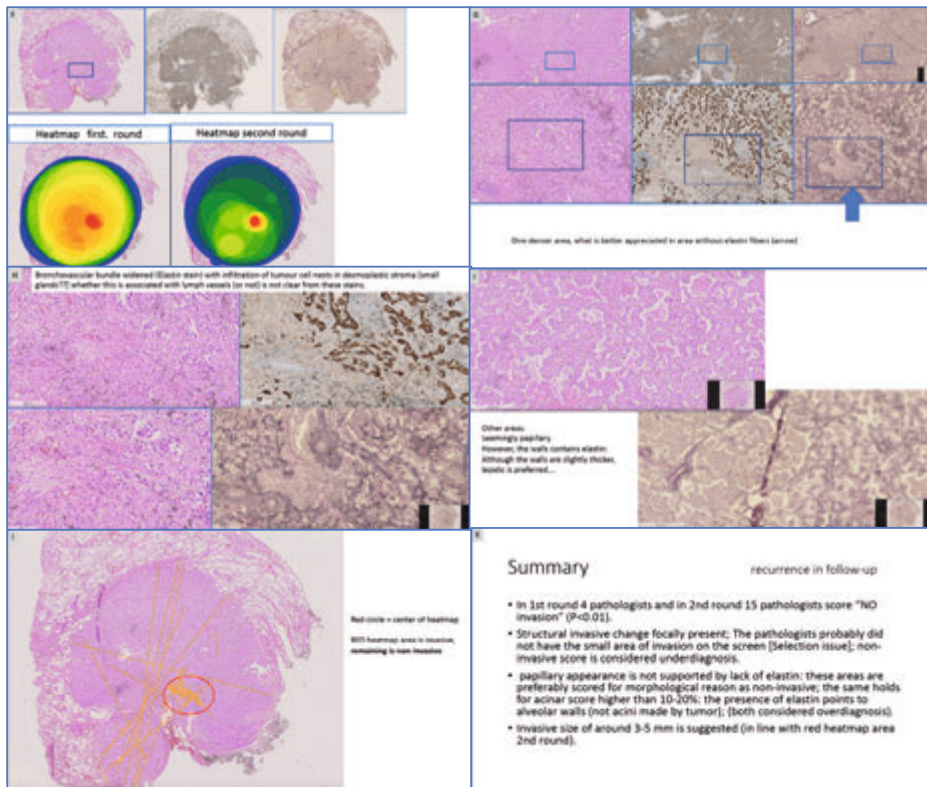
■ **Figure 5.** An example is shown of heatmap analysis in a case with a uniform diagnosis of invasion. In addition, the measurements and variations are discussed as well as the underlying histology. (continued)

Case 80. A: case number 1st and 2nd rounds; heatmap, invasion scores 1st and 2nd round and invasion measurements (mean, sd, CV-inv R1=round1, R2=round 2; B: overlay of invasive lines drawn (orange); C: 6 individual scores and lines denoting invasive area (emphasized in red); D: Boxplot distribution of the pattern scores in 1st (red) and 2nd round (blue); E-P: description of underlying histology in relation to assigned invasive lines and assigned patterns; R: Summary

For a mean invasive size smaller than the mean tumor size a round hotspot frequently pointed to a smaller area of invasion. In some of these cases where other pathologists scored 'no-invasion', underlying histological details suggest likely criteria being used as indicators of invasion (Figure 6).



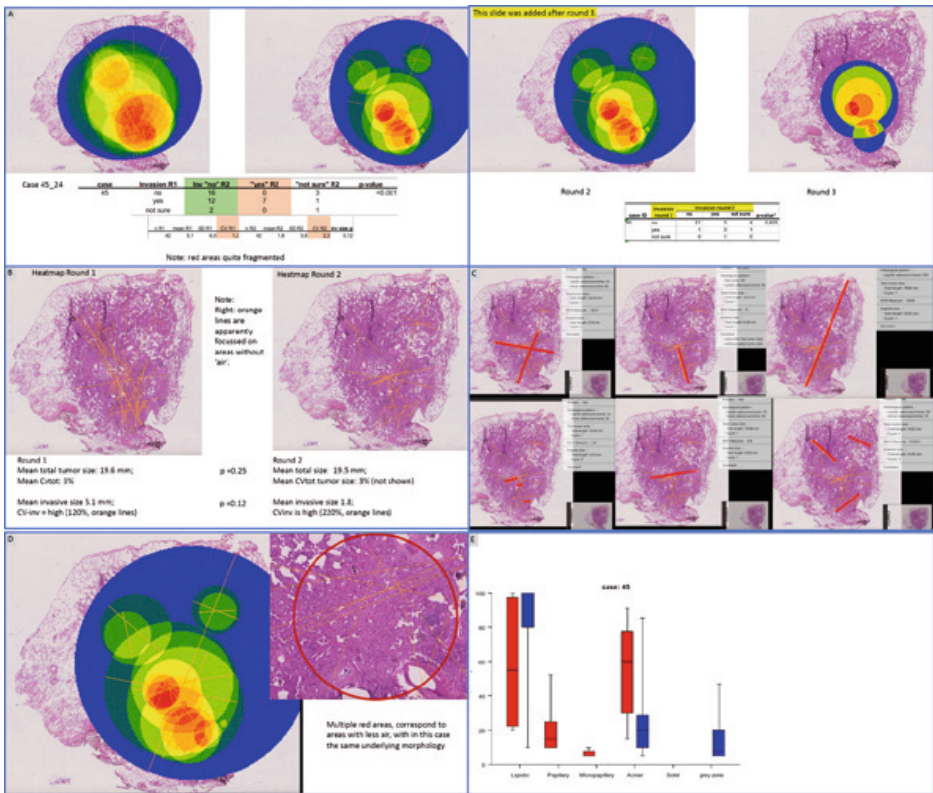
■ **Figure 6.** An example is shown of heatmap analysis in case with diagnosis of invasion and non-invasion, where the 1st and 2nd round measurements are provided as well as the underlying histology. The diagnosis is focal invasion



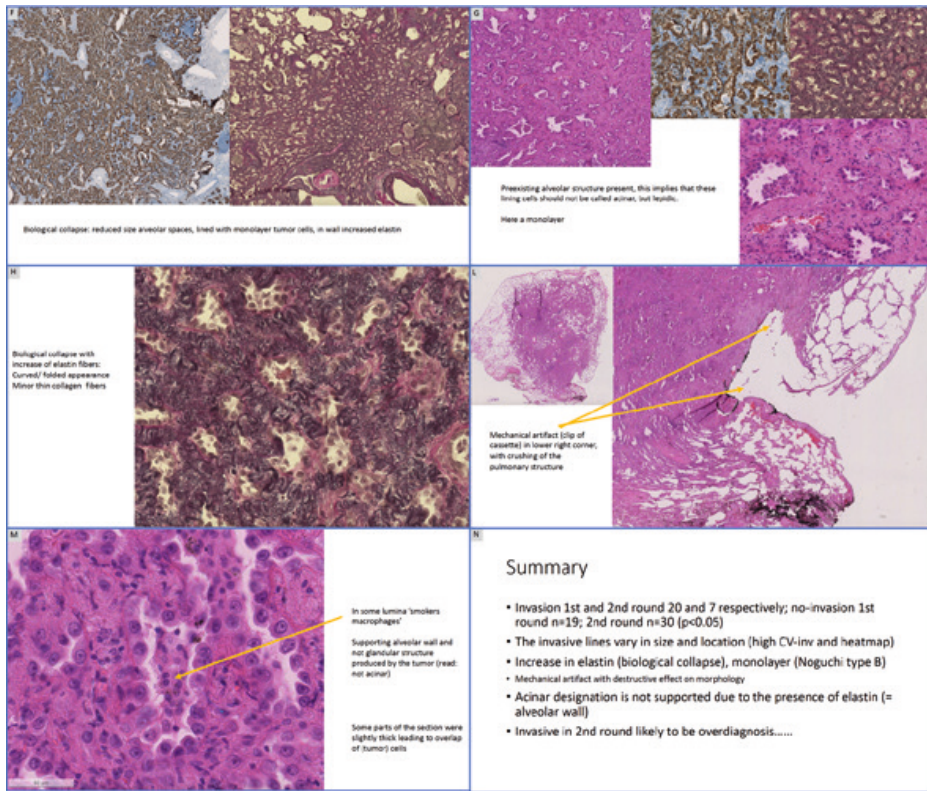
■ **Figure 6.** An example is shown of heatmap analysis in case with diagnosis of invasion and non-invasion, where the 1st and 2nd round measurements are provided as well as the underlying histology. The diagnosis is focal invasion (continued)

Case 41. A: heatmap, invasion scores and measurements; B: overlay of invasive lines drawn (orange); C: 6 individual scores and lines denoting invasive area (emphasized in red); D: Boxplot distribution of the pattern scores in the 1st (red) and 2nd rounds (blue); E-I: description of underlying histology in relation to assigned invasive lines and assigned patterns; J: Likely invasive area; K: Summary.

Examples of overlap in invasive and non-invasive diagnoses and angular shapes of the hot spot, denoting a difference in location and length of the invasive lines, supports a diagnosis of 'non-invasion' (read AIS) (Figure 7).



■ **Figure 7.** An example is shown of heatmap analysis in case with diagnoses of invasion and non-invasion, where 1st and 2nd round measurements are provided as well as the underlying histology. The diagnosis is no-invasion (read AIS).



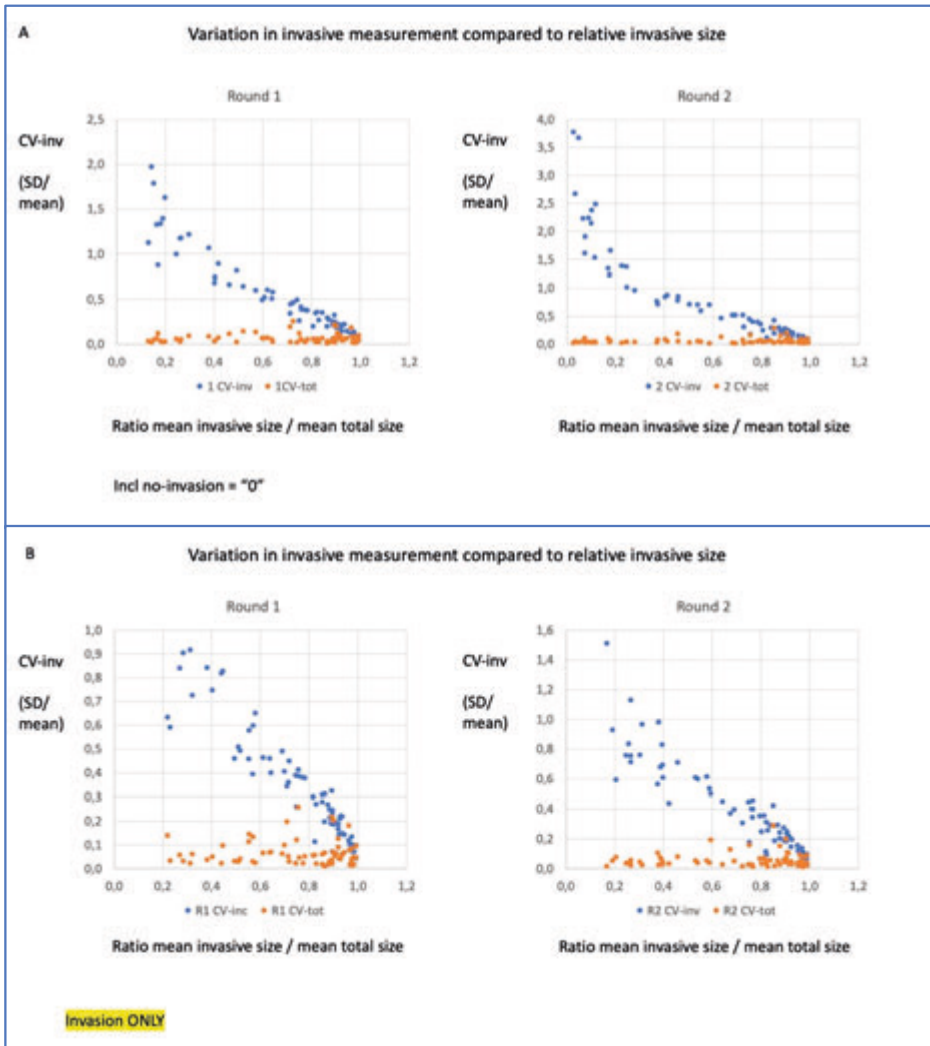
■ **Figure 7.** An example is shown of heatmap analysis in case with diagnoses of invasion and non-invasion, where 1st and 2nd round measurements are provided as well as the underlying histology. The diagnosis is no-invasion (read AIS). (continued)

Case 45. A: heatmap, invasion scores and measurements; B: overlay of invasive lines drawn (orange); C: 6 individual scores and lines denoting invasive area (emphasized in red); D: heatmap 2nd round and underlying histology; E: Boxplot distribution of the pattern scores in 1st (red) and 2nd round (blue); F-M: description of underlying histology in relation to assigned invasive lines and assigned patterns; N: Summary.

Uncertainty about invasion

In order to obtain more insight into the invasive assignments the following aspects were examined.

Firstly, we investigated the relationship between invasive size and variation in assessment of invasion. The relationship between the invasive size ratio (mean invasive size divided by mean total tumor size) and the mean variation coefficient of invasion (CV_{inv}) per case is in the 1st and 2nd rounds (including invasive size of "0" if a case was scored as non-invasive) shown in Figure 8.

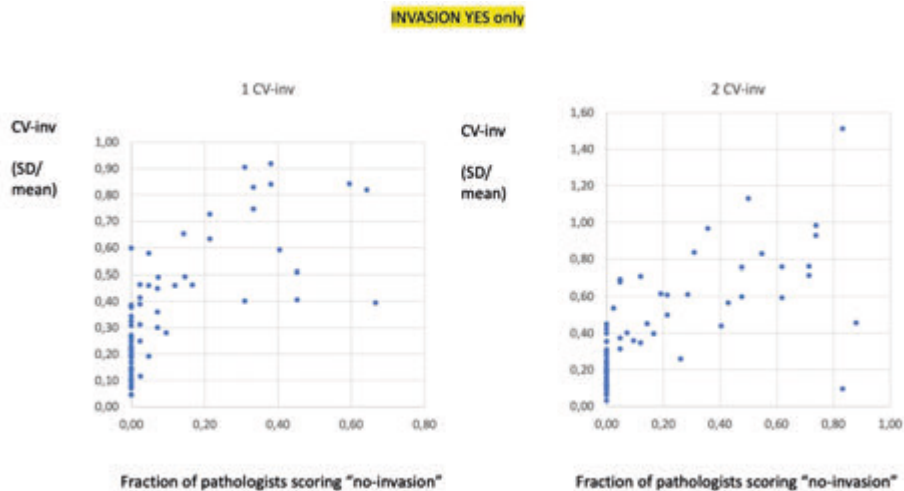


■ **Figure 8.** The relation between invasive size relative to total tumor size (Ratio mean invasive size / mean total size) and mean variation coefficient of invasive measurement (CV-inv) and mean variation coefficient of total tumor size (CV-tot) for the corresponding case is shown in the 1st and 2nd rounds. A: all scores, including invasive size is "0" if invasion was scored as "No"; B: Only invasive size measurement if invasion was scored as "yes". Of note, within the assignment of invasion scores an increasing variation is present for smaller invasive sizes, where the corresponding mean variation for total tumor size remains low (<0.2).

Moreover, the correlation coefficient in round 1 and 2 is high: -0.95, -0.90, respectively. Whereas the correlation between mean total tumor size and invasion size was 0.07 and 0.14 in the 1st and 2nd rounds, respectively. When the analysis was restricted to scores in "invasion present" cases the correlation coefficients were similar: -0.94 and -0.92. No

relevant correlation between invasion size ratio and mean variation in total tumor size measurement was seen (1st and 2nd round <0.001 and 0.11 , respectively). This indicates that for the pathologists who assigned an invasive measurement, variation is relatively low when the invasive size is close to total tumor size, but that there is much greater variation between individuals when perceived invasion is more focal.

Secondly, as the invasive line only provides information about pathologists scoring “invasion present” cases, we subsequently examined the relationship between the fraction of pathologists scoring a case invasive and the CV_{inv} (Figure 9). In cases where most pathologists score “invasion present”, CV_{inv} is low. In contrast, in cases where most pathologists favour “no invasion”, the remaining pathologists tend to assign high variation in size of invasiveness. Thus, there is less consensus in the assessment of invasive areas in cases which most pathologists regard as being wholly *in situ*.



■ **Figure 9.** Relation between fraction of pathologists scoring “no-invasion” and the variation in invasive measurement is shown for rounds 1 and 2. Note that for cases where all 42 pathologists scored “Invasion yes” (fraction = 0) the variation in invasive measurement is relatively low, while for a higher number of pathologists scoring “invasion no” the CV_{inv} for the remaining pathologists is high.

Thirdly, heatmap analyses of cases with low CV_{inv} frequently show a well-defined round hotspot area, as opposed to cases with high CV_{inv}, where the hotspot areas are sometimes angular and assignments are in different locations (Figure 7). Thus, disagreement in the degree of invasiveness (high CV_{inv}) is linked to disagreement about its location.

All three observations point to limited accuracy and precision in the assignment of invasion in some small pulmonary adenocarcinomas. Subsequently, we assessed

pathologist's feeling of (un)certainly about the decision of invasion in each case. The mean and standard deviation of the case uncertainty score was 0.5 ± 0.57 (range 0-2.0). All 25 cases with an uncertainty score >0.4 revealed discordant annotations with invasion "yes" and invasion "no" in round 1 and 2. From the 34 cases with an uncertainty score <0.2 the number of discordant annotations with invasion "yes" and invasion "no" in rounds 1, 2 and 3 were 3, 2 and 0, respectively. The correlation analysis for the average uncertainty score is shown in Table 4.

- Table 4.** The pathologists assigned a score for the feeling of uncertainty regarding the decision of invasion. The spearman rank correlation coefficient for the average uncertainty score per case is shown including *p*-values for several parameters. As expected, the correlation with total tumor size is low. Note that the correlation is high (>0.5 , [$p < 0.001$]) for invasive size measurements (first drawn invasive line: invasive size 1), sum of invasion scores if more than one line was drawn (total invasive size), longest invasive line if more than 1 invasive line was drawn (maximum invasive size), percentage of non-invasive pathologists and a maximum agreement score (irrespective invasion "yes" or "no") score.

	round 1		round 2		Round 3	
	correlation	<i>p</i> -value	correlation	<i>p</i> -value	correlation	<i>p</i> -value
total tumor size	-0,069	0,571	-0,118	0,332	-0,033	0,784
invasive size 1	.824**	<0.001	.849**	<0.001	.847**	<0.001
total invasive size	.831**	<0.001	.852**	<0.001	.835**	<0.001
maximum invasive size	.825**	<0.001	.848**	<0.001	.842**	<0.001
total tumor size (only invasion="yes")	-0,032	0,790	-0,101	0,405	0,021	0,865
invasive size 1 (only invasion="yes")	.556**	<0.001	.481**	<0.001	.462**	<0.001
total invasive size (only invasion="yes")	.777**	<0.001	.734**	<0.001	.692**	<0.001
maximum invasive size (only invasion="yes")	.655**	<0.001	.572**	<0.001	.564**	<0.001
percentage non-invasive pathologists	.802**	<0.001	.871**	<0.001	.804**	<0.001
maximum agreement score	-.823**	<0.001	-.892**	<0.001	-.841**	<0.001

correlation = Spearman's rank correlation with uncertainty score per case

Feedback and Round 3

After round 1 and 2 feedback consisted of i) feedback of the assessments from peers (41 pathologists), ii) case specific heatmaps with underlying histology and comments, iii) detailed comments on areas of likely biological and iatrogenic collapse, iv) a detailed search for foci of invasion, v) assessment of the presence of elastin (usually not associated with papillary or acinar, unless desmoplastic stroma is mixed with tumor cells)²⁰⁶, and vi) information about presence or absence of recurrence in follow-up. To examine if the additional knowledge leads to an improvement in reproducibility a third

round on a reduced set of cases was approved by most pathologists. The 29 cases with unanimous agreement in round 1 and round 2 were discarded in round 3. The remaining 41 cases were again evaluated for the presence of invasion and location and length of invasive line(s). A summary of the general data is shown in Table 1. The kappa score for round 3 is 0.62. The case-based comparison in the invasion scores in 2nd and 3rd round is summarized in Table 5. Out of the 70 cases 42 (60%) were unanimous invasion “yes” and 1 invasion “no”. In 6 cases a significant change was observed towards invasion “yes” and in one case towards invasion “no”. The distribution of pathologists’ scores for ‘invasion’, ‘no invasion’ or ‘not sure’ in round 3 is for each case shown in Figure 3C.

- **Table 5.** Distribution of invasion scores in 2nd and 3rd rounds is shown. Similar scored cases are summarized. The p-value was calculated for a 2X2 table without the ‘not-sure’ category. The discordant scores (false negative) with a recurrence are depicted in red.

Number of cases	Case ID	Invasion round 3	Invasion round 2			p-value*
			“no”	“yes”	“not sure”	
37	5	yes		36		-
1	24	yes		35	1	-
1	68	yes	2	34		-
1	11	yes	2	33	1	-
1	58	yes	4	31	1	-
1	19	yes	8	26	2	-
1	10	yes		35		-
		not sure		1		
1	2	yes	1	34		-
		not sure	0	1		
1	48	yes	0	33	2	-
		not sure	1	0	0	
1	49	no	0	1	0	1,000
		yes	1	31	3	
1	31	no	0	1		0,219
		yes	5	30		
1	26	no	1	0	1	0,250
		yes	3	26	3	
1	69	not sure	2	0	0	1,000
		no	2	2	0	
1	37	yes	2	24	3	0,180
		not sure	1	0	2	
1	37	no	0	2	0	0,180
		yes	7	25	1	
		not sure	0	1	0	

■ **Table 5.** Distribution of invasion scores in 2nd and 3rd rounds is shown. Similar scored cases are summarized. The p-value was calculated for a 2X2 table without the 'not-sure' category. The discordant scores (false negative) with a recurrence are depicted in red. (continued)

Number of cases	Case ID	Invasion round 3	Invasion round 2			p-value*
			"no"	"yes"	"not sure"	
1	33	no	1	0	0	0,063
		yes	5	28	1	
		not sure	0	0	1	
1	74	no	1	1	0	0,012
		yes	10	21	3	
		not sure	0	0	0	
1	43	no	1	0	0	0,031
		yes	6	25	2	
		not sure	2	0	0	
1	57	no	2	0	0	0,008
		yes	8	20	4	
		not sure	1	0	1	
1	41	no	3	0	0	0,004
		yes	9	20	3	
		not sure	0	1	0	
1	63	no	2	1	0	0,003
		yes	12	16	2	
		not sure	0	0	3	
1	62	no	5	1	1	<0.001
		yes	14	9	3	
		not sure	1	1	1	
1	79	no	7	0	0	0,063
		yes	5	13	6	
		not sure	2	1	2	
1	59	no	5	3	2	0,057
		yes	11	9	2	
		not sure	2	0	2	
1	60	no	31	2	3	-
		no	29	2	2	
		yes	0	1	0	
1	38	no	27	1	1	0,500
		yes	0	1	0	
		not sure	1	1	0	
1	3	no	27	1	1	1,000
		yes	2	4	0	
		not sure	1	0	0	

- **Table 5.** Distribution of invasion scores in 2nd and 3rd rounds is shown. Similar scored cases are summarized. The p-value was calculated for a 2X2 table without the 'not-sure' category. The discordant scores (false negative) with a recurrence are depicted in red. (continued)

Number of cases	Case ID	Invasion round 3	Invasion round 2			p-value*
			"no"	"yes"	"not sure"	
1	21	no	25	3	2	0,625
		yes	1	3	0	
		not sure	0	1	1	
1	61	no	24	2	3	1,000
		yes	1	3	1	
		not sure	0	1	1	
1	45	no	23	3	4	0,625
		yes	1	3	1	
		not sure	0	1	0	
1	53	no	14	9	5	0,146
		yes	3	3	0	
		not sure	0	1	1	
1	47	no	21	4	2	0,375
		yes	1	5	2	
		not sure	0	1	0	
1	23	no	15	6	5	0,289
		yes	2	6	1	
		not sure	1	0	0	
1	6	no	17	0	2	0,008
		yes	8	6	1	
		not sure	0	0	2	
1	65	no	15	3	2	0,727
		yes	5	8	0	
		not sure	0	2	1	

Clinical relevance

Fourteen out of the 70 cases recurred after surgical resection. Nine of the recurrences were recorded in the 25 cases with 100% invasive judgements in round 1 and 2. Cases with a recurrence and a diagnosis of "no invasion" are considered discordant judgements. In the 1st round discordant scores occurred in 3 cases with 1, 1 and 6 judgements, respectively. In the 2nd round this occurred in 4 cases with 2, 3, 5 and 15 judgements, respectively (see also Table 3). In the 3rd round this occurred in 2 cases with 1 and 3 judgements.

In the second round >21 pathologists scored "no invasion" in 10 cases, all of which were without a recurrence (mean follow-up time 69.5 months, range 11-132). Survival

analysis (RFS and OS) for cases categorized if ≥ 21 pathologists scored invasion as 'yes' and else 'no' (a score of "not sure" is left out) is shown in Table 6.

- **Table 6.** Survival analysis for cases categorized if ≥ 21 pathologists scored invasion as 'Yes' and else 'No' for rounds 1 and 2. RFS = relapse free survival; OS = overall survival.

Round	Invasion*	n	5-year RFS	p-value	5-year OS	p-value
1	no	4	100% [n.e.]	0,32	100% [n.e.]	0,29
	yes	66	79.3% [69.3 - 89.4%]		76.7% [66.3 - 87.1%]	
2	no	15	100% [n.e.]	0,12	100% [n.e.]	0,021
	yes	55	75.2% [63.4 - 87.0%]		72.2% [60.2 - 84.2%]	

Note an increase from 4 in the 1st round to 15 cases in the 2nd round, all with a 100% RFS and OS for cases categorized as "no invasion". Thus, the consensus ability to identify cases which do not recur was improved following the first tutorial.

The variation in assessment of pT stage, determined by invasive size, is shown in Table 7. In four out of 70 cases pT staging showed unanimous agreement. In 34 cases (49%) stage assignments were divided between pTis (adenocarcinomas *in situ*) and pT1. For invasive tumors an overlap between two adjacent pT categories may be explained if a total tumor size is relatively close to the adjacent category. However, this argument does not hold in cases that span more than two invasive categories.

- **Table 7.** Variation of pT stage distributions (based on invasive size only) within a case is shown for the all 3 rounds. pTis = pathology tumor staging (pT) for adenocarcinoma in situ; pT1a invasive adenocarcinoma ≤ 1 cm; pT1b $>1 - \leq 2$ cm; pT1c: $>2 - \leq 3$ m.

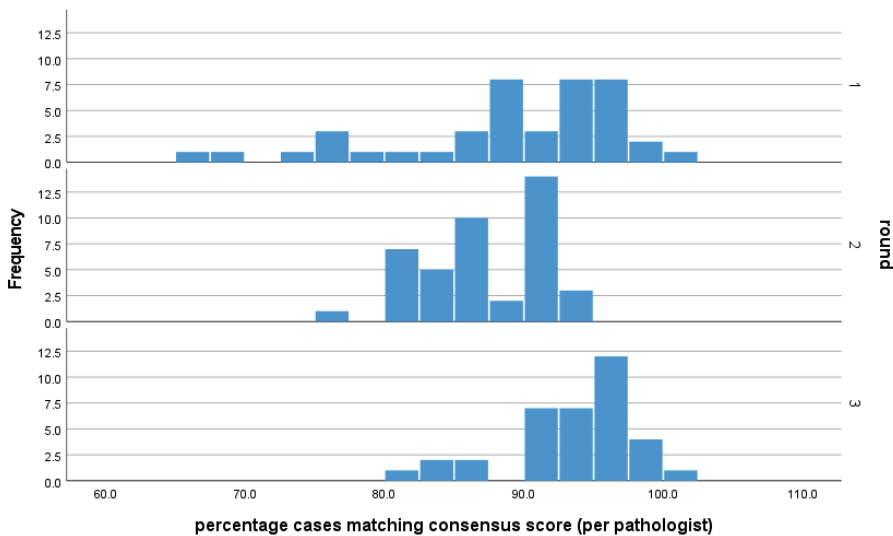
pT-stage	round 1	round 2	round 3
pTis	0	0	1
pT1a	2	3	5
pT1b	6	5	5
pTis+pT1a	7	10	7
pTis+pT1a+pT1b	21	19	14
pTis+pT1a+pT1b+pT1c	4	4	3
pT1a+pT1b	23	22	27
pT1b+pT1c	4	4	5
pT1a+pT1b+pT1c	3	3	3

The viewing time for the three stainings is shown in Table 8. There is an increase in the 2nd round compared to the 1st round for viewing of elastin and CK7 staining.

■ **Table 8.** Viewing time (mean ± standard deviation, range [minutes]) is shown for haematoxylin-eosin (H&E), Cytokeratin 7 (CK7) and elastin staining in the three successive rounds. Viewing time was calculated for 41 pathologists (excluding ET).

Staining	Round		
	1	2	3
H&E	3.9 ± 4.0 (1.5-22.8)	3.5 ± 2.2 (1.1-11.8)	2.0 ± 2.1 (0.4-12.5)
CK7	1.5 ± 0.5 (0.6-3.0)	2.7 ± 3.6 (0.3-24.1)	0.8 ± 0.6 (0.2-3.0)
Elastin	1.2 ± 1.2 (0.3-9.6)	2.4 ± 3.2 (0.2-22.7)	1.5 ± 2.4 (0.1-14.3)

To examine the performance of the pathologist’s perspective with respect to the peers (the 41 other pathologists) a ‘consensus percentage’ was determined by calculating the fraction of cases where the score of the individual pathologist was in agreement with the highest consensus score for each case was calculated and shown in Figure 10. Note the left skewed distribution in the first round, which diminished progressively in 2nd and 3rd round. Ideally, all pathologists reach the 100% consensus percentage. As after the third round there is still improvement possible; more education with the proposal for the revised classification may be beneficial.



■ **Figure 10.** The distribution of ‘consensus percentage’, determined by calculating the fraction of cases where the score of the individual pathologist was in agreement with the highest consensus score for each case, is shown for round 1, 2 and 3, respectively. Note the left skewed distribution in the first round which diminished progressively in 2nd and 3rd round. Ideally, all pathologists reach the 100% consensus percentage.

Discussion

In the present study, unanimous agreement was obtained using the current WHO classification criteria in about half of the small adenocarcinomas. In the other half discordant judgements for invasion “yes” and “no” were frequently present within a case. Moreover, invasive size measurements lead to major differences in pT staging. In round 2 we saw a major shift in the judgement for individual pathologists toward ‘*in situ*’ adenocarcinoma with a revised classification that utilized more precise and standardized criteria, which is in general justified by the clinical follow-up, and is accompanied by a major improvement of interobserver variability from 0.27 in round 1 via 0.45 in round 2 to 0.62 in a ‘coached’ round 3.

Diagnosing invasion in small pulmonary adenocarcinomas is remarkably inexact even among specialized pulmonary pathologists, with disagreement in around 50% of cases leading to differences in pT staging, which is similar to a recent study of the pathology panel of the IASLC³¹⁷. Estimating invasive size in small pulmonary adenocarcinomas may show some overlap between two adjacent categories (e.g., pT1a/b or pT1b/c), especially for tumor sizes around the threshold of the categories. However, two other important aspects are i) the overlap between pT *in situ* and invasive adenocarcinoma, which improved from 46% of the small adenocarcinomas using unaltered WHO guidelines to 34% for the revised classification in round 3. Likewise, for differences in invasive size of more than one category the percentage decreases from 10% to 8,5% in the 3rd round.

The heatmap based on the underlying largest invasive line, taken together with assigned growth patterns, reflects a detailed reflection of the pathologist’s interpretation. This provides a new opportunity for analysis of specific areas and possibly better understanding of the morphological features relevant for the individual pathologist in the assessment of invasion.

On a personal level every pathologist probably has some uncertain feeling about the designation of invasion in about half of the small pulmonary adenocarcinomas. The cases with a high average uncertainty score clearly were also the cases with discordant scores between invasion “yes” and “no” across several samples and individual pathologists. This shared feeling of uncertainty on the same cases implies awareness of the difficulty about the decision of invasion.

In applying the WHO classification of the lung for the assessment of invasion a low kappa score of 0.27 was obtained. Concerning the assessment of invasion, the data from this study match with data from a recent publication from a group of experts in pulmonary pathology. [see Supplementary Figure 2³¹⁷]. In both studies, several pathologists participated from different areas around the globe. This demonstrates that it is a worldwide issue with marked scientific implications. Firstly, i) we (read pathologists) are currently not competent at making a similar decision about invasion in pulmonary adenocarcinomas across the globe. Taking into account the shared feeling of uncertainty about the decision of invasion, after combining the two studies the statement seems valid in terms of learning theory that “we are consciously incompetent

in the assessment of invasion" in half of the pulmonary adenocarcinomas \leq 3cm. Awareness is a part of metacognition (understanding of what our unsolved problems are)³³⁹ This issue may conceptually be solved by education: further learning may increase the performance and confidence again. Secondly, clinicopathological studies on small pulmonary adenocarcinomas may show high variation in subtyping of adenocarcinomas and invasion assessment (see supplementary Table S3³¹⁷). Thirdly, biological studies e.g., those which attempt identify genomic or transcriptomic alterations which drive invasiveness may be hampered.

The study of Boland and colleagues examines reproducibility with distinction between AIS, minimal invasive and invasive adenocarcinoma³¹². They report a kappa score of 0.63. They mention that the agreement data are "likely somewhat falsely inflated because the determination was made by 2 academic pulmonary pathologists practicing at the same large-volume practice". Interestingly, they hint at overdiagnosis: "tumors with disagreement between MIA and IA had survival similar to agreed MIA, and thus, borderline cases can be confidently classified as MIA." The overdiagnosis of invasive adenocarcinoma is in line with our findings of a major shift towards 'no invasion' in the 2nd and 3rd round in discordant cases, all without recurrence.

The term biological collapse denotes a structural change, accompanied by an increased density of curled elastin fibers resulting in marked reduction of the alveolar lumen size, and a monolayer of tumor cells or complete disappearance of the epithelium. In morphological terms the underlying pre-existing architecture is recognizable by the elastin skeleton, where disturbance of the elastin homeostasis has led to an increase in elastin²⁰⁶.

A possible issue in the structural change of biological collapse is the collagen accumulation between tumor cells and elastin without active fibroblasts. More study on this issue is warranted. For the current study collagen accumulation was not used as a decisive morphological argument for invasion. At the edge of the biological collapsed area, small angular epithelial cells can be observed. Occasionally, in the center the epithelial lining may disappear, a process that is pathophysiological not understood. Whether this regards atrophy or apoptosis or something else is unclear. For diagnostic purposes it is important to realize that, if the pre-existing lumen in biological collapsed areas contains focally multilayered tumor cells, this is likely a sign of more adjacent proliferation than usually seen in AIS [i.e., associated with invasion].

Limitations of the study

Several limitations should be mentioned. A) Folding in histological sections may cause larger areas to be out of focus. Few cases were excluded because of the folding. B) Possibly, part of the results was influenced by the fact that we looked at digital slides. Some pathologists lacked experience in reading digital slides. Some of the pathologists have the habit to screen a slide under the microscope in a standard fashion in one direction and move at the one row upwards/ downwards etc. This is not as easy to do on a digital slide. Therefore, we may have missed small foci of invasion in a case

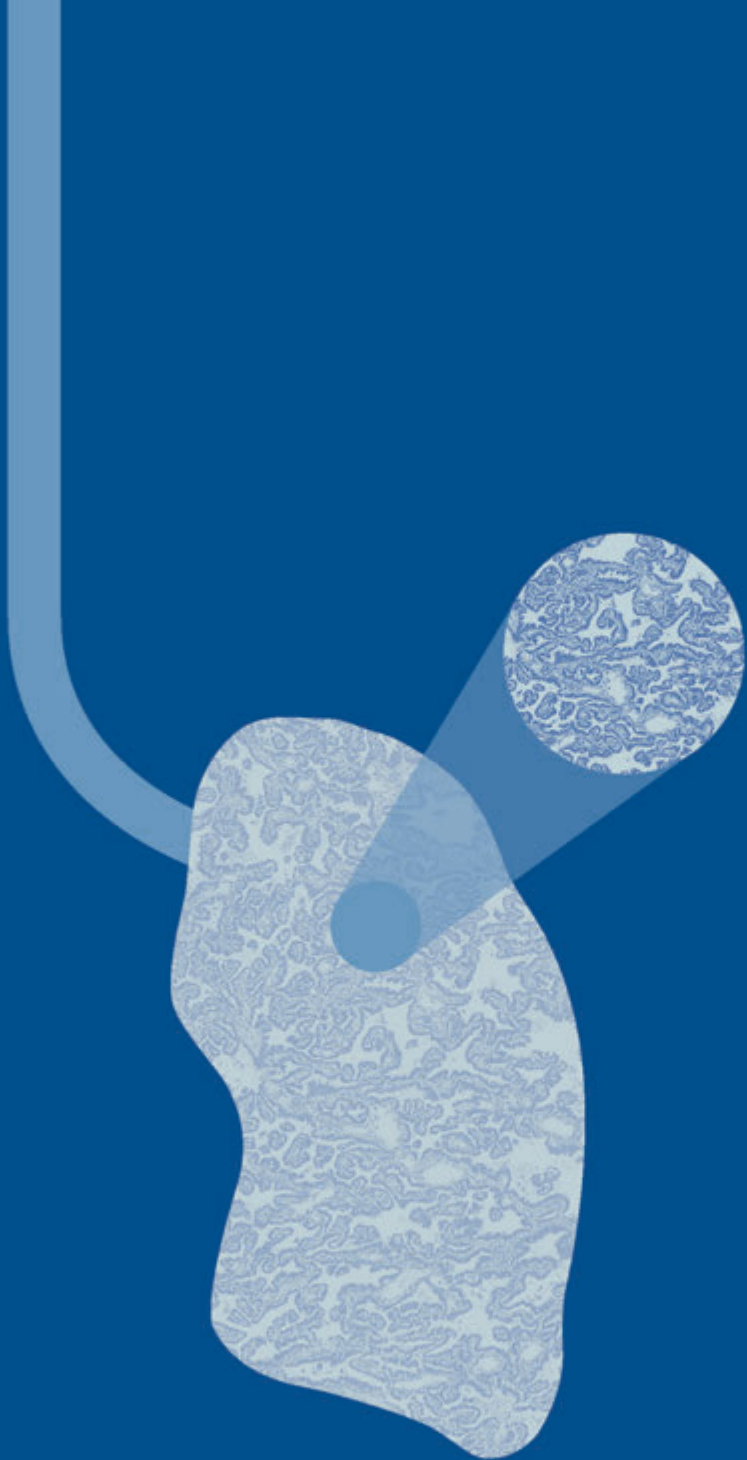
with an otherwise large lepidic component. C) The tutorial before the 2nd round was focusing on recognizing the lepidic component in iatrogenic collapse. Biological collapse was specifically mentioned after the 2nd round before the 3rd round. The best outcome of this study is the kappa of 0.62 in the coached third round, showing promise that better specification and standardization of criteria and better education on the revised classification. may be as a way out of the current situation. However, this was obtained by feedback provided by the peers and the heatmap. This is information that is generally not available. Nevertheless, the content was apparently acceptable for most pathologists and the kappa 0.62 is markedly better than the previous reported scores in intercontinental reproducibility studies¹⁴. Training of pathologists in pulmonary adenocarcinoma may reach high agreement rates³⁴⁰.

D) In the real world, Pathologists hesitate to make the diagnosis of AIS in fear of a possible recurrence and E) possible legal implications. The financial consequences of being sued and a verdict are not affordable.

In summary, there is significant interobserver variation in the measurements of invasive size and assignment of invasive patterns among pathologists. However, using refined morphological criteria along with CK7 and elastin staining can help improve recognition of collapsed AIS. The formal recognition of collapsed AIS can aid in identifying low-risk lesions that are wholly non-invasive.

Acknowledgements

Erik Thunnissen would like to express his great appreciation to all participating pathologists for their commitment and dedication of many hours in reading of the cases for three rounds, of which the third one was not even anticipated beforehand.



16

Arguments for non-mucinous adenocarcinoma in situ of the lung larger than 7 cm.

Hans Blaauwgeers, Onno Mets, Ronald Damhuis,
Birgit Lissenberg-Witte, Idris Bahce, Teodora Radonic,
Chris Dickhoff, Gianluigi Arrigoni, Daniela Finocchiaro,
Erik Thunnissen

Submitted

Abstract

Introduction

The World Health Organization (WHO) recognizes adenocarcinoma *in situ* (AIS) for tumors that are up to 3 cm in size. Tumors with the same growth pattern but larger in diameter are considered invasive and classified as lepidic predominant adenocarcinoma.

The aim of this study was to examine pulmonary adenocarcinomas larger than 7 cm in diameter to see if any cases fit the criteria of AIS.

Materials and Methods

In two cases, where initial histological sampling revealed AIS, while on radiology a pneumonia-like pattern in nearly a whole lobe was present, the whole lobe was histologically embedded. In a parallel, an extension was performed on previously reported nationwide retrospective cohort of 683 patients, who had undergone lung surgical resection for pT3N0M0 NSCLC between 2010 and 2013, on a subset of 112 patients with a tumor size larger than 7 cm and adenocarcinoma histology. Further selection of possible non-invasive cases was based on pathology reports and review of H&E slides and additional elastin and cytokeratin 7 stainings. Follow-up of possible non-invasive cases was obtained, and their radiologic was reviewed along with matched controls.

Results

In two patients the entire lobe was examined, with respectively 130 and 300+ formalin fixed and paraffin embedded tissue blocks. The histological diagnosis supported by additional stainings was AIS, both with a size of 16 cm. In none of the slides criteria for invasion were detected.

In the observational study, 7 out of 112 cases were initially identified as possible non-invasive non-mucinous adenocarcinoma based on H&E staining. Subsequent analysis using additional staining techniques revealed that 3 of these cases could be reclassified as non-invasive/AIS. One of the 7 cases was micropapillary, 2 cases were identified as papillary, and 1 case had a lepidic predominant pattern with an invasive acinar component. Radiological imaging indicated that the non-invasive cases exhibited a consolidation pattern, similar to that seen in pneumonia, while the invasive control cases had a primarily solid appearance, a radiologic pattern that was also seen in the papillary adenocarcinoma. Follow-up showed favorable recurrence-free survival in the patients with AIS.

Conclusion

AIS can be diagnosed in tumors larger than 7cm. The restriction of 3 cm size criterion for AIS in the current World Health classification of pulmonary adenocarcinomas may be reconsidered.

Introduction

The prognosis of lung cancer is largely determined by its stage, with the diameter being one of the components of the TNM classification. Typically, the larger the tumor, the higher the stage⁷⁹. However, if a large tumor has a complete non-invasive, *in situ* growth pattern, then the relationship between tumor size and prognosis is not applicable in theory.

In the 2015 revision of non-small cell lung cancer by the World Health Organization (WHO), a new histologic classification for adenocarcinoma of the lung was proposed, wherein the term “bronchioloalveolar carcinoma” (BAC) was replaced by “adenocarcinoma *in situ*” (AIS) and “minimally invasive adenocarcinoma” (MIA) in cases with an invasive area smaller than 0.5cm. When completely resected, these entities both exhibit 100% recurrence-free survival¹³⁴¹. AIS is characterized by the growth of a monolayer of tumor cells along pre-existing alveolar structures in tumors that are 3cm or smaller, without invasive features³¹⁶. Adenocarcinomas larger than 3 cm, with an invasive component exceeding 0.5cm are called lepidic predominant adenocarcinoma (LPA). So far, there is no category for non-invasive adenocarcinoma larger than 3 cm, since at the time of the 2015 revision no such cases were documented.

The aim of this study was to explore the existence of AIS with a size greater than 7 cm. To this end we i) histologically analyzed in two cases the whole lobe, where initial histological sampling revealed AIS while on radiology a pneumonia-like pattern in nearly a whole lobe was present and ii) conducted a comprehensive search in a previous published pT3N0 cohort with adenocarcinomas > 7cm cm³⁴² to identify potential cases with a pure *in situ* growth pattern.

Materials and methods

Two cases from separate institutes were included in this study, where the entire lobe was examined histologically due to the suspected presence of AIS. One from Vrije Universiteit medical center (VUmc), Amsterdam and one from San Raffaele Scientific Institute, Milan, Italy. Selected slides of both cases were besides hematoxylin and eosin (H&E) stainings, also stained with Elastin von Gieson (EvG) and cytokeratin 7 (CK7). Clinical data, including follow-up were obtained. In parallel an observational study was performed on a previous reported nationwide retrospective cohort of 683 patients, who underwent lung surgical resection for pT3N0M0 NSCLC (TNM 7th edition) from 2010 to 2013³⁴². This study cohort gave us the opportunity to investigate our hypothesis that adenocarcinomas *in situ* larger than 3 cm might exist, especially if we could demonstrate their presence in cases with a diameter larger than 7 cm, related to adequate follow-up.

Therefore, a subgroup of 112 cases was selected based on the combination of tumor diameter larger than 7 cm, and adenocarcinoma histology. A further selection

was made based on the available anonymous pathology reports, which mentioned lepidic or (micro)papillary growth. These cases were considered possible non-invasive adenocarcinomas. H&E-stained slides and paraffin blocks of all adenocarcinoma cases were retrieved from the various pathology departments. After review of the H&E slides (HB, ET, both with over 30 years of experience in pulmonary pathology), a representative paraffin block from the putative non-invasive cases was selected. Areas of suspected invasion were selected when choosing a representative block. Additional staining, including EvG and immunohistochemical stainings for CK7, TTF1, and p40 were performed. The presence of TTF-1 and absence of p40 confirmed the diagnosis of adenocarcinoma. Adenocarcinoma in-situ (AIS) was defined as a monolayer of tumor cells on the alveolar wall with or without collapse, using H&E, EvG, and CK7, as was recently described³⁴³.

For every potential pulmonary non-mucinous adenocarcinoma in-situ case, an age, gender, and date (by year) of surgical resection matched invasive control was selected from the same institute.

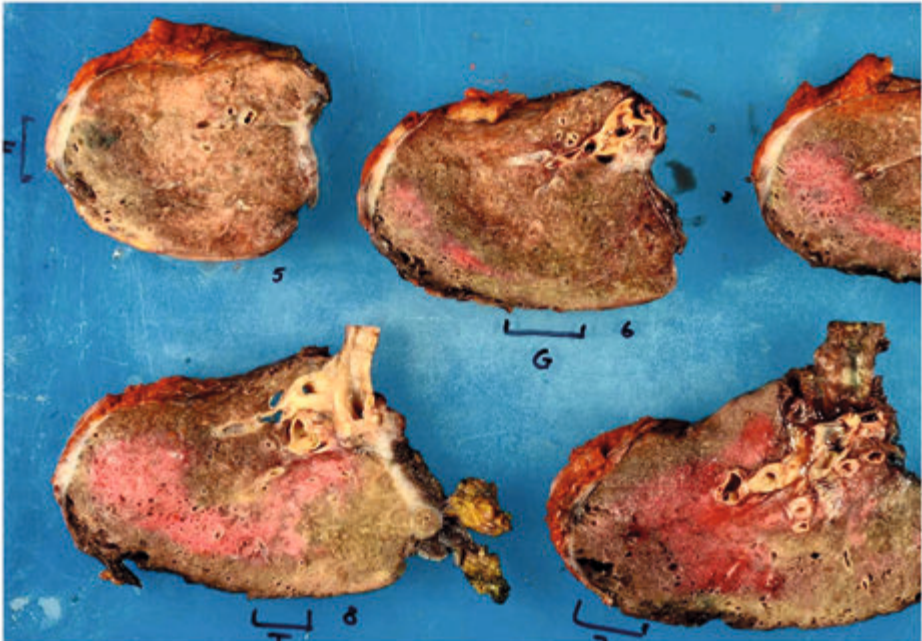
Pre-operative CT imaging, obtained in anonymous form on CD-ROM from different radiology departments, were reviewed by a radiologist (OM) to assess tumor diameter, presence of ground glass opacities or semi-solid areas/consolidations and solid areas. If present the diameter of solid components in ground glass areas was estimated. We categorized three groups of tumor morphology: i) completely solid mass, ii) mass with partial ground glass as well as solid component(s) (subsolid), and iii) more diffuse consolidation with varying amounts of ground glass and solid components (also called 'pneumonia-like'). The correlation between the radiology findings and histology was evaluated using these three categories.

Due to the retrospective nature of the study, only selective blocks were obtained for diagnostic purposes, rather than including the entire tumor or a significant portion of it. Radiological and pathological examination of the retrospective study cases was performed blinded for the other diagnostic technique and for follow-up.

Comprehensive follow-up data of all selected cases were collected from various hospitals, including cases that had been referred to other centers. Data retrieval of the T3N0 cohort was approved by the IKNL privacy review board and performed in accordance with the regulations of the Central Committee on Research involving Human Subjects as well as the ethical committee of PALGA (IKNL No K14.250; PALGA lzv1142/2019-4-A2). The study was conducted according to the criteria set by the 1964 Declaration of Helsinki and later Amendments and in accordance with the Strengthening the Reporting of Observational Studies in Epidemiology Statement (STROBE) guidelines. Due to the retrospective nature of the study, approval by the ethical committee in Milan was waived. No identifying details of the patients were mentioned in this study, all information were anonymized, and the images included may not be identified persons.

Results

The patient from VUmc was a 75-year-old male (Table 1, case 1) showed on CT-scan of the thorax (persistent) diffuse areas of consolidation in his left lower lobe, resulting in a differential diagnosis of infection, localized fibrotic disease or lepidic predominant adenocarcinoma. CT-guided transthoracic biopsy showed adenocarcinoma with a lepidic growth pattern. Surgery was planned and the left lower lobe completely resected. The resection specimen showed a lepidic growth pattern in 12/19 H&E slides from the initially sampled tissue blocks, with no invasive component. As a sharply outlined tumor was lacking and palpation was not supportive in recognizing tumor (Figure 1), additional tissue sampling was performed in the search for possible invasive areas. Eventually, nearly the whole lobe was processed for histologic examination. Including the initial 19 slides, a total of 312 blocks were evaluated. In 281/293 additional slides a similar lepidic growth pattern compatible with AIS as in the initial slides was observed in a background of emphysematous lung (Figure 2A-E). There were no signs of true, nor surrogate markers of, invasion, such as multi-layering or more alveolar filling. In the remaining 12/293 blocks no tumor cells were observed.



- **Figure 1.** Gross appearance of case 1. Note on cross sections, no large sharply circumscribed tumor nodule is present, but small greyish-white pinheads, some white fibrosis on the pleural side (left) as well as preexisting emphysematous lung tissue. The red ink on the surface is added during gross examination supporting the analysis of the resection margins in microscopy. The red parenchyma in the middle is not fixed after 1 day submerging in fixative (low diffusion rate⁶⁶)

The second patient was diagnosed in San Raffaele Scientific Institute. After initial wedge resection of the left lower lobe, that did not reveal a gross tumor, lobectomy of the left lower lobe was performed. Gross examination showed a diffuse thickening of the pulmonary parenchyma, brownish or greyish in color, in which there was a nodular lesion of 1.1 cm palpable. Initial histologic slides (28 blocks) showed a lepidic growth on thin alveolar walls without signs of invasion, compatible with AIS (Noguchi type A¹⁰) in most of the blocks and on the palpable lesion a focus with increased elastin (Noguchi type B¹⁰). Subsequently the remaining of the lobe was extensively sampled with in total 130 tissue blocks. In 111 blocks (85%) AIS Noguchi type A was present. In three sections small foci of slight multilayering fitting with extensive epithelial proliferation³¹⁷. Beside a small pneumocytoma in one slide, the sections also showed signs of emphysema, pigment depositions, focal smooth muscle hyperplasia, intimal fibrosis in pulmonary artery, minor focal lymphocytic infiltrate, focal bleeding and clamping edema.

From the pT3N0 cohort of 683 patients³⁴², 112 (16%) patients with an adenocarcinoma larger than 7 cm were selected. After analyzing the pathology reports, and reviewing the pathology slides, 87 cases were definitely invasive. Another 18 cases were excluded because of mucinous subtype, of which 10 cases had clearly invasive components. The remaining 7 cases were classified on H&E as possibly non-invasive non-mucinous adenocarcinoma and selected for this further analysis. Patient- and tumor characteristics of selected cases and their matched controls are shown in table 1.

■ **Table 1.** Characteristics of the 2 completely histologically examined cases* as well as the 7 possible non-invasive cases from the T3N0 cohort and their invasive controls

Case #	Gender	Age	Hospital	Resected lobe / diameter tumor	slide #	# tumor blocks	Selection H&E staining only	Diagnosis after revision on H&E, CK7, elastin staining
1*	m	75	G	LLL /16 cm	312	293	Possible in-situ	In situ
2*	f	77	H	LUL / 16 cm	159	130	Possible in situ	In situ
3	f	72	A	LUL /whole lobe	8	6	Possible in-situ	In situ
4	m	68	C	RLL/20 cm	7	5	Possible in-situ	In situ
5	m	65	E	LLL /9.0 cm			Possible in-situ	In situ
6	m	76	A	RUL/RML / 9.5 cm	10	7	Possible in-situ	Papillary carcinoma
7	f	70	B	LUL /12.0 cm	10	5	Possible in-situ	Invasive, lepidic predominant + acinar
8	f	63	D	RML /7.1 cm	9	5	Possible in-situ	Papillary carcinoma
9	m	57	F	LUL /11.0 cm	8	5	Possible in-situ	Micropapillary
10	m	76	A	Pneumonectomy Left /9.0 cm	12	6	Invasive control	Invasive, solid
11	m	80	B	LLL /8.0 cm	7	4	Invasive control	Invasive, acinar
12	m	60	C	Pneumonectomy Right/8.5 cm	8	4	Invasive control	Invasive, solid

- **Table 1.** Characteristics of the 2 completely histologically examined cases* as well as the 7 possible non-invasive cases from the T3NO cohort and their invasive controls (continued)

Case #	Gender	Age	Hospital	Resected lobe / diameter tumor	slide #	# tumor blocks	Selection H&E staining only	Diagnosis after revision on H&E, CK7, elastin staining
13	f	75	D	RUL+RML /7.5 cm	16	7	Invasive control	Invasive, Acinar and papillary
14	m	61	E	RUL+RML /9.0 cm	8	6	Invasive control	Invasive, solid
15	f	64	F	RLL /8.0 cm	7	4	Invasive control	Invasive, solid

= number

Three of the 7 cases (case 3, 4 and 5), just as the two above-described cases revealed a regular pattern in the CK7 staining with preserved elastin fibers in the relatively thin stromal components. Therefore, these were considered pre-existing collapsed alveolar septa (Figure 1A-E) and classified as 100% lepidic adenocarcinoma i.e., AIS.

Two cases (case 6 and 8) were, considered true papillary carcinoma²⁰⁶, based on the absence of elastin in papillae (Figure 2F-L). One case (case 7) was classified as lepidic predominant with an invasive acinar component. Another case (case 9) was diagnosed as micropapillary carcinoma based on a mixture of large lepidic and smaller multifocal micropapillary component in several adjacent alveoli.

Radiology

Details of preoperative imaging of the retrospective T3NO cohort are shown in table 2.

- **Table 2.** Radiologic of the 2 completely histologically examined cases* as well as the 7 possible non-invasive cases from the pT3NO cohort and matched invasive controls.

Case	Histology invasive yes/no	Type of images	Diameter Tumor (cm)	GGO yes/no	GGO Diameter (cm)	Solid Diameter (cm)	Radiologic Invasive yes/no	Radiologic remarks
1*	no	PET-CT	19	yes	19	16	yes	GGO + consolidations; emphysematous cysts
2*	no	PET/CT	16	yes	15	8	n/m	GGO + consolidations
3	no	PET-CT	>7	yes	>7	2.6	yes	Pneumonic type + subsolid nodules
4	no	CT-thorax	15.3	yes	15.3	9.3	yes	Pneumonic type
5	no	PET-CT	17.4	yes	17.4	10.1	yes	Pneumonic type + subsolid nodules
6	yes	PET-CT	8	no	n/a	8	yes	Solid nodule

Table 2. Radiologic of the 2 completely histologically examined cases* as well as the 7 possible non-invasive cases from the pT3N0 cohort and matched invasive controls. (continued)

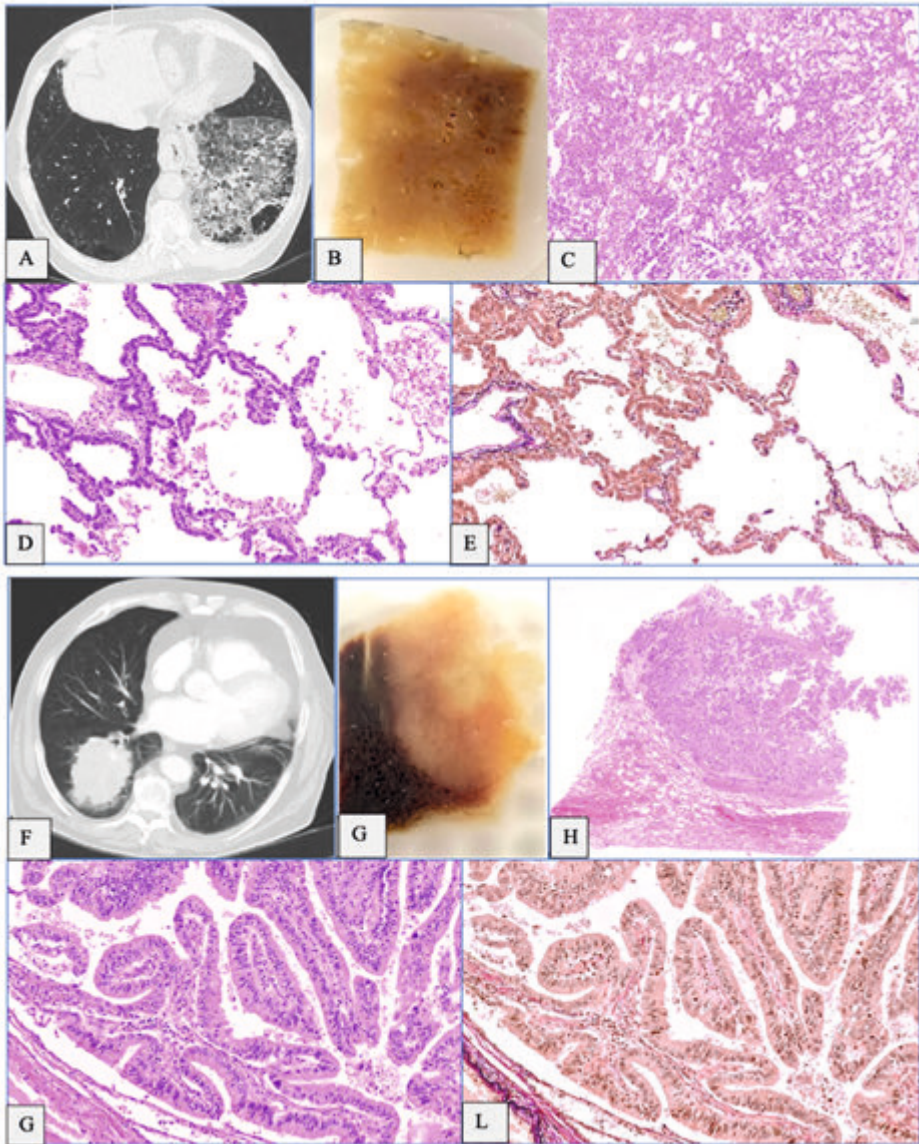
Case	Histology invasive yes/no	Type of images	Diameter Tumor (cm)	GGO yes/no	GGO Diameter (cm)	Solid Diameter (cm)	Radiologic Invasive yes/no	Radiologic remarks
7	yes	PET-CT	14.7	yes	14.1	10.8	yes	Pneumonic type + solid mass surrounding GGO
8	yes	CT-aorta	12.3	yes	12.3	11.1	yes	Solid and consolidations
9	yes	PET-CT	10.4	no	n/a	10.4	yes	Pneumonic type and solid
10	yes	not available	n/a	n/a	n/a	n/a	n/a	n/a
11	yes	CT-thorax	13.6	no	n/a	13.6	yes	Mainly solid
12	yes	CT-thorax	> 7 cm	no	n/a	> 7 cm	yes	Solid mass
13	yes	CT-thorax	10.1	yes	9.3	10.1	yes	Mainly solid
14	yes	PET-CT	9.1	no	n/a	9.1	yes	Solid mass
15	yes	CT-thorax	8.0	no	n/a	5.9	yes	Solid mass

GGO= Ground glass opacity; n/a = not applicable; n/m = not mentioned

The retrieved preoperative imaging had varying imaging protocols, and consisted in 5 cases of a chest CT with relative thick image slides (3-5 mm), consistent with standard imaging quality in the study period. In 8 cases a PET-CT scan was retrieved, with unenhanced thick slice CT imaging available. Of 1 case a CT-Angiography (CTA) of the aorta was retrieved.

In all 3 histologically non-invasive cases, radiology showed a pneumonia-like tumor morphology with multiple subsolid nodules. In 2 of 3 histologic non-invasive cases, the tumor occupied nearly the whole lobe, with diameters larger than 15 cm on CT-imaging.

The lepidic predominant but focal micropapillary case, also showed a pneumonia-like tumor morphology. Surprisingly, one of the control cases with invasive tumor (case 7) also showed a pneumonia-like tumor morphology. However, after pathological revision, this control case showed, beside distinct invasion, large areas with lepidic growth pattern, explaining the imaging appearance. The 2 papillary carcinoma cases showed a solid mass on CT imaging (Figure 2F). The other invasive control cases also showed a predominantly solid tumor morphology.



■ **Figure 2.** Radiological, gross and microscopic aspects of two cases.

A-E. Case 1. In situ adenocarcinoma. Note the pneumonia-like consolidative pattern on the CT-thorax (A). Paraffin block showing a granular pattern without a circumscribed tumor mass (B). On H&E (both overview and detail, 200x): an in situ, partly pseudopapillary pattern (C, D). In Elastin staining preserved fragmented elastin fibers in the alveolar septa, 200x (E).

F-L. Case 6. Papillary carcinoma. Note the solid aspect on the CT-thorax and paraffin block (F, G). On H&E, a papillary pattern both in overview (H) and in detail, 200x (K). In Elastin staining absence in the stromal papillae, 200x (L).

Follow-up

The general follow-up data of the possible *in situ* cases, as well as their controls, are shown in Table 3.

■ **Table 3.** General follow-up data of the 2 completely histologically examined cases* as well as the 7 possible non-invasive cases from the pT3N0 cohort and matched invasive controls.

Case	Gender	Age	Revision diagnosis	Recurrence yes/no (years)	Type of recurrence	Cause of death	Status (years after primary)
1*	m	75	In situ	no	n/a	COVID19	DND (1.5y)
2*	f	77	In situ	no	n/a	n/a	AND (< 1y)
3	f	72	In situ	no	SPLC	Diabetes mellitus Second primary	DND (6y)
4	m	68	In situ	no	SPLC	n/a	AND (10y)
5	m	65	In situ	no	SPLC (no histology)	SPLC	DND (4y)
6	m	76	Papillary carcinoma	yes < 1y	Bone, lung and brain	Lung cancer	DOD (1y)
7	f	70	Lepidic predominant+ acinar	no		Pancreas carcinoma	DND (3y)
8	f	63	Papillary carcinoma	yes 3y	Mediastinum Different lobe same site	n/a	AND (9y)
9	m	57	micropapillary	yes 1y	Recurrence?	Lung cancer	DOD 1y
10	m	76	Invasive solid	yes <1y	Liver metastases	Lung cancer	DOD 10
11	m	80	Invasive acinar	yes <1y	Lung metastases	Lung cancer	DOD 1y
12	m	60	Invasive solid	yes 3y	Brain metastases	Lung cancer	DOD 4y
13	f	75	Invasive Acinar and papillary	yes 3y	Lung metastases	Lung cancer	DOD 3y
14	m	61	Invasive solid	yes 2y	Brain metastases	Lung cancer	DOD 2y
15	f	64	Invasive solid	yes 2y	Lung metastases	Lung cancer	DOD 2y

SPLC = second primary lung cancer; AND = alive, no disease (no lung cancer); AWD = alive with disease (lung cancer); DND = death, no disease (no lung cancer); DOD = death of disease (lung cancer); n/a = not applicable

Here, we describe in detail the follow-up data of the 5 cases with large (>7 cm) non-invasive adenocarcinomas:

Case 1

A 75-year-old male showed a persistent lobar consolidation in the left lower lobe with extensive ground-glass and small cystic changes on CT-imaging. A differential diagnosis of localized interstitial lung disease or malignancy was made, and a biopsy confirmed the presence of adenocarcinoma with a lepidic growth pattern, without invasive features. He underwent a left lower lobectomy. The gross pathology examination did not show tumor nodules, and confirmed focal bullous cysts (Figure 1). The initial histology identified several areas of non-mucinous lepidic adenocarcinoma without invasion, with an estimated diameter of 16 cm. In search for possible invasive areas, comprehensive histopathological examination was performed and nearly the entire lobe was sampled, resulting in over 300 formalin fixed and paraffin embedded blocks and corresponding slides. The cystic formations observed on imaging could be attributed to areas of bullous emphysema covered by the lepidic growth of tumor cells. Histology showed extensive AIS.

The patient successfully recovered from surgery without any major complications. However, 18 months after the resection, he was infected by COVID-19 and required intubation. In a few days, he died due to complications. His status was classified as “death, no evidence of disease” (DND).

Case 2

A 77-year-old female showed in the left lower lobe extensive parenchymal consolidations and ground glass areas on CT-imaging. An initial diagnosis in favor of infection was made, but despite antibiotic therapy. A second CT after six months revealed more extensive parenchymal consolidation and ground glass areas. Subsequent bronchoalveolar lavage that showed presence of adenocarcinoma. PET was negative. She recently (2023) underwent left lower lobectomy. The gross pathology examination did not show tumor nodules. The initial histology identified several areas of non-mucinous lepidic adenocarcinoma without invasion, with an estimated diameter of 16 cm. In search for possible invasive areas, comprehensive histopathological examination was performed and nearly the entire lobe was sampled, resulting in additional 130 formalin fixed and paraffin embedded blocks and corresponding slides. Histology showed extensive AIS.

The patient successfully recovered from surgery without any major complications.

Case 3

In 2010, a woman aged 72, with a history of diabetes mellitus and related vascular disease, underwent a left upper lobectomy for pneumonia-like tumor, with multiple surrounding semisolid nodules. The lobe (diameter 18 cm) showed confluent areas of non-mucinous lepidic adenocarcinoma without invasion. Resection was complete, and uneventful.

Six years later, she experienced severe weight loss (20 kg), and was found to have 2 intrapulmonary ground glass opacities in the left lower lobe with diffuse pulmonary nodules on PET-CT imaging. In the differential diagnosis of a second primary lung

cancer and metastasis, metastases of breast cancer were suspected, due to a right breast mass and regional lymphadenopathy, but further diagnostic testing was not pursued because of her dismal clinical condition. She passed away, and the cause of death was attributed to a metastasized second primary malignancy, most likely breast cancer, based on radiology. Her status related to the initial tumor was therefore, also considering the 6 years' time interval classified as "death, no evidence of disease" (DND).

Case 4

In 2011, a man aged 68 underwent a resection of his right lower lobe for a pneumonia-like tumor > 15 cm. The histology of the whole lobe revealed a non-invasive tumor with lepidic growth pattern. In 2013, the middle and upper lobe were resected, with the middle lobe showing a non-mucinous lepidic adenocarcinoma of 12 cm without any invasive areas. The upper lobe exhibited an lepidic area of 2 cm, similar to that of both tumors in the lower and middle lobes which had the same KRAS mutation. No treatment was initiated. In 2014, he underwent stereotactic radiotherapy for a growing ground-glass lesion in the left lower lobe without solid areas. Following this, multiple ground-glass lesions developed in the left lung. In 2016, he began chemoradiation with a platinum-based regimen. In 2017, he was transferred to a different hospital for experimental immunotherapy, after which chemotherapy was discontinued. However, a year later, immunotherapy was stopped, and chemotherapy was resumed. The lesions have remained relatively stable. Ten years after his initial resection, the status of his initial tumor was classified as "alive with no evidence of disease" (AND).

Case 5

In 2011, a man aged 65 underwent a left upper lobectomy for a 17 cm tumor found on CT. The gross specimen at pathology revealed a recognizable tumor of 9 cm, consistent with a more solid area of about 10 cm seen on radiology. Both this area as well as the ground glass areas surrounding this, but on gross examination non-remarkable were histologically classified as a lepidic growth pattern and therefore non-invasive adenocarcinoma. Approximately 1 year later, consolidations in the left lower lobe were found and on biopsy adenocarcinoma with a lepidic growth pattern was diagnosed. The patient received treatment with radiotherapy and angiogenesis inhibitors. In mid-2014, after a 2-year interval, progressive bilateral lung densities emerged with ground-glass morphology. In the beginning of 2015 the areas became denser, and the patient passed away without establishing the nature of the lung lesions, however, these were presumed metastases or invasive areas from the second primary lung malignancy in the left lower lobe. His status was for his primary tumor was established as "death, no evidence of disease" (DND).

Discussion

This study provides arguments that non-mucinous adenocarcinomas in situ with a size > 7cm exist. In two patients the entire resected lobe was histologically examined, revealing tumors both with diameters of 16 cm, without histological criteria of invasion. Three additional cases from a nationwide T3N0 cohort with tumor sizes exceeding 7 cm, yet displaying an AIS-pattern on histological analysis are also described, including extensive follow-up data, supporting the non-invasive nature of the initially resected tumors.

The prevalence of AIS in this pT3N0 cohort would be 3 in 112 (2.6%). In all three cases, no evidence of invasive growth was observed in the available retrospective material. Although the follow-up showed in 2 cases similar radiologic disease in other lobes, interpreted as another primary. Although we had for most cases no histological prove, the clinical most likely explanation was that none of the AIS patients had recurrences from or died of their initial disease.

Our findings are in line with the study of Inafuku and colleagues, who found 277 cases that showed a non-invasive pattern consistent with AIS³⁴⁴ in 2115 resection specimen. Twenty-two of these (7.9%) had a diameter larger than 3 cm, with a mean of 40,1 mm \pm 6,9 mm.

Boland et al investigated the interobserver variation between 2 pathologists with respect to AIS and minimal invasive adenocarcinoma (MIA) in 296 resection specimens. They agreed on 1 case of AIS, that had a diameter of 3,5 cm (0.3%)³¹². Although not purely lepidic, Strand et al found in 5 of 131 resection specimens an adenocarcinoma with more than 95% lepidic pattern, a tumor diameter larger than 3 cm, in 1 of them larger than 5 cm³⁴⁵. These non-invasive tumor sizes are however well below the tumor sizes up to 16 cm that we now present, which to the best of our knowledge has not been reported before.

In our study, all five cases of AIS were characterized by tumors with just areas of lepidic growth. However, during gross examination, it was challenging to identify specific tumor nodules as there was no clear demarcation and palpation did not provide any support due to the lack of firm consistency (Figure 1). After a follow-up period of 10 years, one patient (patient 4) is still alive, but suffering from the same type of non-invasive disease in their other lung. Patient 1 died due to a COVID19 infection, patient 3 due to presumed metastatic breast cancer, and the fifth patient died from lung cancer in different lobes. This patient exhibited similar manifestations as the primary tumor, with progressive consolidation patterns in other parts of the lung, which were also believed to be non-invasive based on radiological findings of diffuse ground-glass, similar to patient 4. Despite dying from respiratory insufficiency, there were no clear signs of invasive cancer, though no biopsies were performed. It is possible that extensive AIS deposits throughout large areas of the lung led to reduced ventilation and respiratory insufficiency. However, no pulmonary function tests were conducted to support this hypothesis of impaired diffusion capacity.

Large sized AIS tumors have extensive growth of tumor cells with 20+ μ m height on alveolar walls. In pathophysiologic terms, this leads to a 20+ fold increase of the diffusion distance in the gas exchange of oxygen and carbon dioxide. Since large sized AIS tumors involve large alveolar surface areas, this effect might be measurable by a decrease in a diffusion test. We surmise that patients with this form of lung cancer may have a different clinical course than those with the more frequent form of invasive and palpable lung cancer.

The blinded revision of the radiologic images did show an at least partly pneumonic-type tumor morphology^{346 347} in all 7 possible in situ cases of the retrospective cohort. In two of these cases with papillary carcinoma, the tumor had a more predominant solid appearance with minor areas of surrounding (ground-glass) consolidation.

One control patient with invasive carcinoma showed a pneumonic-type tumor morphology on CT-scan, which could be explained by a significant lepidic component accompanying otherwise clearly invasive carcinoma. All other invasive cases did not show pneumonic-type tumor morphology, but were all mainly solid masses.

Pneumonic-type adenocarcinoma has been described as two different types: localized pneumonic-type lung adenocarcinoma (L-PLADC) and a diffuse variant (D-PLADC)³⁴⁸. The diffuse variant usually is a mucinous adenocarcinoma on histology. Non-mucinous pneumonic-type adenocarcinomas seem rare^{349, 350}, but this may also be due the fact they are not diagnosed as such. Our current study not only shows several cases that were consistent with PLADC on CT, but also were non-mucinous and non-invasive on histology.

Some of the patients had a discrepancy regarding tumor diameter between imaging and gross examination on pathology, which is consistent with the difficult-to-see-and-palpate non-solid, spongy consistency of an in-situ carcinoma. Discrepancy between a suggested solid component on CT but absent invasive component on histology may be explained by *in vivo* tumor collapse²⁷⁹.

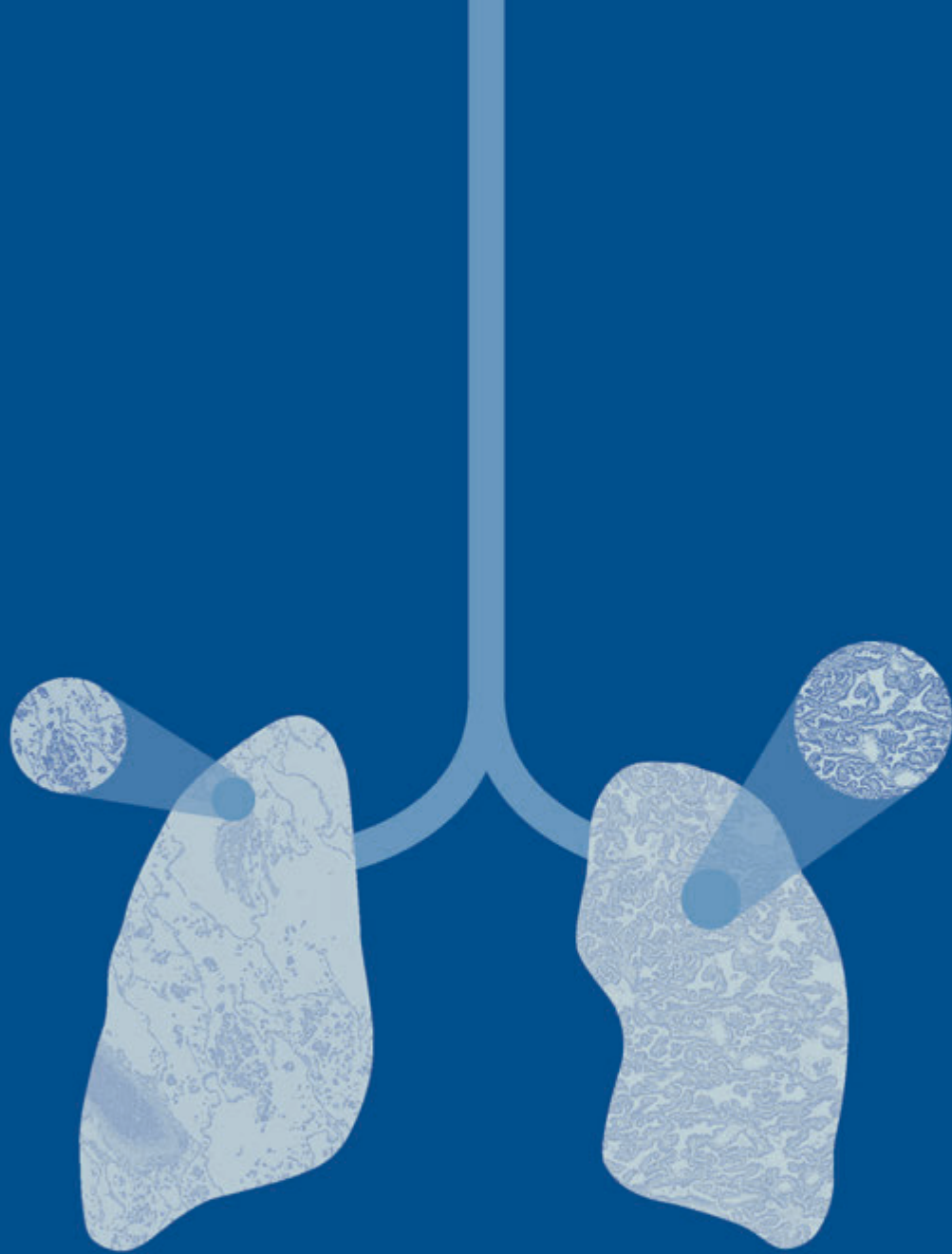
Interestingly, two cases that initially were "possibly non-mucinous AIS" on H&E staining, were reclassified as papillary carcinoma based on elastin staining. Both showed a solid mass morphology on radiology, without significant pneumonia-like features. Visual inspection of the paraffin block after cutting the slides showed a clearly delineated tumor (Figure 1G). The fact that these orthogonal methods of radiology and gross aspect on the paraffin block points in the same direction is a strong support in the differential diagnosis between (collapsed) AIS and papillary carcinoma, and should probably be included in a modified classification.

The limitations of this study include for the pT3N0 cohort, i) its retrospective nature, which prohibits re-examining the resection specimen, since the remaining resection specimen is not stored (which is standard procedure as soon as a few weeks after resection); ii) the number of available histologic slides per case is limited even for tumors that occupy a relatively large portion of a lobe; iii) we did not select cases that were reported as acinar adenocarcinoma as possible non-invasive cases, nor cases with multiple nodules in the same lobe, larger than 3 cm. So, we might have missed some

additional cases of large AIS; iv) the radiologic images available in the study were limited in quality due to varying imaging protocols and relative thick slices. Nevertheless, we believe it is unlikely that this leads to misclassification of cases between solid or pneumonia-type tumor morphology. For the two cases with complete histologically examination of the resected lobes the follow-up time is limited.

Conclusion

Adenocarcinoma in situ > 7cm does exist and can be diagnosed. The restriction of 3 cm size criterion for AIS in the current World Health classification of pulmonary adenocarcinomas may be reconsidered. Sampling in large AIS the whole tumor area for histologic examination is advised.



17

General discussion and
future perspectives

This thesis investigated three histopathological aspects in resected NSCLC specimens, relevant to diagnosis, prognosis, and staging.

In **part I**, the aim was to establish criteria for the pathologic response effect after neoadjuvant therapy by examining whether histopathological findings such as the percentage of tumor rest, proliferative activity, as well as including morphometric properties may lead to a refinement in the prognosis of patients with NSCLC. In addition, the modified criteria from TNM-7 to TNM-8 were examined in a Dutch cohort as a kind of validation.

Neoadjuvant therapy and postoperative pathologic staging

Approximately 25-30% of non-small cell lung cancer (NSCLC) patients are diagnosed in the early stage (IA-IIIB), and most of them undergo surgical treatment with a curative intention². Also, patients with stage IIIA can be treated by surgery. However, a significant number of these patients will during follow-up develop distant metastases, resulting in a low 5-year overall survival (OS) rate (<35%) for those with stage IIIA disease¹⁶. Platinum-based adjuvant chemotherapy showed a positive impact, raising the 5-year survival rate by an additional 5%³⁵¹.

In the absence of randomized studies to compare both of them, adjuvant and neoadjuvant approaches could be valid. Several studies have compared adjuvant treatment to neoadjuvant (preoperative) treatment in different study populations, but they have not shown any significant differences in effectiveness between the two approaches. Both adjuvant and neoadjuvant chemotherapy for resected NSCLC increase the 5 years OS by 4% to 5%^{352 353}. Importantly, neoadjuvant treatment has several advantages over adjuvant therapy, such as reducing the tumor size and stage (thereby increasing the possibility of complete surgical removal), treating micrometastatic disease early, after resection evaluating the response to systemic therapy in the surgical specimen, and improving the patient's preoperative performance status, which may improve adherence to the treatment plan^{354 355}. The introduction of immune checkpoint inhibitors, which have been shown to significantly prolong survival in many patients, is changing the treatment options for advanced NSCLC^{356,357}. Recently, Forde et al. reported the Checkmate 816 trial, showing a significant increase in the median event free survival in patients treated with chemotherapy combined with immunotherapy (Nivolumab) compared to chemotherapy alone (31.6 vs 20.8 months)³⁵⁸. Thorough investigation is warranted to examine the histopathologic effects of these changes in adjuvant schemes.

Also, for patients with more advanced stage III disease, such as those with a Pancoast tumor in the upper lung sulcus, neoadjuvant therapy can be advantageous. This type of treatment may change the status of the tumor from irresectable to resectable. The standard of care for these patients still involves trimodality therapy, which involves concurrent chemotherapy and radiotherapy with cisplatin/etoposide, followed by surgery⁶³. It is likely that immunotherapy will also play a part in altering

this trimodality approach. In a case report, Tang et al. reported a complete pathologic response after neoadjuvant chemo-immunotherapy followed by surgery³⁵⁹.

In **chapter 2**, we investigated in one of the first more detailed retrospective studies on the pathologic response in a series of 46 patients who underwent tri-modality therapy for a sulcus superior tumor. To estimate the pathologic response, we used a modification of the cut-off points suggested by Junker et al²⁷, creating a four-tiered grading system, similar to the one used by Dworak for colorectal cancers³³. A cut-off point of less than 10% viable tumor cells in our study confirmed the favorable prognosis.

This was later-on suggested as the cut-off for a major pathologic response (MPR) in the IASLC multidisciplinary recommendations for pathologic assessment of lung cancer resection specimens after neoadjuvant therapy⁴⁵. They formulated 11 recommendations concerning among others the necessary clinical information, such as the type of neoadjuvant therapy and the way the specimen has to be sampled to optimize comprehensive gross and histologic assessment of the lung tumor bed for pathologic response. Subsequently, another group described a major pathologic response calculator tool, and proposed this for standardized, comprehensive collection of percentages of viable tumor, necrosis, and stroma in the tumor bed. MPR and pathologic complete response (pCR), defined as less than or equal to 10% and 0% viable tumor cells, respectively, are investigated in NSCLC clinical trials to examine if they can be used as surrogate end points for efficacy to shorten time to outcome³⁶⁰³⁶¹. An interesting aspect of estimating the pathologic response after neoadjuvant therapy, is whether this is also applicable in cases where immunotherapy was added to the neoadjuvant scheme. The question is whether there should be a different way to estimate the residual viable tumor (RVT) by including the tumor bed with its inflammatory response³⁶². The Checkmate 816 results showed at least a significant increase in the number of cases with an complete pathologic response (CPR) in those that received immunotherapy as part of their neoadjuvant treatment compared to those who received chemotherapy only (24.0% vs 2.2%)³⁵⁸.

When comparing the recommendations as proposed by the IASLC committee⁴⁵ and Saqi et al³⁶⁰ to our study, we would in hindsight more explicitly describe and illustrate how the handling of the resection specimen was performed and from what areas slides were taken as well as taken more slides than was done, maintaining the 3-dimensional orientation¹⁹⁸. This could lead to an even more reliable estimation of the viable tumor rest. With the current data of our study, the major pathologic response calculator tool can't be used. A small nest was really a small nest, and probably marked lower than the 10% of the gross size. We also experienced that when initial sampling for microscopy (roughly one block per 1-2 cm) did not reveal vital tumor cells, subsequent additional sampling occasionally resulted in areas with vital tumor cells, emphasizing that generous sampling for estimating MPR may aid in the reliability of MPR assessment.

Further studies are needed to establish reliable criteria for the pathologic response associated with various types of adjuvant therapy. Artificial intelligence may potentially

contribute to accurately determining the percentages of different tissue reaction compartments (e.g., viable tumor, necrosis, and stromal reaction) in the tumor bed. This subject requires further investigation^{363 364}.

In **chapter 3**, we found that a high expression of PDL-1 and high proliferation activity (marker MIB-1), were related to a worse outcome. Also, in a later study by Vrankar et al., high PD-L1 expression was a negative prognostic factor for PFS and OS after concurrent CRT in locally advanced NSCLC. As only small number of patients had enough tissue for the IHC testing, no firm conclusions could be made⁵⁷. On the contrary, Zens et al. discovered that PD-L1 expression did not have a significant correlation with longer survival in 53 cases of resected NSCLC after neoadjuvant chemotherapy. Their study demonstrated that after neoadjuvant therapy, PD-L1 expression was lower in 7 out of 53 cases and higher in 12 out of 53 cases. However, the sample size of cases with changed PD-L1 expression was too small to draw conclusions on any prognostic value³⁶⁵. As these findings may be of value for further refinement of the assessment of pathologic response, more studies are needed, probably also taking other variables (e.g., histologic subtypes and IHC of p53 and PD-L1) into account. Tsao et al. for instance, found in an adjuvant setting lower recurrence free survival in high grade subtypes like solid and micropapillary adenocarcinoma, compared to lepidic and acinar predominant patterns³⁶⁶.

The T-descriptor in the pTNM staging

In the transition from TNM-7 to TNM-8, a tumour with a diameter larger than 7 cm moved from the T3 to the T4 category, based on follow-up data of the several international researchers, with a major contribution from Japan (79%)⁷⁹. The IASLC database for the TNM8 staging project did not contain information from Dutch lung cancer patients. Since we had already collected the overview data for the study in chapter 16, and the T-descriptors of T3 in the TNM-7 are quite variable, we investigated in **chapter 4** several staging related parameters in a nationwide population of patients with a pT3N0 NSCLC. We demonstrated that following the implementation of TNM-7 and subsequent modifications made in TNM-8 within the Dutch population, while some data remained consistent, there were also findings that did not fully endorse all the alterations made in TNM-8. As a result, we suggest that further refinement may be feasible. To begin with, we observed that the group of patients with tumor diameters larger than 7 cm should not necessarily be reclassified as category pT4. Furthermore, our findings indicate that a “mixed group of two pT3 descriptors”, not previously described, merits migration to pT4. Additionally, in the pT3N0 subcategory of “two or more nodules,” the histologic type is a relevant descriptor. Based on the Dutch population, patients with adenocarcinoma in this subcategory have a more favorable outcome compared to other subtypes and could be reclassified as a pT2 category. This histologic prognostic correlation was supported by Grosu et al., studying patients with stage I NSCLC and found that those with squamous histology have a higher mortality risk than those with adenocarcinoma histology³⁶⁷. Our study suggests that besides using

the anatomical tumor location(s), other reproducible parameters could be employed to enhance the most commonly used clinical prognostic system, which has relied so far solely on those anatomical data for staging. To improve the prognostic ability of the coming 9th edition of the TNM classification, the latest data collection could probably include molecular information such as genetic biomarkers, copy number alterations, and protein alterations. Adding highly reproducible histologic parameters, such as the distinction between adenocarcinoma and squamous cell carcinomas is simple and informative. Bertoglio et al. showed that pT1 micropapillary and solid subtypes, considered as high grade patterns²⁵², had a prognosis comparable to pT2a tumors³⁶⁸. However, the reproducibility of pattern recognition is low¹⁴. Integration of reproducible parameters with clinical, biological, and anatomical factors may form prognostic groups that will enhance our capacity to refine prognosis and hopefully personalized therapeutic planning.

Rami-Porta suggests that in future editions of the TNM classification, the results of liquid biopsy may play a role in complementing it³⁶⁹. The suggestion of adding the letter B for blood was made, to describe the presence of cancer material in the blood and so leading to a TNMB classification³⁷⁰. He further states that other cancer cells should also be included in future editions of the classification³⁶⁹, namely, those of spread through air spaces (STAS), that have been identified in all types of lung cancer and are associated with a worse prognosis. This last statement seems very premature, because there is still debate on the true nature of STAS and the reproducibility of diagnosing STAS is low and sampling variation high.

In **part II**, the focus was on this phenomenon of “STAS”. Since the introduction of spread through air spaces (STAS) as a new invasive pattern in the 2015 WHO classification on non-small cell lung cancer (NSCLC)⁴, there has been a debate on whether STAS is a true biological phenomenon or mainly an artifact. In **chapter 7**, a critical review on the subject is presented, arguing that STAS could well be an inducible phenomenon by surgical and pathology handling of the resected specimen. The basis for this point of view is the in **chapter 6** presented prospective multi-institutional study, in which we demonstrate that the number of loose tissue fragments and cells increases along the path that the dissection knife takes at gross handling of the resection specimen.

“Loose tumor cells” / “STAS” and definition

Although the viewpoint that “loose tumor cells” are an artifact is mainly debated by the initiators of the STAS concept in the 2015 edition of the WHO classification⁴, they already made nuances in the 2021 WHO edition^{19 371}. In this most recent classification, in contrast to the previous version, artifacts as a possible differential diagnosis of STAS is mentioned: *“The following features favor artifactual spread of tumor cells over STAS: (1) randomly situated and ragged-edged clusters of tumor cells often at the edge of the tissue section or out of the plane of section of the tissue; (2) lack of continuous spread in airspaces from the tumor edge to the most distant airspace tumor cells; (3)*

pneumocytes or bronchial cells with benign cytologic features and/or presence of cilia; or (4) linear strips of cells that are lifted off alveolar walls." They state that using these criteria, separation of STAS from artifacts was highly reproducible (average kappa 0.86) in a study of selected images, based on a poster abstract by Baine et al.³⁷². From one of the participants in that study, we learned that it was a highly selected set of easy cases. However, to be applicable in routine practice, the diagnostic criteria must be clearly defined to ensure consistency over time (intra-observer reproducibility) in a consecutive series of cases and lead to the same diagnosis between different pathologists (low inter-observer variability). Research on inter-observer reproducibility can be categorized as either local, involving a few pathologists within an institute or region, or global, involving pathologists from various parts of the world. The latter type of study is considered to be more robust. Informative in this sense are studies examining STAS in frozen sections. Three studies have reported a sensitivity range of 55-86% for STAS^{204 205 172}. Villalba and colleagues, who are regional pathologists with a particular focus on pulmonary pathology, have clearly articulated the concerns regarding STAS analysis in frozen sections in their paper's summary: "As current accepted definitions for STAS and artifactual clusters are variably interpreted by pathologists, more precise criteria should be established and standardized, before the assessment of STAS can be implemented globally in the intraoperative setting to aid surgical decision making"²⁰⁴. Therefore, this "easy distinction" of STAS as mentioned in the 2021 WHO classification³⁷¹ seems far too optimistic.

To better comprehend the discourse surrounding STAS, it is important to note that the WHO provides morphological criteria for artifacts, and if these are absent, a "loose tumor fragment" aligns with the definition of STAS. However, a topological component also plays a role. Quote "The morphological patterns of STAS, namely single cells, micropapillary and solid tumour cell clusters are artifacts if present without continuity with the (invasive) tumor border or are present at a too far distant from this tumor border." Therefore, although "loose tumor fragments" may appear morphologically consistent with STAS, without proper topological annotation, they should be considered an "artifact" under the WHO criteria. This may aid in the confusion among pathologists and could partly account for the low reproducibility of STAS. In conclusion, there are currently no clear and consistent criteria for STAS. This was also the opinion of > 100 responders from a recent questionnaire distributed in the Pulmonary Pathology Society network, presented at USCAP meeting in New Orleans, March 2023.

Possible causes of "STAS"

After our chapter 6 publication in 2017, Metovic and colleagues attempted to validate our findings in a prospective study, comparable to ours, except that they used a fresh knife blade for every cut they made during gross handling of the resection specimen¹⁷⁵. However, they didn't find a correlation between the amount of STAS and the direction of the cuts made, as we did in our study. In chapter 9 we commented on the fact that they also found tumor cells or fragment in the opposite direction the cutting. We argued

that using downforce, also creates an upward force that could explain the presence of tumor cells, but also erythrocyte in other directions than expected. In the CON part of the STAS editorial in chapter 11 most of the alternative explanations for the presence of tumor cells, normal tissue fragments and erythrocytes, distant from the tumor border are presented. The article highlights potential factors such as surgical clamping forces during lobectomy, which could lead to the displacement of lymph fluids, as well as handling of the specimen during pathological examination. The use of a sharp knife for “gentle” cutting may help to reduce mechanical forces, but an underestimated factor is palpation. Last but not least, the pictures taken from a video, kindly provided by Metovic and Papotti (see chapter 11), shows that the fingers of the left hand are strongly compressing the tumor, in order to cut in a stable manner “gentle” with the new sharp knife in the right hand through the tumor. In this context it is not excluded that (the left hand) palpation force is a confounder, and may be an explanation for an essential part of the different outcomes between Metovic’s and our study. A supporting argument is that palpation by the surgeon leads to more circulating tumor cells during resection procedure, as mentioned in chapter 11.

Loose tumor cells in pulmonary artery of resection specimen

In chapter 10, it was suggested that “loose tumor fragments” could be an artifact, and a new argument to support this claim is that there was a relatively high incidence (almost 60% of 70 cases) of cytokeratin 7 positive tumor cells in small pulmonary artery branches. In addition to tumor cells, intravascular alveolar macrophages were also discovered. Overall, the presence of displaced tumor cells in a non-invasive disease is difficult to explain biologically, but could be attributed to artifacts. Furthermore, none of the potential differential diagnostic diseases were morphologically fitting with our observations. In our opinion, the only realistic explanation for the intravascular tumor cells is an artifact, probably by cutting the knife during macroscopic procedure. In our opinion, the loose tumor cells in the pulmonary artery are considered to be another artificial spread of detached tumor cells.

STAS and dissociation

In the debate about the interpretation of “loose tumor cells” as “STAS” there is no controversy about the malignant nature of these cells. In the WHO classification STAS is used as a criterion of “invasion”. In our opinion this is an overinterpretation. In breast cancer cytology dissociation is rightfully used as a criterion of malignancy, but not as “invasion”. The modified adhesion molecules in malignant cells may be used for explanation of the reduced adherence between tumor cells. The shear force on the cells during spreading of the tumor cells on the hard blunt glass slide for cytological examination is probably not much different from the shear forces occurring during cutting with a hard blunt steel knife. In breast cancer ductal carcinoma *in situ*, tumor cells also lead in cytology to dissociation and is rightfully interpreted as characteristic of malignant cells, but not as invasive. In short, the dissociation is a characteristic of

malignant cells. However, directly attaching to STAS the weight of 'invasion' is in our opinion an overinterpretation: a bridge to far.

"STAS" and prognosis

In the literature, it is frequently stated that the presence of STAS is an independent adverse prognosticator. The association with a worse clinical outcome is not debated. But the "independent" character is doubtful, since there are several significant associations with other known pathological features. In this context is useful to know a study of the International Association for the Study of Lung Cancer (IASLC) pathology committee: a series of histologic prognostic indicators, including STAS, were compared aiming for development of a grading system in resected invasive pulmonary adenocarcinoma. Moreira et al. concluded that several histologic parameters such as nuclear grade, mitotic grade and the presence of STAS were associated with recurrence, but in the final proposed grading model, the added prognostic value of STAS was not selected²⁵².

In summary, we provide several arguments (in this general discussion and in chapter 11) that "loose tumor cells" or "STAS" is one of the (inducible) artifacts that can occur during tissue handling of lung specimen. The sampling variation encountered and poor reproducibility of "STAS" should be major issues that need to be solved, before considering the incorporation of STAS in future TNM systems. The biological connotation of "spread through air spaces" implies some exclusivity and danger if true. Luckily, lung cancer is not contagious. It also suggests that we as pathologists are able to add the connotation "spread through air". Peculiarly, morphological identical cells with a not-for-location-fitting alveolar topology are, according to the expert opinion in the WHO interpreted as "artifact". This statement of STAS being an inducible artifact, may, in combination with tumor cells displaced to other microanatomic locations such as pulmonary artery, bronchial or bronchiolar lumen, also provide an alternative explanation for the counterintuitive molecular based suggestion in the recent TRACER-X study that lung adenocarcinomas do not always follow an evolutionary route toward higher-grade patterns but also from "high grade" to "low grade"³⁷³, as during sampling "low grade" tumor cells may be displaced to an area with a "high grade" pattern.

Moreover, the biology of STAS is not solved. Is STAS an energy neutral fly? In the pulmonary artery we limit ourselves with the in chapter 10 provided arguments of 'loose tumor cells' in pulmonary arteries of resection specimen to the following statement: "do not attach a biologic annotation and interpret this phenomenon as an artifact".

In part III, we aimed to refine diagnostic tools that can aid in better distinction between invasion and non-invasion in non-mucinous pulmonary adenocarcinoma. To achieve this, we examined the impact of iatrogenic collapse on pulmonary adenocarcinomas and its effect on invasion assessment and in the associated prognosis.

Biological collapse

In the literature the term 'collapse' has been used in two ways. 'Iatrogenic collapse' for tissue collapse after resection and 'biological collapse' as an *in vivo* phenomenon. In histology of lung tumors two components of a scar are discerned: fibrosis with dense collagen and biological collapse with increase of elastin. The latter is supporting the recognition of the pre-existing pulmonary architecture, and has in 1995 without invasive characteristics been described as Noguchi type B¹⁰ or Type II by Goto et al³²³. Both studies concluded that this so-called 'biologic collapse' is probably non-invasive and was associated with a 100% disease free survival. The biologically collapsed alveolar framework has condensed and curled elastic tissue leading to smaller alveolar spaces²⁶⁵. Important to realize is that elastin is produced by mesenchymal cells and not by epithelial cells. Thus, also not by the functionally crippled tumor cells. In a model study, the presence of elastin induced the production of more elastin²⁰⁶. This may explain the elastin increase in biological collapse. Why epithelial cells may sometimes disappear in the center of biological collapse is unclear. Nevertheless, this should not withhold pathologists to add a connotation of 'no invasion' (AIS), unless there is adjacent multilayering of tumor cells.

Iatrogenic collapse

Another form of collapse, called iatrogenic collapse, is, in contrast to biological collapse, an *ex vivo* phenomenon that affects the appearance of the lung both macroscopically and microscopically. Iatrogenic collapse was initially as described in pneumothorax and atelectasis³¹⁸. This iatrogenic collapse was for the first time described in 2013 as "surgical atelectasis artifact": a possible confusing factor in the distinction between *in situ* carcinoma and papillary adenocarcinoma³³². It was later on called iatrogenic collapse, mentioned in the in chapter 5 presented study on the description of all kinds of *ex-vivo* artifacts in the lung and accepted for the first time in the 2021 WHO classification of lung cancer as "possible source of confusion in the setting of lepidic adenocarcinoma"^{19 371}.

Chapter 14 describes that maximal iatrogenic collapse in peripheral lung tissue is dependent of the epithelial lining thickness, being either the normal, near flat pneumocytes, somewhat larger reactive pneumocytes or tumor cells. We demonstrated that 12 alveolar wall cross sections fit in nearly complete iatrogenic collapsed normal lung parenchyma in a length of 200 μm , as opposed to 4-5 alveolar walls lined with tumor cells. The mathematical model provided arguments for folding of alveolar walls during iatrogenic collapse. This drastic change of normal underlying morphology is not present in any other organ of the body, and the reason that traditional 2-dimensional pattern recognition is without adjustments not applicable.

In hindsight, awareness of this phenomenon during microscopy is crucial for proper diagnosis. The orientation of collapsed alveolar walls is frequently parallel to the pleural surface. Besides that, tangential cutting of alveolar walls will be slightly misleading as the focal multilayering should be neglected. The folded alveolar walls have a regular

pattern. The use of a cytokeratin 7 staining can be of great help in recognizing the regular pattern, especially in collapsed AIS / lepidic adenocarcinoma. Paradoxically, the effect of iatrogenic collapse on pulmonary parenchyma is until today not taken into account by most pathologists across the globe. The expectation management is needed: the pathologist should realize that curved alveolar walls lined with a monolayer of tumor cells with a lepidic seemingly papillary or acinar pattern is a distinct manifestation of AIS, if no other characteristics of invasion are present.

Collapse at the cellular level

The consequence of iatrogenic collapse is pressure on tumor cells. We demonstrated an increased average tumor cell height in severe iatrogenic collapsed AIS areas compared to less iatrogenic collapsed areas. The shift of some cellular content towards the apical side is plausible and a new finding. Associations of cytoplasmic and nuclear flexibility were reported in other disease states, such as small cell lung carcinoma^{59 60}, large cell neuroendocrine carcinoma^{376 377 378}, atypical carcinoid³⁷⁸, typical carcinoid³⁷⁸ and basaloid squamous cell carcinoma³⁷⁹. A further extension of the cellular vulnerability is cytologically and histologically described as "smearing of the tumor cells", "nuclear streaking"³⁷⁶, "crush artifact"³⁷⁹, "Azzopardi phenomenon"³⁷⁷. The small size and the flexibility of the tumor cells and alveolar walls with the lack of desmoplastic stroma make that these tumors are difficult to palpate.

Collapse and tissue handling

The two cohorts in our studies differed in a practical aspect, namely fixation procedure of the resection specimen. Tumor nodules of Milan cohort were cut perpendicular to pleural surface in 1-2 cm slices to allow formalin diffusion, while in the OLVG cohort, the resection specimens were subject to formalin perfusion by filling the lung with as much formalin as possible, through the bronchial tree, using the pressure of a formalin tap or a syringe with formalin. If necessary, transpleural injection with a formalin filled syringe is added. After 12-24 hours subsequent perpendicular cuts are made¹⁹⁸. The different handling of specimens resulted in the following issues: i) more extensive iatrogenic collapse among Milan cases than in OLVG samples; ii) consequently higher difficulty in recognition of lepidic component and iii) more cases with delay in fixation as established by detached tumor cells. Nevertheless, in the selected samples the correlation coefficient obtained with Weibel's method was almost the same in both cohorts: (-0.44 and -0.42). This suggests that elongation and morphological alterations of the tumor cells occurring in iatrogenic collapse is significantly related to amount of air, but independent from the fixation procedure. In Japan perfusion fixation is present in the national guideline²⁸¹. It would be useful if other countries would adopt this approach too.

Collapse and diagnosis

The application of pattern recognition is the heart of pathology and is applied in all organs of the body. Pathologists are masters in pattern recognition.

The word collapse is mentioned in the 5th edition of the WHO classification of Thoracic Tumors¹⁹, but a distinction between iatrogenic and biological collapse is not made. The notion of iatrogenic collapse as a morphological artifact is not mentioned, but possible confusion of collapsed lepidic adenocarcinoma and AIS with acinar or papillary invasive patterns is recognized. More importantly, an explanation how to recognize collapsed AIS and how to differentiate it from invasive adenocarcinoma is lacking. The description of the papillary and acinar patterns in the WHO classification of pulmonary adenocarcinoma with by definition associated invasion overlaps with iatrogenic collapsed AIS. Not surprisingly, different pathologists may diagnose iatrogenic collapsed AIS, as lepidic adenocarcinoma, papillary⁹⁰, acinar adenocarcinoma or minimal invasive adenocarcinoma to the same case. Differentiation between lepidic and invasive patterns is crucial for a practical reason: for invasive size measurement according to the 8th Edition TNM UICC/AJCC of 2017¹⁹ for non-small cell lung cancer all invasive patterns should be incorporated, except the lepidic pattern³⁸⁰.

The categorization of non-mucinous adenocarcinoma subtypes and identification of invasive patterns are both prone to differences in interpretation among different observers. The clinical consequences are large as patients with some invasive subtypes have a worse prognosis³⁶⁸, while *in situ* carcinomas have a survival rate of 100% and patients with AIS do not require any further treatment following resection, because they are cured.

In 2012 a reproducibility study showed that one group of pathologists consistently judged a subset of adenocarcinomas to be invasive, while another group of pathologists consistently judged the same subset to be non-invasive¹⁴. This clearly points toward a necessity for calibration or re-evaluation of the diagnostic criteria. Thus far, this calibration did not evolve.

Recently, Yambayev and colleagues performed a local study with 2 pathologists in the same pulmonary adenocarcinoma domain, defining low malignant potential (LMP) subgroup with a better prognosis³³⁶. Their proposed criteria for LMP adenocarcinoma among non-mucinous adenocarcinoma were: a total size of ≤ 3 cm, exhibiting $\geq 15\%$ lepidic growth, and lacking predominant high-grade patterns ($\geq 10\%$ cribriform, $\geq 5\%$ micro-papillary, $\geq 5\%$ solid), >1 mitosis per 2mm², angiolymphatic or visceral pleural invasion, spread through air spaces or necrosis³³⁶. They largely followed the managerial process of the current WHO classification¹⁹ and selected for low proliferative tumors, but did not attempt to distinguish morphological invasion or not. In our study, a seemingly micropapillary pattern less than three adjacent alveoli is in our study not sufficient for assigning the micropapillary pattern and is not associated with a recurrence. It is likely that cases in our studies may represent the same subgroup as in the study of Yambayev and colleagues. For example, in their figure 1D, which was diagnosed as acinar predominant adenocarcinoma, we would diagnosis this as collapsed AIS, unless

the elastin stain shows otherwise. The Yambayev study provides more granularity in a classification that has proven low reproducibility¹⁴. The revised classification of chapters 14 and 15 is indebted to morphological principles.

In 2012 a reproducibility study showed that one group of pathologists consistently judged a subset of adenocarcinomas to be invasive (Invasive Group, ING), while another group of pathologists consistently judged the same subset to be non-invasive (non-ING)¹⁴. This clearly points toward a necessity for calibration or re-evaluation of the diagnostic criteria. Conceptually, either the ING or the non-ING has the correct diagnosis. If the ING interpretation is correct, then the non-ING are underdiagnosing invasive lung cancer. The non-ING pathologists should have perceived since 2012 a number of patients with recurrences (and in the US heavy juridical consequences). What is not known in the field of pulmonary pathologists. If the non-ING interpretation is correct, the ING pathologists are over-diagnosing *in-situ* lung cancer as invasive lung cancer. Noteworthy, is that pathologists from one country had a higher tendency to belong to the ING group.

Also, in other studies moderate interobserver agreement is found. Shih et al showed in an international panel of 3 pulmonary pathologists, who scored 60 cases of small adenocarcinomas in 3 rounds an interobserver agreement in small lung adenocarcinomas that fair to moderate with kappa scores of 0.44 or lower³¹. The results improved minimally with elastic stains. They concluded that poor agreement is primarily attributable to subjectivity in pattern recognition and that high-grade cytology increases agreement.

The IALSC Pathology Committee recently published that the reproducibility of invasion assessment is still 'suboptimal', with a proposal for improvement, involving morphologic features of invasion in pulmonary non-mucinous adenocarcinoma with lepidic growth, and the effects of collapse on morphology³⁷. Actually, high variation in invasion measurement is present in the group of pathologists that is frequently leading the changes in the WHO classification of pulmonary adenocarcinomas.

In chapter 15 we describe the largest pathology reproducibility study to date on the recognition of non-invasive patterns in lung adenocarcinoma. The new heatmap analysis supported the recognition of larger and smaller common invasive areas in several cases as well as variation in size and location of invasion in other areas (likely non-invasive areas). This study also revealed that pathologists feel the uncertainty in assignment of invasion and together score opposite categories with associated high variation.

Revised histological classification of pulmonary adenocarcinomas

For the diagnosis of iatrogenic collapsed AIS in our studies, presented in the chapters 13-15 several aspects differ from the 2021 WHO classification of pulmonary adenocarcinomas.

Tangential cutting

The extent of stratification needs to be analyzed to avoid inclusion of folds and tangential cutting as features of multilayering. Extensive multilayering is a characteristic of micropapillary pattern. As in AIS the histological section is a cross section of a three-dimensional lesion deformed by iatrogenic collapse, a monolayer may focally show cellular crowding that impresses as multilayering. This pseudostratification is frequently visible close to the top and bottom (angles) of the folds. In essence tangential cutting is present in focal area of the collapsed alveolar space, and not in the whole alveolar space. This focal multilayering should not be interpreted to be beyond a monolayer.

Minimum involvement

For a criterion to be associated with invasion, the underlying collapsed histology is used: i.e. the underlying functional histology of an acinus. A minimum of a few adjacent alveoli must contain the criterion throughout. This minimum approach is in line with the approach taken in other organs like breast diagnosis for lobular carcinoma *in situ*, whereby more than 50% of the acini in a terminal duct lobular unit must be filled and expanded by the neoplastic cells to qualify as lobular carcinoma *in situ*³³³.

Awareness that a focal artificial stratification in this context is not a sign of a highly proliferative tumor and raising the bar for invasion to more than one alveolar space completely filled with stratified cells may avoid overdiagnosis of iatrogenic collapsed AIS as invasive adenocarcinoma.

Regular pattern CK7

The regular pattern of iatrogenic collapsed AIS is easily observed in the CK7 staining. The CK7 positive borders respect the underlying architecture of secondary lobular septa, bronchovascular bundles with surrounding stroma and visceral pleura.

In collapsed AIS CK7 positive pneumocytes type II may also be clearly visible. The difference with tumor cells is easily observed in the accompanying H&E. These CK7 positive cells should not be interpreted as collapsed AIS or part of lepidic adenocarcinoma.

In search of a regular pattern the pathologist should not be immediately happy and diagnose collapsed AIS, as the catch to be missed is the presence of focal invasion. Any irregular area in the CK7 pattern the corresponding area in elastin and H&E stainings should be scrutinized for focal invasion.

Elastin

The original philosophy of WHO classifications that all diagnosis be made on H&E stain because of the worldwide applicability, has been abandoned: for the diagnosis of 'large cell neuroendocrine carcinoma' a positive neuroendocrine immunohistochemical marker is obligatory. The current study uses in the 2nd round morphological criteria derived in three different stains: beside the H&E also an elastin and a cytokeratin 7 stain. This provides crucial additional morphological information, allowing separation

of the overlapping patterns and non-invasive growth on alveolar walls and markedly reduces the variation in assignment of invasion. As the elastin staining is also used as an aid in the assessment of pleural invasion, and CK7 in most laboratories part of the immunohistochemical armamentarium, the using these stainings to support the morphological diagnosis of pulmonary adenocarcinoma *in situ* should not have technical barriers and therefore be easily applicable in routine practice. Technically, for an optimal result, it is important to refresh the Lawson component of the staining at least every 3 weeks, while the von Gieson component should be refreshed every 4 weeks.

A thin wall or relatively thin wall that has at least a clear fragment of elastin is based on morphological reasons part of a pre-existing alveolar wall. The elastin fibers are best recognized at high power microscope objective (40x). As mentioned above elastin is produced by mesenchymal cells and NOT by tumor cells. If the differential diagnosis on H&E stain is between papillary carcinoma and iatrogenic collapsed AIS. The presence of (discontinuous) elastin fibers in a tumor with fibrovascular cores lined by tumor cells denotes the fibrovascular core as a 2-dimensional cross cut of alveolar wall. Without other invasion characteristics the diagnosis is than (iatrogenic collapsed) AIS. Likewise, if a pathologist doubts about a collapsed AIS/ lepidic adenocarcinoma and acinar carcinoma the characteristic findings of continuous or fragmented elastin in the structures lined with tumor cells should suffice to diagnose that area as collapsed AIS/ lepidic adenocarcinoma.

The papillary carcinoma is in the revised classification defined as a papillary tumor without elastin. This definition seems In larger tumors (> 3cm.) to match perfectly with those described in the original work of Silver and Askin¹¹. Probably the in this way defined papillary carcinomas have a similar worse prognosis, as described by Silver and Askin.

Table 1 shows the relationship between those 3-dimensional *in vivo* structures and the 2-dimensional microscopic view the pathologist uses.

Awareness of the cross-sectional appearance of so called "papilla" is important, as this structure has the connotation of invasion according to the WHO classification of pulmonary adenocarcinomas. Realizing that if a so-called "papilla" would be part of a papillary tumor with several papillae, then there must be more oval cross sections than longitudinal appearances. If that is not the case, the likely interpretation is that the seemingly papillary structure is part of a pre-existing alveolar surface structure in the third dimension (see Table 1 and Figure 1). This is a clear example that 2-dimensional pattern recognition as applied in the WHO classification of pulmonary adenocarcinomas is dissociated from the 3-dimensional pulmonary morphology.

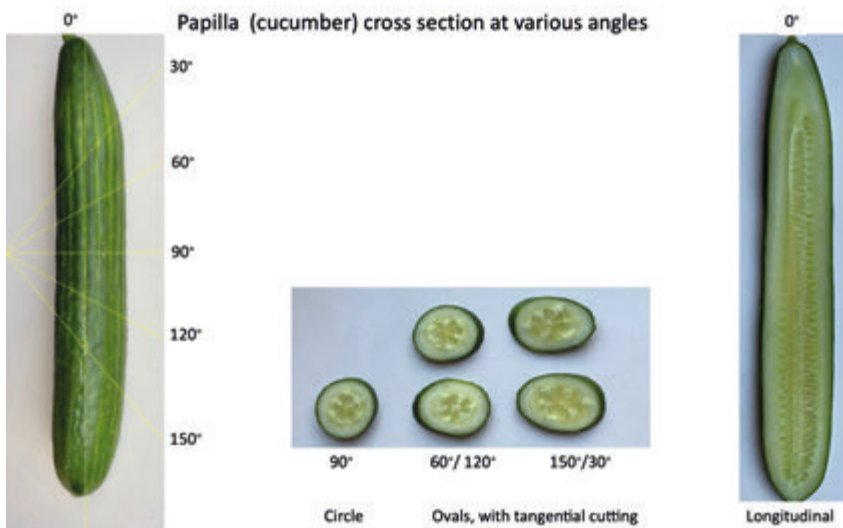
- **Table 1.** Relation between morphologic structures and representation in microscopy (2-dimensional cross section). With unaltered morphology the measurements in microscopy are proportional with the third dimensional measurements, while with altered morphology such as in the lung the surface measurements are disproportional³²¹.

3- dimensional structure		2-dimensional cross section		Stereological relation in vivo	
	Unit		Unit	Other organ ^{*)}	Lung ^{#)}
Alveolar volume	μm^3	Air surface	μm^2	Proportional	Disprop.
Alveolar wall surface	μm^2	Alveolar line / perimeter	μm	Proportional	Proportional
Blood vessel volume	μm^3	Luminal surface	μm^2	Proportional	Disprop.
Blood vessel wall (surface)	μm^2	Inner (endothelial)/ outer (adventitial) perimeter	μm	Proportional	Proportional
Basement membrane surface	μm^2	Basement membrane line	μm	Proportional	Proportional
Elastin fiber	μm	Elastin fragments (dot)		Proportional	Proportional

*) Organs or disease states where the morphology is not altered during the sampling procedure. Here the value of the measured characteristics in the two-dimensional microscopy are proportional to the values in the third dimension.

#) In the periphery of the lung the structure of the underlying morphology is drastically altered during surgery. The amount of air in alveoli and blood and lymph fluid is reduced during iatrogenic collapse. Moreover, the smaller volume requires a smaller surface. Therefore, a relative excess of surface will lead to adaptation. The alveolar basement membrane surface lined with epithelial cells will not reduce during the few minutes of iatrogenic collapse. This will lead to folding of the alveolar wall. The surface measurements in microscopy are not proportional to the volume of the *in vivo* situation, while the measurements of lines will remain proportional to surface in the third dimension.

Disprop. = disproportional



- **Figure 1.** Photographs of a cucumber (papillary) structure taken at various angles. Note i) that if a papillary structure is randomly cut, the chance of observing an oval cross section is much higher than of a longitudinal cut. Note ii) that when in a histological slide a seemingly papillary structure is observed without corresponding oval cross sections, the correct interpretation with respect to the 3-dimensional structure is that the seemingly papillary structure represents a cross section through a structure with a surface (e.g., cross section through alveolar wall). Note iii) that the short axis is the same in all cross sections, while the long axis differs. The short axis is representative of the biology. Note iv) in serial sections the seemingly papillary structure can be continuously followed, as opposed to a true papilla, what disappears in serial sections¹²⁰.

Important is the recognition of desmoplastic stroma in pulmonary adenocarcinomas, what is almost invariably accompanied by isolated or small clusters of tumor cells. Look also at the CK7 staining to confirm the tumor cells in the corresponding area. Desmoplastic stroma may occur not in a pre-existing pulmonary architecture. The elastin staining may show several fragments or continuous lines of elastin, but this should not lead to a non-invasive interpretation as, the desmoplasia trumps the decision in favor of invasive adenocarcinoma.

We established stricter histomorphological criteria for most of the surrogate markers of invasion in non-mucinous adenocarcinomas. These have a form of “alveolar filling growth” in the pre-existing alveolar space. If the lumen is almost completely filled such as in cribriform and solid growth, there will not be remaining air. Consequently, this part of the lung is not able to collapse during surgery. For the other alveolar filling growth patterns, the possible iatrogenic collapse will be related to the amount of remaining air.

Grey zone

As the aim of chapter 13 was to separate patients with definite AIS from clear invasive adenocarcinomas, we defined the AIS as a monolayer and included the tangential cutting effect. However, between the minimum criteria for clear invasive adenocarcinomas and the in this way defined AIS, some adenocarcinomas fall in between. This was called the grey zone. In a recent pathology panel a slightly different approach was followed and the “in between” zone was called “extensive epithelial proliferation”³¹⁷. In the chapters 13 and 14 studies it turned out that “grey” zone was scored in a minority of the cases by some pathologists. In none of the cases the score was 100% grey zone. In contrast, the diagnosis of AIS was favored by the majority of the pathologists in more than 10 cases. Thus, from the two factors described in the IASLC pathology panel paper the recognition of collapsed AIS is more important than the extensive epithelial proliferation or grey zone. The question whether the ‘grey zone’ category will be associated with a 100% 5 years disease free survival or not, is a matter of future studies.

Application of the revised criteria according to the WHO classification has a poor kappa score, also reflected in high variation in ‘consensus percentage’, and high average uncertainty score for the invasion decision. With the revised classification an essential increase in kappa score is possible. for the application of invasiveness in pulmonary adenocarcinomas, established by pathologists covering three major regions in the world. The one-hour training for the revised classification between 1st and 2nd reading focused on recognition of iatrogenic collapsed AIS. In hindsight it is questionable if the content was broad enough. Probably more training including awareness of biological collapse, and emphasis on searching for focal irregularities in the CK7 will lead to a higher agreement than 0.45 obtained in the 2nd round as the kappa score of the ‘coached’ 3rd round was 0.62.

It is likely that the revised diagnostic approach leads to i) a higher fraction of AIS in resected pulmonary adenocarcinomas; ii) in lepidic adenocarcinomas larger non-invasive areas; iii) reduction of number of papillary carcinomas; iv) association of true papillary carcinoma with a worse prognosis; v) reduction of the number of acinar adenocarcinomas and vi) modification of the prognostic associations for papillary and acinar subtypes.

The prevalence of AIS in our cohorts was high with 10 out of 70 resections (14.2%). This is higher than previously reported incidences of AIS in NSCLC (5-8%)³⁸¹ and in the same range as the 16% reported in the adenocarcinoma with low malignant potential study³³⁶, but also as in other series of AIS⁷.

History of WHO classification with a hindsight view

In the 1999 WHO classification the papillary pattern was defined by expert opinion as papillae with secondary and tertiary papillary structures that replace the underlying architecture³². Although this terminology looks like the terminology used in the original manuscript describing papillary carcinoma¹¹, the actual morphologic connotation of “fibroplasia of the papillary fronds or scarring of the supporting stroma (“stromal

invasion”) with associated distortion or destruction of the underlying pulmonary architecture” described in 1997 by Silver and Askin was not incorporated. These descriptions are clearly associated with invasion. However, leaving the fibroplasia out of the definition for 1999 WHO classification turned out to be a catch 22. In hindsight, iatrogenic collapsed AIS also fitted within the description of papillary carcinoma in the 1999 WHO classification and subsequent managerial classifications, the possibility of overdiagnosis as papillary carcinoma (and by definition invasive carcinoma) was created. Aida et al. underscored in 2004 the poor prognosis of papillary carcinoma according to Silver and Askin too and concluded in their paper that the combination of WHO and Silver and Askin criteria (WHO-SA) should be used for prognostic correlation³⁸². However, 10 years after the modified 1999 WHO classification of pulmonary adenocarcinomas the original worse prognosis of papillary carcinoma⁶ turned to become a favorable prognosis in ^{381 383 310 384}. To understand this prognostic reversal, the distinction between papillary adenocarcinoma and papillary mimics, as described above and in chapter 12 is very important.

In the managerial classification of 2012 a new category of “minimally invasive adenocarcinoma”¹³ was described. It is worth highlighting that the aforementioned category was not initially recognized in the seminal paper by Noguchi and colleagues, which described adenocarcinoma in-situ and employed stricter invasion criteria¹⁰. During the 1999-2010 interval, cases with collapsed AIS or biological collapse were likely overdiagnosed as lepidic invasive adenocarcinoma.

Nowadays, pathologists feel that when they use the current WHO classification of pulmonary adenocarcinomas for the assessment of invasion, that they are conscious incompetent. In hindsight 24 years after the 1999 WHO classification the experts of 1999 were probably unconscious incompetent, when they modified the definition of papillary carcinoma.

STAS also was introduced as expert opinion in the WHO classification, while in the preparing sessions only half of the pathologists supported the concept. The effect of the incorporation in the WHO resulted in a tsunami on STAS papers. The process of selection and incorporating of various opinions the WHO classification of pulmonary adenocarcinomas leaves room for improvement.

Currently, the criteria for a modification in the WHO classification are more scientifically defined. There have to be at least two independent peer reviewed studies performing a properly designed case control study with good statistics. The study in chapter 15 is comparing tumors according to the WHO (control) and to a revised classification (case) with statistically estimated sample size before the start of the study. The reduction of variation in and increase in ‘consensus percentage’ as well as the increase in kappa scores from the control (WHO classification 2021; 0.27) compared to case (Revised classification; 0.45-0.62) is the first study at that shines light on the horizon of invasion assessment in pulmonary adenocarcinomas. Despite their current uncertainty, pathologists will become proficient in identifying invasion in pulmonary

adenocarcinomas due to the morphological adjustments in the revised classification. However, there is a clear requirement for additional independent studies on the matter.

Collapsed AIS, and survival

In chapter 13 we described a pilot study to examine the recognition of surgical collapsed AIS with a possible supportive role of CK7 and correlated this to prognosis³²⁰. This pilot study showed that cases reclassified as AIS based on a regular CK7 pattern and the presence of elastin fibers in pre-existing alveolar walls as aids to recognize collapsed AIS, did prevail a 100% recurrence free survival. Subsequently, this study was extended in chapter 14 and confirmed that cases diagnosed as (collapsed) AIS maintain the 100% recurrence free survival. The number of AIS cases in chapter 13 was 7 out of 40 tumors (17.5%), in the same range as the 10 out of 70 cases (14.3%) in chapter 14.

An interesting aspect in the follow-up of lung cancer patients, and therefore also in patients diagnosed with AIS, is the development of a separate primary lung cancer (SPLC) or that of an intrapulmonary metastasis (IPM). The incidence in cases of AIS seems low. Yotsukura et al found in 5.6% of 207 AIS cases an SPLC in the follow-up³¹⁵. Interestingly is the distinction from IPM's, especially in invasive cases. Chang et al used comprehensive next-generation sequencing (NGS) to reliably separate one from the other³⁸⁵. In four cases with a 5-30% lepidic component, an IPM was also discovered, which came as a surprise. However, it's worth noting that these cases were not predominantly lepidic. The argument put forth was that a lepidic component doesn't necessarily indicate that the tumor began as an *in situ* lesion. Instead, the lepidic pattern could be the result of alveolar surface colonization by an invasive tumor that's expanding. Similar cases have been reported where lung metastases from other organs, such as primary pancreas carcinoma, exhibit a lepidic growth pattern²⁴². Even cases with lung metastasis of a malignant melanoma with a lepidic growth pattern have been reported³⁸⁶.

Collapse and patient consequences

The mathematical model presented here, can help to understand iatrogenic collapse and facilitate the diagnostic approach to collapsed AIS. In pulmonary adenocarcinomas this is essential in order not to overestimate AIS as invasive adenocarcinoma, as therapeutic consequences are obviously divergent. Moreover, the message towards the patient is essentially different: being cured of an *in situ* cancer or hoping for the absence of a recurrence in the future with an invasive carcinoma with inherent uncertain feelings.

False negative diagnoses are the most clinically important category: they represent cases which go under-treated and might, if an area of invasive growth is missed, not receive possibly curative adjuvant therapy. Consequences of false negative cases are large for individual pathologists in the USA, as pathologists cannot afford the costs after being juridically sued for a missed diagnosis of malignancy. This explains a more defensive judgment of possible non-invasive cases and is a known phenomenon among

for instance, dermatopathologist in diagnosing melanocytic lesions³⁸⁷, among breast pathologists³⁸⁸ and in diagnosing thyroid lesions³⁸⁹.

Patients whose diagnosis of invasive adenocarcinoma is a false positive and whose tumor size is less than 3cm won't be administered adjuvant treatment. On the other hand, patients with larger AIS lesions that are mistakenly diagnosed as invasive adenocarcinoma could be subjected to unnecessary adjuvant therapy, and therefore to overtreatment.

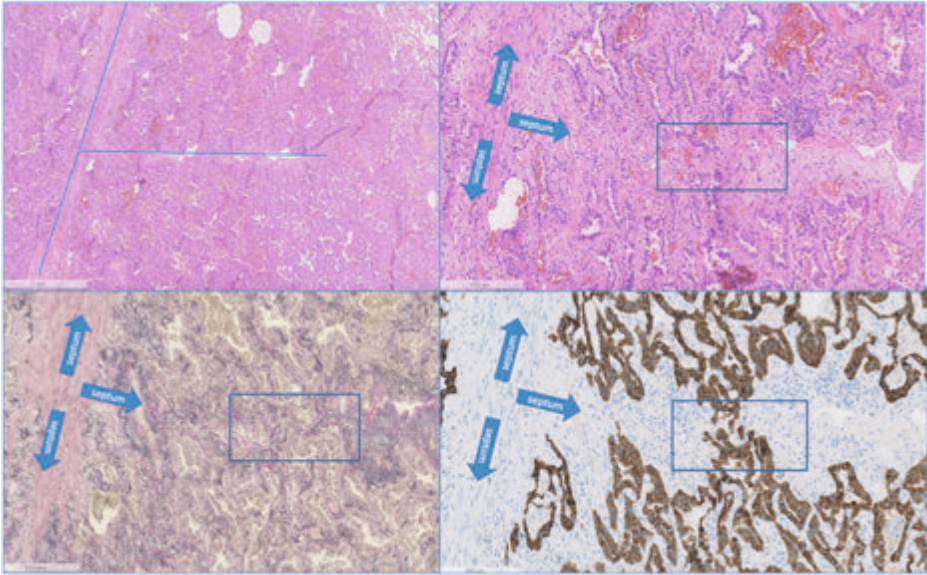
The IASLC Pathology Committee suggests in their paper on defining invasive patterns³¹⁷, that "in case of doubt whether an area should be designated as invasive or noninvasive, most of the group decided in favor of upgrading". In contrast, our study and the study of Boland and colleagues 2016 suggest that downgrading can in this situation reliably be performed. Visca et al commented in an editorial on the upgrading statement in the recent manuscript of the pathology panel of IASLC³⁹⁰, that 'upgrading' is not in line with the TNM's usual approach, which suggests in doubtful cases to downstage lesions instead of upstaging them"¹⁸².

It's probable that AIS is frequently misdiagnosed as invasive adenocarcinoma in routine clinical practice, which is supported by an upsurge in invasive adenocarcinomas detected at lower stages. According to Ganti et al.'s analysis of the US Cancer Statistics database, the incidence of stage I NSCLC rose from 10.8 to 13.2 per 100,000 between 2010 and 2017³⁹¹. In other organs where an *in-situ* category has been recognized a relative survival of 100% is reported in the Netherlands³⁹². In the USA the tendency of overdiagnosis in early stage cancer exists, as the relative survival exceeds 100% (greater longevity compared to an equivalent group from the general population)³⁹³. This favors the premise that these early-stage cancers, which presumably lack metastatic potential and have limited lethal consequences, are generally detected incidentally or via screening in individuals who are otherwise healthier or health-conscious than their counterparts in the general population³⁹⁴. For lung adenocarcinoma *in-situ* these data are not available and probably hidden in the early-stage invasive carcinomas³⁹⁵. This is due to the pattern-recognition approach as opposed to the morphology approach in the revised classification.

Histological detail

All the studies before 1971 about histology (also called microanatomy) of the pulmonary parenchyma have been summarized by a group of Japanese scientists³⁹⁶. Interestingly, the knowledge development of the secondary pulmonary lobule was obtained in lungs of coalminers, where the pigmented macrophages were aligned in the lobular septa and because of the high number of macrophages, this was macroscopically visible, similar to smoker's lungs. The ventilation function of the lung (flow of outside air in and out of the alveolus) has an escape mechanism for focal differences in air pressure. To this end, at the alveolar level the pores of Kohn allow air passage between alveoli. A relatively recent schematic drawing of the lobular architecture shows that the edge of the secondary lobule is a continuous line. In one of the pulmonary adenocarcinomas

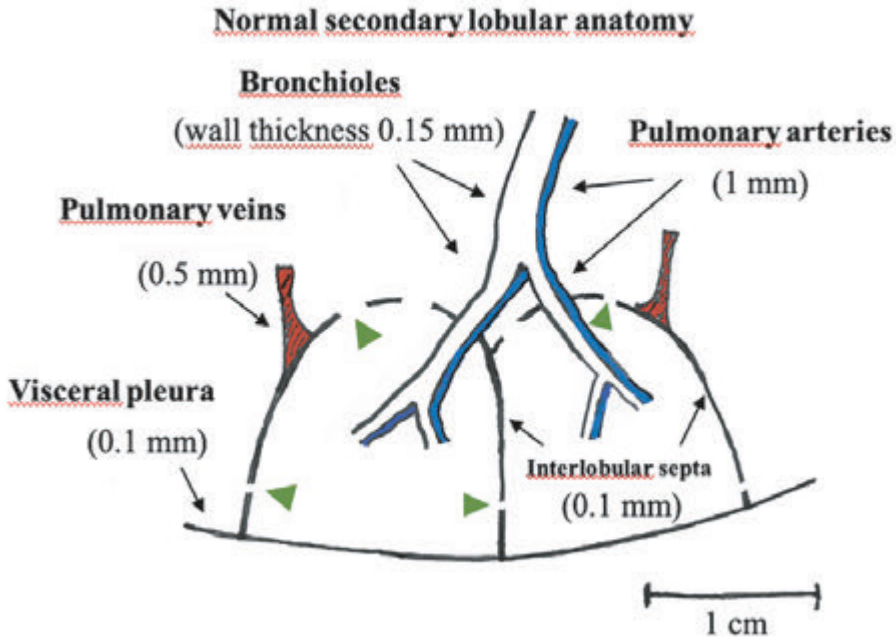
in situ slides we found an alveolar connection between adjacent secondary lobules in H&E staining supported by the elastin fibers in the elastin staining (see Figure 2 and 3)



- **Figure 2.** Upper left and right: hematoxylin & eosin-stained section from adenocarcinoma growing on alveolar walls, monolayer of tumor cells. T-junction of septa is present (blue lines and arrows). Note 'crossing over' of AIS at the septum (blue square).

Lower left and right: same areas as above, showing elastin fibers in all preexisting alveolar septa (left) and in cytokeratin 7 staining the monolayer of tumor cells along the alveolar septa in a regular pattern and crossing over at a small 'hole' in the alveolar septum (blue square).

The function of the alveolar connections in the septa is probably similar as that in the pores of Kohn and might be related to an overflow "pressure relief" function.



- **Figure 3.** Schematic drawing of normal secondary lobular anatomy of the lung. The bronchiole is accompanied by the pulmonary artery (blue). The veins (red) are located in lobular septa. Note the small holes focally in the septa (green arrow head). Note: I) In AIS the tumor cells respect the pre-existing structures and II) Tumor cells may cross the interlobular septa through focal alveolar connections (green arrow head) III) The secondary alveolar lobules have greater and bigger connections with neighboring lobules at their central part.

AIS and size

Finally, AIS has been defined as a non-invasive adenocarcinoma of a diameter of 3 cm or less. In chapter 16 we describe 4 cases with tumors of diameters larger than 7 cm, even much larger, up to 18 cm, that showed on histology a pure, non-invasive lepidic pattern similar to Noguchi type A¹⁰. In addition, we examined in one patient practically the whole lobe with over 300 formalin fixed paraffin embedded blocks and could beside the Noguchi type A pattern not find an invasive focus, rendering an underdiagnosis of AIS due to sampling highly unlikely. Incidental cases with AIS larger 3 cm have also been described. Therefore, we propose that the upper limit of 3 cm for non-invasive non-mucinous adenocarcinoma can be omitted.

Limitations of the studies in this thesis

A disadvantage of the current studies is that most of them were performed in a retrospective way. Furthermore, verifying the hypotheses with the iatrogenic collapsed

AIS with 100% 5-year disease free survival may be limited in two ways. On the one hand resected non-mucinous adenocarcinomas may lead to cure. The presence of invasive characteristics without metastases is not excluded by the disease-free survival rate.

In any managerial classification, thus also the revised adenocarcinomas classification, will have cases that do not fit into the designed categories. Although no system will ever be perfect, a possible improvement in the kappa score from poor reproducibility (0.27) according to the WHO to 0.62 for the revised classification is a major stimulus for further exploration. Borderline cases will always exist and downgrading seems an appropriate approach, also with the Hippocratic oath in mind: "*primum non nocere*" ("first, do no harm")

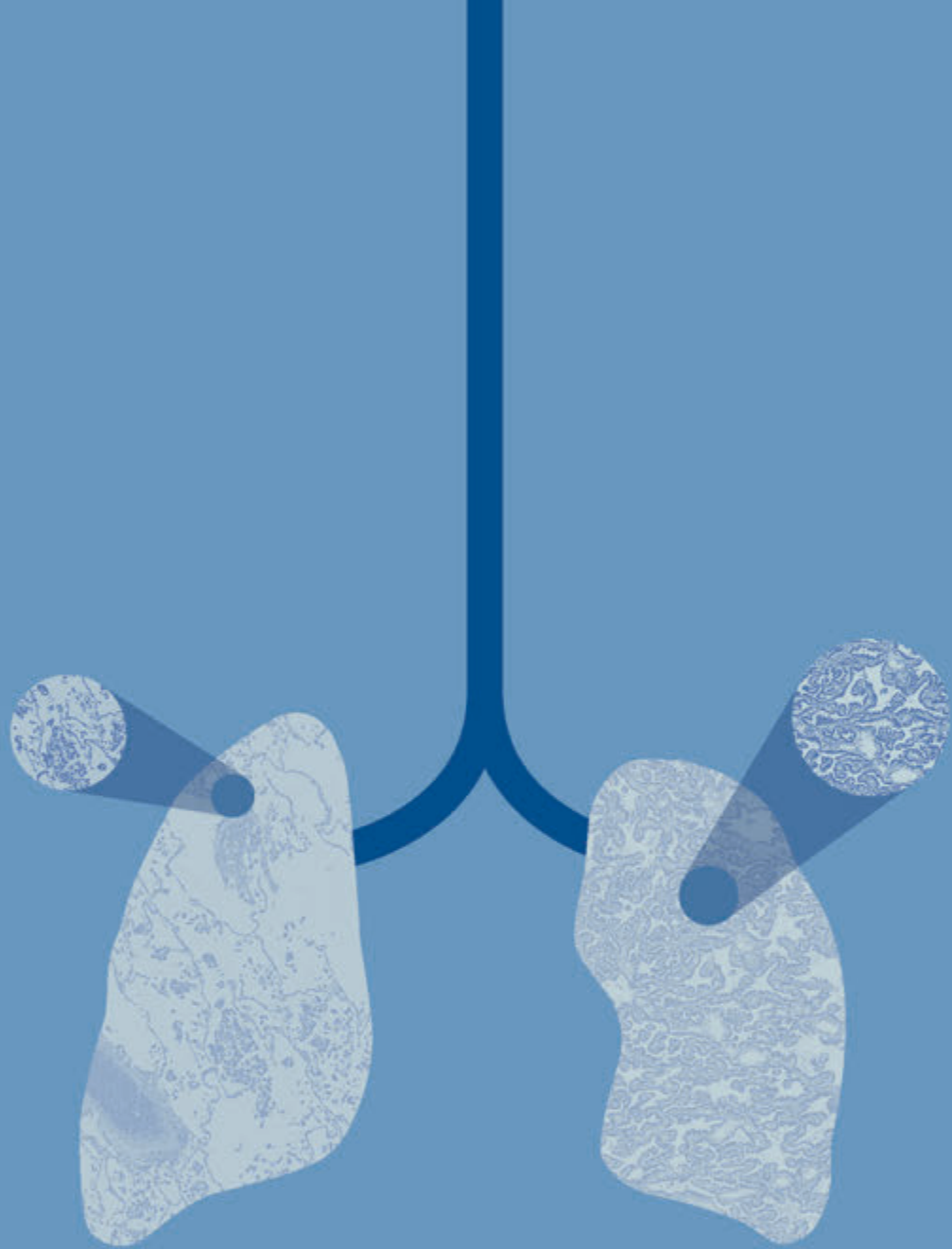
Suggestions for future studies

As two independent studies (the reproducibility study in chapter 15 and the study of the pathology panel of the IASLC³¹⁷) the data show that for the assessment of invasion the pathologists when using the WHO classification in terms of the Dunning-Kruger effect are consciously incompetent³³⁹.

Artificial intelligence is a topic of many studies today. A future analysis of the cases of chapter 14 with an unsupervised AI approach is interesting³⁶⁴. The dream of AI is creating the hope for the ideal solution. In a study of the previous century AI was applied in the differential diagnosis between small cell lung cancer and NSCLC³⁹⁷, what is a problem area in only 5%. To this end the tumor cell nuclei were digitized with scanning stage microscope (resolution 0.42 micron). AI decreased the fraction of problem cases by 50%. In other words, AI may be supportive in reduction of this problem area, but not a perfect solution: drawing lines in a biological system will always have boundary cases. Although expectations may be high, the AI researchers presenting at the last USCAP were modest. Time will tell.

Conclusions

Basic histopathology remains a critical aspect of diagnosing and treating lung cancer. Evaluating the extent of pathologic response in resected specimens after neoadjuvant therapy can be immensely valuable in predicting prognosis. Removing "Spread through air spaces" (STAS) from the WHO classification could potentially alleviate some of the confusion surrounding it since its assumptions of invasion are unproven and we believe it to be an artifact. Identifying a collapsed adenocarcinoma in situ pattern with the help of additional cytokeratin 7 and elastin staining can improve the classification and staging of resected non-mucinous adenocarcinomas. Providing further training on the proposed revised classification may prove advantageous for patients with pulmonary adenocarcinomas worldwide.



Appendices

Supplementary files

References

Summary

Nederlandse samenvatting

List of publications

Dankwoord

Curriculum Vitae

CRedit author statements

Chapter 14

■ Standard Operating Procedure Elastica van Gieson staining (dept. of Pathology, VUmc).

V. Elastica van Gieson: histologische kleuring - analyse pathologie (Versie 12)

1 TITEL
Elastica van Gieson

2 TOEPASSINGSGEBIED / APPLICATIEBEPERKING
De document omschrijft een methode voor het aanbrengen van elastinevezels en bindweefsel.

3 PRINCIPLE
De Leucosin is een modifieerder van de kleuring volgens Hingst met respectie tot elastine. Het fuchsine is verantwoordelijk voor de kleur van het connectief, met name voor de binding met chondrocyten, vóór de kleuring met de elastische vezels met Leucosin oplossing (blauwzwarte/paris blauw) worden de vezels gekleurd met methyleenblauw volgens Mayer.

4 VERANTWOORDELIJKHEID EN BEVOEGDHEDEN
De de lijst "Taken, Bevoegdheden en Verantwoordelijkheden".

5 VEILIGHEID EN MILIEU

Algemeen

- Gedetailleerde informatie vindt u handboeken en indien van toepassing een veiligheidskaart.
- Maak bij een incidentoplossing of overleg met de bevoegde van (zijn) origineel medisch.
- Bij storingen/incidenten/vervalsingen spreken met een voldoende water.
- Bij aanwezigheid van stoffen in goed gevulde ruimte brengen en eventueel een afzuigkap.
- Afvalsoort hangt af van de individuele chemische beschrijving.

Werkplek
De kleuring wordt uitgevoerd in de zaal. Alleen de de afzuigkap te gebruiken of handmatig in de zaal.

Chemicaliën

- Gedetailleerde informatie over chemicaliën inclusief handelingen bij incidenten zijn terug te vinden op de MSD of via de handleidingen van de leverancier. Informatie chemische stoffen. Gebruik voor het opzetten van de kleuring, inclusief beschrijving van het CAS-nummer.
- Brandgevaar en brandwondgevaar stoffen verwijderen houden van warmte, hete oppervlakken, vlammen, open vuur en andere ontstekingsbronnen. Niet roken.
- Bij onopzettelijke contact met de ogen: spoelen met ruim voldoende water. Bij contact in de ogen: contactlenzen verwijderen. Bij aanwezigheid van stoffen in goed gevulde ruimte brengen. Afspoelen met afzuigkap (aan). Afvalsoort hangt af van de individuele chemische beschrijving.

Ethanol, is een ontstekings-, carcinogeen en reproductische vloeistof. Bij incidenten niet laten inademen.

Xyleen, is een ontstekings-, schadelijk, en reproductische vloeistof. Bij incidenten niet laten inademen.

Hematoxyline volgens Mayer, is een ontstekings- en reproductische vloeistof.

Leucosin-oplossing is een brandbaar, giftig, corrosieve vloeistof.

Van Gieson-oplossing, bevindt zich in een fles, opslag, opname door de mond en aanraking met de huid.

Verzadigde waterige fuchsine-oplossing, giftig bij inademing, opname door de mond en aanraking met de huid.

Formosol, giftig, in drager vloeistof oplosbaar. Vóór het meten van een hoeveelheid orgaanweefsel. Giftig bij inademing, opname door de mond en aanraking met de huid.

Zure fuchsine, is een, schadelijk stof. Vermijd aanraking met ogen en huid, met stoffen.

- Van Gieson-oplossing: 75 ml Zure Fuchsine 1%.
- 1 fles verzadigde waterige fuchsine-oplossing [\(zie hier voor details\)](#). Deze oplossing is niet per te gebruiken.
- Xyleen (alcoholoplossing).

7 APPARATUUR EN HULPMIDDELEN

Apparatuur
Apparatuur
Afbreuk
Verwijder

8 WERKWIJZE

Kleuring m.b.v. kleurmachine

De kleurmachine, agitatie en het afsluiten van het apparaat zijn vooraf ingesteld (zie hetgeen H170227). Controleer of de kleurmachine is in de kleurmachine opgenomen en de kleuring is afgevoerd. Controleer of de kleurmachine, standaard op de kleuring, plaats is de afzuigkap.

1. Hang de reagentia met paraffinecoupes, vooraf vervoerd of afgevoerd, in het apparaat. De reagentia worden vervolgens automatisch gemiddeld.
2. Het afsluiten van het apparaat is automatisch ingesteld.
3. Het afsluiten van het apparaat is automatisch ingesteld.
4. Indien de coupes moeten worden gereinigd [\(zie hier voor details\)](#), de coupes na het drogen worden samen drogen en vervolgens in de kleurmachine worden kleuren.

De reagentia worden in het kleurmachine opgenomen, zoals in het tekening H170227 staat vermeld.

Belangrijk bedieningsvoorschrift kleurmachine H170227:

* Keer starten:
• Druk op Start.
• Controleer of het juiste kleuringprogramma is geselecteerd en pas de instellingen aan.
• Houd de knoppen op het display open: de knop van het kleur gebied en plaats het veld in het veld 01, 02 of 03.
• Druk op Start.

Een volgende keer starten:

- Druk op Start.
- Controleer of het juiste kleuringprogramma is geselecteerd en pas de instellingen aan.
- Houd de knoppen op het display open: de knop van het kleur gebied en plaats het veld in het veld 01, 02 of 03.
- Druk op Start.

Einde van programma

- Open de kleurmachine deuren om het afsluiten van.
- Maak de reagentia af, en pas de de kleuring op de kleurmachine.

Voorschrift handmatig kleuren van paraffinecoupes

Na de Van Gieson-oplossing hangt er niet in water geplaatst worden omdat dit invloed heeft op de kleuring.

1.	Deparaffineer en hydrateer de coupes tot en met alcohol 70% (zie hier voor details) .
2.	Dehydratieer indien nodig (zie hier voor details) .

Afval
Niet chemische afval in de daarvoor bestemde afval afvoeren verontreinigd met afval van de kleuring. Verzadigde waterige fuchsine-oplossing, de wordt in een niet afval afvoeren. De handboeken raadplegen voor de afvalsoorten.

9 REAGENTIA, STANDAARDEN EN CONTROLES

Reagentia

Chemicaliënlijst voor het kleuren					
Naam	CAS nr.	Chem.	Formule	Code	Plaats
Formosol	88-1	Chem.	C ₁₂ H ₁₀ O ₄	P-001	Volgend op de MSD
Zure Fuchsine 1%	528-9	Chem.	C ₂₀ H ₁₂ N ₄ O ₆ S ₂	P-004	Volgend op de MSD
Leucosin-oplossing	-	-	-	S-004	Volgend op de MSD
Hematoxyline volgens Mayer	-	-	-	H-014	Volgend op de MSD
Ethanol	64-17-5	Chem.	C ₂ H ₆ O	S-001	Volgend op de MSD
Xyleen	112-95-9	Chem.	C ₈ H ₁₀	S-001	Volgend op de MSD

Chemicaliënlijst voor het kleuren					
Naam	CAS nr.	Chem.	Formule	Code	Plaats
Verzadigde waterige fuchsine-oplossing	-	-	-	P-004	Volgend op de MSD
Zure Fuchsine 1%	528-9	Chem.	C ₂₀ H ₁₂ N ₄ O ₆ S ₂	P-004	Volgend op de MSD
Van Gieson-oplossing	-	-	-	V-004	Volgend op de MSD
Ethanol 70-90%	64-17-5	Chem.	C ₂ H ₆ O	-	Reagentia op de MSD

Reagensbereiding

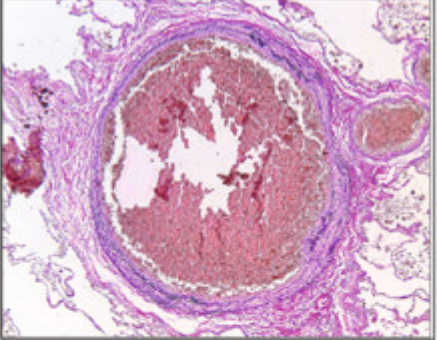
- Leucosin-oplossing is kant en klaar verkrijgbaar. Deze oplossing is te gebruiken tot op de fles, ongeopend bewaren.
- Ethanol 70-90% is kant en klaar verkrijgbaar.
- Zure Fuchsine 1%: 1 g Zure Fuchsine, 100 ml water. Deze oplossing is niet per te gebruiken.
- Verzadigde waterige fuchsine-oplossing: 12 g fuchsine, 1 l water. Deze oplossing is niet per te gebruiken.

3.	Plaats de coupes in Leucosin-oplossing	60 min
4.	Differentieel de coupes in Ethanol 70-90%	3 sec
5.	Differentieel de coupes in Ethanol 70-90%	3 sec
6.	Spoel in leidingwater	-
7.	Plaats de coupes in Hematoxyline volgens Mayer	5 min
8.	Spoel in leidingwater	5 min
9.	Plaats de coupes in Van Gieson-oplossing	5 min
10.	Koel spoelen in Ethanol 100%	-
11.	Koel spoelen in Ethanol 100%	-
12.	Spoel in xyleen	-
13.	Geef de coupes # (zie hier voor details)	-

9 VERWERKING RESULTATEN



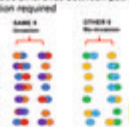
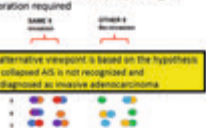
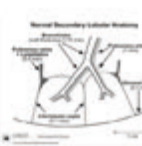
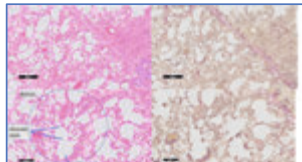
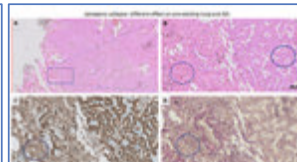
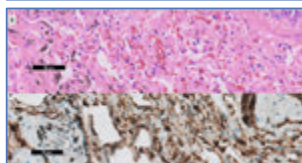



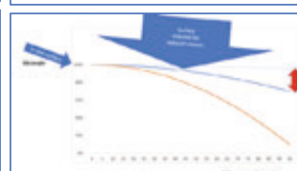
Beoogde resultaat
Elastinevezels: blauw-zwart / zwart
Kern: blauw
Collageen bindweefsel: rood
Opmerking: geen

- Standard Operating Procedure Elastica van Gieson staining (dept. of Pathology, VUmc). (continued)

 <p>Registratie Het resultaat van de kleuring wordt door de assistent patholoog beschreven en getypt. De gekleurde coupes, samen met nummer en kleuringsoede op het juiste deel van de afgedrukte, worden opgeslagen in het computerbestand bij het patiëntencomputerbestand.</p> <p>10 KWALITEITSBEWAKING</p> <p>Controle Bij elke kleuring dient altijd een positieve controlecoupe afgedrukt te worden (megekleurd), waarin het aan te nemen materiaal zeker aanwezig is. De controle coupe wordt getypt in document: Elastica van Gieson in combinatie van de controle coupes, Elastica van Gieson in combinatie van de controle coupes.</p> <p>Acties bij calamiteiten Bij hulp over het resultaat kunnen coupes samen met een eroperv collage of de aanrager worden besproken. Bij een afwijkende controlecoupe wordt het resultaat in het ingboek geïnterpreteerd. Diagnostische coupes worden, indien nodig, herkleurd. Bij structurele afwijkingen wordt het besproken in een technische overleg.</p> <p>11 OPMERKINGEN N.v.t.</p>	<p>12 DEFINITIES EN AFKORTINGEN E.V.G. Elastica van Gieson</p> <p>13 VERWIJZINGEN</p> <p>Literatuur Bancroft, J.D. (1975). Histopathological Techniques and their Diagnostic Uses, 10: 30-47.</p> <p>Verwijzing documenten Elastica van Gieson in combinatie van de controle coupes Elastica van Gieson in combinatie van de controle coupes (ID: 102165) Elastica van Gieson in combinatie van de controle coupes (ID: 102165) Elastica van Gieson in combinatie van de controle coupes (ID: 102165) Elastica van Gieson in combinatie van de controle coupes (ID: 102165) Elastica van Gieson in combinatie van de controle coupes (ID: 102165) Elastica van Gieson in combinatie van de controle coupes (ID: 102165) Elastica van Gieson in combinatie van de controle coupes (ID: 102165) Elastica van Gieson in combinatie van de controle coupes (ID: 102165)</p>
---	---

Chapter 15

■ Slides of the tutorial after round 1

<p>INVASION OR NOT ALTERNATIVE VIEW</p>	<p>Introduction</p>	<p>Reproducibility of histomorphological outcomes and variation in pathologist assessments: An international interobserver study</p> 																																																																																																																																																																																																																																																															
<table border="1"> <thead> <tr> <th>Observer</th> <th>Agree</th> <th>Disagree</th> <th>Agree by 10%</th> <th>Disagree by 10%</th> </tr> </thead> <tbody> <tr><td>1</td><td>100</td><td>0</td><td>0</td><td>0</td></tr> <tr><td>2</td><td>100</td><td>0</td><td>0</td><td>0</td></tr> <tr><td>3</td><td>100</td><td>0</td><td>0</td><td>0</td></tr> <tr><td>4</td><td>100</td><td>0</td><td>0</td><td>0</td></tr> <tr><td>5</td><td>100</td><td>0</td><td>0</td><td>0</td></tr> <tr><td>6</td><td>100</td><td>0</td><td>0</td><td>0</td></tr> <tr><td>7</td><td>100</td><td>0</td><td>0</td><td>0</td></tr> <tr><td>8</td><td>100</td><td>0</td><td>0</td><td>0</td></tr> <tr><td>9</td><td>100</td><td>0</td><td>0</td><td>0</td></tr> <tr><td>10</td><td>100</td><td>0</td><td>0</td><td>0</td></tr> <tr><td>11</td><td>100</td><td>0</td><td>0</td><td>0</td></tr> <tr><td>12</td><td>100</td><td>0</td><td>0</td><td>0</td></tr> <tr><td>13</td><td>100</td><td>0</td><td>0</td><td>0</td></tr> <tr><td>14</td><td>100</td><td>0</td><td>0</td><td>0</td></tr> <tr><td>15</td><td>100</td><td>0</td><td>0</td><td>0</td></tr> <tr><td>16</td><td>100</td><td>0</td><td>0</td><td>0</td></tr> <tr><td>17</td><td>100</td><td>0</td><td>0</td><td>0</td></tr> <tr><td>18</td><td>100</td><td>0</td><td>0</td><td>0</td></tr> <tr><td>19</td><td>100</td><td>0</td><td>0</td><td>0</td></tr> <tr><td>20</td><td>100</td><td>0</td><td>0</td><td>0</td></tr> <tr><td>21</td><td>100</td><td>0</td><td>0</td><td>0</td></tr> <tr><td>22</td><td>100</td><td>0</td><td>0</td><td>0</td></tr> <tr><td>23</td><td>100</td><td>0</td><td>0</td><td>0</td></tr> <tr><td>24</td><td>100</td><td>0</td><td>0</td><td>0</td></tr> <tr><td>25</td><td>100</td><td>0</td><td>0</td><td>0</td></tr> <tr><td>26</td><td>100</td><td>0</td><td>0</td><td>0</td></tr> <tr><td>27</td><td>100</td><td>0</td><td>0</td><td>0</td></tr> <tr><td>28</td><td>100</td><td>0</td><td>0</td><td>0</td></tr> <tr><td>29</td><td>100</td><td>0</td><td>0</td><td>0</td></tr> <tr><td>30</td><td>100</td><td>0</td><td>0</td><td>0</td></tr> <tr><td>31</td><td>100</td><td>0</td><td>0</td><td>0</td></tr> <tr><td>32</td><td>100</td><td>0</td><td>0</td><td>0</td></tr> <tr><td>33</td><td>100</td><td>0</td><td>0</td><td>0</td></tr> <tr><td>34</td><td>100</td><td>0</td><td>0</td><td>0</td></tr> <tr><td>35</td><td>100</td><td>0</td><td>0</td><td>0</td></tr> <tr><td>36</td><td>100</td><td>0</td><td>0</td><td>0</td></tr> <tr><td>37</td><td>100</td><td>0</td><td>0</td><td>0</td></tr> <tr><td>38</td><td>100</td><td>0</td><td>0</td><td>0</td></tr> <tr><td>39</td><td>100</td><td>0</td><td>0</td><td>0</td></tr> <tr><td>40</td><td>100</td><td>0</td><td>0</td><td>0</td></tr> <tr><td>41</td><td>100</td><td>0</td><td>0</td><td>0</td></tr> <tr><td>42</td><td>100</td><td>0</td><td>0</td><td>0</td></tr> <tr><td>43</td><td>100</td><td>0</td><td>0</td><td>0</td></tr> <tr><td>44</td><td>100</td><td>0</td><td>0</td><td>0</td></tr> <tr><td>45</td><td>100</td><td>0</td><td>0</td><td>0</td></tr> <tr><td>46</td><td>100</td><td>0</td><td>0</td><td>0</td></tr> <tr><td>47</td><td>100</td><td>0</td><td>0</td><td>0</td></tr> <tr><td>48</td><td>100</td><td>0</td><td>0</td><td>0</td></tr> <tr><td>49</td><td>100</td><td>0</td><td>0</td><td>0</td></tr> <tr><td>50</td><td>100</td><td>0</td><td>0</td><td>0</td></tr> </tbody> </table>	Observer	Agree	Disagree	Agree by 10%	Disagree by 10%	1	100	0	0	0	2	100	0	0	0	3	100	0	0	0	4	100	0	0	0	5	100	0	0	0	6	100	0	0	0	7	100	0	0	0	8	100	0	0	0	9	100	0	0	0	10	100	0	0	0	11	100	0	0	0	12	100	0	0	0	13	100	0	0	0	14	100	0	0	0	15	100	0	0	0	16	100	0	0	0	17	100	0	0	0	18	100	0	0	0	19	100	0	0	0	20	100	0	0	0	21	100	0	0	0	22	100	0	0	0	23	100	0	0	0	24	100	0	0	0	25	100	0	0	0	26	100	0	0	0	27	100	0	0	0	28	100	0	0	0	29	100	0	0	0	30	100	0	0	0	31	100	0	0	0	32	100	0	0	0	33	100	0	0	0	34	100	0	0	0	35	100	0	0	0	36	100	0	0	0	37	100	0	0	0	38	100	0	0	0	39	100	0	0	0	40	100	0	0	0	41	100	0	0	0	42	100	0	0	0	43	100	0	0	0	44	100	0	0	0	45	100	0	0	0	46	100	0	0	0	47	100	0	0	0	48	100	0	0	0	49	100	0	0	0	50	100	0	0	0	<p>Expectation</p> <ul style="list-style-type: none"> If all cases extremely difficult, <ul style="list-style-type: none"> Train 	<p>Systematic difference between pathologists: calibration required</p>  <p>Calibration needed</p>
Observer	Agree	Disagree	Agree by 10%	Disagree by 10%																																																																																																																																																																																																																																																													
1	100	0	0	0																																																																																																																																																																																																																																																													
2	100	0	0	0																																																																																																																																																																																																																																																													
3	100	0	0	0																																																																																																																																																																																																																																																													
4	100	0	0	0																																																																																																																																																																																																																																																													
5	100	0	0	0																																																																																																																																																																																																																																																													
6	100	0	0	0																																																																																																																																																																																																																																																													
7	100	0	0	0																																																																																																																																																																																																																																																													
8	100	0	0	0																																																																																																																																																																																																																																																													
9	100	0	0	0																																																																																																																																																																																																																																																													
10	100	0	0	0																																																																																																																																																																																																																																																													
11	100	0	0	0																																																																																																																																																																																																																																																													
12	100	0	0	0																																																																																																																																																																																																																																																													
13	100	0	0	0																																																																																																																																																																																																																																																													
14	100	0	0	0																																																																																																																																																																																																																																																													
15	100	0	0	0																																																																																																																																																																																																																																																													
16	100	0	0	0																																																																																																																																																																																																																																																													
17	100	0	0	0																																																																																																																																																																																																																																																													
18	100	0	0	0																																																																																																																																																																																																																																																													
19	100	0	0	0																																																																																																																																																																																																																																																													
20	100	0	0	0																																																																																																																																																																																																																																																													
21	100	0	0	0																																																																																																																																																																																																																																																													
22	100	0	0	0																																																																																																																																																																																																																																																													
23	100	0	0	0																																																																																																																																																																																																																																																													
24	100	0	0	0																																																																																																																																																																																																																																																													
25	100	0	0	0																																																																																																																																																																																																																																																													
26	100	0	0	0																																																																																																																																																																																																																																																													
27	100	0	0	0																																																																																																																																																																																																																																																													
28	100	0	0	0																																																																																																																																																																																																																																																													
29	100	0	0	0																																																																																																																																																																																																																																																													
30	100	0	0	0																																																																																																																																																																																																																																																													
31	100	0	0	0																																																																																																																																																																																																																																																													
32	100	0	0	0																																																																																																																																																																																																																																																													
33	100	0	0	0																																																																																																																																																																																																																																																													
34	100	0	0	0																																																																																																																																																																																																																																																													
35	100	0	0	0																																																																																																																																																																																																																																																													
36	100	0	0	0																																																																																																																																																																																																																																																													
37	100	0	0	0																																																																																																																																																																																																																																																													
38	100	0	0	0																																																																																																																																																																																																																																																													
39	100	0	0	0																																																																																																																																																																																																																																																													
40	100	0	0	0																																																																																																																																																																																																																																																													
41	100	0	0	0																																																																																																																																																																																																																																																													
42	100	0	0	0																																																																																																																																																																																																																																																													
43	100	0	0	0																																																																																																																																																																																																																																																													
44	100	0	0	0																																																																																																																																																																																																																																																													
45	100	0	0	0																																																																																																																																																																																																																																																													
46	100	0	0	0																																																																																																																																																																																																																																																													
47	100	0	0	0																																																																																																																																																																																																																																																													
48	100	0	0	0																																																																																																																																																																																																																																																													
49	100	0	0	0																																																																																																																																																																																																																																																													
50	100	0	0	0																																																																																																																																																																																																																																																													
<p>Systematic difference between pathologists: calibration required</p>  <p>The alternative response is based on the hypothesis that collapsed AS is not recognized and overdiagnosed as invasive adenocarcinoma</p>	<p>Items</p> <ul style="list-style-type: none"> Introduction Micro-anatomy/normal histology Flexibility Tangential cutting Alveolar collapse = mathematical model Criteria for tubogenic collapsed AS Criteria for papillary, solid, solid pattern "Small" acinar adenocarcinoma Flow chart 	<p>Functional unit</p> <ul style="list-style-type: none"> Acinus Secondary lobule 																																																																																																																																																																																																																																																															
	<p>Flexibility of the lung</p>																																																																																																																																																																																																																																																																
		<p>Mathematical Model</p>																																																																																																																																																																																																																																																															
																																																																																																																																																																																																																																																																	

■ Slides of the tutorial after round 1 (continued)

<p>Using an oven temperature for 57 days Reduction in weight of 70%</p>	<p>Using an oven temperature for 57 days Reduction in weight of 70%</p> <p>Any (intermittent) collapse of the specimen is not a problem as long as the specimen is not over-dried.</p>	
<p>Using an oven temperature for 57 days Reduction in weight of 70%</p> <p>Reduction in water mass</p> <p>Long retention of air space</p> <ul style="list-style-type: none"> • High retention of air space • Retention of air space • Retention of air space • Retention of air space • Retention of air space 	<h3>Iatrogenic Collapse</h3> <ul style="list-style-type: none"> • Iatrogenic collapse = (AIRC) disappearance of (thickened) AIR • Conventional acquisition of AIR <p>• Expansion of collapsed AIR should also be:</p>	
<h3>Iatrogenic collapse in the lung</h3> <ul style="list-style-type: none"> • Consequence of collapse is substitution/“filling” appearance of the surface ADEOLAM WALLS • Expansion management: <ul style="list-style-type: none"> • AIR in lung without collapse: large structure seen (as they are expanded) • AIR in collapsed lung: repeat cross sections through arteries with limited air 	<h3>Tangential cut</h3>	<p>Microscopic image showing tangential cutting in the lung, with labels 'Tangential cut' and 'Tangential cut'.</p>
<h3>Iatrogenic collapse in the lung</h3> <ul style="list-style-type: none"> • Consequence of collapse is substitution/“filling” appearance of the surface ADEOLAM WALLS (AIRC) (as they are expanded) • Any histological section is a cross section • Tangential cutting is the term for an oblique cut through (a cluster of) cells • The effect of tangential cutting is: <ul style="list-style-type: none"> • Reduction of the amount of AIR • Reduction of the amount of AIR • Reduction of the amount of AIR 	<ul style="list-style-type: none"> • Expansion • Expansion • Expansion • Expansion • Expansion 	
<ul style="list-style-type: none"> • Expansion • Expansion • Expansion • Expansion • Expansion <p>When it happens contraction between amount of air and tumor cell height: 4:40 When it happens contraction between amount of air and tumor cell height: 4:40</p>	<h3>Collaps</h3> <p>compressed tissue: reduction of amount of "AIR"</p>	<h3>Iatrogenic collapse in the lung</h3> <ul style="list-style-type: none"> • Consequence of collapse is substitution/“filling” appearance of the surface ADEOLAM WALLS • In maximal collapse the tumor cells are better than in less collapsed areas • Any histological section is a cross section, in collapsed state more chance on tangential cut • Tangential cutting is the term for an oblique cut through (a cluster of) cells, causes shrinkage • To avoid overdiagnosis: Any diagnostic criterion should be present in at least a few adjacent areas (morphological action unit)
<h3>Items</h3> <ul style="list-style-type: none"> • Introduction • Micro anatomy/ normal histology • Fixation • Tangential cutting • Iatrogenic collapse = mathematical model • Criteria for iatrogenic collapsed AIR • Criteria for papillary, acinar, solid patterns • “Small” acinar elements/intra • Pleural space 	<h3>AIS in Iatrogenic collapsed specimen</h3>	

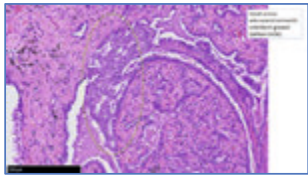
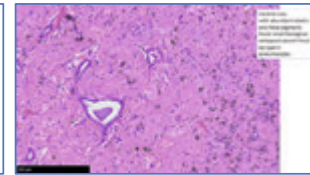

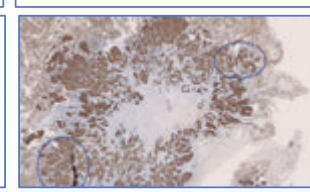

Slides of the tutorial after round 1 (continued)

<p>CK7 regular pattern: AIS respects pre-existing borders (bronchovascular borders and interlobular septa [arrows])</p>		
	<p>Compared to normal lung with discontinuous elastic (AE), the amount of elastic is in this area slightly increased in the anterior septa of AIS Staining with CK7 (brown) in alveolar wall (arrows) shows that the pattern is irregular</p>	<p>Diagnostic thought process in this case</p> <ul style="list-style-type: none"> • Monoclonal tumor cell growth on alveolar wall (CK7 regular pattern) • Slight increase in elastic • Respecting the physiological borders (lobular septa, bronchovascular bundle) • Central area without CK positive cells, leucocytoclastic alveolar pattern (hemorrhagic collapse); increase in elastic • Conclusion: leucocytoclastic AIS (leucocytocytic type II, not biological collapse)
<p>AIS in collapse</p> <ul style="list-style-type: none"> • Regular CK7 pattern, respecting borders • Monoclonal (except for tangential cut) • Alveolar wall contains elastic, may be thin, slightly thicker 	<p>CK7 Regular Irregular</p>	<p>CK7 irregular</p>
<p>Items</p> <ul style="list-style-type: none"> • Introduction • Micro-anatomy/ normal histology • Features • Tangential cutting • Idiogenic collapse + mathematical model • Criteria for leucocytoclastic AIS • Criteria for collapsing, atypical solid pattern • "Small" atypical adenocarcinoma • Flow chart 		<p>DIAGNOSIS ?</p> <ol style="list-style-type: none"> 1. Papillary adenocarcinoma 2. Micropapillary adenocarcinoma 3. Adenocarcinoma in situ 4. Atypical adenocarcinoma
<p>DIAGNOSIS ?</p> <ol style="list-style-type: none"> 1. Papillary adenocarcinoma 2. Micropapillary adenocarcinoma 3. Adenocarcinoma in situ 4. Atypical adenocarcinoma 		<p>Papillary carcinoma</p> <ul style="list-style-type: none"> • Original diagnosis included desmoplastic stroma (Jain, Aden, ASP 1997) • WHO 1999 copied criteria of this paper, except desmoplastic stroma! • Prognostic change: Silver stain gone, WHO 1999 etc much better • Now Papillary carcinoma has no stroma in the center of papilla (Levin-Brown Histopathology 2002), also to be used in the 2nd round of testing
		<p>Items</p> <ul style="list-style-type: none"> • Introduction • Micro-anatomy/ normal histology • Features • Tangential cutting • Idiogenic collapse + mathematical model • Criteria for leucocytoclastic AIS • Criteria for collapsing, atypical solid pattern • "Small" atypical adenocarcinoma • Flow chart

■ Slides of the tutorial after round 1 (continued)

	<p>Micropapillary</p> <ul style="list-style-type: none"> • Minimum criteria at least in relevant part of acinus unit: continuous presence in 2-3 adjacent acini, e.g. micropapillary • Micropapillary is growth on fibrovascular core with stromal desmoplasia. • Thus no real morphological invasion, but an accepted surrogate marker for invasion <p>• The minimum criterion used in the 2nd round exists independently but is tangential cutting</p> <p>• Important to avoid the implication that this is growth of acinar units</p>	<p>Items</p> <ul style="list-style-type: none"> • Introduction • Micro-anatomy/normal histology • Function • Tangential cutting • Intragenic collapse = mathematical model • Criteria for intragenic collapsed AIS • Criteria for papillary, cribriform, acinar, solid pattern • "Small" acinar adenocarcinoma • Flow chart
	<p>Cribriform pattern</p> <ul style="list-style-type: none"> • Cribriform is growth in alveolar space with gland formation. • Thus no real morphological invasion, but an accepted surrogate marker for invasion • Part of acinar adenocarcinoma (Zellicky Modern Pathology 2014) 	<p>Items</p> <ul style="list-style-type: none"> • Introduction • Micro-anatomy/normal histology • Function • Tangential cutting • Intragenic collapse = mathematical model • Criteria for intragenic collapsed AIS • Criteria for papillary, acinar, solid pattern • "Small" acinar adenocarcinoma • Flow chart
<p>Solid pattern</p>		<p>High magnification images of AIS in AIS: cribriform and micropapillary patterns only growth in the acinus (AIS) AIS: cribriform and micropapillary patterns only growth in the acinus (AIS) AIS: cribriform and micropapillary patterns only growth in the acinus (AIS)</p>
<p>• Solid pattern and cribriform may be present in same case</p>	<p>Items</p> <ul style="list-style-type: none"> • Introduction • Micro-anatomy/normal histology • Function • Tangential cutting • Intragenic collapse = mathematical model • Criteria for intragenic collapsed AIS • Criteria for papillary, acinar, solid pattern • "Small" acinar adenocarcinoma • Flow chart 	<p>"Small" acinar adenocarcinoma</p>

■ Slides of the tutorial after round 1 (continued)

	<p>scar</p>	
<p>Items</p> <ul style="list-style-type: none"> • Introduction • Micro-analysis/ normal histology <ul style="list-style-type: none"> • Features • Tangential cutting • Intraluminal collapse = mathematical model • Criteria for papillary, solid, solid pattern • "Small" versus adenocarcinoma • Flow chart 		<ul style="list-style-type: none"> • RNA evolved in 2009, not recognized (present) in 2005 • Due to overdiagnosis of collapsed DCIS pathologists "underread" "nodular adenocarcinoma" with an excellent prognosis (200% DFS in 5 years) • In the 2nd round we will not use RNA • If there is a minimal area of invasion, it is invasive, irrespective of the size of invasion
<p>Debate about STAS</p> <ul style="list-style-type: none"> • This is not an unambiguous topic. • Adds more confusion than a solution. • In other regions dissociation is used as a characteristic of malignancy, not as characteristic of invasion (e.g. breast cytology) • In the 2nd round we will not use STAS 	<p>Invasion measurement</p> <ul style="list-style-type: none"> • Ruler: 3rd space bar; then left mouse button draw line. • Measure area of invasion: the line encompasses a circle • Aerial overlapping area's total measure size = true total tumor size 	
	<ul style="list-style-type: none"> • We need to think outside the box for the second part • Do not be afraid of underdiagnosis, this is only research to figure out an approach to minimize the variation in our readings. • Use the flow chart and provide feedback, please in the comment section • Methodology: randomized cases from 2 different institutions (total n=24); n=12 in 2nd round; 2nd round embedded again; names, decoding for known by Andreas Lind by (T) 	

REFERENCES

1. IKNL. Incidence of Lung Cancer in the Netherlands. <https://iknl.nl/kankersoorten/longkanker/registratie/incidentie>.
2. Hendriks LEL, Dingemans AMC, De Ruyscher DKM, et al. Lung Cancer in the Netherlands. *J Thorac Oncol*. 2021;16(3):355-365. doi:10.1016/j.jtho.2020.10.012
3. Beasley MB, Brambilla E, Travis WD. The 2004 World Health Organization classification of lung tumors. *Semin Roentgenol*. 2005;40(2):90-97. doi:10.1053/j.ro.2005.01.001
4. Travis WD, Brambilla E, Nicholson AG, et al. The 2015 World Health Organization Classification of Lung Tumors. *J Thorac Oncol*. 2015;10(9):1243-1260. doi:10.1097/JTO.0000000000000630
5. Wang B-Y, Huang J-Y, Chen H-C, et al. The comparison between adenocarcinoma and squamous cell carcinoma in lung cancer patients. *J Cancer Res Clin Oncol*. 2020;146(1):43-52. doi:10.1007/s00432-019-03079-8
6. Russell PA, Wainer Z, Wright GM, Daniels M, Conron M, Williams RA. Does lung adenocarcinoma subtype predict patient survival?: A clinicopathologic study based on the new international association for the study of lung cancer/American thoracic society/European respiratory society international multidisciplinary lung adeno. *J Thorac Oncol*. 2011;6(9):1496-1504. doi:10.1097/JTO.0b013e318221f701
7. Murakami S, Ito H, Tsubokawa N, et al. Prognostic value of the new IASLC/ATS/ERS classification of clinical stage IA lung adenocarcinoma. *Lung Cancer*. 2015;90(2):199-204. doi:10.1016/j.lungcan.2015.06.022
8. Yang F, Dong Z, Shen Y, et al. Cribriform growth pattern in lung adenocarcinoma: More aggressive and poorer prognosis than acinar growth pattern. *Lung Cancer*. 2020;147(May):187-192. doi:10.1016/j.lungcan.2020.07.021
9. Liebow AA. Bronchiolo-alveolar carcinoma. *Adv Intern Med*. 1960;10:329-358.
10. Noguchi M, Morikawa A, Kawasaki M, et al. Small adenocarcinoma of the lung. Histologic characteristics and prognosis. *Cancer*. 1995;75(12):2844-2852. doi:10.1002/1097-0142(19950615)75:12<2844::AID-CNCR2820751209>3.0.CO;2-#
11. Silver SA, Askin FB. True papillary carcinoma of the lung: a distinct clinicopathologic entity. *Am J Surg Pathol*. 1997;21(1):43-51. doi:10.1097/00000478-199701000-00005
12. Travis W, Colby T V. *Histological Typing of Lung and Pleural Tumors*. 3rd ed. Springer; 1999.
13. Travis WD, Brambilla E, Noguchi M, et al. International association for the study of lung cancer/american thoracic society/european respiratory society international multidisciplinary classification of lung adenocarcinoma. *J Thorac Oncol*. 2011;6(2):244-285. doi:10.1097/JTO.0b013e318206a221
14. Thunnissen E, Beasley MB, Borczuk AC, et al. Reproducibility of histopathological subtypes and invasion in pulmonary adenocarcinoma. An international interobserver study. *Mod Pathol*. 2012;25(12):1574-1583. doi:10.1038/modpathol.2012.106
15. Mountain C. Revisions in the International System for Staging Lung Cancer. *Chest*. 1997;110:1710-1717. doi:10.1378/chest.111.6.1710
16. Goldstraw P, Chansky K, Crowley J, et al. The IASLC lung cancer staging project: Proposals for revision of the TNM stage groupings in the forthcoming (eighth) edition of the TNM Classification for lung cancer. *J Thorac Oncol*. 2016;11(1):39-51. doi:10.1016/j.jtho.2015.09.009
17. Nicholson AG, Tsao MS, Travis WD, et al. Eighth Edition Staging of Thoracic Malignancies: Implications for the Reporting Pathologist. *Arch Pathol Lab Med*. 2018;142(5):645-661. doi:10.5858/arpa.2017-0245-RA

18. Detterbeck FC. The eighth edition TNM stage classification for lung cancer: What does it mean on main street? *J Thorac Cardiovasc Surg.* 2018;155(1):356-359. doi:10.1016/j.jtcvs.2017.08.138
19. Borczuk AC, Cooper WA, Dacic S, et al. Tumours of the lung. In: WHO_Editorial_Board, ed. *WHO Classification of Tumours Editorial Board. Thoracic Tumours. Lyon (France): International Agency for Research on Cancer; 2021. (WHO Classification of Tumours Series, 5th Ed.; Vol. 5).* 5th ed. IARC; 2021:19-189.
20. Chansky K, Sculier JP, Crowley JJ, Giroux D, Meerbeeck J Van, Goldstraw P. The international association for the study of lung cancer staging project: Prognostic factors and pathologic TNM stage in surgically managed non-small cell lung cancer. *J Thorac Oncol.* 2009;4(7):792-801. doi:10.1097/JTO.0b013e3181a7716e
21. Takeda S ichi, Maeda H, Okada T, et al. Results of pulmonary resection following neoadjuvant therapy for locally advanced (IIIA-IIIB) lung cancer. *Eur J Cardio-thoracic Surg.* 2006;30(1):184-189. doi:10.1016/j.ejcts.2006.03.054
22. Caglar HB, Baldini EH, Othus M, et al. Outcomes of patients with stage III nonsmall cell lung cancer treated with chemotherapy and radiation with and without surgery. *Cancer.* 2009;115(18):4156-4166. doi:10.1002/cncr.24492
23. Kappers I, van Sandick JW, Burgers JA, et al. Results of combined modality treatment in patients with non-small-cell lung cancer of the superior sulcus and the rationale for surgical resection. *Eur J Cardio-thoracic Surg.* 2009;36(4):741-746. doi:10.1016/j.ejcts.2009.04.069
24. Peedell C, Dunning J, Bapusamy a. Is there a standard of care for the radical management of non-small cell lung cancer involving the apical chest wall (Pancoast tumours)? *Clin Oncol (R Coll Radiol).* 2010;22(5):334-346. doi:10.1016/j.clon.2010.03.001
25. Pourel N, Santelmo N, Naafa N, et al. Concurrent cisplatin/etoposide plus 3D-conformal radiotherapy followed by surgery for stage IIB (superior sulcus T3NO)/III non-small cell lung cancer yields a high rate of pathological complete response. *Eur J Cardiothorac Surg.* 2008;33(5):829-836. doi:10.1016/j.ejcts.2008.01.063
26. Rusch VW, Giroux DJ, Kraut MJ, et al. Induction chemoradiation and surgical resection for superior sulcus non-small-cell lung carcinomas: long-term results of Southwest Oncology Group Trial 9416 (Intergroup Trial 0160). *J Clin Oncol.* 2007;25(3):313-318. doi:10.1200/JCO.2006.08.2826
27. Junker K, Thomas M, Schulmann K, Klink F, Bosse U, Müller KM. Tumour regression in non-small-cell lung cancer following neoadjuvant therapy. Histological assessment. *J Cancer Res Clin Oncol.* 1997;123(9):469-477. <http://www.ncbi.nlm.nih.gov/pubmed/9341895>
28. Liu-Jarin X, Stoopler MB, Raftopoulos H, Ginsburg M, Gorenstein L, Borczuk AC. Histologic Assessment of Non-Small Cell Lung Carcinoma after Neoadjuvant Therapy. *Mod Pathol.* 2003;16(11):1102-1108. doi:10.1097/01.MP.0000096041.13859.AB
29. Yamane Y, Ishii G, Goto K, et al. A novel histopathological evaluation method predicting the outcome of non-small cell lung cancer treated by neoadjuvant therapy: The prognostic importance of the area of residual tumor. *J Thorac Oncol.* 2010;5(1):49-55. doi:10.1097/JTO.0b013e3181c0a1f8
30. Detterbeck FC. Changes in the treatment of Pancoast tumors. *Ann Thorac Surg.* 2003;75(6):1990-1997. doi:10.1016/S0003-4975(03)00134-6
31. Eisenhauer EA, Therasse P, Bogaerts J, et al. New response evaluation criteria in solid tumours: Revised RECIST guideline (version 1.1). *Eur J Cancer.* 2009;45(2):228-247. doi:10.1016/j.ejca.2008.10.026
32. Brambilla E, Travis WD, Colby T V., Corrin B, Shimosato Y. The new World Health Organization classification of lung tumours. *Eur Respir J.* 2001;18(6):1059-1068. doi:10.1183/09031936.01.00275301
33. Dworak O, Keilholz L, Hoffmann A. Pathological features of rectal cancer after preoperative radiochemotherapy. *Int J Colorectal Dis.* 1997;12(1):19-23. doi:10.1007/s003840050072

34. Goldstraw P. Editorial Rx. In: *The IASLC Staging Manual in Thoracic Oncology*. Orange Park; 2009:37-38.
35. Rami-Porta R, Crowley JJ, Goldstraw P. The revised TNM staging system for lung cancer. *Ann Thorac Cardiovasc Surg Off J Assoc Thorac Cardiovasc Surg Asia*. 2009;15(1):4-9.
36. Curtin F, Schulz P. Multiple correlations and Bonferroni's correction. *Biol Psychiatry*. 1998;44(8):775-777. doi:10.1016/s0006-3223(98)00043-2
37. Thunnissen FBJM, Schuurbiens OCJ, Den Bakker MA. A critical appraisal of prognostic and predictive factors for common lung cancers. *Histopathology*. 2006;48(7):779-786. doi:10.1111/j.1365-2559.2006.02386.x
38. Fischer S, Darling G, Pierre AF, et al. Induction chemoradiation therapy followed by surgical resection for non-small cell lung cancer (NSCLC) invading the thoracic inlet. *Eur J Cardiothorac Surg*. 2008;33(6):1129-1134. doi:10.1016/j.ejcts.2008.03.008
39. Bollschweiler E, Metzger R, Drebber U, et al. Histological type of esophageal cancer might affect response to neo-adjuvant radiochemotherapy and subsequent prognosis. *Ann Oncol*. 2009;20(2):231-238. doi:10.1093/annonc/mdn622
40. Harrison L, Blackwell K. Hypoxia and Anemia: Factors in Decreased Sensitivity to Radiation Therapy and Chemotherapy? *Oncologist*. 2004;9(S5):31-40. doi:10.1634/theoncologist.9-90005-31
41. Brown JM. Tumor microenvironment and the response to anticancer therapy. *Cancer Biol Ther*. 2002;1(5):453-458. doi:10.4161/cbt.1.5.157
42. Becker K, Mueller JD, Schulmacher C, et al. Histomorphology and grading of regression in gastric carcinoma treated with neoadjuvant chemotherapy. *Cancer*. 2003;98(7):1521-1530. doi:10.1002/cncr.11660
43. Blaauwgeers JL, Kappers I, Klomp HM, et al. Complete pathological response is predictive for clinical outcome after tri-modality therapy for carcinomas of the superior pulmonary sulcus. *Virchows Arch*. 2013;462(5):547-556. doi:10.1007/s00428-013-1404-6
44. Song Z, Yu X, Zhang Y. Altered expression of programmed death-ligand 1 after neo-adjuvant chemotherapy in patients with lung squamous cell carcinoma. *Lung Cancer*. 2016;99:166-171. doi:10.1016/j.lungcan.2016.07.013
45. Travis WD, Dacic S, Wistuba I, et al. IASLC Multidisciplinary Recommendations for Pathologic Assessment of Lung Cancer Resection Specimens After Neoadjuvant Therapy. *J Thorac Oncol*. 2020;15(5):709-740. doi:10.1016/j.jtho.2020.01.005
46. Fleege, JC, Diest, PJ van, Baak J. Reliability of quantitative pathological assessments, standards, and quality control measurement of nuclei. In: *Manual of Quantitative Pathology in Cancer Diagnosis and Prognosis*. ; 1991:155-167.
47. Jakobsen JN, Sørensen JB. Clinical impact of ki-67 labeling index in non-small cell lung cancer. *Lung Cancer*. 2013;79(1):1-7. doi:10.1016/j.lungcan.2012.10.008
48. Wei D ming, Chen W jie, Meng R mei, et al. Augmented expression of Ki-67 is correlated with clinicopathological characteristics and prognosis for lung cancer patients: An updated systematic review and meta-analysis with 108 studies and 14,732 patients. *Respir Res*. 2018;19(1):1-19. doi:10.1186/s12931-018-0843-7
49. Butter R, Hart't NA, Hooijer GKJ, et al. Multicentre study on the consistency of PD-L1 immunohistochemistry as predictive test for immunotherapy in non-small cell lung cancer. *J Clin Pathol*. Published online 2019:423-430. doi:10.1136/jclinpath-2019-205993
50. Thunnissen E, Kerr KM, Dafni U, et al. Programmed death-ligand 1 expression influenced by tissue sample size. Scoring based on tissue microarrays' and cross-validation with resections, in patients with, stage I-III, non-small cell lung carcinoma of the European Thoracic Oncology Platform Lungs. *Mod Pathol*. 2020;33(5):792-801. doi:10.1038/s41379-019-0383-9

51. Corzani R, Luzzi L, Spina D, et al. The prognostic significance of proliferative indices in surgically resected IIIA-N2 Non-small cell lung cancer after induction chemotherapy. *J Cardiovasc Surg (Torino)*. 2014;58(5):763-769. doi:10.23736/S0021-9509.16.08232-X
52. Wen S, Zhou W, Li C ming, et al. Ki-67 as a prognostic marker in early-stage non-small cell lung cancer in Asian patients: A meta-analysis of published studies involving 32 studies. *BMC Cancer*. 2015;15(1). doi:10.1186/s12885-015-1524-2
53. Li LT, Jiang G, Chen Q, Zheng JN. Predic Ki67 is a promising molecular target in the diagnosis of cancer (Review). *Mol Med Rep*. 2015;11(3):1566-1572. doi:10.3892/mmr.2014.2914
54. Uramoto H, Tanaka F. Prediction of recurrence after complete resection in patients with NSCLC. *Anticancer Res*. 2012;32(9):3953-3960.
55. Gennen K, Käsmann L, Taugner J, et al. Prognostic value of PD-L1 expression on tumor cells combined with CD8+ TIL density in patients with locally advanced non-small cell lung cancer treated with concurrent chemoradiotherapy. *Radiat Oncol*. 2020;15(1). doi:10.1186/s13014-019-1453-3
56. Tokito T, Azuma K, Kawahara A, et al. Predictive relevance of PD-L1 expression combined with CD8+ TIL density in stage III non-small cell lung cancer patients receiving concurrent chemoradiotherapy. *Eur J Cancer*. 2016;55:7-14. doi:10.1016/j.ejca.2015.11.020
57. Vrankar M, Zwitter M, Kern I, Stanic K. PD-L1 expression can be regarded as prognostic factor for survival of non-small cell lung cancer patients after chemoradiotherapy. *Neoplasma*. 2018;65(1):140-146. doi:10.4149/neo_2018_170206N77
58. Yoneda K, Kuwata T, Kanayama M, et al. Alteration in tumoural PD-L1 expression and stromal CD8-positive tumour-infiltrating lymphocytes after concurrent chemo-radiotherapy for non-small cell lung cancer. *Br J Cancer*. 2019;121(6):490-496. doi:10.1038/s41416-019-0541-3
59. Fujimoto D, Uehara K, Sato Y, et al. Alteration of PD-L1 expression and its prognostic impact after concurrent chemoradiation therapy in non-small cell lung cancer patients. *Sci Rep*. 2017;7(1):11373. doi:10.1038/s41598-017-11949-9
60. van den Ende T, van den Boorn HG, Hoonhout NM, et al. Priming the tumor immune microenvironment with chemo(radio)therapy: A systematic review across tumor types. *Biochim Biophys Acta - Rev Cancer*. 2020;1874(1). doi:10.1016/j.bbcan.2020.188386
61. Herbst RS, Baas P, Kim D-W, et al. Pembrolizumab versus docetaxel for previously treated, PD-L1-positive, advanced non-small-cell lung cancer (KEYNOTE-010): a randomised controlled trial. *Lancet (London, England)*. 2016;387(10027):1540-1550. doi:10.1016/S0140-6736(15)01281-7
62. Chen Q, Fu Y-Y, Yue Q-N, et al. Distribution of PD-L1 expression and its relationship with clinicopathological variables: an audit from 1071 cases of surgically resected non-small cell lung cancer. *Int J Clin Exp Pathol*. 2019;12(3):774-786. <http://www.ncbi.nlm.nih.gov/pubmed/31933885> <http://www.pubmedcentral.nih.gov/articlerender.fcgi?artid=PMC6945142>
63. Vos CG, Hartemink KJ, Blaauwgeers JLG, et al. Trimodality therapy for superior sulcus tumours: Evolution and evaluation of a treatment protocol. *Eur J Surg Oncol*. 2013;39(2):197-203. doi:10.1016/j.ejso.2012.09.002
64. Formenti SC, Rudqvist N, Golden E, et al. Radiotherapy induces responses of lung cancer to CTLA-4 blockade. *Nat Med*. 2018;24(12):1845-1851. doi:10.1038/s41591-018-0232-2. Radiotherapy
65. Tsao MS, Kerr KM, Kockx M, et al. PD-L1 Immunohistochemistry Comparability Study in Real-Life Clinical Samples: Results of Blueprint Phase 2 Project. *J Thorac Oncol*. 2018;13(9):1302-1311. doi:10.1016/j.jtho.2018.05.013
66. van Seijen M, Brcic L, Gonzales AN, et al. Impact of delayed and prolonged fixation on the evaluation of immunohistochemical staining on lung carcinoma resection specimen. *Virchows Arch*. 2019;475(2):191-199. doi:10.1007/s00428-019-02595-9

67. Dickhoff C, Senan S, Schneiders FL, et al. Ipilimumab plus nivolumab and chemoradiotherapy followed by surgery in patients with resectable and borderline resectable T3-4N0-1 non-small cell lung cancer: The INCREASE trial. *BMC Cancer*. 2020;20(1):1-10. doi:10.1186/s12885-020-07263-9
68. Underwood JCE, Crocker J. *Pathology of the Nucleus*. Springer; 1990.
69. Uhler C, Shivashankar G V. Nuclear Mechanopathology and Cancer Diagnosis. *Trends in Cancer*. 2018;4(4):320-331. doi:10.1016/j.trecan.2018.02.009
70. Fajardo LP BM. Radiation injury in surgical pathology. Part 1. *Am J Surg Pathol*. 1978;(2):159-199.
71. Poeze M, Von Meyenfeldt MF, Peterse JL, et al. Increased proliferative activity and p53 expression in normal glandular breast tissue after radiation therapy. *J Pathol*. 1998;185(1):32-37. doi:10.1002/(SICI)1096-9896(199805)185:1<32::AID-PATH43>3.0.CO;2-Q
72. Buhmeida A, Ålgars A, Ristamäki R, Collan Y, Syrjänen K, Pyrhönen S. Nuclear size as prognostic determinant in stage II and stage III colorectal adenocarcinoma. *Anticancer Res*. 2006;26(1 B):455-462.
73. Kadota K, Miyai Y, Katsuki N, et al. Nuclear grade based on transbronchial cytology is an independent prognostic factor in patients with advanced, unresectable non-small cell lung cancer. *Cancer Cytopathol*. 2016;124(9):630-640. doi:10.1002/cncy.21736
74. Siva S, Lobachevsky P, MacManus MP, et al. Radiotherapy for non-small cell lung cancer induces DNA damage response in both irradiated and out-of-field normal tissues. *Clin Cancer Res*. 2016;22(19):4817-4826. doi:10.1158/1078-0432.CCR-16-0138
75. Eriksson D, Stigbrand T. Radiation-induced cell death mechanisms. *Tumor Biol*. 2010;31(4):363-372. doi:10.1007/s13277-010-0042-8
76. Sellers AH. The clinical classification of malignant tumours: the TNM system. *Can Med Assoc J*. 1971;105(8):836 passim. <http://www.pubmedcentral.nih.gov/articlerender.fcgi?artid=1931208&tool=pmcentrez&rendertype=abstract>
77. Goldstraw P, Crowley J, Chansky K, et al. The IASLC Lung Cancer Staging Project: Proposals for the Revision of the TNM Stage Groupings in the Forthcoming (Seventh) Edition of the TNM Classification of Malignant Tumours. *J Thorac Oncol*. 2007;2(8):706-714. doi:10.1097/JTO.0b013e31812f3c1a
78. Rami-Porta R, Ball D, Crowley J, et al. The IASLC Lung Cancer Staging Project: Proposals for the Revision of the T Descriptors in the Forthcoming (Seventh) Edition of the TNM Classification for Lung Cancer. *J Thorac Oncol*. 2007;2(7):593-602. doi:10.1097/JTO.0b013e31807a2f81
79. Rami-Porta R, Bolejack V, Crowley J, et al. The IASLC Lung Cancer Staging Project: Proposals for the Revisions of the T Descriptors in the Forthcoming Eighth Edition of the TNM Classification for Lung Cancer. *J Thorac Oncol*. 2015;10(7):990-1003. doi:10.1097/JTO.0000000000000559
80. Casparie M, Tiebosch ATMG, Burger G, et al. Pathology databanking and biobanking in The Netherlands, a central role for PALGA, the nationwide histopathology and cytopathology data network and archive. *Cell Oncol*. 2007;29(1):19-24. doi:10.1155/2007/971816
81. Ueda K, Tanaka T, Hayashi M, et al. Compensation of pulmonary function after upper lobectomy versus lower lobectomy. *J Thorac Cardiovasc Surg*. 2011;142(4):762-767. doi:10.1016/j.jtcvs.2011.04.037
82. CBS. CBS data 2016. <http://statline.cbs.nl/Statweb/publication/?DM=SLNL&PA=03743&D1=0&D2=0,2&D3=0,8-206&D4=0,4,9,14,18-20&HDR=T,G1,G3&STB=G2&VW=T>.
83. Oncoline. No Title. <https://www.oncoline.nl/niet-kleincellig-longcarcinoom>.
84. Postmus PE, Kerr KM, Oudkerk M, et al. Early and locally advanced non-small-cell lung cancer (NSCLC): ESMO Clinical Practice Guidelines for diagnosis, treatment and follow-up. *Ann Oncol*. 2017;28(June):iv1-iv21. doi:10.1093/annonc/mdx222

85. Psaty BM, Koepsell TD, Lin D, et al. Assessment and control for confounding by indication in observational studies. *J Am Geriatr Soc.* 1999;47(6):749-754. doi:10.1111/j.1532-5415.1999.tb01603.x
86. Salazar MC, Rosen JE, Wang Z, et al. Association of delayed adjuvant chemotherapy with survival after lung cancer surgery. *JAMA Oncol.* 2017;3(5):610-619. doi:10.1001/jamaoncol.2016.5829
87. Rodrigues G, Choy H, Bradley J, et al. Adjuvant radiation therapy in locally advanced non-small cell lung cancer: Executive summary of an American Society for Radiation Oncology (ASTRO) evidence-based clinical practice guideline. *Pract Radiat Oncol.* 2015;5(3):149-155. doi:10.1016/j.prro.2015.02.013
88. Zhang Z, Gao S, Mao Y, et al. Surgical Outcomes of Synchronous Multiple Primary Non-Small Cell Lung Cancers. *Sci Rep.* 2016;6:1-11. doi:10.1038/srep23252
89. Leslie K, Yousem S, Colby T. Lungs. In: *Histology for Pathologists*. 4th ed. Wolters-Kluwer/ Lippincott Williams & Wilkins; 2012:505-540.
90. Thunnissen E, Beliën JAM, Kerr KM, et al. In compressed lung tissue microscopic sections of adenocarcinoma in situ may mimic papillary adenocarcinoma. *Arch Pathol Lab Med.* 2013;137(12):1792-1797. doi:10.5858/arpa.2012-0613-SA
91. Simons DJ, Chabris CF. Gorillas in our midst: Sustained inattentive blindness for dynamic events. *Perception.* 1999;28:1059-1074. doi:10.1068/p2952
92. Heerd D, Triantafyllou A, Yao F. Bronchoscopy, mediastinoscopy, and thoracotomy. In: Yao ff, ed. *Anesthesiology: Problem-Oriented Patient Management*. Lippincott Williams & Wilkins; 2003:32-49.
93. Wilson W, Benumof J. (1) Anesthesia. 6th ed.; 2005. p. . In: Miller RD, ed. *Anesthesia*. Philadelphia: Elsevier; 2005:1847-1940.
94. Kambouchner M. [The small airways: normal histology and the main histopathological lesions]. *Rev Mal Respir.* 2013;30(4):286-301. doi:10.1016/j.rmr.2012.12.017
95. Figueira de Mello GC, Ribeiro Carvalho CR, Adib Kairalla R, et al. Small airway remodeling in idiopathic interstitial pneumonias: a pathological study. *Respiration.* 2010;79(4):322-332. doi:10.1159/000235722
96. King MS, Eisenberg R, Newman JH, et al. Constrictive bronchiolitis in soldiers returning from Iraq and Afghanistan. *N Engl J Med.* 2011;365(3):222-230. doi:10.1056/NEJMoa1101388
97. Burgel P-R, Bergeron A, de Blic J, et al. Small airways diseases, excluding asthma and COPD: an overview. *Eur Respir Rev.* 2013;22(128):131-147. doi:10.1183/09059180.00001313
98. Jones KD, Urisman A. Histopathologic approach to the surgical lung biopsy in interstitial lung disease. *Clin Chest Med.* 2012;33(1):27-40. doi:10.1016/j.ccm.2012.01.003
99. Couture C, Colby T V. Histopathology of bronchiolar disorders. *Semin Respir Crit Care Med.* 2003;24(5):489-498. doi:10.1055/s-2004-815600
100. Visscher DW, Myers JL. Bronchiolitis: the pathologist's perspective. *Proc Am Thorac Soc.* 2006;3(1):41-47. doi:10.1513/pats.200512-124JH
101. Colombat M, Holifanjaniaina S, Hirschi S, Mal H, Stern M. Histologic reconstruction of bronchiolar lesions in lung transplant patients with bronchiolitis obliterans syndrome. *Am J Surg Pathol.* 2014;38(8):1157-1158. doi:10.1097/PAS.0000000000000181
102. Layfield LJ, Witt BL, Metzger KG, Anderson GM. Extraneous tissue: A potential source for diagnostic error in surgical pathology. *Am J Clin Pathol.* 2011;136(5):767-772. doi:10.1309/AJCP4FFSBPHAU8IU
103. Gephardt GN, Zarbo RJ. Extraneous tissue in surgical pathology: A College of American Pathologists Q-probes study of 275 laboratories. *Arch Pathol Lab Med.* 1996;120(11):1009-1014.

104. Thunnissen FBJM, Tilanus MGJ, Ligtenberg MJL, et al. Quality control in diagnostic molecular pathology in the Netherlands; proficiency testing for patient identification in tissue samples. *J Clin Pathol.* 2004;57(7):717-720. doi:10.1136/jcp.2003.011973
105. Hunt JL, Swalsky P, Sasatomi E, Niehouse L, Bakker A, Finkelstein SD. A microdissection and molecular genotyping assay to confirm the identity of tissue floaters in paraffin-embedded tissue blocks. *Arch Pathol Lab Med.* 2003;127(February):213-217. doi:10.1043/0003-9985(2003)127<213:MAMGAT>2.O.CO;2
106. Platt E, Sommer P, McDonald L, Bennett A, Hunt J. Tissue floaters and contaminants in the histology laboratory. *Arch Pathol Lab Med.* 2009;133:973-978. doi:10.1016/S1077-9108(09)79301-6
107. Hirota N, Martin JG. Mechanisms of airway remodeling. *Chest.* 2013;144(3):1026-1032. doi:10.1378/chest.12-3073
108. An SS, Bai TR, Bates JHT, et al. Airway smooth muscle dynamics: a common pathway of airway obstruction in asthma. *Eur Respir J.* 2007;29(5):834-860. doi:10.1183/09031936.00112606
109. Ward C, De Soyza A, Fisher AJ, Pritchard G, Forrest I, Corris P. A descriptive study of small airway reticular basement membrane thickening in clinically stable lung transplant recipients. *J Hear Lung Transplant.* 2005;24:533-537. doi:10.1016/j.healun.2004.02.018
110. James AL, Green FH, Abramson MJ, et al. Airway basement membrane perimeter distensibility and airway smooth muscle area in asthma. *J Appl Physiol.* 2008;104(6):1703-1708. doi:10.1152/jappphysiol.00169.2008
111. Stephenson A, Flint J, English J, et al. Interpretation of transbronchial lung biopsies from lung transplant recipients: inter- and intraobserver agreement. *Can Respir J.* 2005;12(2):75-77.
112. Travis W, Brambilla E, Burke A, Marx A, Nicholson A. *WHO Classification of Tumours of the Lung, Pleura, Thymus and Heart.* 4th ed. (Travids W, Brambilla E, Burke A, Marx A, Nicholson A, eds.). IARC; 2015.
113. Watanabe M, Yokose T, Tetsukan W, et al. Micropapillary components in a lung adenocarcinoma predict stump recurrence 8 years after resection: A case report. *Lung Cancer.* 2013;80(2):230-233. doi:10.1016/j.lungcan.2013.01.011
114. Sardari Nia P, Colpaert C, Vermeulen P, et al. Different Growth Patterns of Non-Small Cell Lung Cancer Represent Distinct Biologic Subtypes. *Ann Thorac Surg.* 2008;85(2):395-405. doi:10.1016/j.athoracsur.2007.08.054
115. Onozato ML, Kovach AE, Yeap BY, et al. Tumor islands in resected early-stage lung adenocarcinomas are associated with unique clinicopathologic and molecular characteristics and worse prognosis. *Am J Surg Pathol.* 2013;37(2):287-294. doi:10.1097/PAS.0b013e31826885fb
116. Sardari Nia P, Van Marck E, Weyler J, Van Schil P. Prognostic value of a biologic classification of non-small-cell lung cancer into the growth patterns along with other clinical, pathological and immunohistochemical factors. *Eur J Cardiothorac Surg.* 2010;38(5):628-636. doi:10.1016/j.ejcts.2010.03.015
117. Kadota K, Nitadori J, Sima CS, et al. Tumor Spread through Air Spaces is an Important Pattern of Invasion and Impacts the Frequency and Location of Recurrences after Limited Resection for Small Stage I Lung Adenocarcinomas. *J Thorac Oncol.* 2015;10(5):806-814. doi:10.1097/JTO.0000000000000486
118. Warth A, Muley T, Kossakowski CA, et al. Prognostic Impact of Intra-alveolar Tumor Spread in Pulmonary Adenocarcinoma. *Am J Surg Pathol.* 2015;39(6):793-801. doi:10.1097/PAS.0000000000000409
119. Diaz LK, Wiley EL, Venta L a. Are Malignant ofthe Breast ? Needle Displaced by Core Biopsy. 1999;(November):1303-1313.

120. Thunnissen E, Blaauwgeers HJLG, De Cuba EM V, Yick CY, Flieder DB. Ex vivo artifacts and histopathologic pitfalls in the lung. *Arch Pathol Lab Med*. 2016;140(3):212-220. doi:10.5858/arpa.2015-0292-OA
121. Liebens F, Carly B, Cusumano P, et al. Breast cancer seeding associated with core needle biopsies: a systematic review. *Maturitas*. 2009;62(2):113-123. doi:10.1016/j.maturitas.2008.12.002
122. Nair KS, Naidoo R, Chetty R. Expression of cell adhesion molecules in oesophageal carcinoma and its prognostic value. *J Clin Pathol*. 2005;58(4):343-351. doi:10.1136/jcp.2004.018036
123. Zhao S, Guo T, Li J, Deng W, Gu C. Expression and prognostic value of GalNAc-T3 in patients with completely resected small (# 2 cm) peripheral lung adenocarcinoma after IASLC / ATS / ERS classification. Published online 2015:3143-3152.
124. Bertolini G, D'Amico L, Moro M, et al. Microenvironment-modulated metastatic CD133+/CXCR4+/EpCAM-lung cancer-initiating cells sustain tumor dissemination and correlate with poor prognosis. *Cancer Res*. 2015;75(17):3636-3649. doi:10.1158/0008-5472.CAN-14-3781
125. Zhang B, Zhang H, Shen G. Metastasis-associated protein 2 (MTA2) promotes the metastasis of non-small-cell lung cancer through the inhibition of the cell adhesion molecule Ep-CAM and E-cadherin. *Jpn J Clin Oncol*. 2015;45(8):755-766. doi:10.1093/jjco/hyv062
126. Augustin F, Fiegl M, Schmid T, Pomme G, Sterlacci W, Tzankov A. Receptor for hyaluronic acid-mediated motility (RHAMM, CD168) expression is prognostically important in both nodal negative and nodal positive large cell lung cancer. *J Clin Pathol*. 2015;68(5):368-373. doi:10.1136/jclinpath-2014-202819
127. Yao X, Williamson C, Adalsteinsson VA, et al. Tumor cells are dislodged into the pulmonary vein during lobectomy. *J Thorac Cardiovasc Surg*. 2014;148(6):3224-3231. doi:10.1016/j.jtcvs.2014.06.074
128. Sawabata N, Funaki S, Hyakutake T, Shintani Y, Fujiwara A, Okumura M. Perioperative circulating tumor cells in surgical patients with non-small cell lung cancer: does surgical manipulation dislodge cancer cells thus allowing them to pass into the peripheral blood? *Surg Today*. 2016;46(12):1402-1409. doi:10.1007/s00595-016-1318-4
129. Okada S, Mizuguchi S, Izumi N, et al. Prognostic value of the frequency of vascular invasion in stage I non-small cell lung cancer. *Gen Thorac Cardiovasc Surg*. 2017;65(1):32-39. doi:10.1007/s11748-016-0720-6
130. Hamanaka R, Yokose T, Sakuma Y, et al. Prognostic impact of vascular invasion and standardization of its evaluation in stage I non-small cell lung cancer. *Diagn Pathol*. 2015;10(1):1-10. doi:10.1186/s13000-015-0249-5
131. Van Wyk HC, Foulis AK, Roxburgh CS, Orange C, Horgan PG, McMillan DC. Comparison of Methods to Identify Lymphatic and Blood Vessel Invasion and their Prognostic Value in Patients with Primary Operable Colorectal Cancer. *Anticancer Res*. 2015;35(12):6457-6463.
132. Onozato ML, Klepeis VE, Yagi Y, Mino-Kenudson M. A role of three-dimensional (3D)-reconstruction in the classification of lung adenocarcinoma. *Anal Cell Pathol*. 2012;35(2):79-84. doi:10.3233/ACP-2011-0030
133. Lu S, Tan KS, Kadota K, et al. Spread through Air Spaces (STAS) Is an Independent Predictor of Recurrence and Lung Cancer? Specific Death in Squamous Cell Carcinoma. *J Thorac Oncol*. 2017;12(2):223-234. doi:10.1016/j.jtho.2016.09.129
134. Morimoto J, Nakajima T, Suzuki H, et al. Impact of free tumor clusters on prognosis after resection of pulmonary adenocarcinoma. *J Thorac Cardiovasc Surg*. 2016;152(1):64-72. doi:10.1016/j.jtcvs.2016.03.088
135. Dirschmid K, Kiesler J, Mathis G, Beller S, Stoss F SB. Epithelial misplacement after biopsy of colorectal adenomas. *Am J Surg Pathol*. 1993;17(12):1262-1265.

136. Kitahara S, Walsh C, Frumovitz M, Malpica A, Silva EG. Vascular pseudoinvasion in laparoscopic hysterectomy specimens for endometrial carcinoma: A grossing artifact? *Am J Surg Pathol*. 2009;33(2):298-303. doi:10.1097/PAS.0b013e31818a01bf
137. Logani S, Herdman A V., Little J V., Moller KA. Vascular "pseudo Invasion" in laparoscopic hysterectomy specimens: A diagnostic pitfall. *Am J Surg Pathol*. 2008;32(4):560-565. doi:10.1097/PAS.0b013e31816098f0
138. Boerner S. and Asa S. *Biopsy Interpretation of the Thyroid*. (Scott L. SL, ed.). Lippincott Williams and Wilkins Philadelphia, PA; 2010.
139. Clayton F. Bronchioloalveolar carcinomas. Cell types, patterns of growth, and prognostic correlates. *Cancer*. 1986;57(8):1555-1564. doi:10.1002/1097-0142(19860415)57:8<1555::AID-CNCR2820570820>3.0.CO;2-N
140. Barsky SH, Grossman DA, Ho J, Holmes EC. The multifocality of bronchioloalveolar lung carcinoma: evidence and implications of a multiclonal origin. *Mod Pathol*. 1994;7(6):633-640. http://www.ncbi.nlm.nih.gov/entrez/query.fcgi?cmd=Retrieve&db=PubMed&dopt=Citation&list_uids=7527541
141. Masai K, Sukeda A, Yoshida A, et al. P3.01-006 Prognostic Impact of Tumor Spread through Air Spaces in Limited Resection for pStage I Lung Cancer: Topic: Morphology. *J Thorac Oncol*. 2017;12(1):S1122-S1122. doi:10.1016/j.jtho.2016.11.1572
142. Uruga H, Fujii T, Fujimori S, Kohno T, Kishi K. Semiquantitative Assessment of Tumor Spread through Air Spaces (STAS) in Early-Stage Lung Adenocarcinomas. *J Thorac Oncol*. 2017;12(7):1046-1051. doi:10.1016/j.jtho.2017.03.019
143. Dai C, Xie H, Su H, et al. Tumor Spread through Air Spaces Affects the Recurrence and Overall Survival in Patients with Lung Adenocarcinoma >2 to 3 cm. *J Thorac Oncol*. 2017;12(7):1052-1060. doi:10.1016/j.jtho.2017.03.020
144. Shiono S, Yanagawa N. Spread through air spaces is a predictive factor of recurrence and a prognostic factor in stage I lung adenocarcinoma. *Interact Cardiovasc Thorac Surg*. Published online 2016:1-6. doi:10.1093/icvts/ivw211
145. Morales-Oyarvide V, Mino-Kenudson M. Tumor islands and spread through air spaces: Distinct patterns of invasion in lung adenocarcinoma. *Pathol Int*. 2016;66(1):1-7. doi:10.1111/pin.12368
146. Toyokawa G, Yamada Y, Tagawa T, et al. Significance of Spread Through Air Spaces in Resected Pathological Stage I Lung Adenocarcinoma. *Ann Thorac Surg*. Published online 2018. doi:10.1016/j.athoracsur.2018.01.037
147. Warth A. Spread through air spaces (STAS): prognostic impact of a semi-quantitative assessment. *J Thorac Dis*. 2017;9(7):1792-1795. doi:10.21037/jtd.2017.06.53
148. Warth A, Beasley MB, Mino-Kenudson M. Breaking New Ground: The Evolving Concept of Spread through Air Spaces (STAS). *J Thorac Oncol*. 2017;12(2):176-178. doi:10.1016/j.jtho.2016.10.020
149. Chen H-Z, Bertino EM, He K. Tumor spread through air space (STAS) is an important predictor of clinical outcome in stage IA lung adenocarcinoma. *J Thorac Dis*. 2017;9(8):2283-2285. doi:10.21037/jtd.2017.07.69
150. Warth A. Spread through air spaces (STAS): a comprehensive update. *Transl lung cancer Res*. 2017;6(5):501-507. doi:10.21037/jtd.2017.06.53
151. Morales-Oyarvide V, Mino-Kenudson M. Taking the measure of lung adenocarcinoma: towards a quantitative approach to tumor spread through air spaces (STAS). *J Thorac Dis*. 2017;9(9):2756-2761. doi:10.21037/jtd.2017.07.97
152. Beasley MB, Dembitzer FR, Flores RM. Surgical pathology of early stage non-small cell lung carcinoma. *Ann Transl Med*. 2016;4(12):238-238. doi:10.21037/atm.2016.06.13

153. Kadota K, Kushida Y, Katsuki N, et al. Tumor Spread Through Air Spaces Is an Independent Predictor of Recurrence-free Survival in Patients With Resected Lung Squamous Cell Carcinoma. *Am J Surg Pathol*. 2017;41(8):1077-1086. doi:10.1097/PAS.0000000000000872
154. Abdel-Wanis MES, Tsuchiya H, Kawahara N, Tomita K. Tumor growth potential after tumoral and instrumental contamination: An in-vivo comparative study of T-saw, Gigli saw, and scalpel. *J Orthop Sci*. 2001;6(5):424-429. doi:10.1007/s007760170009
155. Scotti V, Di Cataldo V, Falchini M, et al. Isolated chest wall implantation of non-small cell lung cancer after fine-needle aspiration: a case report and review of the literature. *Tumori*. 98(5):126e-129e. doi:10.1700/1190.13213
156. McDonald CF, Baird L. Risk of needle track metastasis after fine needle lung aspiration in lung cancer--a case report. *Respir Med*. 1994;88(8):631-632. Accessed March 23, 2018. <http://www.ncbi.nlm.nih.gov/pubmed/7991890>
157. Matsuguma H, Nakahara R, Kondo T, Kamiyama Y, Mori K, Yokoi K. Risk of pleural recurrence after needle biopsy in patients with resected early stage lung cancer. *Ann Thorac Surg*. 2005;80(6):2026-2031. doi:10.1016/j.athoracsur.2005.06.074
158. Smith BD, Kapur D, Esfahanian S, Dhami MS, Fischer JJ. Challenging problems in malignancy: case 2. Isolated needle-track recurrence following fine needle aspiration for non-small-cell lung cancer. *J Clin Oncol*. 2004;22(18):3828-3829. doi:10.1200/JCO.2004.11.058
159. Valle LGM, Rocha RD, Mendes GF, Succi JE, de Andrade JR. Tumor seeding along the needle track after percutaneous lung biopsy. *J Bras Pneumol*. 2016;42(1):71. doi:10.1590/S1806-37562016000000280
160. Adams RF, Gray W, Davies RJO, Gleeson F V. Percutaneous image-guided cutting needle biopsy of the pleura in the diagnosis of malignant mesothelioma. *Chest*. 2001;120(6):1798-1802.
161. Gerrand CH, Rankin K. The hazards of biopsy in patients with malignant primary bone and soft-tissue tumors. In: *Classic Papers in Orthopaedics*. ; 2014:491-493. doi:10.1007/978-1-4471-5451-8_129
162. Blaauwgeers H, Flieder D, Warth A, et al. A Prospective Study of Loose Tissue Fragments in Non-Small Cell Lung Cancer Resection Specimens. *Am J Surg Pathol*. 2017;41(9):1226-1230. doi:10.1097/PAS.0000000000000889
163. Persson C. Primary lysis of eosinophils in severe desquamative asthma. *Clin Exp Allergy*. 2014;44(2):173-183. doi:10.1111/cea.12255
164. Kamiya K, Hayashi Y, Douguchi J, et al. Histopathological features and prognostic significance of the micropapillary pattern in lung adenocarcinoma. *Mod Pathol*. 2008;21(8):992-1001. doi:10.1038/modpathol.2008.79
165. Zhao S, Guo T, Li J, et al. Expression and prognostic value of GalNAc-T3 in patients with completely resected small (≤ 2 cm) peripheral lung adenocarcinoma after IASLC/ATS/ERS classification. *Onco Targets Ther*. 2015;8:3143-3152. doi:10.2147/OTT.S93486
166. Trzpis M, McLaughlin PMJ, de Leij LMFH, Harmsen MC. Epithelial cell adhesion molecule: more than a carcinoma marker and adhesion molecule. *Am J Pathol*. 2007;171(2):386-395. doi:10.2353/ajpath.2007.070152
167. Bofin AM, Lydersen S, Hagmar BM. Cytological criteria for the diagnosis of intraductal hyperplasia, ductal carcinoma in situ, and invasive carcinoma of the breast. *Diagn Cytopathol*. 2004;31(4):207-215. doi:10.1002/dc.20098
168. Zhan B, Lu D, Luo P, Wang B. Prognostic value of expression of microRNAs in non-small cell lung cancer: A systematic review and meta-analysis. *Clin Lab*. 2016;62(11):2203-2211. doi:10.7754/Clin.Lab.2016.160426
169. Zhu CQ, Shih W, Ling CH, Tsao MS. Immunohistochemical markers of prognosis in non-small cell lung cancer: A review and proposal for a multiphase approach to marker evaluation. *J Clin Pathol*. 2006;59(8):790-800. doi:10.1136/jcp.2005.031351

170. Gaikwad A, Souza CA, Inacio JR, et al. Aerogenous metastases: a potential game changer in the diagnosis and management of primary lung adenocarcinoma. *Am J Roentgenol*. 2014;203(6):W570-W582. doi:10.2214/AJR.13.12088
171. Aly RG, Rekhtman N, Li X, et al. Spread Through Air Spaces (STAS) Is Prognostic in Atypical Carcinoid, Large Cell Neuroendocrine Carcinoma, and Small Cell Carcinoma of the Lung. *J Thorac Oncol Off Publ Int Assoc Study Lung Cancer*. 2019;14(9):1583-1593. doi:10.1016/j.jtho.2019.05.009
172. Walts AE, Marchevsky AM. Current Evidence Does Not Warrant Frozen Section Evaluation for the Presence of Tumor Spread Through Alveolar Spaces. *Arch Pathol Lab Med*. 2018;142(1):59-63. doi:10.5858/arpa.2016-0635-OA
173. Blaauwgeers H, Russell PA, Jones KD, Radonic T, Thunnissen E. Pulmonary loose tumor tissue fragments and spread through air spaces (STAS): Invasive pattern or artifact? A critical review. *Lung Cancer*. 2018;123(July):107-111. doi:10.1016/j.lungcan.2018.07.017
174. Pelosi G, Nesa F, Taietti D, et al. Spread of hyperplastic pulmonary neuroendocrine cells into air spaces (S.H.I.P.M.E.N.T.S): A proof for artifact. *Lung Cancer*. 2019;137:43-47. doi:10.1016/j.lungcan.2019.09.006
175. Metovic J, Falco EC, Vissio E, et al. Gross Specimen Handling Procedures Do Not Impact the Occurrence of Spread through Air Spaces (STAS) in Lung Cancer. *Am J Surg Pathol*. 2021;45(2):215-222. doi:10.1097/PAS.0000000000001642
176. Cha SI, Shin KM, Lim JK, et al. Pulmonary embolism concurrent with lung cancer and central emboli predict mortality in patients with lung cancer and pulmonary embolism. *J Thorac Dis*. 2018;10(1):262-272. doi:10.21037/jtd.2017.12.32
177. Price LC, Seckl MJ, Dorfmueller P, Wort SJ. Tumoral pulmonary hypertension. *Eur Respir Rev*. 2019;28(151):1-15. doi:10.1183/16000617.0065-2018
178. Miyano S, Izumi S, Takeda Y, et al. Pulmonary Tumor Thrombotic Microangiopathy. *J Clin Oncol*. 2007;25(5):597-599. doi:10.1200/JCO.2006.09.0670
179. Price LC, Wells AU, Wort SJ. Pulmonary tumour thrombotic microangiopathy. *Curr Opin Pulm Med*. 2016;22(5):421-428. doi:10.1097/MCP.0000000000000297
180. Mainardi AS, Trow T. Tumor Emboli: A Rare Cause of Acute Pulmonary Hypertension. *Am J Med*. 2017;130(4):e137-e139. doi:10.1016/j.amjmed.2016.11.023
181. Vincenten JPL, Smit EF, Grünberg K, et al. Is the current diagnostic algorithm reliable for selecting cases for EGFR- and KRAS-mutation analysis in lung cancer? *Lung Cancer*. 2015;89(1):19-26. doi:https://doi.org/10.1016/j.lungcan.2015.04.005
182. Brierley JD, Gospodarowicz M, Wittekind C. *TNM Classification of Malignant Tumors*. 8th ed. John Wiley & Sons, Inc.; 2017.
183. Al-Mehisen R, Al-Halees Z, Alnemri K, Al-Hemayed W, Al-Mohaissen M. Primary pulmonary artery sarcoma: A rare and overlooked differential diagnosis of pulmonary embolism. Clues to diagnosis. *Int J Surg Case Rep*. 2019;65:15-19. doi:10.1016/j.ijscr.2019.10.014
184. Mehta RI, Mehta RI, Choi JM, Mukherjee A, Castellani RJ. Hydrophilic polymer embolism and associated vasculopathy of the lung: prevalence in a retrospective autopsy study. *Hum Pathol*. 2015;46(2):191-201. doi:10.1016/j.humpath.2014.09.011
185. Miyaoka M, Hatanaka K, Uekusa T, Nakamura N. Clinicopathological features of hydrophilic polymer emboli in Japanese autopsy cases. *Apmis*. 2018;126(11):838-841. doi:10.1111/apm.12891
186. Hickey TB, Honig A, Ostry AJ, et al. Iatrogenic embolization following cardiac intervention: postmortem analysis of 110 cases. *Cardiovasc Pathol*. 2019;40:12-18. doi:10.1016/j.carpath.2019.01.003
187. Maly V, Maly O, Kolostova K, Bobek V. Circulating tumor cells in diagnosis and treatment of lung cancer. *In Vivo (Brooklyn)*. 2019;33(4):1027-1037. doi:10.21873/invivo.11571

188. Crosbie PAJ, Shah R, Krysiak P, et al. Circulating tumor cells detected in the tumor-draining pulmonary vein are associated with disease recurrence after surgical resection of NSCLC. *J Thorac Oncol*. 2016;11(10):1793-1797. doi:10.1016/j.jtho.2016.06.017
189. Pechet TTV, Carr SR, Collins JE, Cohn HE, Farber JL. Arterial invasion predicts early mortality in stage I non-small cell lung cancer. *Ann Thorac Surg*. 2004;78(5):1748-1753. doi:10.1016/j.athoracsur.2004.04.061
190. Al-Alao BS, Gately K, Nicholson S, McGovern E, Young VK, O'Byrne KJ. Prognostic impact of vascular and lymphovascular invasion in early lung cancer. *Asian Cardiovasc Thorac Ann*. 2014;22(1):55-64. doi:10.1177/0218492313478431
191. Maeda R, Yoshida J, Ishii G, Hishida T, Nishimura M, Nagai K. Prognostic impact of intratumoral vascular invasion in non-small cell lung cancer patients. *Thorax*. 2010;65(12):1092-1098. doi:10.1136/thx.2010.141861
192. Mete O, Asa SL. Pathological definition and clinical significance of vascular invasion in thyroid carcinomas of follicular epithelial derivation. *Mod Pathol*. 2011;24(12):1545-1552. doi:10.1038/modpathol.2011.119
193. Kryvenko ON, Epstein JI. Histologic criteria and pitfalls in the diagnosis of lymphovascular invasion in radical prostatectomy specimens. *Am J Surg Pathol*. 2012;36(12):1865-1873. doi:10.1097/PAS.0b013e318262c3d0
194. Leijssen LGJ, Dinaux AM, Amri R, et al. Impact of intramural and extramural vascular invasion on stage II-III colon cancer outcomes. *J Surg Oncol*. 2019;119(6):749-757. doi:10.1002/jso.25367
195. Van Eeghen EE, Flens MJ, Mulder MMR, Loffeld RJLF. Extramural venous invasion as prognostic factor of recurrence in stage 1 and 2 colon cancer. *Gastroenterol Res Pract*. 2017;2017:1-6. doi:10.1155/2017/1598670
196. Metovic J, Falco EC, Vissio E, et al. Gross Specimen Handling Procedures Do Not Impact the Occurrence of Spread Through Air Spaces (STAS) in Lung Cancer. *Am J Surg Pathol*. 2021;45(2):215-222. doi:10.1097/PAS.0000000000001642
197. Blaauwgeers H, Thunnissen E. Spread Through Air Spaces (STAS): Can an Artifact Really be Excluded? *Am J Surg Pathol*. 2021;145(10):1439. doi:10.1097/PAS.0000000000001787
198. Radonic T, Dickhoff C, Mino-Kenudson M, Lely R, Paul R, Thunnissen E. Gross handling of pulmonary resection specimen: Maintaining the 3-dimensional orientation. *J Thorac Dis*. 2019;11(S1):S37-S44. doi:10.21037/jtd.2018.12.36
199. Gross DJ, Hsieh MS, Li Y, et al. Spread Through Air Spaces (STAS) in Non-Small Cell Lung Carcinoma: Evidence Supportive of an In Vivo Phenomenon. *Am J Surg Pathol*. 2021;45(11):1509-1515. doi:10.1097/PAS.0000000000001788
200. Eguchi T, Kameda K, Lu S, et al. Lobectomy Is Associated with Better Outcomes than Sublobar Resection in Spread through Air Spaces (STAS)-Positive T1 Lung Adenocarcinoma: A Propensity Score-Matched Analysis. *J Thorac Oncol Off Publ Int Assoc Study Lung Cancer*. 2019;14(1):87-98. doi:10.1016/j.jtho.2018.09.005
201. Kadota K, Kushida Y, Kagawa S, et al. Limited Resection Is Associated With a Higher Risk of Locoregional Recurrence than Lobectomy in Stage I Lung Adenocarcinoma With Tumor Spread Through Air Spaces. *Am J Surg Pathol*. 2019;43(8):1033-1041. doi:10.1097/PAS.0000000000001285
202. Ikeda T, Kadota K, Go T, Haba R, Yokomise H. Current status and perspectives of spread through air spaces in lung cancer. *Thorac cancer*. 2021;12(11):1639-1646. doi:10.1111/1759-7714.13918
203. Qi L, Xue K, Cai Y, Lu J, Li X, Li M. Predictors of CT Morphologic Features to Identify Spread Through Air Spaces Preoperatively in Small-Sized Lung Adenocarcinoma. *Front Oncol*. 2020;10:548430. doi:10.3389/fonc.2020.548430

204. Villalba JA, Shih AR, Sayo TMS, et al. Accuracy and Reproducibility of Intraoperative Assessment on Tumor Spread Through Air Spaces in Stage 1 Lung Adenocarcinomas. *J Thorac Oncol.* 2021;16(4):619-629. doi:10.1016/j.jtho.2020.12.005
205. Zhou F, Villalba JA, Sayo TMS, et al. Assessment of the feasibility of frozen sections for the detection of spread through air spaces (STAS) in pulmonary adenocarcinoma. *Mod Pathol an Off J United States Can Acad Pathol Inc.* Published online July 2021. doi:10.1038/s41379-021-00875-x
206. Thunnissen E, Motoi N, Minami Y, et al. Elastin in pulmonary pathology: relevance in tumours with a lepidic or papillary appearance. A comprehensive understanding from a morphological viewpoint. *Histopathology.* 2022;80(3):457-467. doi:10.1111/his.14537
207. Hiller JG, Perry NJ, Pouligiannis G, Riedel B, Sloan EK. Perioperative events influence cancer recurrence risk after surgery. *Nat Rev Clin Oncol.* 2018;15(4):205-218. doi:10.1038/nrclinonc.2017.194
208. Scheinin T, Koivuniemi A. Factors influencing the occurrence of circulating malignant cells in lung cancer. *Cancer.* 1963;16:639-645. doi:10.1002/1097-0142(196305)16:5<639::aid-cncr2820160515>3.0.co;2-a
209. Hashimoto M, Tanaka F, Yoneda K, et al. Significant increase in circulating tumour cells in pulmonary venous blood during surgical manipulation in patients with primary lung cancer. *Interact Cardiovasc Thorac Surg.* 2014;18(6):775-783. doi:10.1093/icvts/ivu048
210. Song PP, Zhang W, Zhang B, Liu Q, Du JJ. Effects of different sequences of pulmonary artery and vein ligations during pulmonary lobectomy on blood micrometastasis of non-small cell lung cancer. *Oncol Lett.* 2013;5(2):463-468. doi:10.3892/ol.2012.1022
211. Chudasama D, Burnside N, Beeson J, Karteris E, Rice A, Anikin V. Perioperative detection of circulating tumour cells in patients with lung cancer. *Oncol Lett.* 2017;14(2):1281-1286. doi:10.3892/ol.2017.6366
212. Murlidhar V, Reddy RM, Fouladdel S, et al. Poor Prognosis Indicated by Venous Circulating Tumor Cell Clusters in Early-Stage Lung Cancers. *Cancer Res.* 2017;77(18):5194-5206. doi:10.1158/0008-5472.CAN-16-2072
213. Duan X, Zhu Y, Cui Y, et al. Circulating tumor cells in the pulmonary vein increase significantly after lobectomy: A prospective observational study. *Thorac Cancer.* 2019;10(2):163-169. doi:10.1111/1759-7714.12925
214. Lv C, Zhao B, Wang L, et al. Detection of circulating tumor cells in pulmonary venous blood for resectable non-small cell lung cancer. *Oncol Lett.* 2018;15(1):1103-1112. doi:10.3892/ol.2017.7405
215. Kurusu Y, Yamashita J, Ogawa M. Detection of circulating tumor cells by reverse transcriptase-polymerase chain reaction in patients with resectable non-small-cell lung cancer. *Surgery.* 1999;126(5):820-826. doi:10.1016/S0039-6060(99)70020-6
216. Hashimoto M, Tanaka F, Yoneda K, et al. Positive correlation between postoperative tumor recurrence and changes in circulating tumor cell counts in pulmonary venous blood (pvCTC) during surgical manipulation in non-small cell lung cancer. *J Thorac Dis.* 2018;10(1):298-306. doi:10.21037/jtd.2017.12.56
217. Funaki S, Sawabata N, Abulaiti A, et al. Significance of tumour vessel invasion in determining the morphology of isolated tumour cells in the pulmonary vein in non-small-cell lung cancer. *Eur J Cardio-Thoracic Surg.* 2013;43(6):1126-1130. doi:10.1093/ejcts/ezs553
218. Sienel W, Seen-Hibler R, Mutschler W, Pantel K, Passlick B. Tumour cells in the tumour draining vein of patients with non-small cell lung cancer: detection rate and clinical significance. *Eur J Cardio-Thoracic Surg.* 2003;23(4):451-456. doi:10.1016/S1010-7940(02)00865-5
219. Yao X, Williamson C, Adalsteinsson VA, et al. Tumor cells are dislodged into the pulmonary vein during lobectomy. *J Thorac Cardiovasc Surg.* 2014;148(6):3224-3231. doi:10.1016/j.jtcvs.2014.06.074

220. Yagi Y, Aly RG, Tabata K, et al. Three-Dimensional Histologic, Immunohistochemical, and Multiplex Immunofluorescence Analyses of Dynamic Vessel Co-Option of Spread Through Air Spaces in Lung Adenocarcinoma. *J Thorac Oncol*. 2020;15(4):589-600. doi:10.1016/j.jtho.2019.12.112
221. Bridgeman VL, Vermeulen PB, Foo S, et al. Vessel co-option is common in human lung metastases and mediates resistance to anti-angiogenic therapy in preclinical lung metastasis models. *J Pathol*. 2017;241(3):362-374. doi:10.1002/path.4845
222. Yamamoto M, Kunugi S, Ishikawa A, Fukuda Y. Considerations on the mechanisms of alveolar remodeling in centriacinar emphysema. *Virchows Arch*. 2010;456(5):571-579. doi:10.1007/s00428-010-0903-y
223. Linden MD. Histology for Pathologists. Mills S, ed. *Am J Surg Pathol*. 2008;32(7):1109-1110. doi:10.1097/pas.0b013e3181659143
224. Metovic J, Volante M, Righi L, Papotti M. Reply: Spread Through Air Spaces. STAS Can an artifact really be excluded? *Am J Surg Pathol*. 2021;45(10):1439-1440. doi:10.1097/PAS.0000000000001791
225. Xie H, Su H, Zhu E, et al. Morphological Subtypes of Tumor Spread Through Air Spaces in Non-Small Cell Lung Cancer: Prognostic Heterogeneity and Its Underlying Mechanism. *Front Oncol*. 2021;11:608353. doi:10.3389/fonc.2021.608353
226. Doxtader EE, Pijuan L, Lepe M, et al. Displaced Cartilage Within Lymph Node Parenchyma Is a Novel Biopsy Site Change in Resected Mediastinal Lymph Nodes Following EBUS-TBNA. *Am J Surg Pathol*. 2019;43(4):497-503. doi:10.1097/PAS.0000000000001197
227. Toyokawa G, Yamada Y, Tagawa T, et al. P3.16-033 Significance of Spread through Air Spaces in Resected Pathological Stage I Lung Adenocarcinoma. *J Thorac Oncol*. 2017;12(11):S2355. doi:10.1016/j.jtho.2017.09.1839
228. Uruga H, Fujii T, Fujimori S, Kohno T, Kishi K. Semiquantitative Assessment of Tumor Spread through Air Spaces (STAS) in Early-Stage Lung Adenocarcinomas. *J Thorac Oncol Off Publ Int Assoc Study Lung Cancer*. 2017;12(7):1046-1051. doi:10.1016/j.jtho.2017.03.019
229. Shiono S, Endo M, Suzuki K, Yarimizu K, Hayasaka K, Yanagawa N. Spread Through Air Spaces Is a Prognostic Factor in Sublobar Resection of Non-Small Cell Lung Cancer. *Ann Thorac Surg*. 2018;106(2):354-360. doi:10.1016/j.athoracsur.2018.02.076
230. Hu S-Y, Hsieh M-S, Hsu H-H, et al. Correlation of tumor spread through air spaces and clinicopathological characteristics in surgically resected lung adenocarcinomas. *Lung Cancer*. 2018;126:189-193. doi:10.1016/j.lungcan.2018.11.003
231. Qiu X, Chen D, Liu Y, et al. Relationship between stromal cells and tumor spread through air spaces in lung adenocarcinoma. *Thorac cancer*. 2019;10(2):256-267. doi:10.1111/1759-7714.12945
232. Shiono S, Endo M, Suzuki K, Hayasaka K, Yanagawa N. Spread through air spaces in lung cancer patients is a risk factor for pulmonary metastasis after surgery. *J Thorac Dis*. 2019;11(1):177-187. doi:10.21037/jtd.2018.12.21
233. Ren Y, Xie H, Dai C, et al. Prognostic Impact of Tumor Spread Through Air Spaces in Sublobar Resection for 1A Lung Adenocarcinoma Patients. *Ann Surg Oncol*. 2019;26(6):1901-1908. doi:10.1245/s10434-019-07296-w
234. Liu A, Hou F, Qin Y, et al. Predictive value of a prognostic model based on pathologic features in lung invasive adenocarcinoma. *Lung Cancer*. 2019;131:14-22. doi:10.1016/j.lungcan.2019.03.002
235. Song T, Jiang L, Zhuo Z, et al. Impacts of thoracoscopic surgery and high grade histologic subtypes on spread through air spaces in small stage I lung adenocarcinomas. *J Cancer Res Clin Oncol*. 2019;145(9):2375-2382. doi:10.1007/s00432-019-02972-6
236. Vaghjiani RG, Takahashi Y, Eguchi T, et al. Tumor Spread Through Air Spaces Is a Predictor of Occult Lymph Node Metastasis in Clinical Stage IA Lung Adenocarcinoma. *J Thorac Oncol Off Publ Int Assoc Study Lung Cancer*. 2020;15(5):792-802. doi:10.1016/j.jtho.2020.01.008

237. Jia M, Yu S, Yu J, Li Y, Gao H, Sun P-L. Comprehensive analysis of spread through air spaces in lung adenocarcinoma and squamous cell carcinoma using the 8th edition AJCC/UICC staging system. *BMC Cancer*. 2020;20(1):705. doi:10.1186/s12885-020-07200-w
238. Yi E, Lee JH, Jung Y, Chung JH, Lee Y, Lee S. Clinical implication of tumour spread through air spaces in pathological stage I lung adenocarcinoma treated with lobectomy. *Interact Cardiovasc Thorac Surg*. 2021;32(1):64-72. doi:10.1093/icvts/ivaa227
239. Zhang Z, Liu Z, Feng H, et al. Predictive value of radiological features on spread through air space in stage cIA lung adenocarcinoma. *J Thorac Dis*. 2020;12(11):6494-6504. doi:10.21037/jtd-20-1820
240. Han YB, Kim H, Mino-Kenudson M, et al. Tumor spread through air spaces (STAS): prognostic significance of grading in non-small cell lung cancer. *Mod Pathol an Off J United States Can Acad Pathol Inc*. 2021;34(3):549-561. doi:10.1038/s41379-020-00709-2
241. Lee MA, Kang J, Lee HY, et al. Spread through air spaces (STAS) in invasive mucinous adenocarcinoma of the lung: Incidence, prognostic impact, and prediction based on clinoradiologic factors. *Thorac cancer*. 2020;11(11):3145-3154. doi:10.1111/1759-7714.13632
242. Zeng Q, Wang B, Li J, et al. Solid Nodule Appearance as a Predictor of Tumor Spread Through Air Spaces in Patients with Lung Adenocarcinoma: A Propensity Score Matching Study. *Cancer Manag Res*. 2020;12:8197-8207. doi:10.2147/CMAR.S266750
243. Shiono S, Yanagawa N. Spread through air spaces is a predictive factor of recurrence and a prognostic factor in stage I lung adenocarcinoma. *Interact Cardiovasc Thorac Surg*. 2016;23(4):567-572. doi:10.1093/icvts/ivw211
244. Masai K, Sakurai H, Sukeda A, et al. Prognostic Impact of Margin Distance and Tumor Spread Through Air Spaces in Limited Resection for Primary Lung Cancer. *J Thorac Oncol*. 2017;12(12):1788-1797. doi:10.1016/j.jtho.2017.08.015
245. Lee JS, Kim EK, Kim M, Shim HS. Genetic and clinicopathologic characteristics of lung adenocarcinoma with tumor spread through air spaces. *Lung Cancer*. 2018;123:121-126. doi:10.1016/j.lungcan.2018.07.020
246. Terada Y, Takahashi T, Morita S, et al. Spread through air spaces is an independent predictor of recurrence in stage III (N2) lung adenocarcinoma. *Interact Cardiovasc Thorac Surg*. 2019;29(3):442-448. doi:10.1093/icvts/ivz116
247. Suh JW, Jeong YH, Cho A, et al. Stepwise flowchart for decision making on sublobar resection through the estimation of spread through air space in early stage lung cancer(1). *Lung Cancer*. 2020;142:28-33. doi:10.1016/j.lungcan.2020.02.001
248. Cao L, Jia M, Sun P-L, Gao H. Histopathologic features from preoperative biopsies to predict spread through air spaces in early-stage lung adenocarcinoma: a retrospective study. *BMC Cancer*. 2021;21(1):913. doi:10.1186/s12885-021-08648-0
249. Tian Y, Feng J, Jiang L, et al. Integration of clinicopathological and mutational data offers insight into lung cancer with tumor spread through air spaces. *Ann Transl Med*. 2021;9(12):985. doi:10.21037/atm-21-2256
250. Alvarez Moreno JC, Aljamal AA, Bahmad HF, et al. Correlation between spread through air spaces (STAS) and other clinicopathological parameters in lung cancer. *Pathol Res Pract*. 2021;220:153376. doi:10.1016/j.prp.2021.153376
251. Wen Y, Qiu G, Liu Z, Liang H, He J, Liang W. P2.09-04 The Clinicopathological Characteristics and Prognosis of Lung Cancer with Tumor Spread Through Air Spaces: A Meta-Analysis. *J Thorac Oncol*. 2019;14(10):S769-S770. doi:10.1016/j.jtho.2019.08.1653
252. Moreira AL, Ocampo PSS, Xia Y, et al. A Grading System for Invasive Pulmonary Adenocarcinoma: A Proposal From the International Association for the Study of Lung Cancer Pathology Committee. *J Thorac Oncol*. 2020;15(10):1599-1610. doi:10.1016/j.jtho.2020.06.001
253. Starcher BC. Lung elastin and matrix. *Chest*. 2000;117(5 Suppl 1):229S-34S. doi:10.1378/chest.117.5_suppl_1.229s-a

254. Toshima M, Ohtani Y, Ohtani O. Three-dimensional architecture of elastin and collagen fiber networks in the human and rat lung. *Arch Histol Cytol.* 2004;67(1):31-40. doi:10.1679/aohc.67.31
255. Thomson J, Singh M, Eckersley A, Cain SA, Sherratt MJ, Baldock C. Fibrillin microfibrils and elastic fibre proteins: Functional interactions and extracellular regulation of growth factors. *Semin Cell Dev Biol.* 2019;89:109-117. doi:10.1016/j.semcdb.2018.07.016
256. Rifkin DB, Rifkin WJ, Zilberberg L. LTBP in biology and medicine: LTBP diseases. *Matrix Biol.* 2018;71-72:90-99. doi:10.1016/j.matbio.2017.11.014
257. Vindin H, Mithieux SM, Weiss AS. Elastin architecture. *Matrix Biol.* 2019;84:4-16. doi:10.1016/j.matbio.2019.07.005
258. Godwin ARF, Singh M, Lockhart-Cairns MP, Alanazi YF, Cain SA, Baldock C. The role of fibrillin and microfibril binding proteins in elastin and elastic fibre assembly. *Matrix Biol.* 2019;84:17-30. doi:10.1016/j.matbio.2019.06.006
259. Dabovic B, Robertson IB, Zilberberg L, Vassallo M, Davis EC, Rifkin DB. Function of latent TGF β binding protein 4 and fibulin 5 in elastogenesis and lung development. *J Cell Physiol.* 2015;230(1):226-236. doi:10.1002/jcp.24704
260. Uversky VN. Unusual biophysics of intrinsically disordered proteins. *Biochim Biophys Acta.* 2013;1834(5):932-951. doi:10.1016/j.bbapap.2012.12.008
261. Mecham RP. Elastin in lung development and disease pathogenesis. *Matrix Biol.* 2018;73:6-20. doi:10.1016/j.matbio.2018.01.005
262. Shapiro SD, Endicott SK, Province MA, Pierce JA, Campbell EJ. Marked longevity of human lung parenchymal elastic fibers deduced from prevalence of D-aspartate and nuclear weapons-related radiocarbon. *J Clin Invest.* 1991;87(5):1828-1834. doi:10.1172/JCI115204
263. Campbell E, Pierce J, Endicott S, Shapiro S. Evaluation of extracellular matrix turnover. Methods and results for normal human lung parenchymal elastin. *Chest.* 1991;99(3 Suppl):49S. doi:10.1378/chest.99.3_supplement.49s
264. Uehara T, Honda T, Sano K, Hachiya T, Ota H. A three-dimensional analysis of blood vessels in bronchioloalveolar carcinoma. *Lung.* 2004;182(6):343-353. doi:10.1007/s00408-004-2515-2
265. Honda T, Ota H, Sano K, et al. Alveolar shrinkage in bronchioloalveolar carcinoma without central fibrosis. *Lung Cancer.* 2002;36(3):283-288. doi:10.1016/s0169-5002(02)00002-8
266. Sakurai H, Maeshima A, Watanabe SI, et al. Grade of Stromal Invasion in Small Adenocarcinoma of the Lung: Histopathological Minimal Invasion and Prognosis. *Am J Surg Pathol.* 2004;28(2):198-206. doi:10.1097/00000478-200402000-00007
267. Chao C-M, Moiseenko A, Zimmer K-P, Bellusci S. Alveologenesis: key cellular players and fibroblast growth factor 10 signaling. *Mol Cell Pediatr.* 2016;3(1). doi:10.1186/s40348-016-0045-7
268. Dickie R, Wang YT, Butler JP, Schulz H, Tsuda A. Distribution and quantity of contractile tissue in postnatal development of rat alveolar interstitium. *Anat Rec.* 2008;291(1):83-93. doi:10.1002/ar.20622
269. Blaauboer ME, Smit TH, Hanemaaijer R, Stoop R, Everts V. Cyclic mechanical stretch reduces myofibroblast differentiation of primary lung fibroblasts. *Biochem Biophys Res Commun.* 2011;404(1):23-27. doi:10.1016/j.bbrc.2010.11.033
270. Brandsma C-A, van den Berge M, Postma DS, et al. A large lung gene expression study identifying fibulin-5 as a novel player in tissue repair in COPD. *Thorax.* 2015;70(1):21-32. doi:10.1136/thoraxjnl-2014-205091
271. Tsubosaka A, Matsushima J, Ota M, et al. Whole-lung pathology of pleuroparenchymal fibroelastosis (PPFE) in an explanted lung: Significance of elastic fiber-rich, non-specific interstitial pneumonia-like change in chemotherapy-related PPFE. *Pathol Int.* 2019;69(9):547-555. doi:10.1111/pin.12833

272. Matsubara D, Morikawa T, Goto A, Nakajima J, Fukayama M, Niki T. Subepithelial myofibroblast in lung adenocarcinoma: A histological indicator of excellent prognosis. *Mod Pathol*. 2009;22(6):776-785. doi:10.1038/modpathol.2009.27
273. Eto T, Suzuki H, Honda A, Nagashima Y. The changes of the stromal elastotic framework in the growth of peripheral lung adenocarcinomas. *Cancer*. 1996;77(4):646-656. doi:10.1002/(SICI)1097-0142(19960215)77:4<646::AID-CNCR10>3.0.CO;2-0
274. Fukushima M, Fukuda Y, Kawamoto M, Yamanaka N. Elastosis in lung carcinoma: immunohistochemical, ultrastructural and clinical studies. *Pathol Int*. 2000;50(8):626-635. doi:10.1046/j.1440-1827.2000.01103.x
275. Kung IT, Lui IO, Loke SL, et al. Pulmonary scar cancer. A pathologic reappraisal. *Am J Surg Pathol*. 1985;9(6):391-400. doi:10.1097/00000478-198506000-00001
276. Shimosato Y, Suzuki A, Hashimoto T, et al. Prognostic implications of fibrotic focus (scar) in small peripheral lung cancers. *Am J Surg Pathol*. 1980;4(4):365-373. doi:10.1097/00000478-198008000-00005
277. Yamashiro K, Yasuda S, Nagase A, Hirata T, Nojima T, Nagashima K. Prognostic significance of an interface pattern of central fibrosis and tumor cells in peripheral adenocarcinoma of the lung. *Hum Pathol*. 1995;26(1):67-73. doi:10.1016/0046-8177(95)90116-7
278. Kumar V, Abbas A, Fausto N. *Robbins and Cotran Pathologic Basis of Disease*. 7th ed.; 2005.
279. Ambrosi F, Lissenberg-Witte B, Comans E, et al. Tumor Atelectasis Gives Rise to a Solid Appearance in Pulmonary Adenocarcinomas on High-Resolution Computed Tomography. *JTO Clin Res Reports*. 2020;1(2):100018. doi:10.1016/j.jtocrr.2020.100018
280. Honda T, Ishida K, Hayama M, Kubo K, Katsuyama T. Type II pneumocytes are preferentially located along thick elastic fibers forming the framework of human alveoli. *Anat Rec*. 2000;258(1):34-38. doi:10.1002/(SICI)1097-0185(20000101)258:1<34::AID-AR4>3.0.CO;2-7
281. Japanese Lung Cancer Society, ed. *Japanese Lung Cancer Society, Ed. General Rules for Clinical and Pathological Records of Lung Cancer*. 8th ed. Kanehara Press; 2017.
282. Hasleton PS. Incidence of emphysema. *Thorax*. 1972;27(5):552-556.
283. Satoh K, Kobayashi T, Ohkawa M, Tanabe M. Preparation of human whole lungs inflated and fixed for radiologic-pathologic correlation. *Acad Radiol*. 1997;4(5):374-379. doi:10.1016/s1076-6332(97)80120-1
284. Kobayashi T, Satoh K, Kojima K, Ohkawa M, Tanabe M. [An improved method of preparation of autopsied human inflated-fixed whole lungs for radiologic-pathologic correlation]. *Nihon Igaku Hoshasen Gakkai Zasshi*. 1993;53(11):1301-1312.
285. Boers JE, Ambergen AW, Thunnissen FBJM. Number and proliferation of basal and parabasal cells in normal human airway epithelium. *Am J Respir Crit Care Med*. 1998;157:2000-2006. doi:10.1164/ajrccm.159.5.9806044
286. Boers JE, den Brok JL, Koudstaal J, Arends JW, Thunnissen FB. Number and proliferation of neuroendocrine cells in normal human airway epithelium. *Am J Respir Crit Care Med*. 1996;154(3 Pt 1):758-763. doi:10.1164/ajrccm.154.3.8810616
287. Pratt PC, Vollmer RT, Miller JA. Prevalence and severity of morphologic emphysema and bronchitis in non-textile and cotton-textile workers. *Chest*. 1980;77(2 Suppl):323-325. doi:10.1378/chest.77.2.323
288. Wright JL, Hobson JE, Wiggs B, Pare PD, Hogg JC. Airway inflammation and peribronchiolar attachments in the lungs of nonsmokers, current and ex-smokers. *Lung*. 1988;166(5):277-286. doi:10.1007/BF02714058
289. Kawabata Y, Hoshi E, Murai K, et al. Smoking-related changes in the background lung of specimens resected for lung cancer: a semiquantitative study with correlation to postoperative course. *Histopathology*. 2008;53(6):707-714. doi:10.1111/j.1365-2559.2008.03183.x

290. Fukuda Y, Basset F, Soler P, Ferrans VJ, Masugi Y, Crystal RG. Intraluminal fibrosis and elastic fiber degradation lead to lung remodeling in pulmonary Langerhans cell granulomatosis (histiocytosis X). *Am J Pathol.* 1990;137(2):415-424.
291. Mariani TJ, Crouch E, Roby JD, Starcher B, Pierce RA. Increased elastin production in experimental granulomatous lung disease. *Am J Pathol.* 1995;147(4):988-1000.
292. Honda T, Ota H, Arai K, et al. Three-dimensional analysis of alveolar structure in usual interstitial pneumonia. *Virchows Arch.* 2002;441(1):47-52. doi:10.1007/s00428-001-0567-8
293. Starcher B, Sauter E, Ho C. Elastin turnover in malignant solid tumors. *Connect Tissue Res.* 2013;54(4-5):313-318. doi:10.3109/03008207.2013.820723
294. Lagstein A. Pulmonary apical cap-what's old is new again. *Arch Pathol Lab Med.* 2015;139(10):1258-1262. doi:10.5858/arpa.2015-0224-RA
295. Von Der Thüsen JH, Hansell DM, Tominaga M, et al. Pleuroparenchymal fibroelastosis in patients with pulmonary disease secondary to bone marrow transplantation. *Mod Pathol.* 2011;24(12):1633-1639. doi:10.1038/modpathol.2011.114
296. Kinoshita Y, Watanabe K, Ishii H, Kushima H, Fujita M, Nabeshima K. Proliferation of elastic fibres in idiopathic pulmonary fibrosis: a whole-slide image analysis and comparison with pleuroparenchymal fibroelastosis. *Histopathology.* 2017;71(6):934-942. doi:10.1111/his.13312
297. Parra ER, Kairalla RA, De Carvalho CRR, Capelozzi VL. Abnormal deposition of collagen/elastic vascular fibres and prognostic significance in idiopathic interstitial pneumonias. *Thorax.* 2007;62(5):428-437. doi:10.1136/thx.2006.062687
298. Kawabata Y, Hoshi E, Takayanagi N, Sugita Y. [Pathological study of the natural history of pulmonary infarction mainly seen in lung tumors--pulmonary infarction begins with alveolar wall bleeding]. *Nihon Kokyuki Gakkai Zasshi.* 2009;47(10):851-857.
299. Groshong S, Tomaszewski J, Cool C. Pulmonary vascular disease. In: Tomaszewski J, Cagle P, Farver C, eds. *Dail and Hammer's Pulmonary Pathology.* 3rd ed. Springer NewYork; 2008:1053-1055.
300. Kondo T, Nakazawa T, Murata S, Katoh R. Stromal elastosis in papillary thyroid carcinomas. *Hum Pathol.* 2005;36(5):474-479. doi:10.1016/j.humpath.2005.03.006
301. Chen Y, Klingen TA, Wik E, et al. Breast cancer stromal elastosis is associated with mammography screening detection, low Ki67 expression and favourable prognosis in a population-based study. *Diagn Pathol.* 2014;9:230. doi:10.1186/s13000-014-0230-8
302. Rasmussen BB, Pedersen B V, Thorpe SM, Rose C. Elastosis in relation to prognosis in primary breast carcinoma. *Cancer Res.* 1985;45(3):1428-1430.
303. Ishikawa Y, Miyoshi T, Satoh Y, Okumura S, Nakagawa K. P-659 Noninvasive papillary adenocarcinoma of the lung: A proposal of a new entity. *Lung Cancer.* 2005;49:S291. doi:10.1016/S0169-5002(05)81152-3
304. Barsky S, Huang S, Bhuta S. Extracellular matrix of pulmonary scar carcinomas is suggestive of a desmoplastic origin. *Am J Pathol.* 1986;124:412-419.
305. Yotsukura M, Asamura H, Suzuki S, et al. Prognostic impact of cancer-associated active fibroblasts and invasive architectural patterns on early-stage lung adenocarcinoma. *Lung Cancer.* 2020;145(April):158-166. doi:10.1016/j.lungcan.2020.04.023
306. Travis WD, Brambilla E, Nicholson AG, et al. WHO Classification of Tumours of the Lung, Pleura, Thymus and Heart. Travis W., Brambilla E, Burke AP, Marx A, Nicholson AG, eds. *J Thorac Oncol.* 2015;10(9):1243-1260. <http://content.wkhealth.com/linkback/openurl?sid=WKPTLP:landingpage&an=01243894-900000000-98927%5Cnhttp://www.ncbi.nlm.nih.gov/pubmed/26291008>
307. Travis WD, Asamura H, Bankier AA, et al. The IASLC lung cancer staging project: Proposals for coding T categories for subsolid nodules and assessment of tumor size in part-solid tumors in the forthcoming eighth edition of the TNM classification of lung cancer. *J Thorac Oncol.* 2016;11(8):1204-1223. doi:10.1016/j.jtho.2016.03.025

308. Thunnissen E, Motoi N, Minami Y, et al. Elastin in pulmonary pathology: relevance in tumors with lepidic or papillary appearance. A comprehensive understanding from a morphological viewpoint. *Histopathology*. Published online August 2021. doi:10.1111/his.14537
309. Borczuk AC. Assessment of invasion in lung adenocarcinoma classification, including adenocarcinoma in situ and minimally invasive adenocarcinoma. *Mod Pathol*. 2012;25 Suppl 1(S1):S1-S10. doi:10.1038/modpathol.2011.151
310. Yim J, Zhu L-C, Chiriboga L, Watson HN, Goldberg JD, Moreira AL. Histologic features are important prognostic indicators in early stages lung adenocarcinomas. *Mod Pathol*. 2007;20(2):233-241. doi:10.1038/modpathol.3800734
311. Shih A. Problems in the Reproducibility of Classification of Small Lung Adenocarcinoma: An International Interobserver Study. *Histopathology*. Published online 2019.
312. Boland JM, Froemming AT, Wampfler JA, et al. Adenocarcinoma in situ, minimally invasive adenocarcinoma, and invasive pulmonary adenocarcinoma - Analysis of interobserver agreement, survival, radiographic characteristics, and gross pathology in 296 nodules. *Hum Pathol*. 2016;51:41-50. doi:10.1016/j.humpath.2015.12.010
313. Nicholson AG, Tsao MS, Travis WD, et al. Eighth edition staging of thoracic malignancies: Implications for the reporting pathologist. *Arch Pathol Lab Med*. 2018;142(5):645-661. doi:10.5858/arpa.2017-0245-RA
314. Travis WD. Invasive non-mucinous adenocarcinoma of the lung. In: *WHO Classification of Tumours Editorial Board. Thoracic Tumours [Internet]. Lyon (France): International Agency for Research on Cancer. ; 2021.*
315. Yotsukura M, Asamura H, Motoi N, et al. Long-Term Prognosis of Patients With Resected Adenocarcinoma In Situ and Minimally Invasive Adenocarcinoma of the Lung. *J Thorac Oncol*. 2021;16(8):1312-1320. doi:10.1016/j.jtho.2021.04.007
316. Kadota K, MacMahon H, Matsubara D, Mino-Kenudson M MT. Adenocarcinoma in situ. In: *WHO Classification of Tumours Editorial Board. Thoracic Tumours [Internet]. Lyon (France): International Agency for Research on Cancer; 2021. (WHO Classification of Tumours Series, 5th Ed.; Vol. 5). Available from: <https://tumourclassification.iarc.who.in.> ; 2021.*
317. Thunnissen E, Beasley MB, Borczuk A, et al. Defining morphologic features of invasion in pulmonary non-mucinous adenocarcinoma with lepidic growth - A proposal by the IASLC Pathology Committee. *J Thorac Oncol*. Published online December 2022. doi:10.1016/j.jtho.2022.11.026
318. Nagaiushi C. Bronchoalveolar System. In: Nagaiushi C, ed. *Functional Anatomy and Histology of the Lung*. 1st ed. ; 1972:1-65.
319. Min Kung IT, Lin Lui IO, Loke SL, et al. Pulmonary scar cancer. A pathologic reappraisal. *Am J Surg Pathol*. 1985;9(6):391-400. doi:10.1097/00000478-198506000-00001
320. Blaauwgeers H, Radonic T, Lissenberg-Witte B, et al. P06.02 Incorporating Surgical Collapse in the Pathological Assessment of Resected Adenocarcinoma in situ of the Lung. A Proof of Principle Study. *J Thorac Oncol*. 2021;16(10):S985. doi:10.1016/j.jtho.2021.08.281
321. Weibel ER. *Stereological Methods for Biological Morphometry: 001*. 1st ed. Academic Press Inc.; 1979.
322. Nakazato Y, Minami Y, Kobayashi H, et al. Nuclear grading of primary pulmonary adenocarcinomas: Correlation between nuclear size and prognosis. *Cancer*. 2010;116(8):2011-2019. doi:10.1002/cncr.24948
323. Goto K, Yokose T, Kodama T, et al. Detection of early invasion on the basis of basement membrane destruction in small adenocarcinomas of the lung and its clinical implications. *Mod Pathol*. 2001;14(12):1237-1245. doi:10.1038/modpathol.3880468
324. Mackinnon AC, Luevano A, De Araujo LC, Rao N, Le M, Suster S. Cribriform adenocarcinoma of the lung: Clinicopathologic, immunohistochemical, and molecular analysis of 15 cases of a distinctive morphologic subtype of lung adenocarcinoma. *Mod Pathol*. 2014;27(8):1063-1072. doi:10.1038/modpathol.2013.227

325. Kadota K, Yeh YC, Sima CS, et al. The cribriform pattern identifies a subset of acinar predominant tumors with poor prognosis in patients with stage I lung adenocarcinoma: A conceptual proposal to classify cribriform predominant tumors as a distinct histologic subtype. *Mod Pathol*. 2014;27(5):690-700. doi:10.1038/modpathol.2013.188
326. Nakajima N, Yoshizawa A, Rokutan-Kurata M, et al. Prognostic significance of cribriform adenocarcinoma of the lung: validation analysis of 1,057 Japanese patients with resected lung adenocarcinoma and a review of the literature. *Transl lung cancer Res*. 2021;10(1):117-127. doi:10.21037/tlcr-20-612
327. Kamiya K, Hayashi Y, Douguchi J, et al. Histopathological features and prognostic significance of the micropapillary pattern in lung adenocarcinoma. *Mod Pathol*. 2008;21(8):992-1001. doi:10.1038/modpathol.2008.79
328. Pyo JS, Kim JH. Clinicopathological Significance of Micropapillary Pattern in Lung Adenocarcinoma. *Pathol Oncol Res*. 2018;24(3):547-555. doi:10.1007/s12253-017-0274-7
329. Travis WD, Brambilla E, Noguchi M, et al. International Association for the Study of Lung Cancer/ American Thoracic Society/European Respiratory Society: International multidisciplinary classification of lung adenocarcinoma - An executive summary. *Proc Am Thorac Soc*. 2011;8(5):381-385. doi:10.1513/pats.201107-042ST
330. Butter R, Halfwerk H, Radonic T, Lissenberg-Witte B, Thunnissen E. The impact of impaired tissue fixation in resected non-small-cell lung cancer on protein deterioration and DNA degradation. *Lung Cancer*. 2023;178(January):108-115. doi:10.1016/j.lungcan.2023.02.007
331. Kadota K, Villena-Vargas J, Yoshizawa A, et al. Prognostic significance of adenocarcinoma in situ, minimally invasive adenocarcinoma, and nonmucinous lepidic predominant invasive adenocarcinoma of the lung in patients with stage I disease. *Am J Surg Pathol*. 2014;38(4):448-460. doi:10.1097/PAS.0000000000000134
332. Thunnissen E, Beliën JAM, Kerr KM, et al. In compressed lung tissue microscopic sections of adenocarcinoma in situ may mimic papillary adenocarcinoma. *Arch Pathol Lab Med*. 2013;137(12):1792-1797. doi:10.5858/arpa.2012-0613-SA
333. Shin SS, Sasano H, Kristiansen G et al. *Invasive Lobular Carcinoma*. In: *WHO Classification of Tumours Editorial Board. Breast Tumours [Internet]. Lyon (France): International Agency for Research on Cancer; 2021. (WHO Classification of Tumours Series, 5th Ed.; Vol. 2). Available from: <https://tu.who.int>; 2022.*
334. Suzuki K, Yokose T, Yoshida J, et al. Prognostic significance of the size of central fibrosis in peripheral adenocarcinoma of the lung. *Ann Thorac Surg*. 2000;69(3):893-897. doi:10.1016/S0003-4975(99)01331-4
335. Bittar HE, Jerome JA, Hartman D, Pantanowitz L, Mehrad M, Dacic S. Prognostic significance of microscopic size in peripherally located scar-associated clinical stage I lung carcinomas. *Lung Cancer*. 2020;143(February):12-18. doi:10.1016/j.lungcan.2020.03.004
336. Yambayev I, Sullivan TB, Suzuki K, et al. Pulmonary Adenocarcinomas of Low Malignant Potential: Proposed Criteria to Expand the Spectrum beyond Adenocarcinoma in Situ and Minimally Invasive Adenocarcinoma. *Am J Surg Pathol*. 2021;45(4):567-576. doi:10.1097/PAS.0000000000001618
337. Zugazagoitia J, Enguita AB, Nuñez JA, Iglesias L, Ponce S. The new IASLC/ATS/ERS lung adenocarcinoma classification from a clinical perspective: Current concepts and future prospects. *J Thorac Dis*. 2014;6:S526-S536. doi:10.3978/j.issn.2072-1439.2014.01.27
338. Krishnamoorthy K, Lee M. Improved tests for the equality of normal coefficients of variation. *Comput Stat*. 2014;29(1-2):215-232. doi:10.1007/s00180-013-0445-2
339. Kruger J, Dunning D. Unskilled and unaware of it: how difficulties in recognizing one's own incompetence lead to inflated self-assessments. *J Pers Soc Psychol*. 1999;77(6):1121-1134. doi:10.1037//0022-3514.77.6.1121

340. Noguchi M, Minami Y, Iijima T, Matsuno Y. Reproducibility of the diagnosis of small adenocarcinoma of the lung and usefulness of an educational program for the diagnostic criteria. *Pathol Int*. 2005;55(1):8-13. doi:10.1111/j.1440-1827.2005.01782.x
341. Travis WD, Brambilla E, Nicholson AG, et al. The 2015 World Health Organization Classification of Lung Tumors: Impact of Genetic, Clinical and Radiologic Advances since the 2004 Classification. Travis W., Brambilla E, Burke AP, Marx A, Nicholson AG, eds. *J Thorac Oncol*. 2015;10(9):1243-1260. doi:10.1097/JTO.0000000000000630
342. Blaauwgeers H, Damhuis R, Lissenberg-Witte BI, de Langen AJ, Senan S, Thunnissen E. A Population-Based Study of Outcomes in Surgically Resected T3N0 Non-Small Cell Lung Cancer in The Netherlands, Defined Using TNM-7 and TNM-8; Justification of Changes and an Argument to Incorporate Histology in the Staging Algorithm. *J Thorac Oncol*. 2019;14(3):459-467. doi:10.1016/j.jtho.2018.10.164
343. Filipello F, Blaauwgeers H, Lissenberg-Witte B, et al. 3-dimensional reflection aids in understanding the fog of 2-dimensional pattern recognition in pulmonary adenocarcinomas with emphasis on collapsed adenocarcinoma in situ and a proposal for a revised classification. 2023;submitted.
344. Inafuku K, Yokose T, Ito H, et al. Should Pathologically Noninvasive Lung Adenocarcinoma Larger Than 3 cm Be Classified as T1a? *Ann Thorac Surg*. 2019;108(6):1678-1684. doi:10.1016/j.athoracsur.2019.06.055
345. Strand TE, Rostad H, Strøm EH, Hasleton P. The percentage of lepidic growth is an independent prognostic factor in invasive adenocarcinoma of the lung. *Diagn Pathol*. 2015;10(1):1-7. doi:10.1186/s13000-015-0335-8
346. Ji H, Liu Q, Chen Y, et al. Combined model of radiomics and clinical features for differentiating pneumonic-type mucinous adenocarcinoma from lobar pneumonia: An exploratory study. *Front Endocrinol (Lausanne)*. 2023;13(January):1-12. doi:10.3389/fendo.2022.997921
347. Decavèle M, Parrot A, Duruisseaux M, et al. Diagnosis and prognosis of acute respiratory distress syndrome related to diffuse pneumonic-type adenocarcinoma: a single-center case series study. *J Thorac Dis*. 2022;14(8):2812-2825. doi:10.21037/jtd-22-12
348. Huo J wen, Huang X tao, Li X, Gong J wei, Luo T you, Li Q. Pneumonic-type lung adenocarcinoma with different ranges exhibiting different clinical, imaging, and pathological characteristics. *Insights Imaging*. 2021;12(1). doi:10.1186/s13244-021-01114-2
349. Shui Y, Wang H. Metagenomic next-generation sequencing as an unconventional approach to warn of tumor cells in a patients with non-mucinous pneumonic-type lung adenocarcinoma: Case report. *Med (United States)*. 2022;101(51). doi:10.1097/MD.00000000000032448
350. Nakamura S, Ashizawa K, Fukuda M, Uetani M. Mucinous and nonmucinous pneumonic-type adenocarcinoma: CT classification and clinical outcome. *J Clin Oncol*. 2011;29(15_suppl):e18073-e18073. doi:10.1200/jco.2011.29.15_suppl.e18073
351. Stewart LA, Pignon JP. Chemotherapy in non-small cell lung cancer: A meta-analysis using updated data on individual patients from 52 randomised clinical trials. *Br Med J*. 1995;311(7010):899-909. doi:10.1016/0169-5002(96)85918-6
352. Lim E, Harris G, Patel A, Adachi I, Edmonds L, Song F. Preoperative versus postoperative chemotherapy in patients with resectable non-small cell lung cancer: Systematic review and indirect comparison meta-analysis of randomized trials. *J Thorac Oncol*. 2009;4(11):1380-1388. doi:10.1097/JTO.0b013e3181b9ecca
353. Provencio M, Calvo V, Romero A, Spicer JD, Cruz-Bermúdez A. Treatment Sequencing in Resectable Lung Cancer: The Good and the Bad of Adjuvant Versus Neoadjuvant Therapy. *Am Soc Clin Oncol Educ B*. 2022;(42):711-728. doi:10.1200/edbk_358995
354. Blumenthal GM, Bunn PA, Chaft JE, et al. Current Status and Future Perspectives on Neoadjuvant Therapy in Lung Cancer. *J Thorac Oncol*. 2018;13(12):1818-1831. doi:10.1016/j.jtho.2018.09.017

355. Cuppens K, Baas P. The path forward in early-stage lung cancer. *Transl Lung Cancer Res.* 2023;12(1):11-13. doi:10.21037/tlcr-22-546
356. Aguado C, Chara L, Antofianzas M, et al. Neoadjuvant treatment in non-small cell lung cancer: New perspectives with the incorporation of immunotherapy. *World J Clin Oncol.* 2022;13(5):314-322. doi:10.5306/wjco.v13.i5.314
357. Chen X, Ma K. Neoadjuvant therapy in lung cancer: What is most important: Objective response rate or major pathological response? *Curr Oncol.* 2021;28(5):4129-4138. doi:10.3390/curroncol28050350
358. Forde PM, Spicer J, Lu S, et al. Neoadjuvant Nivolumab plus Chemotherapy in Resectable Lung Cancer. *N Engl J Med.* 2022;386(21):1973-1985. doi:10.1056/nejmoa2202170
359. Tang WF, Xu W, Huang WZ, et al. Pathologic complete response after neoadjuvant tislelizumab and chemotherapy for Pancoast tumor: A case report. *Thorac Cancer.* 2021;12(8):1256-1259. doi:10.1111/1759-7714.13910
360. Saqi A, Leslie KO, Moreira AL, et al. Assessing Pathologic Response in Resected Lung Cancers: Current Standards, Proposal for a Novel Pathologic Response Calculator Tool, and Challenges in Practice. *JTO Clin Res Reports.* 2022;3(5):100310. doi:10.1016/j.jtocrr.2022.100310
361. Hellmann MD, Chaft JE, William WN, et al. Pathological response after neoadjuvant chemotherapy in resectable non-small-cell lung cancers: Proposal for the use of major pathological response as a surrogate endpoint. *Lancet Oncol.* 2014;15(1):42-50. doi:10.1016/S1470-2045(13)70334-6
362. Rojas F, Parra ER, Wistuba II, Haymaker C, Solis Soto LM. Pathological Response and Immune Biomarker Assessment in Non-Small-Cell Lung Carcinoma Receiving Neoadjuvant Immune Checkpoint Inhibitors. *Cancers (Basel).* 2022;14(11):1-22. doi:10.3390/cancers14112775
363. Dacic S, Travis WD, Giltner JM, et al. Artificial intelligence (AI)-powered pathologic response (PathR) assessment of resection specimens after neoadjuvant atezolizumab in patients with non-small cell lung cancer: Results from the LCADC3 study. *J Clin Oncol.* 2021;39(15_suppl):106. doi:10.1200/JCO.2021.39.15_suppl.106
364. Ahmad Z, Rahim S, Zubair M, Abdul-Ghfar J. Artificial intelligence (AI) in medicine, current applications and future role with special emphasis on its potential and promise in pathology: present and future impact, obstacles including costs and acceptance among pathologists, practical and philosoph. *Diagn Pathol.* 2021;16(1):1-16. doi:10.1186/s13000-021-01085-4
365. Zens P, Bello C, Scherz A, et al. The effect of neoadjuvant therapy on PD-L1 expression and CD8+lymphocyte density in non-small cell lung cancer. *Mod Pathol.* 2022;35(12):1848-1859. doi:10.1038/s41379-022-01139-y
366. Tsoo MS, Marguet S, Le Teuff G, et al. Subtype classification of lung adenocarcinoma predicts benefit from adjuvant chemotherapy in patients undergoing complete resection. *J Clin Oncol.* 2015;33(30):3439-3446. doi:10.1200/JCO.2014.58.8335
367. Grosu HB, Manzanera A, Shivakumar S, Sun S, Noguras Gonzalez G, Ost DE. Survival disparities following surgery among patients with different histological types of non-small cell lung cancer. *Lung Cancer.* 2020;140:55-58. doi:10.1016/j.lungcan.2019.12.007
368. Bertoglio P, Aprile V, Ventura L, Cattoni M, Nachira D, Lococo F. Impact of High - Grade Patterns in Early - Stage Lung Adenocarcinoma : A Multicentric Analysis. *Lung.* 2022;(0123456789).
369. Rami-Porta R. Fifty-Five Years of Lung Cancer Staging. What to do Next? *Arch Bronconeumol.* 2021;58:111-112. doi:10.1016/j.arbres.2021.06.011
370. Yang M, Forbes ME, Bitting RL, et al. Incorporating blood-based liquid biopsy information into cancer staging: Time for a TNMB system? *Ann Oncol.* 2018;29(2):311-323. doi:10.1093/annonc/mdx766

371. Nicholson AG, Tsao MS, Beasley MB, et al. The 2021 WHO Classification of Lung Tumors: Impact of Advances Since 2015. *J Thorac Oncol.* 2022;17(3):362-387. doi:10.1016/j.jtho.2021.11.003
372. Baine M, Beasley MB, Buonocore. The distinction between spread through air spaces (STAS) and artifacts in selected images is highly reproducible. *Mod Pathol.* 2020;(33):S1754-S1755.
373. Karasaki T, Moore DA, Veeriah S, et al. Evolutionary characterization of lung adenocarcinoma morphology in TRACERx. *Nat Med.* 2023;29(April). doi:10.1038/s41591-023-02230-w
374. Khalbuss WE, Yang H, Lian Q, Elhosseiny A, Pantanowitz L, Monaco SE. The cytomorphologic spectrum of small-cell carcinoma and large-cell neuroendocrine carcinoma in body cavity effusions: A study of 68 cases. *Cytojournal.* 2011;8:18. doi:10.4103/1742-6413.86816
375. Kim L, Choi SJ, Park IS, Han JY, Kim JM, Chu YC. Cytomorphologic features of small cell carcinoma of lung in effusion fluid using a liquid-based cytology technique. *Diagn Cytopathol.* 2020;48(3):203-210. doi:10.1002/dc.24365
376. Kakinuma H, Mikami T, Iwabuchi K, et al. Diagnostic findings of bronchial brush cytology for pulmonary large cell neuroendocrine carcinomas: Comparison with poorly differentiated adenocarcinomas, squamous cell carcinomas, and small cell carcinomas. *Cancer.* 2003;99(4):247-254. doi:10.1002/cncr.11220
377. Sun L, Sakurai S, Sano T, Hironaka M, Kawashima O, Nakajima T. High-grade neuroendocrine carcinoma of the lung: Comparative clinicopathological study of large cell neuroendocrine carcinoma and small cell lung carcinoma: Original Article. *Pathol Int.* 2009;59(8):522-529. doi:10.1111/j.1440-1827.2009.02402.x
378. Huang CC, Collins BT, Flint A, Michael CW. Pulmonary neuroendocrine tumors: An entity in search of cytologic criteria. *Diagn Cytopathol.* 2013;41(8):689-696. doi:10.1002/dc.22933
379. Crapanzano JP, Loukeris K, Borczuk AC, Saqi A. Cytological, histological, and immunohistochemical findings of pulmonary carcinomas with basaloid features. *Diagn Cytopathol.* 2011;39(2):92-100. doi:10.1002/dc.21335
380. Tsutani Y, Miyata Y, Mimae T, et al. The prognostic role of pathologic invasive component size, excluding lepidic growth, in stage I lung adenocarcinoma. *J Thorac Cardiovasc Surg.* 2013;146(3):580-585. doi:10.1016/j.jtcvs.2013.04.032
381. Yoshizawa A, Motoi N, Riely GJ, et al. Impact of proposed IASLC/ATS/ERS classification of lung adenocarcinoma: prognostic subgroups and implications for further revision of staging based on analysis of 514 stage I cases. *Mod Pathol.* 2011;24(5):653-664. doi:10.1038/modpathol.2010.232
382. Aida S, Shimazaki H, Sato K, et al. Prognostic analysis of pulmonary adenocarcinoma subclassification with special consideration of papillary and bronchioloalveolar types. *Histopathology.* Published online 2004:468-476.
383. Warth A, Muley T, Meister M, et al. The novel histologic International Association for the Study of Lung Cancer/American Thoracic Society/European Respiratory Society classification system of lung adenocarcinoma is a stage-independent predictor of survival. *J Clin Oncol.* 2012;30(13):1438-1446. doi:10.1200/JCO.2011.37.2185
384. Borczuk AC, Qian F, Kazeros A, et al. Invasive size is an independent predictor of survival in pulmonary adenocarcinoma. *Am J Surg Pathol.* 2009;33(3):462-469. doi:10.1097/PAS.0b013e318190157c
385. Chang JC, Alex D, Bott MJ, et al. Comprehensive Next-Generation Sequencing Unambiguously Distinguishes Separate Primary Lung Carcinomas From Intrapulmonary Metastases: Comparison with Standard Histopathologic Approach. *Clin Cancer Res.* 2019;25(23):7113-7125. doi:10.1158/1078-0432.CCR-19-1700.Comprehensive
386. Mizuuchi H, Suda K, Kitahara H, et al. Solitary pulmonary metastasis from malignant melanoma of the bulbar conjunctiva presenting as a pulmonary ground glass nodule: Report of a case. *Thorac Cancer.* 2015;6(1):97-100. doi:10.1111/1759-7714.12124

387. Titus LJ, Reisch LM, Tosteson ANA, et al. Malpractice Concerns, Defensive Medicine, and the Histopathology Diagnosis of Melanocytic Skin Lesions. *Am J Clin Pathol*. 2018;150(4):338-345. doi:10.1093/ajcp/aqy057
388. Reisch LM, Carney PA, Oster N V, et al. Medical malpractice concerns and defensive medicine: a nationwide survey of breast pathologists. *Am J Clin Pathol*. 2015;144(6):916-922. doi:10.1309/AJCP80LYIM00UJIF
389. Schnadig VJ. Overdiagnosis of Thyroid Cancer: Is This Not an Ethical Issue for Pathologists As Well As Radiologists and Clinicians? *Arch Pathol Lab Med*. 2018;142(9):1018-1020. doi:10.5858/arpa.2017-0510-ED
390. Visca P, Gallo E, Marino M. New Morphologic Findings Support Invasiveness Criteria in Small-Sized Nonmucinous Lepidic Adenocarcinoma : Commenting a Proposal From the International Association for the Study of Lung Cancer Pathology Committee. *J Thorac Oncol*. 2023;18(4):387-389. doi:10.1016/j.jtho.2023.01.001
391. Ganti AK, Klein AB, Cotarla I, Seal B, Chou E. Update of Incidence, Prevalence, Survival, and Initial Treatment in Patients with Non-Small Cell Lung Cancer in the US. *JAMA Oncol*. 2021;7(12):1824-1832. doi:10.1001/jamaoncol.2021.4932
392. Dinmohamed AG, Lemmens VEPP, De Hingh IHJT, Visser O. Relative survival in early-stage cancers in the Netherlands: A population-based study. *J Hematol Oncol*. 2020;13(1):1-4. doi:10.1186/s13045-020-00888-0
393. Marcadis AR, Marti JL, Ehdaie B, Hakimi AA, Davies L, Morris LGT. Characterizing Relative and Disease-Specific Survival in Early-Stage Cancers. *JAMA Intern Med*. 2020;180(3):461-463. doi:10.1001/jamainternmed.2019.6120
394. Welch HG, Kramer BS, Black WC. Epidemiologic Signatures in Cancer. *N Engl J Med*. 2019;381(14):1378-1386. doi:10.1056/nejmsr1905447
395. de Koning HJ, van der Aalst CM, de Jong PA, et al. Reduced Lung-Cancer Mortality with Volume CT Screening in a Randomized Trial. *N Engl J Med*. 2020;382(6):503-513. doi:10.1056/nejmoa1911793
396. Nagaiushi C, Okada Y. The structure of the bronchoalveolar system with special reference to its fine structure. *Acta Tuberc Jpn*. 1960;10:20-38.
397. Thunnissen FB, Diegenbach PC, van Hattum AH, et al. Further evaluation of quantitative nuclear image features for classification of lung carcinomas. *Pathol Res Pract*. 1992;188(4-5):531-535. doi:10.1016/s0344-0338(11)80050-6

Summary

This thesis is the result of the doctoral research of Dr. J.L.G. Blaauwgeers on various histopathological aspects in lung resections, removed for the treatment of non-small cell lung carcinoma, entitled "Histopathological aspects of resected non-small cell lung carcinoma, with emphasis on spread through air spaces and collapsed adenocarcinoma in situ."

The role of the pathologist in lung cancer is important in several ways. Firstly, in making a diagnosis of a lesion detected by imaging in the lung. It is important to determine whether it is a malignant tumor, then whether it is primary lung cancer, and then which variant it is. A diagnosis on tissue from another part of the body can confirm suspicion of metastases. With lung cancer variants, it is particularly important to distinguish between "non-small cell carcinoma" (NSCLC) and "small cell carcinoma." In the case of non-small cell carcinoma, it is important to differentiate between squamous cell carcinoma and adenocarcinoma. With adenocarcinoma, it is also relevant to determine whether it is an invasive tumor or a precursor (in situ) carcinoma, and in the case of an invasive tumor, what the main, dominant growth pattern is. Both have an impact in terms of the patient's prognosis. A non-invasive tumor does not metastasize, and the patient is cured after removal (resection), while some subtypes of invasive carcinoma, such as those with a solid or micropapillary growth pattern, have a potentially worse prognosis with a greater chance of metastases. A relatively recent described phenomenon, the presence of loose tumor cells in the air spaces (alveoli) of the lung (spread through air spaces, STAS), is interpreted as a new form of invasive growth and is thought to be related to an unfavorable prognosis. Although, incorporated in the WHO classification of pulmonary adenocarcinomas, its exact significance is still unclear.

In addition to determining whether there is an invasive tumor and which variant it is, the pathologist also plays a role in evaluating tumors that are removed after pre-treatment (neoadjuvant therapy). The assessment of the response to this pre-treatment is a determining factor for the further prognosis of the patient.

This thesis investigates three aspects in lung resections with non-small cell carcinoma that are relevant for diagnosis, prognosis, and staging. Firstly, the pathological response after neoadjuvant therapy was examined. Secondly, research was conducted on the so-called "STAS" with the hypothesis that this phenomenon may be an artifact rather than a biological phenomenon. Thirdly, attempts were made to refine diagnostic tools that can help distinguish invasion from non-invasion in non-mucinous adenocarcinoma, with particular attention to the effect of collapsed lung tissue on tumor morphology.

In chapter 2 of Part I, the histological changes after neoadjuvant therapy are described in a study cohort of 46 patients with a sulcus superior tumor who underwent chemoradiation followed by surgical resection. Complete pathological response was identified in 20 patients (43%) who underwent induction chemoradiotherapy. A

complete response was associated with an essentially better favorable prognosis, namely a 70% 5-year overall survival versus 20% ($p=0.001$). Patients with a near-complete response (defined as less than 10% vital tumor residue) also had significantly better survival than patients with more than 10% vital tumor residue (65% 5-year overall survival versus 18%; $p<0.001$). This threshold of less than 10% vital tumor residue is now referred to as a criterion for “major pathologic response” (MPR).

In chapter 3, additional morphological prognostic characteristics of tumors were sought in the same patient group as in chapter 2, namely in 33 patients with residual tumor after neoadjuvant treatment for a sulcus superior tumor. The study examined whether proliferation (with the biomarker MIB1), PD-L1 (a biomarker related to the immune system), and nuclear size after chemoradiation compared to pre-treatment measurements are related to prognosis. This study showed an increase in tumor nuclear size after chemoradiotherapy, but without prognostic significance. Importantly, low MIB-1 expression was associated with improved survival and disease-free survival, while negative PD-L1 expression also predicted better survival. Further research may be useful to see how these findings can be applied in larger and prospectively followed patient groups in daily practice.

The TNM system classifies tumors based on their characteristics, usually the tumor diameter (T), whether there are lymph node metastases (“Node”, N), and whether there are metastases via the bloodstream (metastases, M). The transition from TNM version 7 to version 8 involves a shift of some T descriptors to a different category based on follow-up data from a large international patient group. Chapter 4 presents the results of a national study on T3N0 NSCLC, which was conducted in preparation for Chapter 16, which includes various tumor categories, including those with parietal pleural invasion or a diameter greater than 7 cm. The study in Chapter 4 had two objectives: to assess the validity of this shift in the Dutch population and to investigate whether the inclusion of additional morphological factors could improve staging accuracy.

In the group of 683 patients, the 3- and 5-year overall survival (OS) percentages for the subgroup with a tumor diameter greater than 7 cm were 59.9% and 47.2%, respectively. This is comparable to the percentages for 3- and 5-year survival of the subgroup with pleural invasion (50.4% and 45.3%), a group that remained in the T3 category. These findings do not support the relocation of the group with a tumor diameter greater than 7 cm to the pT4 category in the 8th edition of the TNM classification, as is now the case. A newly defined group of patients with 2 or more T characteristics was found, mainly greater than 7 cm in combination with pleural invasion. This group showed worse 3- and 5-year OS percentages (37.5% and 28.7%, respectively), which were comparable to the outcomes for TNM 8th edition stage IIIB and pT4 cases.

For the subtype with two or more nodules, the 3- and 5-year OS percentages were 70.6% and 62.8%, respectively, with patients with adenocarcinoma having a significantly better OS than patients with squamous cell carcinoma: a 5-year OS percentage of 65.1% versus 47.2% ($p<0.001$). This suggests that the prognosis for the

adenocarcinoma variant may be similar to that for the pT2 category, while squamous cell carcinoma with multiple nodules may remain pT3. This population analysis of overall survival for the pT3N0 subcategory for NSCLC suggests that histological variant is a relevant description for the category of two or more nodules, provides no support for the shift of tumors larger than 7 cm to the pT4 category, and suggests that a combination of two pT3 descriptions (the mixed group) deserves migration to pT4. However, the TNM classification currently only uses anatomical locations in the classification. Adding orthogonal characteristics may further refine the prognostic classification.

Part II focuses on the phenomenon of Spread Through Air Spaces (STAS). This has been described as a new way of metastases since the 2015 WHO classification, but it may be an artifact. Chapter 5 describes various histopathological artifacts related to tissue treatment after removal and upon receipt at the pathology department. It explains the effect of surgical collapse, which is the collapse of lung tissue after removal from the thoracic cavity. Additionally, spreading of tumor tissue by a knife during the cutting of the resection specimen is described as a possible explanation for the presence of loose tumor cells or cell clusters in alveolar spaces away from the tumor's border. This finding is referred to as spread through a knife surface (STAKS) instead of STAS and is considered an artifact.

In Chapter 6, a prospective multicenter study is described that suggests that STAS is an inducible phenomenon. In 44 resection specimens, the number of loose tumor cells and/or cell clusters was counted in four sections taken through the tumor without cleaning the preparation knife. The number of loose cells and/or clusters increased from the first section that was cut without going through the tumor to the last section where the knife had been used twice through the tumor. The number of cells was significantly greater between the first section and sections 2-4. Cells were also found in the alveoli originating from benign bronchial epithelium, also referred to as dragging by the knife. These findings were independent of the institution. Based on this study, it was concluded that it is highly likely that STAS is an inducible artifact.

Chapter 7 is a critical evaluation of the STAS phenomenon, discussing the literature up until then and explaining alternative explanations for STAS, suggesting that it should be considered more as an artifact than a new way of metastasis. This chapter does not deny the association between STAS and prognosis, but rather suggests that it is a result of STAS being more common in high-grade tumors, such as micropapillary adenocarcinoma, where the cohesion between tumor cells is less.

Chapters 8 and 9 provide commentary on this topic, related to a study on neuroendocrine tumors of the lung and the findings in a similar study as described in Chapter 6. This commentary emphasizes alternative explanations for finding loose tumor cells in alveoli other than the preparation knife during macroscopic processing at the pathology department, such as manipulation by the surgeon during lung lobe removal or manipulation by the pathologist.

In Chapter 10, another possible artifact is investigated, namely the presence of individual tumor cells and tumor cell clusters, as well as macrophages in branches of the pulmonary artery in histological sections of lung resection specimens. In a small pilot study of 33 patients, this was observed in 23 patients (70%), with no relationship between this presence and overall survival. This result was confirmed in two validation cohorts (total of 70 patients) from two institutions in Amsterdam and Milan, where the phenomenon was observed in 41 patients (58%), again without a relationship with recurrence-free or overall survival. Particularly noteworthy was that in cases diagnosed as non-invasive, this observation was seen in 8 out of 10 cases. These findings were considered a strong argument that this is also an artifact rather than a biological phenomenon.

Chapter 11 contains the most recent arguments together about STAS as an artifact in the CON part of a Pro-Con editorial.

In Part III, the focus is on iatrogenic and biological collapse as a possible pitfall in the assessment of invasion in small adenocarcinomas. Chapter 12 describes the importance of elastin in pulmonary pathology and its potential usefulness in recognizing collapsed lung and non-invasive growth along alveolar walls. In particular, emphasis is placed on the presence of elastin in the alveolar septa and its absence in the septa of a true papillary invasive variant in the case of collapse in an *in-situ* carcinoma.

Chapter 13 discusses a proof-of-principle study that investigated whether consideration of surgical collapse leads to a more frequent diagnosis of AIS. In this study, cytokeratin 7 is used as an immunohistochemical marker to better recognize the regular growth pattern of a monolayer of tumor cells in AIS. In the patient group of the pilot study in Chapter 10, a diagnosis of AIS was made in 33 out of 38 patients, including 5 patients whose tumors were previously considered invasive. The revised diagnosis did not affect the 100% 5-year survival rate. Based on this, it was considered plausible that recognition of collapsed AIS, including with the help of a CK7 staining, can lead to better diagnosis of non-invasive patterns.

Chapter 14 describes the morphological features of iatrogenic and biological collapsed AIS, where lessons are learned from a mathematical model, and cytokeratin 7 and elastin stains are used to assess invasiveness. Two independent cohorts of resected adenocarcinomas of 3 cm or less were examined to investigate these aspects, and their relationship with disease-free and overall survival was analyzed. In the Amsterdam and Milan cohorts, as also described in Chapter 10, a diagnosis of AIS was made in 10 patients based on proposed criteria, 9 of whom were originally diagnosed as invasive. As in the proof-of-principle study in Chapter 13, these patients had 100% disease-free and overall survival. This chapter also suggests additional morphological criteria with other intra-alveolar growth patterns than the monolayer in AIS, which can be used as surrogate markers for invasion.

Chapter 15 concerns the largest international interobserver study with pathologists ever, in which the presence of iatrogenic and biological collapse in the assessment of

invasion of lung adenocarcinoma using elastin and cytokeratin 7 staining to diagnose (collapsed) AIS more reliably and reduce variation between assessors of invasive patterns in small pulmonary adenocarcinomas was investigated.

A total of 42 pathologists from 13 countries scored all 70 cases in the first 2 rounds, while 36 pathologists scored 41 non-unanimous cases in the 3rd round. The kappa values for rounds 1, 2, and 3 were 0.27, 0.45, and 0.62, respectively. A kappa score ranges from "0" to "1". A score of 0 means that tossing a coin is as good, while a score of "1" shows perfect uniformity. This reproducibility study confirms the difficulty in assessing invasion in pulmonary adenocarcinomas on full histological sections, supporting the notion that pathologists worldwide are consciously incompetent in assessing invasion according to WHO criteria. Heatmap analysis showed differences and variation in the location and size of invasion. In contrast, the revised classification obtained a significantly higher kappa score in blind assessment (0.45) or coached assessment (0.62), demonstrating a substantial increase in competence. No recurrence was demonstrated in the group of patients with "no invasion" scores (100% survival). Additional support for these findings, for example, through biomarker research, could further support the results.

According to the WHO, the non-invasive adenocarcinoma variant (AIS) has a maximum size of 3 cm. Given the above findings, it is theoretically possible for AIS to occur as a larger tumor. In Chapter 16, this hypothesis was investigated in the national subgroup of T3N0 NSCLC from Chapter 4. In the subgroup of 112 adenocarcinomas larger than 7 cm, three patients were identified in whom the tumors were assessed as non-invasive based on the available sections. Radiological correlation showed a pneumonia-like image in these cases. Strikingly, in potentially non-invasive cases, which were supported by elastin staining as papillary carcinoma, a solid tumor aspect was seen radiologically and pathologically. Two later additional case, not from the T3N0 cohort, in which the entire lung lobe was histologically evaluated with more than 300 and 130 tissue blocks, showed in the sections a non-invasive tumor in this entire lobe (both 16 cm). Follow-up showed no tumor recurrence. The study provides strong arguments for abandoning the diameter limit of 3 cm for AIS.

Nederlandse samenvatting

Dit proefschrift is het resultaat van het promotieonderzoek van drs J.L.G. Blaauwgeers naar diverse histopathologische aspecten in longresecties, verwijderd voor behandeling van een niet-kleincellig longcarcinoom, met de naar het Nederlands vertaalde titel: Histopathologische aspecten van het geresecteerde niet-kleincellige longcarcinoom met nadruk op verspreiding door luchtruimtes en gecollabeerd adenocarcinoom in situ.

De rol van de patholoog bij longkanker is in meerdere opzichten van belang. Allereerst in het stellen van een diagnose op een bij beeldvorming vastgestelde haard in de long. Belangrijk is het vaststellen of het gaat om een kwaadaardige tumor, vervolgens of het primair longkanker betreft en daarna om welke variant het gaat. Een diagnose op weefsel afkomstig van een andere plaats in het lichaam kan verdenking op uitzaaiingen bevestigen. Bij de longkankervarianten gaat het er met name om of het een "niet-kleincellig carcinoom" (non-small cell lung cancer, NSCLC) dan wel een "kleincellig carcinoom" is. In geval van niet-kleincellig carcinoom is het dan van belang om onderscheid te maken tussen een plaveiselcelcarcinoom en adenocarcinoom. Bij het adenocarcinoom wordt gevraagd om te bepalen of het een invasieve tumor betreft of een voorstadium (in situ) carcinoom en in geval van een invasieve tumor wat het belangrijkste, dominante groeipatroon is. Beide zijn van belang in verband met de prognose voor de patiënt. Een niet invasieve tumor zaait niet uit en patiënt is na verwijdering ervan (resectie) genezen, terwijl sommige subtypes van het invasieve carcinoom, zoals die met een solide of micro-papillaire groeiwijze potentieel een slechtere prognose hebben met grotere kans op uitzaaiingen. Een vrij recent apart benoemd fenomeen, namelijk de aanwezigheid van losse tumorcellen in de luchtruimtes (alveoli) van de long (spread through air spaces, STAS), wordt beschreven als een nieuwe vorm van invasieve groei en zou gerelateerd zijn aan een ongunstige prognose. De exacte betekenis ervan is echter nog onduidelijk.

Naast het vaststellen of er sprake is van een invasieve tumor en welke variant, heeft de patholoog ook een rol bij de beoordeling van tumoren, die na voorbehandeling (neoadjuvante therapie) alsnog verwijderd worden. De beoordeling van de reactie op deze voorbehandeling, is medebepalend voor de verdere prognose van de ziekte.

In dit proefschrift worden 3 van die aspecten in longresecties met een niet-kleincellig carcinoom onderzocht, aspecten die relevant zijn voor diagnose, prognose en stadiering. Allereerst is gekeken naar het pathologische respons-effect na neoadjuvante therapie.

Ten tweede is onderzoek gedaan naar het zogenaamde "STAS" met de hypothese dat dit fenomeen mogelijk een artefact, eerder dan een biologisch fenomeen is.

En ten derde is geprobeerd diagnostische hulpmiddelen te verfijnen die kunnen helpen bij het onderscheid tussen invasie en niet-invasie bij het niet-mucineuze adenocarcinoom, waarbij er met name gekeken is naar het effect van de bij de verwijdering samengevouwen (collaps) long op de morfologie van tumoren.

In hoofdstuk 2 van deel I worden de histologische veranderingen na neoadjuvante therapie beschreven, in een studiecohort van 46 patiënten met een longtop, een zgn. sulcus superior tumor, die chemoradiatie behandeling gevolgd door chirurgische resectie hebben ondergaan. Een complete pathologische respons werd geïdentificeerd bij 20 patiënten (43%), die een behandeling met inductie chemoradiotherapie ondergingen. Een complete respons was geassocieerd met een gunstiger prognose, namelijk een 70% 5-jaars overall survival vs. 20% ($p=0.001$). Maar ook patiënten met een bijna complete response (gedefinieerd als minder dan 10% vitale tumorrest) hadden een significant betere overleving dan patiënten bij wie meer dan 10% vitale tumorrest werd gevonden (65% 5-jaars overall survival versus 18%; $p<0.001$). Deze grens van minder dan 10% vitale tumor, wordt heden ten dage als een criterium voor “major pathologic response” (MPR) benoemd.

In hoofdstuk 3 is gezocht naar aanvullende morfologische prognostische kenmerken van tumoren in dezelfde soort patiëntengroep als in hoofdstuk 2, namelijk in 33 patiënten met rest tumor na neoadjuvante behandeling voor een sulcus superior tumor. Er is gekeken of proliferatie (met biomarker MIB1), PD-L1 (een biomarker gerelateerd aan de eigen afweer) en grootte van de celkern na chemoradiatie in vergelijking met voorbehandelingsmetingen gerelateerd zijn aan prognose. Deze studie toont een toename in de grootte van de celkern van tumoren na chemoradiotherapie, echter zonder prognostische betekenis. Belangrijk is dat een lage MIB-1-expressie geassocieerd werd met een verbeterde overleving en ziektevrije overleving, terwijl een negatieve PD-L1-expressie ook een betere overleving voorspelt. Aanvullend onderzoek kan nuttig zijn om in een grotere en ook prospectief gevolgde patiëntengroep te zien hoe de bevindingen in de dagelijkse praktijk toegepast kunnen worden.

In het TNM-systeem worden tumoren geassocieerd op basis van tumorkenmerk (meestal een diameter van de tumor, T), of er uitzaaiingen via de lymfklier (“Node”, N) en uitzaaiingen via de bloedbaan zijn (metastasen, M). De overgang van stadium indeling TNM- versie 7 naar TNM-versie 8 op basis van een grote internationale patiëntengroep, waar follow-up gegevens van bekend zijn, omvat een verschuiving van sommige T-descriptoren naar een andere categorie. Hoofdstuk 4 presenteert de resultaten van een landelijke studie naar T3N0 NSCLC, die werd gestart ter voorbereiding op hoofdstuk 16, die verschillende tumorcategorieën omvat, waaronder die met pariëtale pleura-invasie of een diameter groter dan 7 cm. Het doel van de studie in hoofdstuk 4 was tweeledig: de validiteit van deze verschuiving in de Nederlandse populatie beoordelen en onderzoeken of de inclusie van aanvullende morfologische factoren de nauwkeurigheid van de stadiëring kon verbeteren.

In de groep van 683 patiënten was 3- en 5-jaars algehele overleving (OS) percentages voor het subgroep met een tumordiameter groter dan 7 cm respectievelijk 59,9% en 47,2%. Dit is vergelijkbaar is met de percentages voor 3- en 5 jaars overleving van de subgroep met pleurale invasie (50,4% en 45,3%), een groep welke in de T3 categorie is gebleven. Deze bevindingen ondersteunen niet de verplaatsing van de groep met een tumordiameter groter dan 7 cm naar de categorie pT4 in de 8e editie

van de TNM-classificatie, zoals nu wel gebeurd is. Een nieuw gedefinieerde groep van patiënten met 2 of meer T-kenmerken werd gevonden, voornamelijk groter dan 7 cm in combinatie met pleurale invasie. Deze groep toonde slechtere 3- en 5-jaars OS-percentages (respectievelijk 37,5% en 28,7%), wat vergelijkbaar was met de uitkomsten voor TNM 8e editie-stadium IIIB en pT4 gevallen.

Voor het subtype met twee of meer nodules waren de 3- en 5-jaars OS-percentages respectievelijk 70,6% en 62,8%, waarbij patiënten met adenocarcinoom een significant betere OS hadden dan patiënten met plaveiselcelcarcinoom: een 5-jaars OS-percentage van 65,1% versus 47,2% ($p < 0,001$). Dit suggereert dat de prognose voor het adenocarcinoom variant vergelijkbaar kan zijn met die voor de pT2 categorie, terwijl plaveiselcelcarcinoom met meerdere nodules pT3 kunnen blijven.

Deze populatie analyse van algehele overleving voor de pT3N0 subcategorie voor NSCLC suggereert dat histologisch variant een relevante beschrijving is voor de categorie van twee of meer nodules, geeft geen steun voor verschuiving van tumoren groter dan 7 cm naar de pT4 categorie en suggereert dat een combinatie van twee pT3 beschrijvingen (de gemengde groep) migratie verdient naar pT4. De TNM-indeling hanteert tot nu toe echter alleen anatomische lokalisaties in de classificatie. Mogelijk levert uitbreiding met andere kenmerken een verdere verfijning van de prognostische indeling op.

Deel II richt zich op het fenomeen Spread Through Air Spaces (STAS). Een fenomeen dat sinds de 2015 WHO classificatie wordt benoemd als een nieuwe manier van metastasering, maar mogelijk een artefact is.

Hoofdstuk 5 beschrijft in het algemeen verschillende histopathologische artefacten gerelateerd aan weefselbehandeling na verwijdering en na ontvangst bij de pathologie. Hierbij wordt met name beschreven wat het effect is van chirurgische collaps, namelijk het in elkaar vallen van het longweefsel na verwijdering uit de thoraxholte. Daarnaast wordt het spreiden van (tumor) weefsel door een mes tijdens het snijden van het resectiepreparaat beschreven als mogelijke verklaring voor de aanwezigheid van losse tumorcellen of celgroepen in alveolaire ruimtes op afstand van de grens van de tumorhaard. Deze bevinding wordt in plaats van als STAS benoemd als spread through a knife surface (STAKS) en daarmee als een artefact.

In hoofdstuk 6 wordt een prospectieve multicenterstudie beschreven, waarin aannemelijk wordt gemaakt dat STAS een induceerbaar verschijnsel is. In 44 resectiepreparaten werd het aantal losse tumorcellen en/of celclusters geteld in 4 doorsneden door de tumorhaard uitgenomen zonder het prepareermes schoon te maken. Het aantal losse cellen en/of clusters nam toe vanaf de eerste coupe zonder eerst door de tumor gesneden te hebben tot de laatste coupe waar met het mes twee keer door de tumor was gesneden. Het aantal cellen was significant groter tussen de eerste coupe en de coupes 2-4. Daarbij werden er ook cellen in de alveoli aangetroffen afkomstig van o.a. (benigne) bronchusepitheel, ook geïdentificeerd als versleping door het

mes. Deze bevindingen waren instituut onafhankelijk. Op basis van deze studie werd geconcludeerd dat het zeer aannemelijk is dat STAS een induceerbaar artefact is.

Hoofdstuk 7 is een kritische evaluatie over het onderwerp STAS, waarin de literatuur tot dan wordt besproken en alternatieve verklaringen worden toegelicht, op basis waarvan STAS veeleer benoemd dient te worden als een artefact, dan als een nieuwe manier van metastasering. Hierin wordt niet ontkend dat er een associatie bestaat tussen STAS en prognose, maar dat die veeleer het gevolg is van de bevinding dat STAS vaker voorkomt bij hooggradige tumoren, zoals micro-papillair adenocarcinoom, waarbij de onderlinge cohesie van de tumorcellen minder is.

In hoofdstuk 8 en 9 wordt commentaar gegeven op dit onderwerp, gerelateerd aan een studie naar neuro-endocriene tumoren van de long en aan de bevindingen in een vergelijkbare studie als beschreven in hoofdstuk 6. In dit commentaar ligt de nadruk op alternatieve verklaringen voor het vinden van losse tumorcellen in alveoli, anders dan het prepareermes bij de macroscopische bewerking bij de pathologie, zoals manipulatie door de chirurg bij de verwijdering van de longkwab of manipulatie door de patholoog.

In hoofdstuk 10 is een ander mogelijk artefact onderzocht, namelijk de aanwezigheid van individuele tumorcellen en tumorcelclusters, alsmede cellen als macrofagen in takken van de pulmonale arterie in histologische secties van longresectiepreparaten. In een kleine proef-studie bij 33 patiënten wordt dit bij 23 patiënten (70%), waarbij er geen relatie is tussen deze aanwezigheid en overall survival. Dit resultaat wordt bevestigd in 2 validatie cohorten (met totaal 70 patiënten) uit twee instituten in Amsterdam en Milaan. In deze cohorten wordt het fenomeen in 41 patiënten gezien (58%), ook hier zonder relatie met recidievrije of overall overleving. Bijzonder hierbij was dat ook in gevallen, die als niet-invasief werden gediagnosticeerd, deze waarneming in 8 van de 10 gevallen werd gezien. Deze bevindingen werden beschouwd als sterk argument dat het ook hier gaat om een artefact en niet om een biologisch fenomeen.

Hoofdstuk 11 bevat de meest recente argumenten samen over STAS als een artefact in het CON-deel van een Pro-Con-editorial.

In deel III ligt de nadruk op iatrogene en biologische collaps als een mogelijke valkuil bij de beoordeling van invasie in kleine adenocarcinomen. In hoofdstuk 12 wordt het belang van elastine in de pulmonale pathologie en de mogelijke bruikbaarheid ervan bij de herkenning van samengevallen (gecollabeerde) long en (niet-invasieve) groei langs alveolaire wanden beschreven. Met name ligt hier de nadruk op de aanwezigheid van elastine in de alveolaire septa en in geval van collaps bij een in situ carcinoom, terwijl het bij een reëel papillaire invasieve variant elastine afwezig is in de septa.

Hoofdstuk 13 bespreekt een "proof-of-principle" studie waarin onderzocht is de overweging van chirurgische collaps leidt tot het vaker stellen van de diagnose AIS. In deze studie wordt hiervoor cytokeratine 7 als een immunohistochemische marker toegepast om het regelmatig groeipatroon van een monolayer van tumorcellen bij AIS beter te herkennen. In de patiëntengroep van de pilotstudie in hoofdstuk 10 werd bij 33 van de patiënten bij 7 patiënten de diagnose AIS gesteld, daar waar bij 5 hiervan

eerder de tumor als invasief werd beoordeeld. De gewijzigde diagnose had geen invloed op de 100% 5-jaarsoverleving. Op basis hiervan werd het aannemelijk gevonden dat herkenning van gecollabeerd AIS, o.a. met behulp van een CK7 kleuring kan leiden tot betere diagnostiek van niet-invasieve patronen.

Hoofdstuk 14 beschrijft de morfologische kenmerken van iatrogene en biologische gecollabeerde AIS, waarbij lessen worden geleerd uit een wiskundig model en cytokeratine 7 en elastine kleuringen worden gebruikt om invasiviteit te beoordelen. Twee onafhankelijke cohorten van geresecteerde adenocarcinomen van 3 cm of kleiner werden onderzocht om deze aspecten te onderzoeken en hun relatie met ziektevrije- en totale overleving werd geanalyseerd.

In de 2 cohorten uit Amsterdam en Milaan, als ook beschreven in hoofdstuk 10, werd op basis van voorgestelde criteria bij 10 patiënten de diagnose AIS gesteld, daar waar 9 hiervan oorspronkelijk als invasief waren gediagnosticeerd. Net als in de "proof-of-principle" studie uit hoofdstuk 13 was er bij deze patiënten een 100% ziektevrije en totale overleving. In dit hoofdstuk worden ook suggesties gedaan voor aanvullende morfologische criteria met andere intra-alveolaire groeipatronen dan de monolayer bij AIS, die gebruikt kunnen worden als surrogaatmarkers voor invasie.

Hoofdstuk 15 betreft de grootste internationale interobserver studie met pathologen ooit, waarin werd gekeken of het bewust worden van de aanwezigheid van iatrogene en biologische collaps in de beoordeling van de invasie van longadenocarcinoom met behulp van elastine- en cytokeratine 7 kleuringen (gecollabeerde) AIS betrouwbaarder kan diagnosticeren en de variatie tussen beoordelaars van invasieve patronen in kleine pulmonale adenocarcinomen kan verminderen.

Een totaal van 42 pathologen uit 13 landen hebben alle 70 gevallen gescoord in de eerste 2 rondes, terwijl 36 pathologen 41 niet-unanieme gevallen scoorden in de 3e ronde. De kappa waarden voor ronde 1, 2 en 3 waren respectievelijk 0,27, 0,45 en 0,62. Een kappa score ligt tussen de "0" en "1". Een score van 0 betekent dat het opgooien van een muntje net zo goed is, terwijl de score "1" perfectie uniformiteit laat zien. Deze reproduceerbaarheidsstudie bevestigt de moeilijkheid bij het beoordelen van invasie in pulmonale adenocarcinomen op volledige histologische coupes, wat de notie ondersteunt dat pathologen wereldwijd bewust onbekwaam zijn in de beoordeling van invasie volgens de WHO-criteria. Heatmap-analyse toonde verschillen en variatie in locatie en grootte van invasie. In tegenstelling daarmee werd met de herziene classificatie een belangrijke hogere kappa-score verkregen bij blind beoordelen (0,45) of gecoacht beoordelen (0,62), wat een essentiële toename van competentie aantoont. In de groep met patiënten met "geen invasie" scores werd geen recidief aangetoond (100% overleving). Aanvullende steun voor deze bevindingen, bijvoorbeeld middels biomarker onderzoek, zou de resultaten verder kunnen ondersteunen.

Volgens de WHO heeft de niet-invasieve adenocarcinoom variant (AIS) een maximale grootte van 3 cm. Gezien bovenstaande bevindingen is het in ieder geval in theorie mogelijk dat AIS kan voorkomen als een grotere tumor. In hoofdstuk 16 is deze hypothese onderzocht in de nationale subgroep van T3N0 NSCLC uit hoofdstuk 4. In de subgroep

van 112 adenocarcinomen groter dan 7 cm worden 3 patiënten geïdentificeerd waarbij op basis van de beschikbare coupes de tumoren als niet-invasief werden beoordeeld. De radiologische correlatie toonde een longontstekingsachtig beeld (“pneumonia-like”) in deze gevallen. Opvallend was dat bij potentieel niet-invasieve casus, die met elastine kleuring onderbouwd als papillair carcinoom werden beoordeeld, radiologisch en pathologisch een solide tumor aspect werd gezien. Twee latere extra casus, niet uit het T3N0 cohort, waarbij de hele longkwab histologisch werd beoordeeld met meer dan 300 coupes, toonde in deze hele kwab (beide 16 cm) een niet-invasieve tumor. De follow-up toonde geen tumor recidief. De studie toont harde argumenten om de diametergrens van 3 cm voor AIS te laten vervallen.

List of publications

1. Blaauwgeers H, Lissenberg-Witte BI, Dickhoff C, Duin S, Thunnissen E. Prognostic value of proliferation, PD-L1 and nuclear size in patients with superior sulcus tumours treated with chemoradiotherapy and surgery. *J Clin Pathol*. 2023;76(2):111-5.
2. Blaauwgeers H, Radonic T, Lissenberg-Witte B, Bahce I, Vincenten J, Dickhoff C, et al. P06.02 Incorporating Surgical Collapse in the Pathological Assessment of Resected Adenocarcinoma in situ of the Lung. A Proof of Principle Study. *J Thorac Oncol* [Internet]. 2021;16(10):S985. Available from: <https://doi.org/10.1016/j.jtho.2021.08.281>
3. Butter R, Hondelink L, van Elswijk L, Blaauwgeers JLG, Bloemena E, Britstra R, et al. The impact of a pathologist's personality on the interobserver variability and diagnostic accuracy of predictive PD-L1 immunohistochemistry in lung cancer. *Lung Cancer* [Internet]. 2022;166(December 2021):143-9. Available from: <https://doi.org/10.1016/j.lungcan.2022.03.002>
4. Thunnissen E, Motoi N, Minami Y, Matsubara D, Timens W, Nakatani Y, Ishikawa Y, Baez-Navarro X, Radonic T, Blaauwgeers H, Borczuk A and Noguchi M. Elastin in pulmonary pathology: relevance in tumours with a lepidic or papillary appearance. A comprehensive understanding from a morphological viewpoint. Vol. 80, *Histopathology*. John Wiley and Sons Inc; 2022. p. 457-67.
5. Blaauwgeers H, Thunnissen E. Spread Through Air Spaces (STAS): Can an Artifact Really be Excluded? *Am J Surg Pathol*. 2021 Jul;145(10):1439.
6. Theelen WSME, Krijgsman O, Monkhorst K, Kuilman T, Peters DDGC, Cornelissen S, Blaauwgeers H et al. Presence of a 34-gene signature is a favorable prognostic marker in squamous non-small cell lung carcinoma. *J Transl Med* [Internet]. 2020;18(1):1-12. Available from: <https://doi.org/10.1186/s12967-020-02436-3>
7. Thunnissen E, Marchevsky A, Rossi G, Russell PA, Blaauwgeers H, Radonic T, et al. RE: Spread Through Air Spaces (STAS) is Prognostic in Atypical Carcinoid, Large Cell Neuroendocrine Carcinoma, and Small Cell Carcinoma of the Lung. Vol. 15, *Journal of thoracic oncology : official publication of the International Association for the Study of Lung Cancer*. United States; 2020. p. e116-7.
8. Wolf JL, van Nederveen F, Blaauwgeers H, Marx A, Nicholson AG, Roden AC, et al. Interobserver variation in the classification of thymic lesions including biopsies and resection specimens in an international digital microscopy panel. *Histopathology*. 2020;734-41.
9. Theelen WSME, Kuilman T, Schulze K, Zou W, Krijgsman O, Peters DDGC, Blaauwgeers H et al. Absence of PD-L1 expression on tumor cells in the context of an activated immune infiltrate may indicate impaired IFN γ signaling in non-small cell lung cancer. *PLoS One*. 2019;14(5):e0216864.
10. Blaauwgeers H, Damhuis R, Lissenberg-Witte BI, de Langen AJ, Senan S, Thunnissen E. A Population-Based Study of Outcomes in Surgically Resected T3N0 Non-Small Cell Lung Cancer in The Netherlands, Defined Using TNM-7 and TNM-8; Justification of Changes and an Argument to Incorporate Histology in the Staging Algorithm. *J Thorac Oncol* [Internet]. 2019;14(3):459-67. Available from: <https://doi.org/10.1016/j.jtho.2018.10.164>
11. Oja AE, Piet B, van der Zwan D, Blaauwgeers H, Mensink M, de Kivit S, et al. Functional Heterogeneity of CD4(+) Tumor-Infiltrating Lymphocytes With a Resident Memory Phenotype in NSCLC. *Front Immunol*. 2018;9:2654.
12. Blaauwgeers H, Russell PA, Jones KD, Radonic T, Thunnissen E. Pulmonary loose tumor tissue fragments and spread through air spaces (STAS): Invasive pattern or artifact? A critical review. Vol. 123, *Lung Cancer*. 2018. p. 107-11.

13. Oja AE, Piet B, Helbig C, Stark R, van der Zwan D, Blaauwgeers H, et al. Trigger-happy resident memory CD4(+) T cells inhabit the human lungs. *Mucosal Immunol*. 2018 May;11(3):654-67.
14. Blaauwgeers H, Flieder D, Warth A, Harms A, Monkhorst K, Witte B, et al. A Prospective Study of Loose Tissue Fragments in Non-Small Cell Lung Cancer Resection Specimens. *Am J Surg Pathol* [Internet]. 2017;41(9):1226-30.
15. Theelen WS, Mittempergher L, Willems SM, Bosma AJ, Peters DD, van der Noort V, Blaauwgeers H et al. FGFR1, 2 and 3 protein overexpression and molecular aberrations of FGFR3 in early stage non-small cell lung cancer. *J Pathol Clin Res*. 2016 Oct;2(4):223-33.
16. Thunnissen E, Blaauwgeers HJLG, De Cuba EM V, Yick CY, Flieder DB. Ex vivo artifacts and histopathologic pitfalls in the lung. *Arch Pathol Lab Med*. 2016;140(3):212-20.
17. van Ierland-van Leeuwen M, Peringa J, Blaauwgeers H, van Dam A. Cat scratch disease, a rare cause of hypodense liver lesions, lymphadenopathy and a protruding duodenal lesion, caused by *Bartonella henselae*. *BMJ Case Rep*. 2014 Oct;2014.
18. Huiberts AAM, Donkervoort SC, Blok WL, Blaauwgeers HLG. Enterocolic lymphocytic phlebitis: an oncologic surgical resection without a preoperative pathologic diagnosis. Vol. 2014, *Journal of surgical case reports*. England; 2014.
19. van den Broek R, van Balen M, Blaauwgeers J, ten Wolde M. A 28-year-old pregnant woman with a very rare cause of jugular vein thrombosis. *Neth J Med*. 2014 May;72(4):224-6.
20. Keijzers M, Dingemans AMC, Blaauwgeers H, Van Suylen RJ, Hochstenbag M, Van Garsse L, et al. 8 Years' experience with robotic thymectomy for thymomas. *Surg Endosc Other Interv Tech*. 2014;28(4):1202-8.
21. Willems SM, Engelsman-Theelen W, Blaauwgeers JLGH. [Molecular pathology in tumour classification: the present and future molecular revolution]. *Ned Tijdschr Geneeskd*. 2014;158:A7364.
22. Salguero FJ, Belderbos JSA, Rossi MMG, Blaauwgeers JLG, Stroom J, Sonke JJ. Microscopic disease extensions as a risk factor for loco-regional recurrence of NSCLC after SBRT. *Radiother Oncol*. 2013;109(1):26-31.
23. Blaauwgeers JL, Kappers I, Klomp HM, Belderbos JS, Dijkstra LM, Smit EF, et al. Complete pathological response is predictive for clinical outcome after tri-modality therapy for carcinomas of the superior pulmonary sulcus. *Virchows Arch*. 2013;462(5):547-56.
24. Vos CG, Hartemink KJ, Blaauwgeers JLG, Oosterhuis JWA, Senan S, Smit EF, et al. Trimodality therapy for superior sulcus tumours: Evolution and evaluation of a treatment protocol. *Eur J Surg Oncol*. 2013;39(2):197-203.
25. Blaauwgeers JLGH. [Task differentiation, in pathology as well]. *Ned Tijdschr Geneeskd*. 2013;157(19):A6187.
26. Blaauwgeers JLGH, van Rijn RR. [Virtual autopsy--why not?]. *Ned Tijdschr Geneeskd*. 2012;156(19):A4786.
27. Van Loon J, Siedschlag C, Stroom J, Blaauwgeers H, Van Suylen RJ, Kneijens J, et al. Microscopic disease extension in three dimensions for non-small-cell lung cancer: Development of a prediction model using pathology-validated positron emission tomography and computed tomography features. *Int J Radiat Oncol Biol Phys*. 2012;82(1):448-56.
28. Blaauwgeers JLGH. [Pathology also subject to RCTs]. *Ned Tijdschr Geneeskd*. 2010;154:A2274.
29. Siedschlag C, van Loon J, van Baardwijk A, Rossi MMG, van Pei R, Blaauwgeers JLG, et al. Analysis of the relative deformation of lung lobes before and after surgery in patients with NSCLC. *Phys Med Biol*. 2009 Sep;54(18):5483-92.
30. Leenarts MFE, Blaauwgeers HLG, Hoekzema R. [A clinically unrecognised and persistent facial folliculitis: herpes folliculitis]. *Ned Tijdschr Geneeskd*. 2009;153:A285.

31. de Jong WK, Schaapveld M, Blaauwgeers JLG, Groen HJM. Pulmonary tumours in the Netherlands: focus on temporal trends in histology and stage and on rare tumours. *Thorax* [Internet]. 2008;63(12):1096-102. Available from: <http://www.ncbi.nlm.nih.gov/pubmed/18678702>
32. Tuinman PR, de Nes LCF, Blaauwgeers JLG, Koene HR, Peters SHA, Hart W. [Clinical reasoning and decision-making in practice. A man with hip pain and fever]. *Ned Tijdschr Geneeskd*. 2008 Jul;152(28):1560-7.
33. Buiter HJC, Blaauwgeers JLG, van der Spoel JI, Franssen EJF. Erythromycin precipitation in vena femoralis: investigation of crystals found in postmortem material of an intensive care unit patient. *Ther Drug Monit*. 2008 Feb;30(1):125-9.
34. de Jong WK, Blaauwgeers JLG, Schaapveld M, Timens W, Klinkenberg TJ, Groen HJM. Thymic epithelial tumours: A population-based study of the incidence, diagnostic procedures and therapy. *Eur J Cancer*. 2008;44(1):123-30.
35. Stroom J, Blaauwgeers H, van Baardwijk A, Boersma L, Lebesque J, Theuws J, et al. Feasibility of pathology-correlated lung imaging for accurate target definition of lung tumors. *Int J Radiat Oncol Biol Phys*. 2007 Sep;69(1):267-75.
36. Casparie M, Tiebosch ATMG, Burger G, Blaauwgeers H, van de Pol A, van Krieken JHJM, et al. Pathology databanking and biobanking in The Netherlands, a central role for PALGA, the nationwide histopathology and cytopathology data network and archive. *Cell Oncol*. 2007;29(1):19-24.
37. Donkervoort SC, Baak LC, Blaauwgeers JLG, Gerhards MF. Laparoscopic resection of a symptomatic gastric diverticulum: a minimally invasive solution. *JSL S J Soc Laparoendosc Surg*. 2006;10(4):525-7.
38. Wieringa RE, Blaauwgeers HJ, van Andel G. Pseudomelanosis of the bladder: a case report. *Acta Cytol*. 2006;50(4):473-5.
39. Post PN, Casparie MK, Blaauwgeers JLG, de Blok S. Reduced risk of ovarian cancer after hysterectomy. Vol. 84, *Acta obstetrica et gynecologica Scandinavica*. United States; 2005. p. 1024; author reply 1024-5.
40. Liesker KR, Blaauwgeers JLG. [Diagnostic image (220). A young man with an obstructing lung tumor]. *Ned Tijdschr Geneeskd*. 2004 Dec;148(51):2539.
41. Blaauwgeers JLG, Omtzigt AWJ. [Diagnostic image (210). A young woman suffering from abdominal pain]. *Ned Tijdschr Geneeskd*. 2004 Oct;148(41):2020.
42. Blaauwgeers JLG, van den Blink B, Hart W. [Diagnostic image (203). A woman with hypercalcaemia and osteolytic lesions caused by primary hyperparathyroidism]. *Ned Tijdschr Geneeskd*. 2004 Aug;148(34):1685-6.
43. Novotny VMJ, van der Hulst VPM, van der Wouw PA, Blaauwgeers JLG, Frissen PHJ. An unusual presentation and way to diagnose hepatocellular carcinoma. *Neth J Med*. 2004;62(7):254-6.
44. Blaauwgeers JL, Wagtmans MJ. [Diagnostic image (179). A woman with abdominal pain and weight loss. Intestinal infection with *Strongyloides stercoralis*]. *Ned Tijdschr Geneeskd*. 2004 Mar;148(10):479.
45. van der Maten J, Blaauwgeers JLG, Sutedja TG, Kwa HB, Postmus PE, Wagenaar SS. Granular cell tumors of the tracheobronchial tree. *J Thorac Cardiovasc Surg*. 2003 Sep;126(3):740-3.
46. De Blok S, De Vries C, Prinssen HM, Blaauwgeers HLG, Jorna-Meijer LB. Fatal sepsis after uterine artery embolization with microspheres. *J Vasc Interv Radiol*. 2003;
47. Warmerdam FARM, Blaauwgeers JLG, de Valk B, Roozendaal KJ. [A gastric signet ring cell carcinoma as the first expression of a breast carcinoma]. *Ned Tijdschr Geneeskd*. 2003 May;147(20):980-4.

48. Alderliesten ME, Peringa J, Van Der Hulst VPM, Blaauwgeers HLG, Van Lith JMM. Perinatal mortality: Clinical value of postmortem magnetic resonance imaging compared with autopsy in routine obstetric practice. *BJOG An Int J Obstet Gynaecol.* 2003;
49. Meijer-Jorna LB, Roos D, Blaauwgeers JLG. A soft tissue nodule on the foot. *Neth J Med.* 2003 Apr;61(4):127-8.
50. Bisschop PH, Peringa J, Blaauwgeers JLG. Photo quiz. Bilateral adrenal tumour. *Neth J Med.* 2003 Feb;61(2):49,62.
51. Blaauwgeers JLG, de Blok S. Virilisation. *Neth J Med.* 2002 Dec;60(11):428,448.
52. Olde Scholtenhuis MAG, Bakker RW, Blaauwgeers JLG. Non-Hodgkin lymphoma of the female genital tract. A five case series. *Eur J Obstet Gynecol Reprod Biol.* 2002 Aug;104(1):49-51.
53. Meijer-Jorna LB, Slingerland ACH, Blaauwgeers JLG. [Diagnostic image (93). A boy with a painful leg swelling. Osteoid osteoma]. *Ned Tijdschr Geneeskd.* 2002 Jun;146(25):1179.
54. Blaauwgeers JL, Hart W. [Diagnostic image(44). Sheep tick (*Ixodes ricinus*)]. *Ned Tijdschr Geneeskd.* 2001 Jun;145(26):1248.
55. Blaauwgeers JL, Hoekzema R, Hart W. [Diagnostic image (41). *Molluscum contagiosum*]. *Ned Tijdschr Geneeskd.* 2001 Jun;145(23):1113.
56. Blaauwgeers JL, Hart W. [Diagnostic image (34). Echinococcal cysts in the liver]. *Ned Tijdschr Geneeskd.* 2001 Apr;145(16):779.
57. Blaauwgeers JL, Hart W. [Diagnostic image (32). Gout tophus]. *Ned Tijdschr Geneeskd.* 2001 Apr;145(14):685.
58. Blaauwgeers JL, Bais JM. [Diagnostic image (28). Hydatidiform mole]. *Ned Tijdschr Geneeskd.* 2001 Mar;145(10):477.
59. Blaauwgeers JL, Hart W. [Diagnostic image (24). Ovary with a mature teratoma (so-called dermoid cyst)]. *Ned Tijdschr Geneeskd.* 2001 Feb;145(6):265.
60. Blaauwgeers JL, Hart W. Diagnostic image (21). Small intestine necrosis due to mesenteric venous thrombosis. *Ned Tijdschr Geneeskd.* 2001;
61. Blaauwgeers JL, Hart W. [Diagnostic image (8). Amebic colitis]. *Ned Tijdschr Geneeskd.* 2000 Oct;144(43):2056.
62. Blaauwgeers JL, Hart W. [Diagnostic image (5) (Ileum pathology)]. *Ned Tijdschr Geneeskd.* 2000 Sep;144(40):1914.
63. Blaauwgeers JL, Hart W. [Diagnostic image (1). Staphylococcal endocarditis]. *Ned Tijdschr Geneeskd.* 2000 Sep;144(36):1731.
64. van Triest B, Pinedo HM, Blaauwgeers JL, van Diest PJ, Schoenmakers PS, Voorn DA, et al. Prognostic role of thymidylate synthase, thymidine phosphorylase/platelet-derived endothelial cell growth factor, and proliferation markers in colorectal cancer. *Clin Cancer Res.* 2000 Mar;6(3):1063-72.
65. van Eeden S, Offerhaus GJ, Peterse HL, Dingemans KP, Blaauwgeers HL. Gangliocytic paraganglioma of the appendix. *Histopathology.* 2000 Jan;36(1):47-9.
66. van Beurden M, de Craen AJ, de Vet HC, Blaauwgeers JL, Drillenburger P, Gallee MP, et al. The contribution of MIB 1 in the accurate grading of vulvar intraepithelial neoplasia. *J Clin Pathol.* 1999 Nov;52(11):820-4.
67. Blaauwgeers JL, Hoitsma HF, Geraedts AA, Wagenaar SS. [Nonspecific symptoms due to gastrointestinal stromal tumors]. *Ned Tijdschr Geneeskd.* 1999 Jun;143(24):1241-5.
68. Swartjes JM, de Blok S, Blaauwgeers JL. Abdominal wall metastases after surgical resection of an immature teratoma of the ovary. *Eur J Obstet Gynecol Reprod Biol.* 1997 Jul;74(1):41-3.
69. Schouwink JH, Weigel HM, Blaauwgeers JL, Schreurs AJ. Aspergilloma formation in a pneumatocele associated with *Pneumocystis carinii* pneumonia. Vol. 11, *AIDS (London, England).* England; 1997. p. 135-7.

70. Toben FM, Blaauwgeers JL. [Echinococcus cyst in a young Dutch woman]. *Ned Tijdschr Geneeskd*. 1995 Dec;139(52):2739-41.
71. Zeebregts CJ, Geraedts AA, Blaauwgeers JL, Hoitsma HF. Intussusception of the sigmoid colon because of an intramuscular lipoma. Report of a case. *Dis Colon Rectum*. 1995 Aug;38(8):891-2.
72. Schreurs AJ, Blaauwgeers JL, Wagenaar JP, Mahadewsingh J V. Coexistence of hydatid and foregut cysts in the lung: a diagnostic problem. *Pediatr Pulmonol*. 1995 Jun;19(6):389-92.
73. Vleeming R, Blaauwgeers HL, Karthaus PP, Sobotka MR, Schaafsma HE. Pulmonary tumour and inferior vena cava tumour thrombus: rare presentation of renal transitional cell carcinoma. Case report. *Scand J Urol Nephrol*. 1994 Dec;28(4):419-23.
74. Kok I, Veenstra J, Rietra PJGM, Dirks-Go S, Blaauwgeers JLG, Weigel HM. Disseminated *Penicillium marneffei* infection as an imported disease in HIV-1 infected patients. Description of two cases and a review of the literature. *Neth J Med*. 1994;
75. Blaauwgeers JL, Bleker OP, Veltkamp S, Weigel HM. Langerhans cell histiocytosis of the vulva. *Eur J Obstet Gynecol Reprod Biol*. 1993 Feb;48(2):145-8.
76. van Ginkel CJ, Sang RT, Blaauwgeers JL, Schattenkerk JK, Mooi WJ, Hulsebosch HJ. Multiple primary malignant melanomas in an HIV-positive man. *J Am Acad Dermatol*. 1991 Feb;24(2 Pt 1):284-5.
77. de Jonge HK, Steinmetz PA, Blaauwgeers JG, van Merkesteyn JP. [Gardner's syndrome: report of a case]. *Ned Tijdschr Tandheelkd*. 1990 Jun;97(6):252-4.
78. Blaauwgeers JL, Allema JH, Bosma A, Brummelkamp WH. Early adenoid cystic carcinoma of the upper oesophagus. *Eur J Surg Oncol*. 1990 Feb;16(1):77-81.
79. Romijn JA, Blaauwgeers JL, van Lieshout JJ, Vijverberg PL, Reekers JA, Krediet RT. Bilateral kidney rupture with severe retroperitoneal bleeding in polyarteritis nodosa. *Neth J Med*. 1989 Dec;35(5-6):260-6.
80. Blaauwgeers JL, Troost D, Dingemans KP, Taat CW, Van den Tweel JG. Multifocal rhabdomyoma of the neck. Report of a case studied by fine-needle aspiration, light and electron microscopy, histochemistry, and immunohistochemistry. *Am J Surg Pathol*. 1989 Sep;13(9):791-9.
81. Pietroletti R, Blaauwgeers JL, Taat CW, Simi M, Brummelkamp WH, Becker AE. Intestinal endocrine cells in radiation enteritis. *Surg Gynecol Obstet* [Internet]. 1989;169(2):127-30. Available from: <http://eutils.ncbi.nlm.nih.gov/entrez/eutils/elink.fcgi?dbfrom=pubmed&id=2474204&retmode=ref&cmd=prlinks%5Cnpapers3://publication/uuid/F4DF6FEO-014F-41B3-9688-EAF2C1A74A01>
82. Blaauwgeers JL, Das PK, Slob AW, Houthoff HJ. Human gut wall reactivity to monoclonal antibodies against *M. avium* glycolipid in relation to Crohn's disease (preliminary results). *Acta Leprol*. 1989;7 Suppl 1:138-40.
83. Blaauwgeers JL, Troost D. A midline cerebral primitive neuroectodermal tumor: immunohistochemical evidence for a germinal matrix origin. *Clin Neuropathol*. 1988;7(2):73-6.

Dankwoord

Wetenschap en het schrijven van een proefschrift is teamwork. In mijn geval een klein team. Mijn dankwoord is dus kort, maar niet minder gemeend.

Erik, zonder jou was dit proefschrift er niet. Toen jij mij in 2008 benaderde met de vraag om samen onderzoek te doen dat zou kunnen leiden tot een proefschrift, wisten wij beiden niet hoelang dat zou duren, maar ook niet waar we precies zouden uitkomen. Jouw kennis en ideeën hebben in 15 jaar geleid van een begin met beoordeling van resectiepreparaten na neoadjuvante behandeling tot een uitgesproken mening over STAS en AIS. Met name na mijn bestuurlijke activiteiten waren er vele vrijdagen, zowel bij jou thuis als in VUmc, waarin met koffie en een flesje sap deze mening rijpte en vorm kreeg. De voortgang was niet altijd zo snel als jij wilde, maar ik ben je dankbaar voor je geduld en vertrouwen.

In die 15 jaar zijn er veel dingen, met name ook op het persoonlijke vlak gebeurd met verlies van dierbaren, maar ook de geboorte van onze kleinkinderen. We zagen onszelf ouder worden, maar we hebben vaak relativerend samen hierom kunnen lachen, net als over vele andere zaken. Heel veel dank!

Birgit, het vak van patholoog gaat grotendeels over kijken naar coupes en een diagnose daarop stellen. Bij wetenschappelijk onderzoek komen daar vrijwel altijd getallen bij van groepen patiënten. En zonder de analyse van die getallen zou het onderzoek zijn betekenis missen. Kennis van statistiek is vaak niet de sterkste kant van dokters, ook niet die van mij. Ik ben daarom zeer blij dat jij dit met grote betrokkenheid en nauwgezetheid hebt willen doen. Jouw bijdrage aan mijn proefschrift is groot en ik ben dan ook zeer blij dat jij een van mijn copromotors bent.

Elisabeth, dank dat jij mijn promotor wil zijn. Jouw betrokkenheid was wat meer op afstand, meer organisatorisch dan puur inhoudelijk. Maar niet minder geïnteresseerd, zo heb ik dat gevoeld.

Prof. Suresh Senan, prof. Paul van Schil, prof. Keith Kerr, prof. Sylvie Lantuejoul, dr. Teodora Radonic and prof. Joachim Aerts, thank you for agreeing to serve on my thesis committee to evaluate my dissertation and to act as opponents during its defense. Your presence is greatly appreciated.

Zonder goede technische ondersteuning is onderzoek niet mogelijk. **Sylvia**, als analist van het researchlab heb jij het leeuwendeel van die eindeloze hoeveel paraffineblokjes gesneden en gekleurd. **Analisten van het histotechnisch lab**, vele beoordelaars waren onder de indruk van de Elastica van Gieson kleuring die jullie maken. Dat geldt ook voor de immunohistochemische kleuringen, uitgevoerd onder leiding van jou, **Wim**. Ieder veel dank voor dit kwalitatief zeer goede werk.

Alle **mede-auteurs** van de diverse artikelen, jullie bijdragen in het verzamelen van gegevens, het scoren van preparaten, het kritisch beoordelen van de artikelen was onmisbaar en wordt zeer gewaardeerd.

Anne en Maaïke, ik zie het als weer een van onze mooie gezinsmomenten, dat jullie mijn paranimfen zijn. Leuk! **Mark**, dank voor je hulp bij de festiviteiten.

Rineke, al 50 jaar mijn steun en toeverlaat. Ik hou van je!

CURRICULUM VITAE

Hans Blaauwgeers was born on January 12th, 1957 and grew up in Rijswijk (ZH), Netherlands. After graduating from secondary school at the Gymnasium in Lodewijk Makeblijde College in Rijswijk, he received his medical degree from the Erasmus MC Rotterdam in 1982. After graduation, he completed a non-residency training in internal medicine and surgery at the Bethel Ziekenhuis Delft (now known as the Reinier de Graaf Gasthuis). He then received further training in pathology and medical microbiology at SSDZ Delft before completing his pathology residency at the Academic Medical Centre (AMC) in Amsterdam from 1985 to 1990.

In 1990, Hans joined the OLVG in Amsterdam as a pathologist. Two years later, he also began working as a pathologist for the Flevoziekenhuis in Almere. He worked in this role for more than 33 years, since 2018 at OLVG LAB BV. The department he works in offers diagnostic services to not only the OLVG and Flevoziekenhuis, but also to several other hospitals including BovenIJ Ziekenhuis and Tergooi MC. Additionally, they provide diagnostic services in the areas of skin and gastrointestinal issues to various independent treatment centers.

Throughout his career, Hans has been committed to education and professional development. He served as a trainer for pathology residents in the OLVG from 1995 to 2012.

He was a member of the medical staff board at the OLVG from 2006 to 2010 in the role of secretary. Subsequently, he was chair of the Honorarium Commission OLVG for 5 years.

He has also been actively involved in various professional societies. He was a board member and co-founder of the Dutch Resident Association of Pathology (LPAV) from 1987 to 1990, a board member of the nationwide network and registry of histo- and cytopathology in the Netherlands (PALGA Foundation) from 2002 to 2008, and a member of the supervisory board of the PALGA Foundation from 2009 to 2016.

Hans served as a board member of the Dutch Society of Pathology (NVVP) from 2008 to 2016, serving as treasurer from 2008 to 2011, president-elect from 2011 to 2012, president from 2012 to 2015, and past-president and interim treasurer from 2015 to 2016.

Currently, he is a member of the Committee Legal Affairs (Juridische Commissie) of the NVVP. For his contributions to the NVVP, he received the association's honorary medal, the "Pompe-penning", in 2022.

He served as a sub-editor for pathology at the *Nederlands Tijdschrift voor Geneeskunde* (NTvG) from 2008 to 2014.

His professional areas of interest and expertise include besides pulmonary pathology, also gynecological pathology.

He is married to his high school sweetheart, Rineke, for 44 years and they have 3 children and 4 grandchildren.

CRediT author statements

- **Chapter 2** Complete pathological response is predictive for clinical outcome after tri-modality therapy for carcinomas of the superior pulmonary sulcus
Hans Blaauwgeers: Conceptualization, writing original draft, investigating; **Ingrid Kappers, Houke Klomp, Rick Paul, Koen Hartemink, Erik Phernambucq, Max Dahele:** Investigating, writing & editing; **José Belderbos, Egbert Smit, Piet Postmus, Jan Oosterhuis, Cornelis Vos, Sjaak Burgers:** Writing & editing; **Lea Dijkstra, Birgit Lissenberg-Witte:** Formal analysis, writing & editing; **Erik Thunnissen:** Conceptualization, writing & editing, supervision.

- **Chapter 3** The prognostic value of proliferation, PD-L1 and nuclear size in patients with superior sulcus tumours treated with chemoradiotherapy and surgery.
Hans Blaauwgeers: Conceptualization, writing original draft, investigating; **Birgit Lissenberg-Witte:** Formal analysis; **Chris Dickhoff:** Investigation, Writing and editing; **Sylvia Duin:** Investigating; **Erik Thunnissen:** Conceptualization, writing & editing, supervision

- **Chapter 4** A population-based study of outcomes in surgically resected T3N0 non-small cell lung cancer in the Netherlands, defined using TNM-7 and TNM-8; justification of changes and an argument to incorporate histology in the staging algorithm.
Hans Blaauwgeers: Conceptualization, writing original draft, investigating; **Ronald Damhuis:** Investigating, writing & editing; **Birgit Lissenberg-Witte:** Formal analysis, writing & editing; **Joop de Langen, Suresh Senan:** Writing and editing; **Erik Thunnissen:** Conceptualization, writing & editing, supervision

- **Chapter 5** Ex vivo artifacts and histopathologic pitfalls in the lung
Erik Thunnissen: Conceptualization, writing original draft; **Hans Blaauwgeers, Erienne de Cuba, David Yick, Douglas Flieder:** Writing and editing

- **Chapter 6** A prospective study of loose tissue fragments in non-small cell lung cancer resection specimen. An alternative view to “spread through airspaces”

Hans Blaauwgeers: Conceptualization, writing original draft, investigating; **Douglas Flieder, Arne Warth, Alexander Harms, Kim Monkhorst:** Investigation, writing and editing; **Birgit-Lissenberg-Witte:** Formal analysis, writing & editing; **Erik Thunnissen:** Conceptualization, writing & editing, supervision

- **Chapter 7** Pulmonary loose tumor tissue fragments and spread through air spaces (STAS): invasive pattern or artifact? A critical review.

Hans Blaauwgeers: Conceptualization, writing original draft; **Prudence Russell, Kirk Jones, Teodora Radonic:** Writing and editing; **Erik Thunnissen:** Conceptualization, writing & editing, supervision

- **Chapter 8** To the editor: “Spread through air spaces (STAS) is prognostic in atypical carcinoid, large cell neuroendocrine carcinoma, and small cell carcinoma of the lung”

Erik Thunnissen: Conceptualization, writing original draft; **Alberto Marchevsky, Giulio Rossi, Prudence A. Russell, Hans Blaauwgeers, Teodora Radonic, Jan von der Thüsen, Douglas Flieder, Giuseppe Pelosi:** Writing and editing

- **Chapter 9** To the editor: “Spread through air spaces (STAS); can an artifact really be excluded?”.

Hans Blaauwgeers: Conceptualization, writing original draft; **Erik Thunnissen:** Conceptualization, writing & editing, supervision

- **Chapter 10** Loose tumor cells in pulmonary arteries of lung adenocarcinoma resection specimen; no correlation with survival, despite high prevalence.

Hans Blaauwgeers: Conceptualization, writing original draft, investigating; **Federica Filipello, Arthur Smit, Julien Vincenten:** Investigation, writing and editing; **Birgit Lissenberg-Witte:** Formal analysis, writing & editing; **Claudio Doglioni, Teodora Radonic, Idris Bahce, Yuko Minami, Andreas Schonau, Chris Dickhoff:** Writing and editing; **Erik Thunnissen:** Conceptualization, writing & editing, supervision, investigating

- **Chapter 11** Is Spread Through Air Spaces an in vivo phenomenon or an inducible artifact?
- Hans Blaauwgeers:** Conceptualization, writing original draft; **Chris Dickhoff, Giuseppe Pelosi, Wim Timens, Federica Filipello, Yuko Minami, Giulio Rossi:** Writing and editing; **Erik Thunnissen:** Conceptualization, writing & editing, supervision
- **Chapter 12** Elastin in pulmonary pathology: relevance in tumors with lepidic and/or papillary appearance. A comprehensive understanding from a morphological viewpoint.
- Erik Thunnissen:** Conceptualization, writing original draft; **Noriko Motoi, Yuko Minami, Daisuke Matsubara, Wim Timens, Yukio Nakatani, Yuichi Ishikawa, Ximena Baez- Navarro, Teodora Radonic, Hans Blaauwgeers, Alain C Borczuk, Masayuki Noguchi:** Writing and editing
- **Chapter 13** Incorporating surgical collapse in the pathological assessment of resected adenocarcinoma in situ of the lung. A proof of principle study.
- Hans Blaauwgeers:** Conceptualization, writing original draft, investigating; **Julien P.L. Vincenten:** Investigation, writing and editing; **Birgit I. Lissenberg-Witte:** Formal analysis, writing & editing; **Teodora Radonic, Idris Bahce, Chris Dickhoff:** Writing and editing; **Erik Thunnissen:** Conceptualization, writing & editing, supervision
- **Chapter 14** 3-dimensional reflection aids in understanding the fog of 2-dimensional pattern recognition in pulmonary adenocarcinomas. Proposal for a modified classification.
- Federica Filipello, Hans Blaauwgeers:** Conceptualization, writing original draft, investigating; **Birgit Lissenberg-Witte:** Formal analysis, writing & editing; **Claudio Doglioni, Arthur Smit:** Investigating, writing and editing; **Andreas Schonau, Gianluigi Arrigoni, Teodora Radonic, Idris Bahce, Chris Dickhoff, Antonio Nuccio, Alessandra Bulotta, Yuko Minami, Masayuki Noguchi, Francesca Ambrosi:** Writing and editing; **Erik Thunnissen:** Conceptualization, writing & editing, investigating, supervision

■ Chapter 15

Invasion measurement and adenocarcinoma *in situ* (AIS) in pulmonary adenocarcinomas of 3 cm or less. A reproducibility study according to the WHO and a revised classification.

Erik Thunnissen, Hans Blaauwgeers: Conceptualization, writing original draft, investigating; **Birgit Lissenberg-Witte:** Formal analysis, writing & editing; **Federica Filipello, Yuko Minami, Masayuki Noguchi, Willem Vreuls, Jan H. von der Thüsen, John Le Quesne, Mauro Giulio Papotti, Wim Timens, Irene Sansano, David Moore, Sabina Berezowska, Aleš Ryška, Giuseppe Pelosi, Luka Brcic, Kirk Jones, Noriko Motoi, Yukio Nakatani, Christiane Kuempers, Paul Hofman, Veronique Hofman, Vibeke Grotnes Dale, Giulio Rossi, Francesca Ambrosi, Daisuke Matsubara, Yuichi Ishikawa, Birgit Weynand, Fiorella Calabrese, Izidor Kern, Sven Perner, Diana Gabriela Leonte, Siobhan Nicholson, Douglas Flieder, Marc Ooft, Mariel Brinkhuis, Nicole Bulkman, Shaimaa Al-Janabi, Aino Mutka, Sanja Dacic, Mary Beth Beasley, Gianluigi Arrigoni, Rieneke Britstra, Hendrik Hager, Andreas Schønau, Federica Pezzuto:** Investigating, writing and editing

■ Chapter 16

Arguments for non-mucinous adenocarcinoma *in situ* of the lung larger than 7 cm.

Hans Blaauwgeers: Conceptualization, writing original draft, investigating; **Onno Mets, Birgit Lissenberg-Witte, Ronald Damhuis, Idris Bahce, Teodora Radonic, Chris Dickhoff, Gianluigi Arrigoni, Daniela Finocchiaro:** Investigating, writing and editing; **Erik Thunnissen:** Conceptualization, writing & editing, investigating, supervision

